LIPASE INHIBITORS FROM *DENDROBIUM SENILE*

Miss Myat Pann Phyu

A Thesis Submitted in Partial Fulfillment of the Requirements
for the Degree of Master of Science in Pharmaceutical Sciences and Technology
Common Course
FACULTY OF PHARMACEUTICAL SCIENCES
Chulalongkorn University
Academic Year 2021

สารที่มีฤทธิ์ยับยั้งเอนไซม์ไลเปสจากเอื้องชะนี

น.ส.เมียต พาน พยู

วิทยานิพนธ์นี้เป็นส่วนหนึ่งของการศึกษาตามหลักสูตรปริญญาวิทยาศาสตรมหาบัณฑิต
สาขาวิชาเภสัชศาสตร์และเทคโนโลยี ไม่สังกัดภาควิชา/เทียบเท่า
คณะเภสัชศาสตร์ จุฬาลงกรณ์มหาวิทยาลัย
ปีการศึกษา 2564

Thesis Title	LIPASE INHIBITORS FROM *DENDROBIUM SENILE*
By	Miss Myat Pann Phyu
Field of Study	Pharmaceutical Sciences and Technology
Thesis Advisor	Associate Professor BOONCHOO SRITULARAK, Ph.D.
Thesis Co Advisor	Professor KITTISAK LIKHITWITAYAWUID, Ph.D.

Accepted by the FACULTY OF PHARMACEUTICAL SCIENCES, Chulalongkorn University in Partial Fulfillment of the Requirement for the Master of Science

..... Dean of the FACULTY OF PHARMACEUTICAL SCIENCES

(Professor PORNANONG ARAMWIT, Ph.D.)

THESIS COMMITTEE

..... Chairman

(Assistant Professor TAKSINA CHUANASA, Ph.D.)

..... Thesis Advisor

(Associate Professor BOONCHOO SRITULARAK, Ph.D.)

..... Thesis Co-Advisor

(Professor KITTISAK LIKHITWITAYAWUID, Ph.D.)

..... Examiner

(Assistant Professor CHAISAK CHANSRINIYOM, Ph.D.)

..... External Examiner

(Duangpen Pattamadilok, Ph.D.)

เมียต พาน พยู : สารที่มีฤทธิ์ยับยั้งเอนไซม์ไลเปสจากเอื้องชะนี. (LIPASE INHIBITORS FROM *DENDROBIUM SENILE*) อ.ที่ปรึกษาหลัก : รศ. ภก. ดร.บุญชู ศรีตุลารักษ์, อ.ที่ปรึกษาร่วม : ศ. ภก. ดร.กิตติศักดิ์ ลิขิตวิทยาวุฒิ

โรคอ้วนเป็นภาวะที่มีความผิดปกติของการเผาผลาญไขมันที่เกิดจากความไม่สมดุลระหว่างพลังงานที่รับเข้าสู่ร่างกายและพลังงานที่ใช้ออกไป เอนไซม์ไลเปสจากตับอ่อนทำหน้าที่ย่อยไขมันและไขมันที่ถูกย่อยจะถูกดูดซึมเข้าสู่ลำไส้เล็ก การยับยั้งเอนไซม์ไลเปสจากตับอ่อนจึงช่วยลดการดูดซึมไขมันจากอาหารส่งผลให้น้ำหนักตัวลงและยังมีผลช่วยลดระดับคอเลสเตอรอลและน้ำตาลในเลือด จากส่วนทั้งต้นของเอื้องชะนีสามารถสกัดสารกลุ่มฟีแนนทรีนชนิดใหม่ 1 ชนิด คือ 2,5,7-trihydroxy-4-methoxyphenanthrene (1) ร่วมกับสารที่เคยมีรายงานจำนวน 7 ชนิด ได้แก่ moscatin (2), 2,5-dihydroxy-4,9-dimethoxyphenanthrene (3), moscatilin (4), aloifol I (5), 4,4',8,8'-tetramethoxy[1,1'-biphenanthrene]-2,2',7,7'-tetrol (6), 2,2',7,7'-tetrahydroxy-4,4'-dimethoxy-1,1'-biphenanthrene (7) และ bleformin G (8) การวิเคราะห์โครงสร้างทางเคมีอาศัยเทคนิคทาง NMR, UV, IR และ MS จากการทดสอบฤทธิ์ยับยั้งเอนไซม์ไลเปสของสารที่แยกได้พบว่า moscatin (2) และ 2,5-dihydroxy-4,9-dimethoxyphenanthrene (3) มีฤทธิ์ยับยั้งเอนไซม์ไลเปส โดยมีค่า IC_{50} 57.6 ± 3.3 ไมโครโมลาร์ และ 58.6 ± 3.4 ไมโครโมลาร์ ตามลำดับ เมื่อเปรียบเทียบกับยา orlistat (IC_{50} 0.031 ± 0.004 ไมโครโมลาร์) ที่ใช้เป็นสารควบคุมผลบวก

สาขาวิชา เภสัชศาสตร์และเทคโนโลยี ลายมือชื่อนิสิต .....
ปีการศึกษา 2564 ลายมือชื่อ อ.ที่ปรึกษาหลัก .....
ลายมือชื่อ อ.ที่ปรึกษาร่วม .....

6272010733 : MAJOR PHARMACEUTICAL SCIENCES AND TECHNOLOGY
KEYWORD: obesity pancreatic lipase hypocholesterolemia hypoglycemia Dendrobium senile phenanthrene orlistat

Myat Pann Phyu : LIPASE INHIBITORS FROM *DENDROBIUM SENILE*. Advisor: Assoc. Prof. BOONCHOO SRITULARAK, Ph.D. Co-advisor: Prof. KITTISAK LIKHITWITAYAWUID, Ph.D.

Obesity is characterized as an abnormal lipid metabolism due the imbalance between the energy intake and output. Pancreatic lipase is secreted by the pancreas and plays an important role in the digestion and absorption of lipids in the small intestine. Inhibition of pancreatic lipase enzyme can reduce dietary fat absorption which will lead to loss of weight and finally result in hypocholesterolemia and hypoglycemia. From the whole plant of *Dendrobium senile*, a new phenanthrene derivative was isolated, together with seven known compounds, including 2,5,7-trihydroxy-4-methoxyphenanthrene (1), moscatin (2), 2,5-dihydroxy-4,9-dimethoxyphenanthrene (3), moscatilin (4), aloifol I (5), 4,4',8,8'-tetramethoxy[1,1'-biphenanthrene]-2,2',7,7'-tetrol (6), 2,2',7,7'-tetrahydroxy-4,4'-dimethoxy-1,1'-biphenanthrene (7) and bleformin G (8). Their structures were characterized by NMR, UV, IR and MS spectroscopic methods. All the isolated compounds were evaluated for pancreatic lipase inhibitory activity. Moscatin (2) and 2,5-dihydroxy-4,9-dimethoxyphenanthrene (3) showed recognizable pancreatic lipase inhibitory activity with IC_{50} values of 57.6 ± 3.3 μM and 58.6 ± 3.4 μM, respectively, when compared with the positive control orlistat (IC_{50} 0.031 ± 0.004 μM).

Field of Study:	Pharmaceutical Sciences and Technology	Student's Signature .....
Academic Year:	2021	Advisor's Signature .....
		Co-advisor's Signature .....

ACKNOWLEDGEMENTS

Firstly, I would like to extend my special gratitude to my advisor, Associate Professor BOONCHOO SRITULARAK, Ph.D. and my co-advisor Professor KITTISAK LIKHITWITAYAWUID, Ph.D. for their mercy, guidance and widespread knowledge. It was a fabulous moment doing research under their instruction without any difficulties throughout my research period.

Secondly, I would like to express my appreciation to all the seniors, friends and also staff members of the Department of Pharmacognosy and Pharmaceutical Botany for their considerable support, benevolence and friendliness.

I also wish to show my special thanks to the Pharmaceutical Sciences and Technology Graduate Scholarship Program and CU ASEAN Scholarship for giving me a great chance to study a Master's Degree in Thailand.

Finally, I would like to say thanks to my family for their strong encouragement during my master student life.

Myat Pann Phyu

TABLE OF CONTENTS

Page

LIST OF FIGURES

LIST OF TABLES

LIST OF SCHEMES

ABBREVIATIONS AND SYMBOLS

Acetone-d_6	=	Deuterated acetone
Ara	=	Arabinose
Api	=	Apiose
br s	=	Broad singlet (for NMR spectra)
^{13}C-NMR	=	Carbon-13 Nuclear Magnetic Resonance
$CaCl_2$	=	Calcium chloride
CC	=	Column chromatography
CH_2Cl_2	=	Dichloromethane
COSY	=	^{1}H-^{1}H Correlation Spectroscopy
cm	=	Centimeter
2-D NMR	=	Two-dimensional Nuclear Magnetic Resonance
d	=	Doublet (for NMR spectra)
dd	=	Doublet of doublets (for NMR spectra)
EtoAc	=	Ethyl acetate
ESI-MS	=	Electrospray Ionization Mass Spectrometry
FT-IR	=	Fourier-Transformed Infrared Spectroscopy
Gal	=	Galactose
Glc	=	Glucose
g	=	Gram
^{1}H-NMR	=	Proton Nuclear Magnetic Resonance
HPLC	=	High-Performance Liquid Chromatography
HR-ESI-MS	=	High Resolution Electrospray Ionization Mass Spectrometry
HSQC	=	^{1}H-detected Heteronuclear Single Quantum Coherence
HMBC	=	^{1}H-detected Heteronuclear Multiple Bond Correlation

Hz	=	Hertz
IC_{50}	=	Concentration exhibiting 50% inhibition
IR	=	Infrared
J	=	Coupling constant
Kg	=	Kilogram
λ_{max}	=	Wavelength at maximal absorption
MeOH	=	Methanol
$[M-H]^-$	=	Deprotonated molecular ion
$[M+Na]^+$	=	Sodium-adduct molecular ion
m/z	=	Mass to charge ratio
4-MUO	=	4-Methylumbelliferyl oleate
4-MU	=	4-Methylumbelliferone
M	=	Molar
m	=	Multiplet (for NMR spectra)
mg	=	Milligram
µg	=	Microgram
MHz	=	MegaHertz
min	=	Minute
ml	=	Milliliter
µl	=	Microliter
µM	=	Micromolar
mM	=	Millimolar
mm	=	Millimeter
MS	=	Mass Spectrometry
ν_{max}	=	Wave number at maximal absorption
NaCl	=	Sodium chloride

NMR	=	Nuclear Magnetic Resonance
nm	=	Nanometer
NOESY	=	Nuclear Overhauser Effect Spectroscopy
OH	=	Hydroxy
OMe	=	Methoxy
OPC	=	Open Column Chromatography
pH	=	Potential of Hydrogen ion
ppm	=	Part per million
Rha	=	Rhamnose
s	=	Singlet (for NMR spectra)
SD	=	Standard Deviation
t	=	Triplet (for NMR spectra)
TLC	=	Thin Layer Chromatography
UV	=	Ultraviolet
UV-VIS	=	Ultraviolet and Visible Spectroscopy
VLC	=	Vacuum Liquid Column Chromatography
Xyl	=	Xylose

CHAPTER I

INTRODUCTION

Recently, the epidemic of obesity has significantly been rising in both developed and developing countries, and this metabolic disorder has now been ranked as the fifth leading cause of death (Kojta *et al.*, 2020; Sharma & Sharma, 2020). Due to the tremendous increase in obese population worldwide, the World Health Organization (WHO) has considered obesity, also termed "New World Syndrome", as a global problem (Seyedan *et al.*, 2015). Obesity is becoming a major contributor to health problems over the outbreak of undernutrition and other infectious diseases due to its recent impacts on adolescents and adults (Kopelman, 2000; Lim *et al.*, 2020). Obesity is closely related to lifestyles such as insufficient physical exercise and high caloric food intake. Other factors including family history, health problems such as hypothyroidism or Cushing's syndrome, emotional factors, age, smoking and taking corticosteroids or antidepressants considerably contribute to weight gain (Chedda *et al.*, 2016; Marti *et al.*, 2004).

Obesity is a chronic lipid metabolic disorder that is caused by the imbalance between energy intake and energy expenditure, leading to an excess fat accumulation in adipose tissues (Jung & Choi, 2014). This metabolic illness is consequently associated with the massive range of co-morbidities such as cardiovascular diseases, insulin-resistant diabetes, hypertension, hyperlipidemia, asthma, sleeping disorders, fatty liver disease, gallstones, musculoskeletal disorders (e.g., osteoarthritis), cancers in certain organs (e.g., liver, gallbladder, colon, kidney, breast, ovarian and endometrial cancers) and reproduction deficits such as infertility (Baretić, 2012; Kim *et al.*, 2016; Liu *et al.*, 2020b; Seyedan *et al.*, 2015). In addition, obesity can cause psychological and social problems (Aronne, 2002).

In anatomical study, obesity is classified according to the site of fat distribution and deposition in the body: (1) visceral fat which attributes to serious

health consequences; (2) subcutaneous fat which is not involved in obesity related metabolic disorders. In terms of etiology, obesity that is resulted from the impaired fat homeostasis mechanism is called primary obesity. Obesity that is caused by the adverse effects of certain types of drug treatments (steroids, insulin, antipsychotic drugs, etc.) and endocrine diseases (Cushing syndrome, hypothyroidism, etc.) is classified as secondary obesity (González-Castejón & Rodriguez-Casado, 2011; Lunagariya *et al.*, 2014). Body mass index (BMI) is an important parameter used to assess obesity. BMI is defined as the individual's body weight divided by the square of the height (kg/m^2). BMI values of less than 18.5 and greater than 24.9 are classified as underweight and overweight, respectively. A BMI of above 30 is graded as obesity (Sukhdev & Singh, 2013). Moreover, in terms of BMI intervals, there are three classes of obesity as determined from the levels of mortality risk. Class I (BMI 30-34.9), Class II (BMI 35-39.9) and Class III obesity (BMI above 40) are associated with moderate, high and highest mortality risk, respectively (González-Castejón & Rodriguez-Casado, 2011).

Reduction of overweight and obesity can be accomplished by several methods through central or peripheral pathways. For example, appetite suppression can be induced by centrally stimulating the release of the anorexigenic signals or by blocking the orexigenic signals. Regarding the peripheral mechanisms, there are three approaches. The first strategy aims to reduce energy intake through the inhibition of dietary fat digestion and absorption processes in the gastrointestinal system. The second approach is to reduce fat mass via enhancing fat mobilization and metabolism processes through the inhibition of triacylglycerol synthesis and deposition in the adipose tissue. The last strategy targets the increase in energy expenditure by stimulating lipid oxidation or thermogenesis through peripheral mechanisms (Shi & Burn, 2004).

Currently, four anti-obesity drug therapies have been approved by the US Food and Drug Administration (FDA) for long-term weight loss management, including

orlistat, liraglutide, naltrexone/bupropion and phentermine/topiramate (Kim *et al.*, 2020). All of these except phentermine/topiramate combination therapy have been approved by the European Medicines Agency (EMA) (Patel & Stanford, 2018). During the last decades, several anti-obesity drugs were withdrawn from the market due to their high-risk profiles discovered during post-marketing surveillance. They are fenfluramine (valvular heart disease, in 1997), rimonabant (serious psychiatric problems, in 2008), sibutramine (myocardial infarction and stroke, in 2010) and lorcaserin (cancer risk, in 2020) (Lai *et al.*, 2020; Patel & Stanford, 2018; Rodgers *et al.*, 2012; Tak & Lee, 2021).

Liraglutide, one of the FDA approved anti-obesity drugs, can reduce food intake by acting through both central and peripheral mechanisms. Liraglutide is a glucagon-like peptide-1 (GLP-1) receptor agonist which suppresses appetite by directly stimulating appetite inhibiting anorexigenic pro-opiomelanocortin / cocaine- and amphetamine-regulated transcript (POMC/CART) neurons and indirectly inhibiting appetite stimulating orexigenic neurons such as neuropeptide-Y (NPY) and Agouti-related peptide (AgRP) neurons in the arcuate nucleus of the hypothalamus via gamma-aminobutyric acid-dependent signaling (Alruwaili *et al.*, 2021; Patel & Stanford, 2018). Gallstones and acute pancreatitis are considered as major safety issues in liraglutide treatment while nausea, vomiting, diarrhea, constipation and abdominal pain are common adverse effects of the drug. Liraglutide is administered subcutaneously at a dose of 3 mg daily for weight loss management (Patel & Stanford, 2018). Systemic administration of GLP-1 receptor agonist delays gastric emptying and reduces energy intake resulting in losing body weight. At the dose of 1.8 mg, it can also induce glucose-dependent insulin secretion from the pancreas in the management of type-2 diabetes (Alruwaili *et al.*, 2021; Patel, 2015).

Regarding the Naltrexone/bupropion combination therapy, bupropion, which is a norepinephrine–dopamine reuptake inhibitor and nicotinic acetylcholine receptor

antagonist, decreases the energy intake and energy expenditure through the release of alpha-melanocyte-stimulating hormone (α-MSH) by stimulating the arcuate nucleus based POMC neurons. Naltrexone, an opioid-receptor antagonist, acts as a synergist to bupropion via inhibition of beta-endorphins binding on the mu-opioid receptor thereby increasing POMC activity and facilitating the release of α-MSH. Therefore, this combination therapy may facilitate the appetite suppression process and finally leads to weight loss effect (Patel & Stanford, 2018). Common side effects of naltrexone/bupropion treatment are nausea, headache, constipation, dry mouth, dizziness and insomnia (Woodard *et al.*, 2020). For obesity management, the starting recommended dose of the naltrexone (8 mg)/bupropion (90 mg) combination is one sustained-release tablet daily, and the dose can be gradually titrated up to 2 tablets twice a day over a period of 1 month (Tek, 2016).

The phentermine/topiramate combination therapy is used in chronic weight management. The combined drugs induce appetite suppression by acting as a norepinephrine and gamma-aminobutyric acid (GABA) agonist and also as a glutamate antagonist. However, the exact mechanisms of action are still under elucidation (Woodard *et al.*, 2020). It is recommended to take orally once daily and the starting dose is an extended-release (ER) single capsule of 3.75 mg phentermine and 23 mg topiramate. The dose can be titrated up to 15 mg/92 mg of phentermine/topiramate ER. Dry mouth, depression, insomnia, anxiety, constipation, paresthesia and abnormal taste sensation are common untoward effects of this combination therapy, and the fetal toxic effect of topiramate limits its use in pregnant women (Topaloglu & Sahin, 2021).

Since lipid metabolism plays a major role in developing obesity, inhibition of the digestion and absorption of lipid via pancreatic lipase inhibition seems to be safe and have relatively fewer side effects without unwanted central effects (Birari & Bhutani, 2007; Sridhar *et al.*, 2017). About 90% of the main dietary fat are

triglycerides (TAGs). The structure of a TAG is made up of one glycerol molecule and three fatty acid molecules (Liu *et al.*, 2020b; Shi & Burn, 2004). The breakdown of TAGs into free fatty acids by the enzyme lipase is a necessary step before the lipid absorption by intestinal enterocytes. Tongue lipase, gastric lipase and pancreatic lipase are involved in the hydrolysis of triglycerides which produce diglycerides, monoglycerides, glycerol and fatty acids (Iqbal & Hussain, 2009).

When dietary fats are ingested, the lingual lipase secreted by serous (von Ebner) glands on the tongue digests only one-third of the ingested fat due to its lower expression level (Birari & Bhutani, 2007; Kulkarni & Mattes, 2014). Partial hydrolysis (10-30%) is performed by the acid stable gastric lipase secreted from the gastric mucosal cells in the stomach, and this lipase also acts as synergistic to the pancreatic lipase enzyme in the duodenum to facilitate lipid digestion (Garza *et al.*, 2011; Hamosh, 1990; Lunagariya *et al.*, 2014). Human pancreatic lipase (triacylglycerol acyl hydrolase) is the principle lipolytic enzyme in the small intestine. It plays a significant role in the complete hydrolysis (50-70%) of dietary triglycerides into monoglycerides and free fatty acids and is also important for lipid absorption in the duodenum.

Pancreatic lipase (PL) enzyme is produced by pancreatic acinar cells and is a high molecular weight single chain glycoprotein of 449 amino acids (Birari & Bhutani, 2007; Lunagariya *et al.*, 2014). Two folding units of the polypeptide chain of PL enzyme are a globular N-terminal domain (amino acid residues 1-335) formed by a central β-sheet core and a C-terminal domain (residues 336-449) with a β-sheet sandwich structure (Buchholz & Melzig, 2015; Lowe, 1997). The specific role of N-terminal domain is catalytically active in the presence of a catalytic triad of amino acids serine (152), histidine (263) and aspartic acid (176). The nucleophilic serine (152) is essential for the hydrolytic activity of the enzyme, and the oxyanion hole of the N-terminal domain largely contributes to the catalytic efficiency of the enzyme

(Buchholz & Melzig, 2015; Kumar & Chauhan, 2021; Sarmah *et al.*, 2018). In addition, the lid or flap (peptide stretch C237–C261) covers the active catalytic site by locating non-polar side chains over the catalytic group and polar side chains on the surface of the enzyme in the absence of the lipid micelles (GuyáDodson, 1992; Miled *et al.*, 2000). These lipid micelles are formed by emulsification of the large fat molecules containing dietary triglycerides, diglycerides and bile salts together with phospholipids, polar lipids, oligosaccharides, cholesterol, free fatty acids and denatured proteins (Lunagariya *et al.*, 2014). The mechanism of "interfacial activation" occurs as the lid of the enzyme opens at the oil-water interface by means of which provides a way for the substrate to reach the active catalytic site (Sarmah *et al.*, 2018). This interfacial activation is accelerated by a small non-enzymatic protein, co-lipase which acts as an anchor for lipase adsorption because bile salts inhibit the lipase adsorption onto the substrate by covering the whole water-substrate interface. Therefore, co-lipase is required for the complete function of PL enzyme via preventing bile salts and phosphatidyl choline-mediated inhibitory effects on enzyme-substrate complex (Chapus *et al.*, 1975; Kumar & Chauhan, 2021). Co-lipase is converted from a precursor pro-colipase which is secreted by the exocrine pancreas via tryptic cleavage of an N-terminal pentapeptide known as enterostatin which is responsible for the regulation of food intake process in higher mammals (Bacha *et al.*, 2011).

The adsorption of pancreatic lipase onto the substrate facilitates the formation of Michaelis-Menten adsorption complex in which the oxyanion hole (a pocket in the active site of the enzyme, the catalytic triad and the carboxylic ester group of triglycerides) plays a key role for acylation and de-acylation mechanisms to break down the dietary lipids (Kumar & Chauhan, 2021; Mukherjee, 2014). The catalytic mechanism of the enzyme starts with acylation in which the hydroxyl group of the catalytic serine residue of the catalytic triad becomes activated with a

subsequent increase in nucleophilicity due to the transfer of a proton among the aspartate, histidine and serine residues of the lipase. This nucleophilic attack of serine residue on the carbonyl group of the substrate enables the formation of a tetrahedral intermediate with a negative charge on the oxygen of the carbonyl group. The stabilization of the charge distribution and reduction of the energy state of the tetrahedral intermediate are obtained with the help of the oxyanion hole by forming at least two hydrogen bonds between their backbone amide protons and oxygen ion of negatively charged tetrahedral intermediate. Then, a nucleophile such as water attacks the enzyme resulting in the de-acylation mechanism and releases the lipolytic products (Casas-Godoy *et al.*, 2018).

After hydrolysis, the lipolytic products such as monoglycerides, diglycerides, cholesterol, free fatty acids, bile salts, fat soluble vitamins and lysophosphatidic acid are absorbed by the intestinal enterocytes as chyme, and which in turn induce the secretion of bile salts and pancreatic lipase by stimulating the release of cholecystokinin and secretin hormones of the intestinal tract after entering of the chyme in the duodenum. After the intestinal lipid absorption, free fatty acids and monoglycerides are re-esterified into triglycerides (TAGs) for energy storage in the adipose tissue. Excess fat deposition in the adipose tissue finally leads to obesity (Buchholz & Melzig, 2015).

Although several anti-obesity drugs have reached the market, most of them have been withdrawn at the post-marketing stage due to their serious health consequences (Onakpoya *et al.*, 2016). Until now after approval from US FDA in 1999, Orlistat has been a drug of choice for long-term obesity management of both adolescents (12 years of age) and older people because of its higher safety profiles and therapeutic effects in type-2 diabetes, hypertension, dyslipidemia, non-alcoholic fatty liver disease, polycystic ovary syndrome and breast cancer (Priyadharshini *et al.*, 2019; Woodard *et al.*, 2020). Recently, researchers have uncovered the anti-tumor

effects of orlistat on breast, ovary, prostate, colorectal, bladder, osteosarcoma, non-Hodgkin lymphomas, leukemias and lung cancers via acting as a fatty acid synthase (FASN) inhibitor in preclinical *in vitro* and *in vivo* studies. FAS plays a vital role in carcinogenesis by protecting cells from apoptosis and is also highly expressed in cancer cells (Schcolnik-Cabrera *et al.*, 2018).

Orlistat (tetrahydrolipstatin) is a saturated derivative of lipstatin which is derived naturally from *Streptomyces toxytricini.* Orlistat is a potent gastric and pancreatic lipase inhibitor. It irreversibly inhibits pancreatic lipase with little or no effect on other hydrolases such as amylase, trypsin, chymotrypsin and phospholipases (Qi, 2018). Orlistat inactivates up to 91.4% of these enzymes by forming a covalent bond with the serine residue of the active catalytic site of the lipase thus preventing the dietary fat hydrolysis and inhibiting the absorption of free fatty acids and monoglycerides (McClendon *et al.*, 2009).

The chemical name of orlistat is [(*S*)-2-formylamino-4-methyl-pentanoic acid (*S*)-1-[[(2*S*,3*S*)-3-hexyl-4-oxo-2-oxetanyl] methyl]-dodecyl ester] (Goyal *et al.*, 2020). Its pancreatic lipase inhibitory effect is obtained by forming a long-lived acyl-enzyme complex via the nucleophilic attack on the β-lactone ring of orlistat by the hydroxy group of the active serine 152 of the lipase. The primary product of β-hydroxy carboxylic acid of Orlistat and the active enzymes are further processed by the subsequent hydrolysis of this covalent adduct thereby leading to the inactive δ-lactone final degradation products through isomerization or hydrolysis of the primary product (Bénarouche *et al.*, 2014). Orlistat reduces approximately 30% dietary fat absorption at the recommended dosage (120 mg three times daily during or after meal within 1 hour) (Kim *et al.*, 2018). It produces local inhibitory effect in the gut with no systemic absorption due to its lipophilic nature (Al-Omar *et al.*, 2006). Gastrointestinal side effects such as steatorrhea, fecal spotting, fecal incontinence, abdominal floating and cramping, diarrhea and fat-soluble vitamins (Vitamins A, D, E

and K) deficiencies are common adverse effects of orlistat. A few cases of hepatic adverse effects (cholestatic hepatitis, cholelithiasis and subacute liver failure) and acute pancreatitis have also been reported. Moreover, orlistat is associated with the risk for acute kidney injury due to the excess oxalate formation as the unabsorbed fat binds with calcium in the intestinal lumen (Filippatos *et al.*, 2008).

As mentioned earlier, pancreatic lipase inhibition has recently received much research attention as PL enzyme plays a vital role in dietary fat metabolism, and targeting PL appears to be a safe and effective treatment, with relatively fewer side effects due to its action via the peripheral mechanism (Liu *et al.*, 2020b). Nowadays, several plant, marine, bacterial and fungal species have been screened for their PL inhibitory activity (Buchholz & Melzig, 2015). Among these natural sources, the phytochemicals from plants have potential advantages such as a wide variety of sources, structural diversity, biological friendliness and lower toxicity, the properties of which are suitable for the development of new therapeutic agents (Liu *et al.*, 2020b). In addition, although orlistat is a widely used anti-obesity drug, its usage is compromised due to its unpleasant GI side effects. New PL inhibitors from natural sources without these adverse effects have become attractive targets to explore. Besides, natural products generally have lower toxicity and fewer side effects when compared to the synthetic products (Seyedan *et al.*, 2015). Over the years, a great number of plant extracts and phytoconstituents have been studied for their pancreatic lipase inhibitory activity through *in vitro* or *in vivo* studies (Rajan *et al.*, 2020). Bioactive anti-obesity phytochemicals can be classified according to their chemical structures as phenolics, alkaloids, glycosides, terpenes, saponins, bibenzyls, phenanthrenes, carotenoids and polysaccharides. Flavonoids, phenolic acids and tannins are sometimes collectively called polyphenolic compounds (Inthongkaew *et al.*, 2017; Na Ranong *et al.*, 2019; Singh *et al.*, 2015). Some examples of phytochemicals with PL inhibitory activity are presented in **Table 1** and **Figure 1**.

Table 1 Examples of PL inhibitors from plant sources

Source	Category	Phytochemical	IC_{50}
Glycyrrhiza glabra L. (Fabaceae) Part used – Root (Birari *et al.*, 2011)	Chalcone	Isoliquiritigenin [**1**]	7.3±1.2 μM (Tam *et al.*, 2020)
Erythrina abyssinica Lam. ex DC. (Fabaceae) Part used – Stem bark (Habtemariam, 2012)	Flavanone	Sigmoidin A [**2**]	4.5±0.87 μM (Habtemariam, 2012)
Camellia sinensis L. (Theaceae) Part used – Oolong tea leave (Nakai *et al.*, 2005)	Polyphenol	Oolonghomobisflavan A [**3**]	0.048 μM (Nakai *et al.*, 2005)
Filipendula kamtschatica (Pall.) Maxim. (Rosaceae) Part used – Aerial part (Kato *et al.*, 2012)	Phenolic acid (Hydroxycinnamic acid)	3-*O*-caffeoyl-4-*O*-galloyl-*L*-threonic acid [**4**]	26.00 μM (Kato *et al.*, 2012)

Table 1 (continued)

Source	Category	Phytochemical	IC_{50}
Hemimycale columella (Hymedesmiidae) Part used – Marine sponge (Marmouzi *et al.*, 2021)	Phenolic acid (Hydroxybenzoic acid)	Gallic acid-3-methyl ether [**5**]	91.12±4.7 µg/ml (Marmouzi *et al.*, 2021)
Annona crassiflora Mart. (Annonaceae) Part used – Fruit peel (Pereira *et al.*, 2017)	Aporphine Alkaloid	Stephalagine [**6**]	8.35 µg/ml (Pereira *et al.*, 2017)
Eremochloa ophiuroides (Munro) Hack. (Poaceae) Part used – Leave (Lee *et al.*, 2010)	Flavone Glycoside	Isoorientin-2-*O*-α-*L*-rhamnoside [**7**]	18.5±2.6 µM (Lee *et al.*, 2010)
Cassia auriculata (L.) Roxb. (Fabaceae) Part used – Aerial part (Habtemariam, 2013)	Flavonol Glycoside	Kaempferol-3-*O*-rutinoside [**8**]	2.9±0.50 µM (Habtemariam, 2013)

Table 1 (continued)

Source	Category	Phytochemical	IC_{50}
Actinidia arguta Planchon (Actinidiaceae) Part used – Roots (Jang *et al.*, 2008)	Coumaroyl Triterpene	3-*O*-Trans-*p*-coumaroyl actinidic acid [**9**]	14.95±0.21 μM (Jang *et al.*, 2008)
Salvia officinalis L. (Lamiaceae) Part used – Leave (Ninomiya *et al.*, 2004)	Diterpene	Carnosol [**10**]	13 μM (Ninomiya *et al.*, 2004)
Platycodon grandiflorum (Jacq.) A.DC. (Campanulaceae) Part used – Root (Nyakudya *et al.*, 2014)	Triterpenoid Saponin	Platycodin D [**11**]	2.1±0.03 mM (Zhao & Kim, 2004)
Dioscorea nipponica Makino (Dioscoreaceae) Part used – Root (Kwon *et al.*, 2003)	Steroidal Sapogenin	Diosgenin [**12**]	28 μg/ml (Kwon *et al.*, 2003)
Dendrobium formosum Roxb. ex Lindl. (Orchidaceae) Part used – Whole plant (Inthongkaew *et al.*, 2017)	Bibenzyl	Dendrosinen B [**13**]	295±37.9 μM (Inthongkaew *et al.*, 2017)

Table 1 (continued)

Source	Category	Phytochemical	IC_{50}
Dendrobium infundibulum Lindl. (Orchidaceae) Part used – Whole plant (Na Ranong *et al.*, 2019)	Phenanthrene	5-Methoxy-7-hydroxy-9,10-dihydro-1,4-phenanthrenequinone [**14**]	69.45±10.14 μM (Na Ranong *et al.*, 2019)
Undaria pinnatifida (Alariaceae) Part used – Edible seaweed (Matsumoto *et al.*, 2010)	Carotenoid	Fucoxanthin [**15**]	660 nM (Matsumoto *et al.*, 2010)
Eisenia bicyclis (Laminariaceae) Part used – Brown algae (Eom *et al.*, 2013)	Phlorotannin (Phloroglucinol polymer)	7-Phloroeckol [**16**]	12.7±1.0 μM (Eom *et al.*, 2013)

Several polysaccharides such as pectin (from apples) and algae polysaccharides (carrageenan, agar, chitin, and chitosan), dietary fibers (from wheat bran) and soybean proteins have been studied *in vitro* or *in vivo* for their pancreatic lipase inhibitory activity (Bajes *et al.*, 2020; Lunagariya *et al.*, 2014). Although many candidates of pancreatic lipase inhibitors have been isolated from plants, only a few of them are under clinical investigation. Examples of plant constituents and plant extracts under clinical trials are satiereal, an extract from *Crocus sativus;* an extract of green tea *(Camellia sinensis)*; a *Panax ginseng* extract; and apple polyphenols from *Malus domestica* (Kumar & Chauhan, 2021).

Despite numerous studies on pancreatic lipase inhibitors from several plant species and families, only a few pancreatic lipase inhibitors have been reported from the family Orchidaceae. Several pancreatic lipase inhibitors have been previously reported from the genus *Dendrobium* of this family (Inthongkaew *et al.*, 2017; Na Ranong *et al.*, 2019). Before this study, *Dendrobium senile* was not reported for phytochemicals and biological activities. In this investigation, the plant extracts were prepared from *Dendrobium senile* by extraction methods and then were screened for PL inhibitory activity at a concentration of 100 µg/ml (see the experimental section). The extracts with ≥70% inhibitory effect were considered as active and were subjected to further chemical and biological studies to identify the active principles.

The objective of this study was to search for new anti-obesity molecules from plant sources.

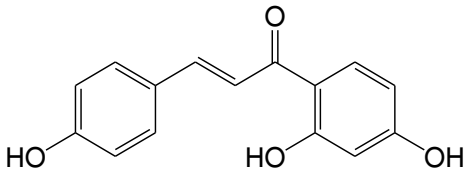

Isoliquiritigenin [**1**]

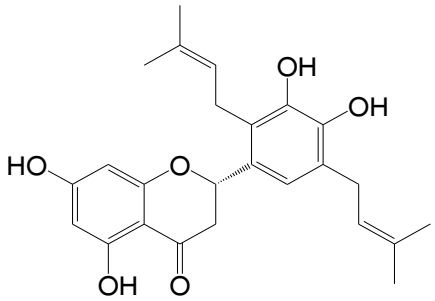

Sigmoidin A [**2**]

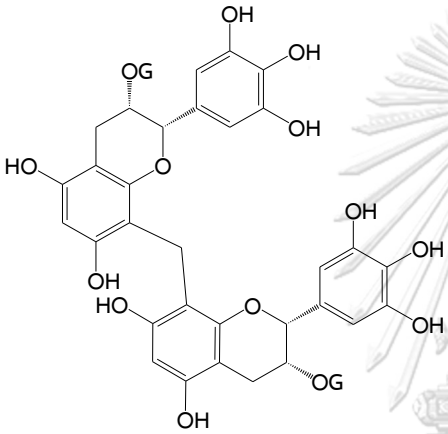

Oolonghomobisflavan A [**3**]

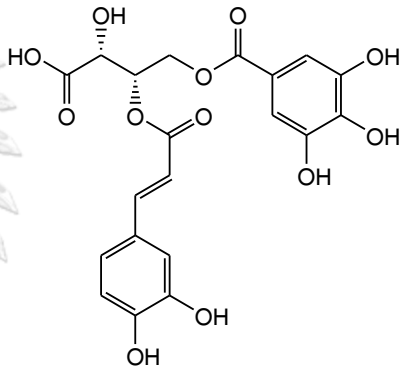

3-*O*-caffeoyl-4-*O*-galloyl-*L*-threonic acid [**4**]

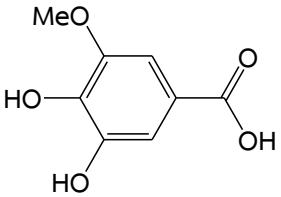

Gallic acid-3-methyl ether [**5**]

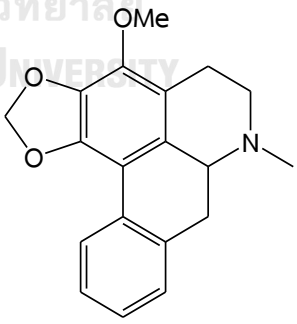

Stephalagine [**6**]

Figure 1 Structures of PL inhibitors from plant sources

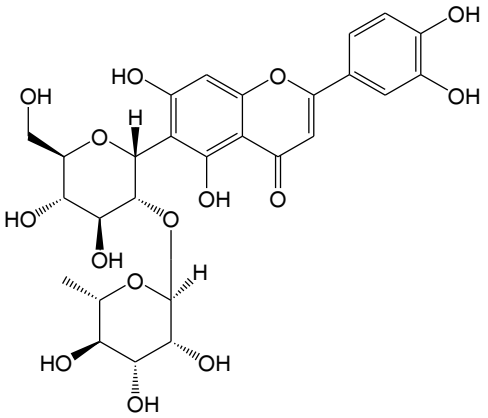

Isoorientin-2-*O*-α-*L*-rhamnoside [**7**]

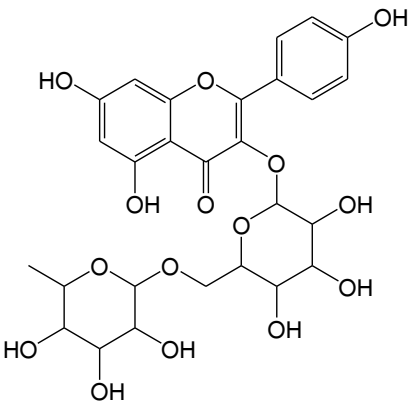

Kaempferol-3-*O*-rutinoside [**8**]

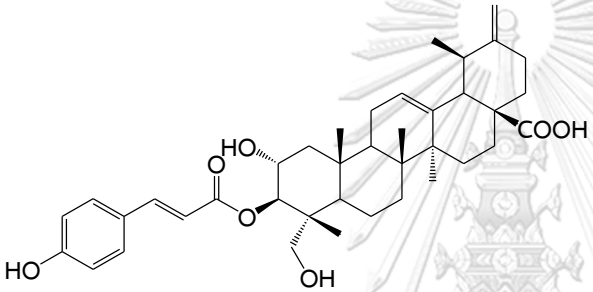

3-*O*-Trans-*p*-coumaroyl actinidic acid [**9**]

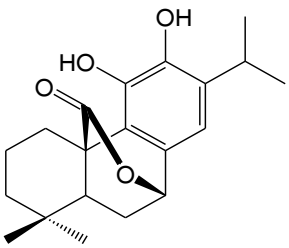

Carnosol [**10**]

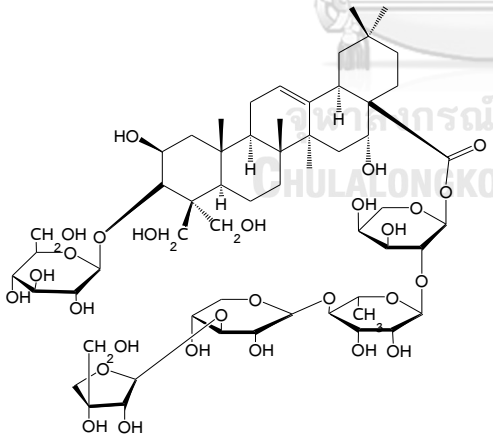

Platycodin D [**11**]

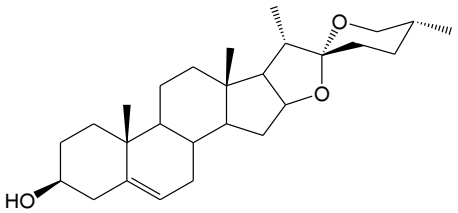

Diosgenin [**12**]

Figure 1 (continued)

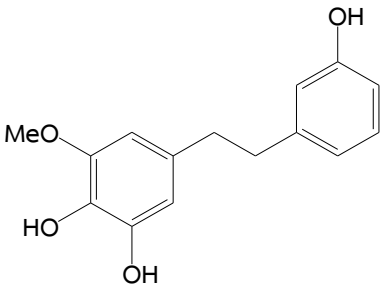

Dendrosinen B [**13**]

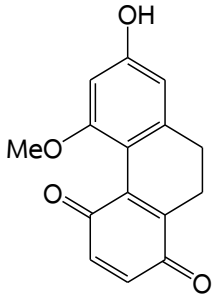

5-Methoxy-7-hydroxy-9,10-dihydro-1,4-phenanthrenequinone [**14**]

Fucoxanthin [**15**]

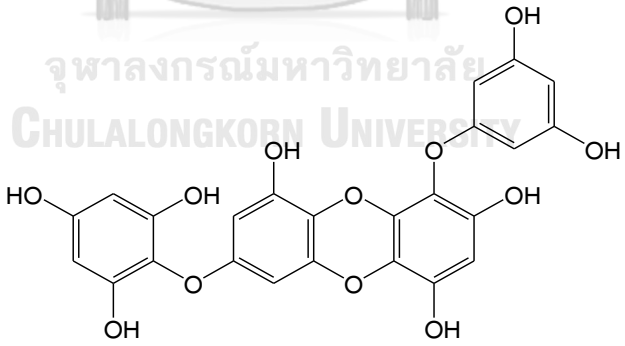

7-Phloroeckol [**16**]

Figure 1 (continued)

CHAPTER II

LITERATURE REVIEW

1. *Dendrobium* species

1.1 Taxonomy and distribution

Orchidaceae is the largest flowering plant family, with approximately 25,000 to 35,000 species under 750 to 900 genera widely distributed throughout the world (Lam *et al.*, 2015). Within this family, *Dendrobium* is the second largest genus with more than 1500 species distributed from Asia to Oceania. More than 150 species of *Dendrobium* have been identified in Thailand while about 129 species and over 80 species grow in Myanmar and China, respectively (Cakova *et al.*, 2017; He *et al.*, 2020; Peyachoknagul *et al.*, 2014; Tang *et al.*, 2017). Mountainous (1400-1600m high) areas with humid and foggy environments are the best geographical locations for the growth of most *Dendrobium* species (Lam *et al.*, 2015).

1.2 Conventional therapy and biological investigations

The name of *Dendrobium* is originated from two Greek words "Dendros" representing trees and "bios" meaning life. They are sympodial epiphytic plants and are commonly used for both ornamental and medicinal purposes. About 30 species out of 80 *Dendrobium* species in China are described in traditional Chinese medicine (TCM). In TCM, they have been traditionally used for nourishing Yin and enhancing longevity and considered as one of the 50 fundamental herbs in China. They also are sources of substances with tonic, astringent, anti-pyretic, analgesic and anti-inflammatory activities. The name "Shi-Hu" is commonly used to represent 30 *Dendrobium* spp., such as *D. chrysotoxum*, *D. fimbriatum*, *D. nobile* and other related *Dendrobium* species (Cakova *et al.*, 2017). Some plants in this genus have also been used in traditional Thai medicine. For example, the dried stem of *D. draconis* has been used for blood nourishing and tonic effects in the form of tea (Na Ranong *et al.*, 2019).

A wide range of biological activities have been reported for *Dendrobium* plants., such as anti-tumor, anti-oxidant, anti-angiogenesis, anti-inflammatory, anti-platelet aggregation, anti-bacterial, anti-malarial, anti-herpetic, anti-fungal, anti-cataractogenic, anti-diabetic, hepatoprotective and neuroprotective activities. They have also been reported for beneficial effects on colon problems and hyperthyroidism (Da Silva & Ng, 2017; Da Silva *et al.*, 2015).

1.3 Chemical investigation

Dendrobium spp. possess a diverse group of secondary metabolites (Lam *et al.*, 2015). They are classified based on their chemical structures. Chemical compounds such as bibenzyls, phenanthrenes, alkaloids, flavonoids, terpenoids, coumarins, fluorenones, fluorenes, lignans, neo-lignans, aliphatic, phenolic compounds and also polysaccharides have been reported in *Dendrobium* species (Xu *et al.*, 2013).

The biosynthesis of bibenzyls, 9,10-dihydrophenanthrenes and phenanthrenes which commonly occurs throughout Orchidaceae family has been first studied through the fungal infection of the orchid tissues (Reinecke & Kindl, 1993). These phenolic compounds are derived from the general phenylpropanoid pathway through the synthesis of *trans*-cinnamic acid or its derivative *p*-coumaric acid from the aromatic amino acids such as phenylalanine or tyrosine, respectively (Dubrovina & Kiselev, 2017).

The catalytic activity of bibenzyl synthase on a dihydro-*m*-coumaroyl-CoA substrate together with the incorporation of three molecules of malonyl-CoA is required in the biosynthesis of bibenzyls. Four key enzymes are involved in the initial biosynthesis of dihydro-*m*-coumaroyl-CoA. The first enzyme is phenylalanine ammonia-lyase (PAL) which catalyzes the phenylalanine molecule to produce a cinnamate molecule. This structure is then incorporated into *m*-coumaric-CoA with the help of the second enzyme, cinnamate 4-hydroxylase (C4H). Then, the third

enzyme, 4-coumarate-CoA ligase (4CL), enhances the synthesis of dihydro-*p*-coumaroyl-CoA from *p*-coumaric-CoA. The incorporation of the fourth enzyme, cytochrome P450 (CYP450), into the *m*-coumaric acid induces the formation of dihydro-*m*-coumaric acid. CYP450 is necessary for the production of secondary metabolites to defense against the environmental stresses. (Adejobi *et al.*, 2021). The linkage of two benzene rings with the ethylene bridge is the structural feature of the bibenzyl derivatives (Gorham, 1989). The chemical composition of bibenzyls from *Dendrobium* and their structures are summarized in **Table 2** and **Figure 2**.

As for the biosynthetic pathways of phenanthrenes, stilbene synthase is generally required for the incorporation of three molecules of malonyl-CoA on a *m*-coumaroyl-CoA substrate to produce the stilbene backbones and then to phenanthrenes, respectively (Reinecke & Kindl, 1993). The structural skeleton of phenanthrenes is formed by the oxidative coupling of the aromatic rings of the stilbene precursors (Bús *et al.*, 2020). The occurrences of monomeric, dimeric phenanthrenes and phenanthraquinones in *Dendrobium* spp., are shown in **Table 3** and **Figure 3**.

The backbone skeleton of flavonoids is comprised of two aromatic rings (ring A and B) linked by three carbons of ring C (Isoda *et al.*, 2014). Depending on the carbon of ring C on which ring B is attached and the degree of oxidation and unsaturation of ring C, flavonoids are subdivided into several subgroups such as flavanones, flavones, flavonols, flavanonols, flavanols or catechins, anthocyanins and chalcones (Panche *et al.*, 2016). All flavonoids are generally derived from a phenylpropanoid intermediate from the shikimic acid pathway. Chalcone synthase (CHS) is the first enzyme in the biosynthetic pathway, which catalyzes the reaction of 4-coumaroyl-CoA and three molecules of malonyl-CoA to form a chalcone. This intermediate is then transformed into different types of flavonoids through the catalytic activity of various enzymes such as chalcone isomerase (CHI), flavanone 3-

hydroxylase (F3H), dihydroflavonol 4-reductase (DFR), flavonol synthase (FLS), flavone synthase (FNS) and anthocyanidin synthase (Da Silva *et al.*) (Ma *et al.*, 2014). The derivatives of flavonoids found in *Dendrobium* are listed in **Table 4** and **Figure 4**.

Table 5 and **Figure 5** show the derivatives of sesquiterpenes and terpenoid alkaloids isolated from *Dendrobium* species. All Terpenoids are synthesized through the condensation of the five-carbon monomer isopentenyl diphosphate (IPP) with its isomer dimethylallyl diphosphate (DMAPP) (Kuzuyama & Seto, 2012). IPP and DMAPP can be produced by two distinct pathways such as the 2*C*-methyl-D-erythritol-4-phosphate (MEP) pathway and the mevalonic acid (MVA) pathway. Sesquiterpenoids (C15), triterpenoids (C30), sterols (C27-C29) and saponin derivatives are synthesized from C5 prenyl diphosphates through the MVA pathway, whereas monoterpenoids (C10), diterpenoids (C20) and tetraterpenoids (C40) are synthesized from the MEP pathway using the same precursors (Bergman *et al.*, 2019).

Alkaloids are low molecular-weight compounds with a nitrogen-atom in a heterocyclic ring. They are mostly derived from amino acids. Alkaloids are generally classified based on their heterocyclic ring system and biosynthetic precursors (Dey *et al.*, 2020). *Dendrobium* alkaloids such as amine alkaloids, pyrrole alkaloids, indolizidine alkaloids, indole and other types of alkaloids are shown in **Table 6** and **Figure 6**.

Coumarins are classified into simple coumarins, furanocoumarins, pyranocoumarins and phenylcoumarins. Simple coumarins, furanocoumarins and pyranocoumarins are originated from the general phenylpropanoid pathway whereas phenylcoumarins are derived from the isoflavone metabolism. Simple coumains are comprised of coumarins, hydroxylated and methoxylated coumarins and minor coumarins. Coumarins are synthesized from the *ortho*-hydroxylation of the cinnamic acid by cinnamic acid 2-hydroxylase (C2H). The other simple coumarins and

furanocoumarins are derived from 4-coumaric acid or its ester derivatives which are also synthesized from cinnamic acid (Bourgaud *et al.*, 2006). The occurrence and structures of coumarin derivatives in *Dendrobium* are presented in **Table 7** and **Figure 7**.

Table 8 and **figure 8** summarize the lignans and neo-lignans found in *Dendrobium*. Lignans are composed of two phenylpropane (C6-C3) units linked together by a C-C bond between C-8 and C-8′. The linkages of the two C6-C3 units by other than the C-8 to C-8′ bond form neo-lignans. Both lignans and neo-lignans are originated from cinnamic acid derivatives, which are derived from phenylalanine through the shikimate pathway (Teponno *et al.*, 2016).

Table 9 and **Figure 9** show fluorenone and fluorene derivatives of *Dendrobium* species. Aliphatic derivatives are summarized in **Table 10** and **Figure 10. Table 11** and **Figure 11** sum up the phenylpropanoids and phenolic derivatives isolated from *Dendrobium* species. Other miscellaneous compounds are shown in **Table 12** and **Figure 12**.

Table 2 Bibenzyl derivatives of *Dendrobium* species

Bibenzyl derivatives			
Phytochemical	**Plant**	**Plant part**	**Reference**
Aloifol I [**17**]	*D. christyanum*	Root	(San *et al.*, 2020)
	D. gibsonii	Whole plant	(Thant *et al.*, 2020)
	D. infundibulum	Whole plant	(Na Ranong *et al.*, 2019)
	D. longicornu	Stem	(Hu *et al.*, 2008a)
	D. scabrilingue	Whole plant	(Sarakulwattana *et al.*, 2020)
	D. williamsonii	Whole plant	(Yang *et al.*, 2018b)
Amoenylin [**18**]	*D. amoenum*	Whole plant	(Majumder *et al.*, 1999)
	D. williamsonii	Whole plant	(Yang *et al.*, 2018b)
Batatasin [**19**]	*D. longicornu*	Stem	(Hu *et al.*, 2008a)
	D. plicatile	Stem	(Yamaki & Honda, 1996)
Batatasin III [**20**]	*D. aphyllum*	Stem	(Yang *et al.*, 2015a)
		Whole plant	(Chen *et al.*, 2008b)
	D. cariniferum	Stem	(Chen *et al.*, 2008d)
	D. chrysotoxum	Whole plant	(Li *et al.*, 2009b)
	D. christyanum	Root	(San *et al.*, 2020)
	D. draconis	Stem	(Sritularak *et al.*, 2011a)
	D. formosum	Whole plant	(Inthongkaew *et al.*, 2017)
	D. gratiosissimum	Stem	(Zhang *et al.*, 2008a)
	D. infundibulum	Whole plant	(Na Ranong *et al.*, 2019)
	D. loddigesii	Stem	(Ito *et al.*, 2010)
	D. rotundatum	Whole plant	(Majumder & Pal, 1992)

Table 2 (continued)

Bibenzyl derivatives			
Phytochemical	**Plant**	**Plant part**	**Reference**
Batatasin III [**20**] (continued)	*D. scabrilingue*	Whole plant	(Sarakulwattana *et al.*, 2020)
	D. venustum	Whole plant	(Sukphan *et al.*, 2014)
Brittonin A [**21**]	*D. secundum*	Stem	(Sritularak *et al.*, 2011b)
Chrysotobibenzyl [**22**]	*D. aurantiacum var. denneanum*	Stem	(Yang *et al.*, 2006b)
	D. capillipes	Stem	(Phechrmeekha *et al.*, 2012)
	D. chrysanthum	Stem	(Yang *et al.*, 2006a)
	D. chryseum	Stem	(Ma *et al.*, 1998)
	D. chrysotoxum	Stem	(Hu *et al.*, 2012)
	D. nobile	Stem	(Zhang *et al.*, 2007b)
	D. pulchellum	Stem	(Chanvorachote *et al.*, 2013)
	D. scabrilingue	Whole plant	(Sarakulwattana *et al.*, 2020)
Chrysotoxine [**23**]	*D. aurantiacum var. denneanum*	Stem	(Yang *et al.*, 2006b)
	D. chrysanthum	Stem	(Yang *et al.*, 2006a)
	D. chryseum	Stem	(Ma *et al.*, 1998)
	D. nobile	Stem	(Zhang *et al.*, 2007b)
	D. pulchellum	Stem	(Chanvorachote *et al.*, 2013)

Table 2 (continued)

Bibenzyl derivatives			
Phytochemical	**Plant**	**Plant part**	**Reference**
Chrysotoxine [**23**] (continued)	*D. lindleyi*	Whole plant	(Khoonrit *et al.*, 2020)
Crepidatin [**24**]	*D. aurantiacum var. denneanum*	Whole plant	(Ying *et al.*, 2009)
	D. capillipes	Stem	(Phechrmeekha *et al.*, 2012)
	D. chrysanthum	Stem	(Yang *et al.*, 2006a)
	D. crepidatum	Whole plant	(Majumder & Chatterjee, 1989)
	D. loddigesii	Stem	(Ma *et al.*, 2019b)
	D. nobile	Stem	(Zhang *et al.*, 2007b)
	D. pulchellum	Stem	(Chanvorachote *et al.*, 2013)
Cumulatin [**25**]	*D. cumulatum*	Whole plant	(Majumder & Pal, 1993)
Dendrobin A [**26**]	*D. nobile*	Stem	(Wang *et al.*, 1985; Ye *et al.*, 2002)
Dendromoniliside E [**27**]	*D. nobile*	Stem	(Miyazawa *et al.*, 1999)
Erianin [**28**]	*D. chrysotoxum*	Stem	(Hu *et al.*, 2012)
Gigantol [**29**]	*D. aphyllum*	Whole plant	(Chen *et al.*, 2008b)
	D. aurantiacum var. denneanum	Whole plant	(Ying *et al.*, 2009)

Table 2 (continued)

Bibenzyl derivatives			
Phytochemical	**Plant**	**Plant part**	**Reference**
Gigantol [**29**] (continued)	*D. brymerianum*	Whole plant	(Klongkumnuankarn *et al.*, 2015)
	D. densiflorum	Stem	(Fan *et al.*, 2001)
	D. devonianum	Whole plant	(Sun *et al.*, 2014)
	D. draconis	Stem	(Sritularak *et al.*, 2011a)
	D. longicornu	Stem	(Hu *et al.*, 2008a)
	D. nobile	Stem	(Zhang *et al.*, 2007b)
	D. officinale	Stem	(Zhao *et al.*, 2018)
	D. palpebrae	Whole plant	(Kyokong *et al.*, 2019)
	D. polyanthum	Stem	(Hu *et al.*, 2009)
	D. scabrilingue	Whole plant	(Sarakulwattana *et al.*, 2020)
	D. trigonopus	Stem	(Hu *et al.*, 2008b)
	D. venustum	Whole plant	(Sukphan *et al.*, 2014)
	D. wardianum	Stem	(Zhang *et al.*, 2017a)
	D. lindleyi	Whole plant	(Khoonrit *et al.*, 2020)
	D. christyanum	Root	(San *et al.*, 2020)
	D. pachyglossum	Whole plant	(Warinhomhoun *et al.*, 2021)
Isoamoenylin [**30**]	*D. amoenum*	Whole plant	(Majumder *et al.*, 1999)
Moniliformine [**31**]	*D. candidum*	Stem	(Li *et al.*, 2008)
	D. signatum	Whole plant	(Mittraphab *et al.*, 2016)
	D. tortile	Whole plant	(Limpanit *et al.*, 2016)

Table 2 (continued)

Bibenzyl derivatives			
Phytochemical	**Plant**	**Plant part**	**Reference**
Moniliformine [**31**] (continued)	*D. williamsonii*	Whole plant	(Yang *et al.*, 2018b)
Moscatilin [**32**]	*D. amoenum*	Whole plant	(Majumder *et al.*, 1999)
	D. aurantiacum var. denneanum	Stem	(Yang *et al.*, 2006b)
	D. brymerianum	Whole plant	(Klongkumnuankarn *et al.*, 2015)
	D. chrysanthum	Stem	(Yang *et al.*, 2006a)
	D. densiflorum	Stem	(Fan *et al.*, 2001)
	D. ellipsophyllum	Whole plant	(Tanagornmeatar *et al.*, 2014)
	D. formosum	Whole plant	(Inthongkaew *et al.*, 2017)
	D. gratiosissimum	Stem	(Zhang *et al.*, 2008a)
	D. infundibulum	Whole plant	(Na Ranong *et al.*, 2019)
	D. loddigesii	Whole plant	(Chen *et al.*, 1994; Ito *et al.*, 2010)
	D. longicornu	Stem	(Hu *et al.*, 2008a)
	D. moscatum	Whole plant	(Majumder & Sen, 1987b)

Table 2 (continued)

Bibenzyl derivatives			
Phytochemical	**Plant**	**Plant part**	**Reference**
Moscatilin [**32**] (continued)	*D. nobile*	Stem	(Miyazawa *et al.*, 1999; Yang *et al.*, 2007c)
	D. palpebrae	Whole plant	(Kyokong *et al.*, 2019)
	D. parishii	Whole plant	(Kongkatitham *et al.*, 2018)
	D. polyanthum	Stem	(Hu *et al.*, 2009)
	D. pulchellum	Stem	(Chanvorachote *et al.*, 2013)
	D. secundum	Stem	(Sritularak *et al.*, 2011b)
	D. wardianum	Stem	(Zhang *et al.*, 2017a)
	D. williamsonii	Whole plant	(Yang *et al.*, 2018b)
	D. lindleyi	Whole plant	(Khoonrit *et al.*, 2020)
	D. christyanum	Root	(San *et al.*, 2020)
	D. pachyglossum	Whole plant	(Warinhomhoun *et al.*, 2021)
Moscatilin diacetate [**33**]	*D. loddigesii*	Stem	(Chen *et al.*, 1994)
Tristin [**34**]	*D. aphyllum*	Stem	(Yang *et al.*, 2015a)

Table 2 (continued)

Bibenzyl derivatives			
Phytochemical	**Plant**	**Plant part**	**Reference**
Tristin [**34**] (continued)	*D. chrysotoxum*	Stem	(Hu *et al.*, 2012)
	D. densiflorum	Stem	(Fan *et al.*, 2001)
	D. gratiosissimum	Stem	(Zhang *et al.*, 2008a)
	D. longicornu	Stem	(Hu *et al.*, 2008a)
	D. officinale	Stem	(Zhao *et al.*, 2018)
	D. trigonopus	Stem	(Hu *et al.*, 2008b)
4-Hydroxy-3,5,3′-trimethoxybibenzyl [**35**]	*D. nobile*	Stem	(Ye *et al.*, 2002)
5-Hydroxy-3,4,3′,4′,5′-pentamethoxybibenzyl [**36**]	*D.* secundum	Stem	(Phechrmeekha *et al.*, 2012)
3,3′-Dihydroxy-4,5-dimethoxybibenzyl [**37**]	*D. williamsonii*	Whole plant	(Rungwichaniwat *et al.*, 2014)
3,4′-Dihydroxy-5-methoxybibenzyl [**38**]	*D. amoenum*	Whole plant	(Majumder *et al.*, 1999)
4,5-Dihydroxy-3,3′,4′-trimethoxybibenzyl [**39**]	*D. lindleyi*	Whole plant	(Khoonrit *et al.*, 2020)
3,4′-Dihydroxy-5,5′-dimethoxydihydrostilbene [**40**]	*D. nobile*	Stem	(Hwang *et al.*, 2010)
3,4′-Dihydroxy-3′,4,5-trimethoxybibenzyl [**41**]	*D. infundibulum*	Whole plant	(Na Ranong *et al.*, 2019)

Table 2 (continued)

Bibenzyl derivatives			
Phytochemical	**Plant**	**Plant part**	**Reference**
5,4′-Dihydroxy-3,4,3′-trimethoxybibenzyl [**42**]	*D. infundibulum*	Whole plant	(Na Ranong *et al.*, 2019)
3,3′,4-Trihydroxybibenzyl [**43**]	*D. longicornu*	Stem	(Hu *et al.*, 2008a)
3,3′,5-Trihydroxybibenzyl [**44**]	*D. cariniferum*	Whole plant	(Chen *et al.*, 2008d)
3,5,4′-Trihydroxybibenzyl (Dihydroresveratrol)* [**45**]	*D. aphyllum*	Stem	(Yang *et al.*, 2015a)
	D. gratiosissimum	Stem	(Zhang *et al.*, 2008a)
4,3′,4′-Trihydroxy-3,5-dimethoxybibenzyl [**46**]	*D. parishii*	Whole plant	(Kongkatitham *et al.*, 2018)
4,5-Dihydroxy-3,3′,4′,α,-tetramethoxybibenzyl [**47**]	*D. lindleyi*	Whole plant	(Shang *et al.*, 2020)
4,4′,5-Trihydroxy-3,3′,α-trimethoxybibenzyl [**48**]	*D. lindleyi*	Whole plant	(Shang *et al.*, 2020)
4,5,4′-Trihydroxy-3,3′-dimethoxybibenzyl [**49**]	*D. ellipsophyllum*	Whole plant	(Tanagornmeatar *et al.*, 2014)
	D. palpebrae	Whole plant	(Kyokong *et al.*, 2019)
	D. parishii	Whole plant	(Kongkatitham *et al.*, 2018)

Table 2 (continued)

Bibenzyl derivatives			
Phytochemical	**Plant**	**Plant part**	**Reference**
4,5,4′-Trihydroxy-3,3′-dimethoxybibenzyl [**49**] (continued)	*D. secundum*	Stem	(Sritularak *et al.*, 2011b)
	D. pachyglossum	Whole plant	(Warinhomhoun *et al.*, 2021)
Dendrophenol [**50**]	*D. candidum*	Stem	(Li *et al.*, 2008)
Loddigesiinol C [**51**]	*D. loddigesii*	Whole plant	(Ito *et al.*, 2010)
3-*O*-Methylgigantol [**52**]	*D. candidum*	Stem	(Li *et al.*, 2008)
	D. plicatile	Stem	(Yamaki & Honda, 1996)
3,4-Dihydroxy-5,4′-dimethoxybibenzyl [**53**]	*D. candidum*	Stem	(Li *et al.*, 2008)
	D. signatum	Whole plant	(Mittraphab *et al.*, 2016)
	D. tortile	Whole plant	(Limpanit *et al.*, 2016)
	D. wardianum	Stem	(Zhang *et al.*, 2017a)
	D. williamsonii	Whole plant	(Yang *et al.*, 2018b)
4,4′-Dihydroxy-3,5-dimethoxybibenzyl [**54**]	*D. candidum*	Stem	(Li *et al.*, 2008)

Table 2 (continued)

Bibenzyl derivatives			
Phytochemical	**Plant**	**Plant part**	**Reference**
4,4′-Dihydroxy-3,5-dimethoxybibenzyl [**54**] (continued)	*D. ellipsophyllum*	Whole plant	(Tanagornmeatar *et al.*, 2014)
	D. williamsonii	Whole plant	(Yang *et al.*, 2018b)
4-[2-(3-Hydroxyphenol)-1-methoxyethyl]-2,6-dimethoxyphenol [**55**]	*D. longicornu*	Stem	(Hu *et al.*, 2008a)
Nobilin A [**56**]	*D. nobile*	Stem	(Zhang *et al.*, 2006a)
Nobilin B [**57**]	*D. nobile*	Stem	(Zhang *et al.*, 2006a)
Nobilin C [**58**]	*D. nobile*	Stem	(Zhang *et al.*, 2006a)
Nobilin D [**59**]	*D. nobile*	Stem	(Zhang *et al.*, 2007b)
Nobilin E [**60**]	*D. nobile*	Stem	(Zhang *et al.*, 2007b)
Dendrocandin A [**61**]	*D. candidum*	Stem	(Li *et al.*, 2008)
	D. wardianum	Stem	(Zhang *et al.*, 2017a)
	D. officinale	Stem	(Tang *et al.*, 2017)
Dendrocandin B [**62**]	*D. candidum*	Stem	(Li *et al.*, 2008)
	D. signatum	Whole plant	(Mittraphab *et al.*, 2016)

Table 2 (continued)

Bibenzyl derivatives			
Phytochemical	**Plant**	**Plant part**	**Reference**
Dendrocandin B [**62**] (continued)	*D. officinale*	Stem	(Yang *et al.*, 2015b)
Dendrocandin C [**63**]	*D. candidum*	Stem	(Li *et al.*, 2009c)
	D. officinale	Stem	(Tang *et al.*, 2017)
Dendrocandin D [**64**]	*D. candidum*	Stem	(Li *et al.*, 2009c)
	D. officinale	Stem	(Tang *et al.*, 2017)
Dendrocandin E [**65**]	*D. candidum*	Stem	(Li *et al.*, 2009c)
	D. officinale	Stem	(Tang *et al.*, 2017)
	D. parishii	Whole plant	(Kongkatitham *et al.*, 2018)
Dendrocandin F (Dendrofalconerol A)* [**66**]	*D. candidum*	Stem	(Li *et al.*, 2009c)
	D. officinale	Stem	(Tang *et al.*, 2017)
	D. falconeri	Stem	(Sritularak & Likhitwitayawuid, 2009)
	D. signatum	Whole plant	(Mittraphab *et al.*, 2016)
	D. tortile	Whole plant	(Limpanit *et al.*, 2016)
Dendrocandin G [**67**]	*D. candidum*	Stem	(Li *et al.*, 2009c)
	D. officinale	Stem	(Tang *et al.*, 2017)
Dendrocandin H [**68**]	*D. candidum*	Stem	(Li *et al.*, 2009c)
	D. officinale	Stem	(Tang *et al.*, 2017)
Dendrocandin I [**69**]	*D. candidum*	Stem	(Li *et al.*, 2009c)
	D. signatum	Whole plant	(Mittraphab *et al.*, 2016)
	D. officinale	Stem	(Tang *et al.*, 2017)

Table 2 (continued)

Bibenzyl derivatives			
Phytochemical	**Plant**	**Plant part**	**Reference**
Dendrocandin J [**70**]	*D. candidum*	Stem	(Li *et al.*, 2014b)
	D. officinale	Stem	(Tang *et al.*, 2017)
Dendrocandin K [**71**]	*D. candidum*	Stem	(Li *et al.*, 2014b)
	D. officinale	Stem	(Tang *et al.*, 2017)
Dendrocandin L [**72**]	*D. candidum*	Stem	(Li *et al.*, 2014b)
	D. officinale	Stem	(Tang *et al.*, 2017)
Dendrocandin M [**73**]	*D. candidum*	Stem	(Li *et al.*, 2014b)
	D. officinale	Stem	(Tang *et al.*, 2017)
Dendrocandin N [**74**]	*D. candidum*	Stem	(Li *et al.*, 2014b)
	D. officinale	Stem	(Tang *et al.*, 2017)
Dendrocandin O [**75**]	*D. candidum*	Stem	(Li *et al.*, 2014b)
	D. officinale	Stem	(Tang *et al.*, 2017)
Dendrocandin P [**76**]	*D. candidum*	Stem	(Li *et al.*, 2014b)
	D. officinale	Stem	(Tang *et al.*, 2017)
Dendrocandin Q [**77**]	*D. candidum*	Stem	(Li *et al.*, 2014b)
	D. officinale	Stem	(Tang *et al.*, 2017)
Dendrocandin T [**78**]	*D. officinale*	Stem	(Yang *et al.*, 2015b)
Dendrocandin U [**79**]	*D. officinale*	Stem	(Yang *et al.*, 2015b)
	D. wardianum	Stem	(Zhang *et al.*, 2017a)

Table 2 (continued)

Bibenzyl derivatives			
Phytochemical	**Plant**	**Plant part**	**Reference**
Dendrocandin V [**80**]	*D. wardianum*	Stem	(Zhang *et al.*, 2017a)
Dendrosinen A [**81**]	*D. sinense*	Whole plant	(Chen *et al.*, 2014)
Dendrosinen B [**82**]	*D. sinense*	Whole plant	(Chen *et al.*, 2014)
	D. infundibulum	Whole plant	(Na Ranong *et al.*, 2019)
	D. christyanum	Root	(San *et al.*, 2020)
Dendrosinen C [**83**]	*D. sinense*	Whole plant	(Chen *et al.*, 2014)
Dendrosinen D [**84**]	*D. sinense*	Whole plant	(Chen *et al.*, 2014)
Crepidatuol A [**85**]	*D. crepidatum*	Stem	(Li *et al.*, 2013)
Crepidatuol B [**86**]	*D. crepidatum*	Stem	(Li *et al.*, 2013)
Dencryol A [**87**]	*D. crystallinum*	Stem	(Wang *et al.*, 2009)
Dencryol B [**88**]	*D. crystallinum*	Stem	(Wang *et al.*, 2009)
Dendropachol [**89**]	*D. pachyglossum*	whole plant	(Warinhomhoun *et al.*, 2021)
Dendroscabrol B [**90**]	*D. scabrilingue*	Whole plant	(Sarakulwattana *et al.*, 2020)
Dendrowillol A [**91**]	*D. williamsonii*	Stem	(Yang *et al.*, 2018b)
Densiflorol A [**92**]	*D. densiflorum*	Stem	(Fan *et al.*, 2001)
Loddigesiinol D [**93**]	*D. loddigesii*	Whole plant	(Ito *et al.*, 2010)

Table 2 (continued)

Bibenzyl derivatives			
Phytochemical	**Plant**	**Plant part**	**Reference**
Longicornuol A [**94**]	*D. longicornu*	Stem	(Hu *et al.*, 2008a)
Trigonopol A [**95**]	*D. trigonopus*	Stem	(Hu *et al.*, 2008b)
Trigonopol B [**96**]	*D. chrysotoxum*	Stem	(Hu *et al.*, 2012)
Dendrofalconerol B [**97**]	*D. falconeri*	Stem	(Sritularak & Likhitwitayawuid, 2009)
Dendrofindlaphenol A [**98**]	*D. findlayanum*	Stem	(Yang *et al.*, 2018a)
6″-De-*O*-methyldendrofindlaphenol A [**99**]	*D. findlayanum*	Stem	(Yang *et al.*, 2018a)
Dendrofindlaphenol B [**100**]	*D. findlayanum*	Stem	(Yang *et al.*, 2018a)
Dendrofindlaphenol C [**101**]	*D. findlayanum*	Stem	(Yang *et al.*, 2018a)
Dengraol A [**102**]	*D. gratiosissimum*	Stem	(Zhang *et al.*, 2008a)
Dengraol B [**103**]	*D. gratiosissimum*	Stem	(Zhang *et al.*, 2008a)

Table 2 (continued)

Bibenzyl derivatives			
Phytochemical	**Plant**	**Plant part**	**Reference**
Aphyllone B [**104**]	*D. aphyllum*	Stem	(Yang *et al.*, 2015a)
Aphyllal C [**105**]	*D. aphyllum*	Stem	(Yang *et al.*, 2015a)
	D. loddigesii	Stem	(Ma *et al.*, 2019b)
Aphyllal D [**106**]	*D. aphyllum*	Stem	(Yang *et al.*, 2015a)
Aphyllal E [**107**]	*D. aphyllum*	Stem	(Yang *et al.*, 2015a)
(*R*) -4,5,4′-Trihydroxy-3,3′,α-trimethoxybibenzyl [**108**]	*D. loddigesii*	Stem	(Ma *et al.*, 2019b)
Gigantol-5-*O*-β-D-glucopyranoside [**109**]	*D. fimbriatum*	Stem	(Xu *et al.*, 2017)
Trisin-5-*O*-β-D-glucopyranoside [**110**]	*D. fimbriatum*	Stem	(Xu *et al.*, 2017)

*represent different names of the same compound

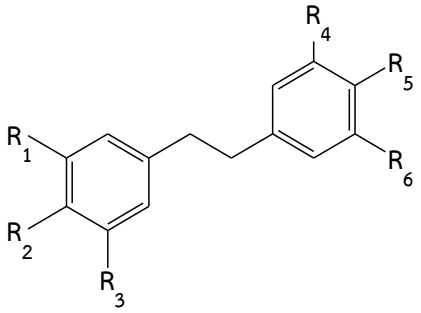

	R_1	R_2	R_3	R_4	R_5	R_6
Aloifol I [**17**]	OMe	OH	OMe	OH	H	H
Amoenylin [**18**]	OMe	OH	OMe	H	OMe	H
Batatasin [**19**]	OMe	H	H	OH	H	OH
Batatasin III [**20**]	OH	H	OMe	H	H	OH
Brittonin A [**21**]	OMe	OMe	OMe	OMe	OMe	OMe
Chrysotobibenzyl [**22**]	OMe	OMe	OMe	OMe	OMe	H
Chrysotoxine [**23**]	OMe	OH	OMe	OMe	OMe	H
Crepidatin [**24**]	OMe	OMe	OMe	OMe	OH	H
Cumulatin [**25**]	OMe	OMe	OH	OH	OMe	OMe
Dendrobin A [**26**]	OH	OH	OMe	H	H	OMe
Dendromoniliside E [**27**]	OGlc	OGlc	OMe	H	OMe	H
Erianin [**28**]	OMe	OMe	H	OMe	OH	OMe
Gigantol [**29**]	OMe	H	H	H	OH	OMe
Isoamoenylin [**30**]	OMe	OMe	OMe	H	H	OH
Moniliformine [**31**]	OH	OH	OMe	H	OMe	H

Figure 2 Structures of bibenzyl derivatives of *Dendrobium* species

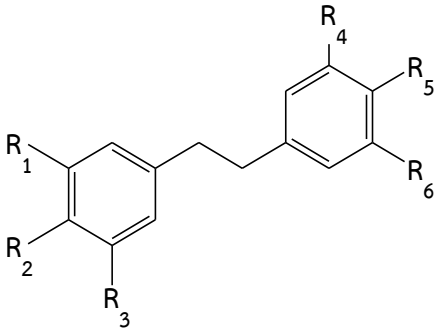

	R_1	R_2	R_3	R_4	R_5	R_6
Moscatilin [**32**]	OMe	OH	OMe	H	OH	OMe
Moscatilin diacetate [**33**]	OMe	OAc	OMe	H	OAc	OMe
Tristin [**34**]	OH	H	OH	H	OH	OMe
4-Hydroxy-3,5,3′-trimethoxy bibenzyl [**35**]	OMe	OH	OMe	H	H	OMe
5-Hydroxy-3,4,3′,4′,5′-pentamethoxybibenzyl [**36**]	OMe	OMe	OH	OMe	OMe	OMe
3,3′-Dihydroxy-4,5-dimethoxybibenzyl [**37**]	OMe	OMe	OH	H	H	OH
3,4′-Dihydroxy-5-methoxybibenzyl [**38**]	OH	H	OMe	H	OH	H
4,5-Dihydroxy-3,3′,4′-trimethoxybibenzyl [**39**]	OMe	OH	OH	OMe	OMe	H

Figure 2 (continued)

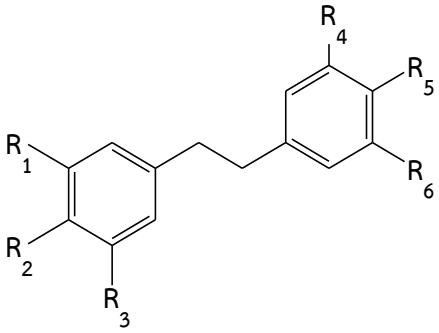

	R_1	R_2	R_3	R_4	R_5	R_6
3,4′-Dihydroxy-5,5′-dimethoxydihydrostilbene [**40**]	OH	H	OMe	OMe	OH	H
3,4′-Dihydroxy-3′,4,5-trimethoxybibenzyl [**41**]	OMe	OMe	OH	H	OH	OMe
5,4′-Dihydroxy-3,4,3′-trimethoxybibenzyl [**42**]	OH	OMe	OMe	OH	OMe	H
3,3′,4-Trihydroxybibenzyl [**43**]	OH	OH	H	H	H	OH
3,3′,5-Trihydroxybibenzyl [**44**]	OH	H	OH	H	H	OH
3,5,4′-Trihydroxybibenzyl (Dihydroresveratrol)* [**45**]	OH	H	OH	H	OH	H
4,3′,4′-Trihydroxy-3,5-dimethoxybibenzyl [**46**]	OMe	OH	OMe	H	OH	OH
4,5,4′-Trihydroxy-3,3′-dimethoxybibenzyl [**49**]	OMe	OH	OH	H	OH	OMe

Figure 2 (continued)

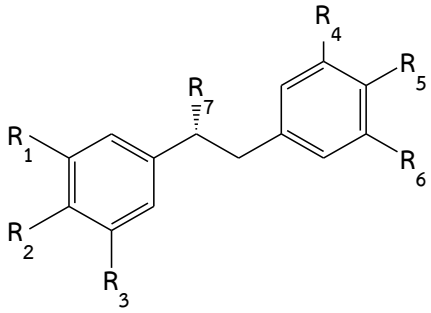

	R_1	R_2	R_3	R_4	R_5	R_6	R_7
4,5-Dihydroxy-3,3′,4′,α,-tetramethoxybibenzyl [**47**]	OMe	OH	OH	H	OMe	OMe	OMe
4,4′,5-Trihydroxy-3,3′,α-trimethoxybibenzyl [**48**]	OMe	OH	OH	H	OH	OMe	OMe
Dendrophenol [**50**]	OMe	OH	OMe	OH	H	OH	H
Loddigesiinol C [**51**]	OMe	OH	OMe	H	OH	OMe	OMe
3-*O*-Methylgigantol [**52**]	OMe	H	OH	OMe	OMe	H	H
3,4-Dihydroxy-5,4′-dimethoxybibenzyl [**53**]	OH	OH	OMe	H	OMe	H	H
4,4′-Dihydroxy-3,5-dimethoxybibenzyl [**54**]	OMe	OH	OMe	H	OH	H	H
4-[2-(3-Hydroxyphenol)-1-methoxyethyl]-2,6-dimethoxyphenol [**55**]	OMe	OH	OMe	H	H	OH	OMe

Figure 2 (continued)

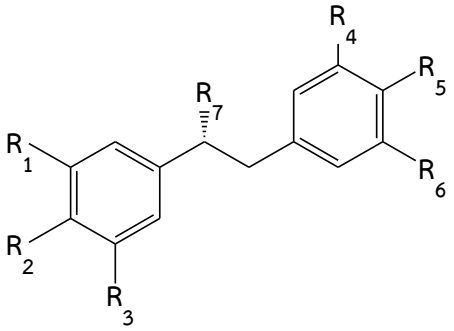

	R_1	R_2	R_3	R_4	R_5	R_6	R_7
Nobilin A [**56**]	OMe	OH	OH	H	H	OMe	OMe
Nobilin B [**57**]	OMe	OH	OMe	H	OH	OMe	OMe
Nobilin C [**58**]	OMe	OH	OMe	H	OMe	OMe	OMe
Nobilin D [**59**]	OMe	OH	H	OMe	OH	OMe	OH
Dendrocandin A [**61**]	OMe	OH	OH	H	OMe	H	OMe
Dendrocandin C [**63**]	OMe	OH	OH	H	OH	H	OMe
Dendrocandin D [**64**]	OMe	OH	OH	H	OH	H	OEt
Dendrocandin E [**65**]	OMe	OH	OH	OH	OH	H	H
Dendrosinen A [**81**]	OMe	OMe	OH	H	OH	H	OH
Dendrosinen B [**82**]	OMe	OMe	OH	H	OH	H	H

Figure 2 (continued)

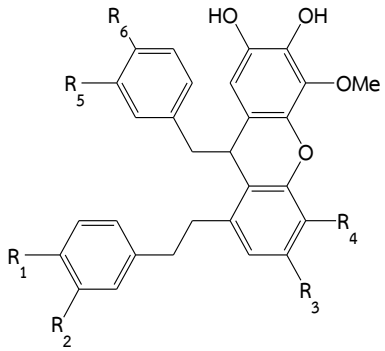

	R_1	R_2	R_3	R_4	R_5	R_6
Nobilin E [**60**]	H	OMe	OMe	OH	OMe	H
Dendrocandin F (Dendrofalconerol A)* [**66**]	OMe	H	OMe	OH	H	OMe
Dendrocandin G [**67**]	OMe	H	OMe	OH	H	OH
Dendrocandin J [**70**]	OH	H	OMe	OH	H	OMe
Dendrocandin K [**71**]	OH	H	OMe	OH	H	OH
Dendrofalconerol B [**97**]	OH	H	OH	H	H	OMe

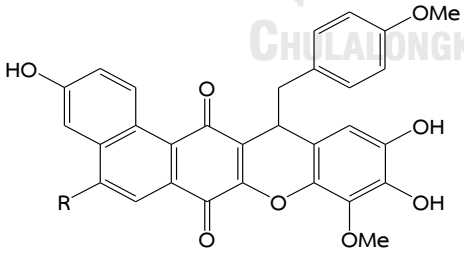

Dendrocandin H [**68**] R = OH

Dendrocandin L [**72**] R = H

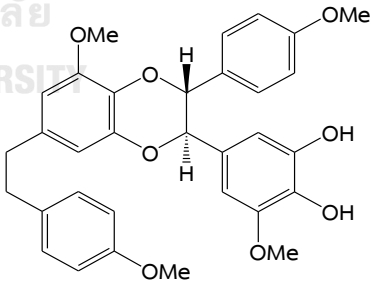

Dendrocandin I [**69**]

Figure 2 (continued)

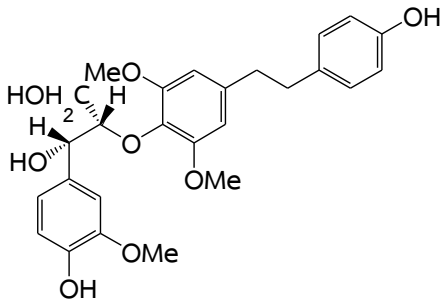

Dendrocandin M [**73**]

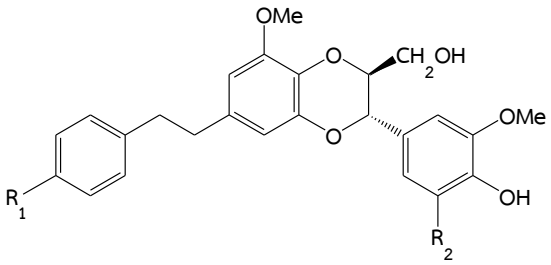

	R_1	R_2
Dendrocandin N [**74**]	OH	H
Dendrocandin O [**75**]	OH	OH

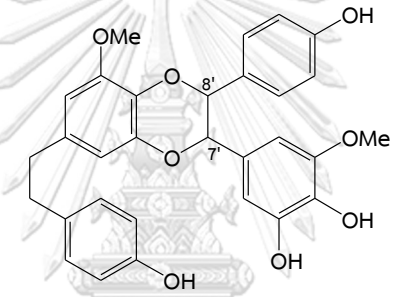

Dendrocandin P [**76**] H-7′, 8′ cis

Dendrocandin Q [**77**] H-7′, 8′ trans

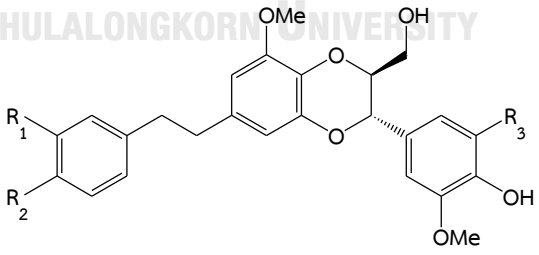

	R_1	R_2	R_3
Dendrocandin B [**62**]	H	OMe	OMe
Dendrocandin T [**78**]	OMe	OH	OMe

Figure 2 (continued)

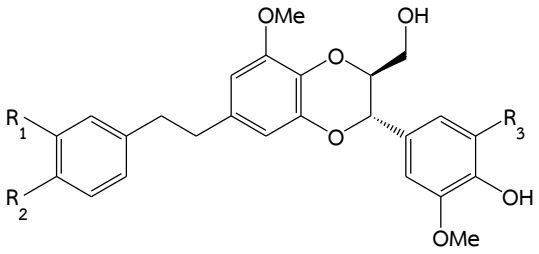

	R_1	R_2	R_3
Dendrocandin U [**79**]	H	OH	OMe
Dendrocandin V [**80**]	H	OMe	H

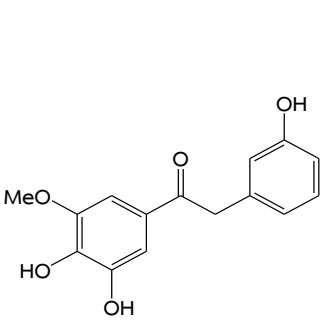

Dendrosinen C [**83**]

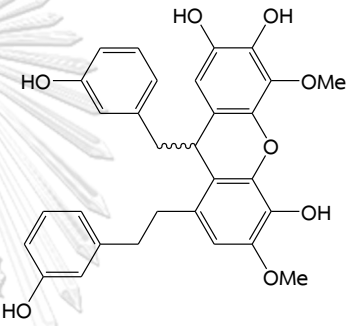

Dendrosinen D [**84**]

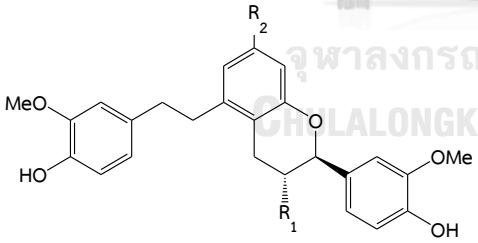

	R_1	R_2
Crepidatuol A [**85**]	H	OMe
Crepidatuol B [**86**]	OH	OMe
Trigonopol B [**96**]	OH	OH

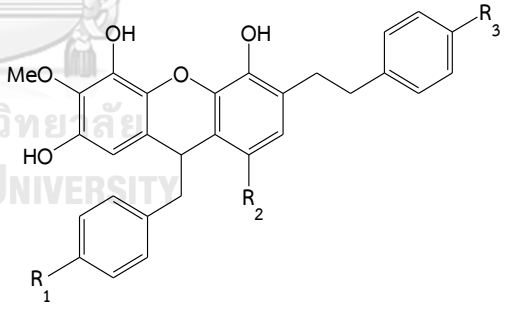

	R_1	R_2	R_3
Dencryol A [**87**]	OMe	OH	OH
Dencryol B [**88**]	OH	OMe	OMe

Figure 2 (continued)

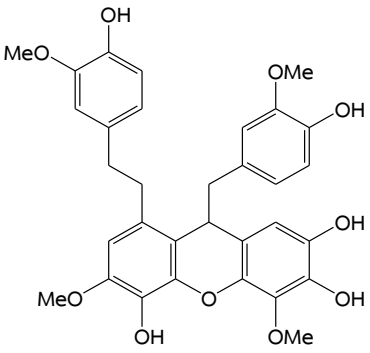

Dendropachol [**89**]

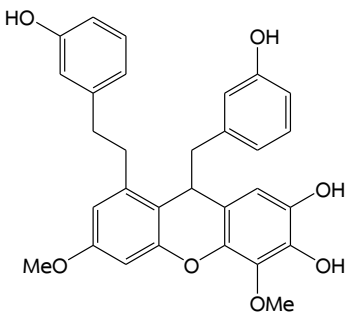

Dendroscabrol B [**90**]

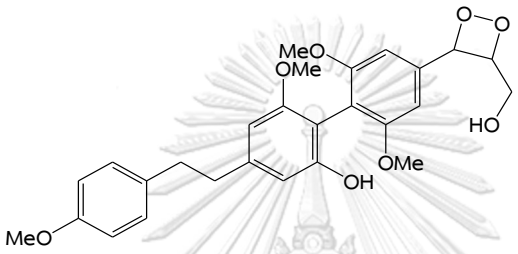

Dendrowillol A [**91**]

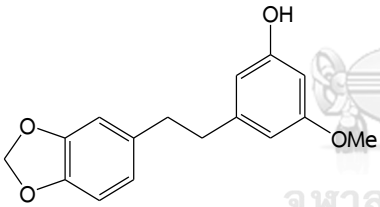

Densiflorol A [**92**]

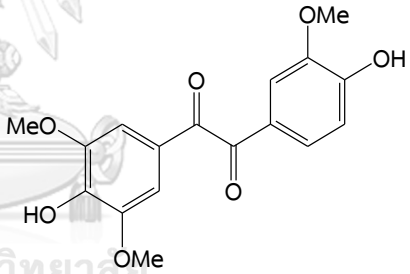

Loddigesiinol D [**93**]

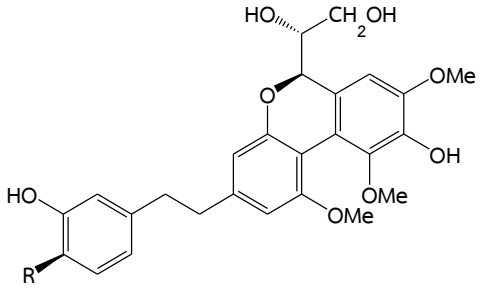

Longicornuol A [**94**] R = H

Trigonopol A [**95**] R = OMe

Figure 2 (continued)

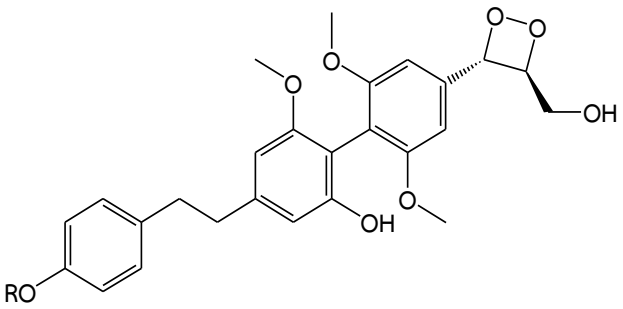

Dendrofindlaphenol A [**98**] R = Me

6″-De-*O*-methyldendrofindlaphenol A [**99**] R = H

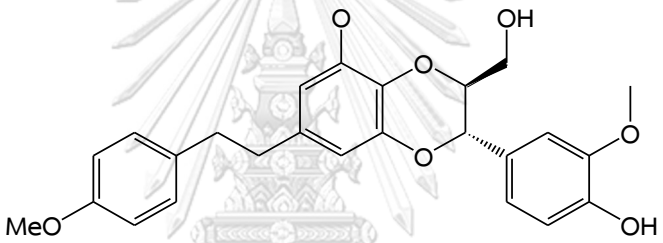

Dendrofindlaphenol B [**100**]

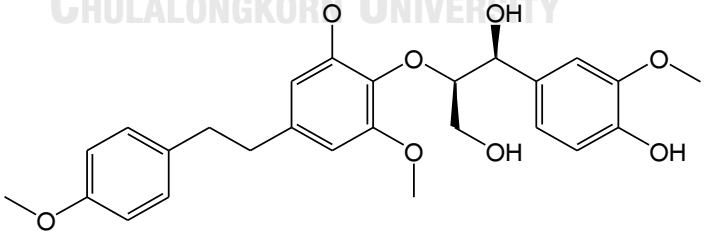

Dendrofindlaphenol C [**101**]

Figure 2 (continued)

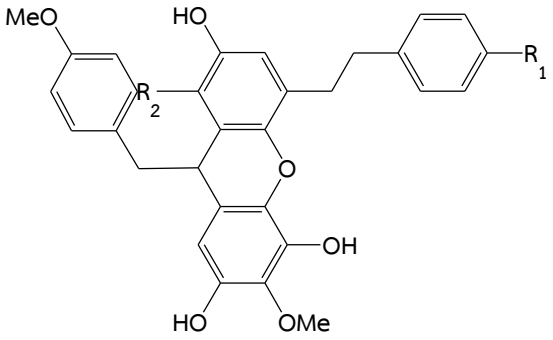

	R_1	R_2
Dengraol A [**102**]	OH	OH
Dengraol B [**103**]	OMe	OMe

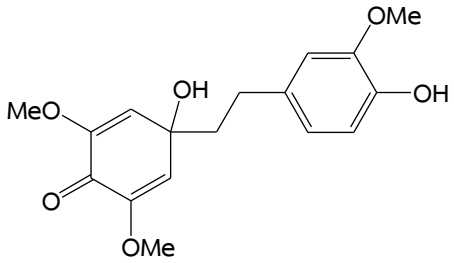

Aphyllone B [**104**]

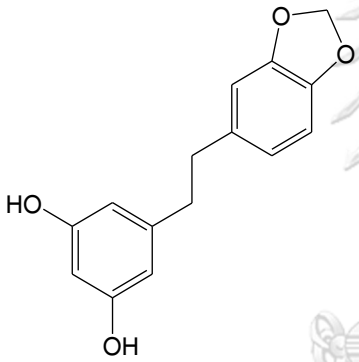

Aphyllal C [**105**]

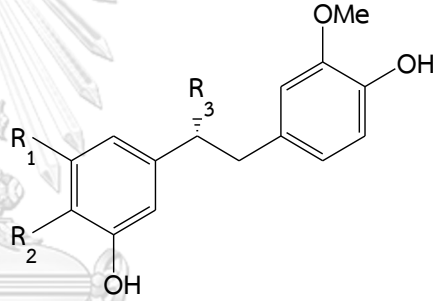

	R_1	R_2	R_3
Aphyllal D [**106**]	OH	H	OH
Aphyllal E [**107**]	OMe	H	OH
(*R*)-4,5,4′-Trihydroxy-3,3′,α-trimethoxy bibenzyl [**108**]	OMe	OH	OMe

Figure 2 (continued)

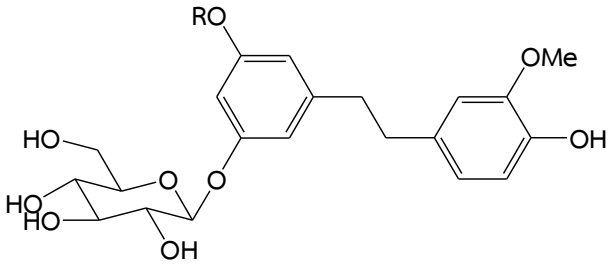

Gigantol-5-*O*-β-D-glucopyranoside [**109**] R = Me

Trisin-5-*O*-β-D-glucopyranoside [**110**] R = H

Figure 2 (continued)

Table 3 Phenanthrene derivatives of *Dendrobium* species

Phenanthrene derivatives			
Phytochemical	**Plant**	**Plant part**	**Reference**
Bulbophyllanthrin [**111**]	*D. nobile*	Stem	(Yang *et al.*, 2007a)
Confusarin [**112**]	*D. chrysotoxum*	Stem	(Hu *et al.*, 2012)
	D. formosum	Whole plant	(Inthongkaew *et al.*, 2017)
	D. nobile	Stem	(Zhang *et al.*, 2008c)
	D. officinale	Stem	(Zhao *et al.*, 2018)
Dendroscabrol A [**113**]	*D. scabrilingue*	Whole plant	(Sarakulwattana *et al.*, 2020)
Dendrosignatol [**114**]	*D. signatum*	Whole plant	(Mittraphab *et al.*, 2016)
Denthyrsinin [**115**]	*D. thyrsiforum*	Stem	(Zhang *et al.*, 2005)
3-Hydroxy-2,4,7-trimethoxyphenanthrene [**116**]	*D. nobile*	Stem	(Yang *et al.*, 2007a)
5-Hydroxy-2,4-dimethoxyphenanthrene [**117**]	*D. loddigesii*	Whole plant	(Ito *et al.*, 2010)
Epheranthol B [**118**]	*D. chrysotoxum*	Stem	(Hu *et al.*, 2012)
	D. plicatile	Stem	(Yamaki & Honda, 1996)
Fimbriol B [**119**]	*D. nobile*	Stem	(Hwang *et al.*, 2010; Yang *et al.*, 2007a)

Table 3 (continued)

Phenanthrene derivatives			
Phytochemical	**Plant**	**Plant part**	**Reference**
Flavanthrinin [**120**]	*D. brymerianum*	Whole plant	(Klongkumnuankarn *et al.*, 2015)
	D. venustum	Whole plant	(Sukphan *et al.*, 2014)
	D. nobile	Stem	(Zhang *et al.*, 2008b)
	D. parishii	Whole plant	(Kongkatitham *et al.*, 2018)
Loddigesiinol A [**121**]	*D. loddigesii*	Whole plant	(Ito *et al.*, 2010)
	D. wardianum	Stem	(Zhang *et al.*, 2017a)
Moscatin [**122**]	*D. aphyllum*	Whole plant	(Yang *et al.*, 2015a)
	D. chrysanthum	Stem	(Yang *et al.*, 2006a)
	D. chrysotoxum	Whole plant	(Li *et al.*, 2009b)
	D. densiflorum	Stem	(Fan *et al.*, 2001)
	D. polyanthum	Stem	(Hu *et al.*, 2009)
Nudol [**123**]	*D. formosum*	Whole plant	(Inthongkaew *et al.*, 2017)
	D. nobile	Stem	(Yang *et al.*, 2007a)
	D. rotundatum	Whole plant	(Majumder & Pal, 1992)
Plicatol A [**124**]	*D. nobile*	Stem	(Yang *et al.*, 2007a)
	D. plicatile	Stem	(Honda & Yamaki, 2000)
Plicatol B [**125**]	*D. plicatile*	Stem	(Honda & Yamaki, 2000)

Table 3 (continued)

Phenanthrene derivatives			
Phytochemical	**Plant**	**Plant part**	**Reference**
2,5-Dihydroxy-3,4-dimethoxyphenanthrene [**126**]	*D. nobile*	Stem	(Yang *et al.*, 2007a)
2,5-Dihydroxy-4,9-dimethoxyphenanthrene [**127**]	*D. nobile*	Stem	(Zhang *et al.*, 2008b)
	D. palpebrae	Whole plant	(Kyokong *et al.*, 2019)
2,6-Dihydroxy-1,5,7-trimethoxyphenanthrene [**128**]	*D. densiflorum*	Stem	(Fan *et al.*, 2001)
	D. palpebrae	Whole plant	(Kyokong *et al.*, 2019)
2,8-Dihydroxy-3,4,7-trimethoxyphenanthrene [**129**]	*D. nobile*	Stem	(Yang *et al.*, 2007a)
1,5,7-Trimethoxyphenanthrene-2-ol [**130**]	*D. nobile*	Stem	(Kim *et al.*, 2015)
2,3,5-Trihydroxy-4,9-Dimethoxyphenanthrene [**131**]	*D. nobile*	Stem	(Yang *et al.*, 2007a)
3,4,8-Trimethoxyphenanthrene-2,5-diol [**132**]	*D. nobile*	Stem	(Hwang *et al.*, 2010)

Table 3 (continued)

Phenanthrene derivatives			
Phytochemical	**Plant**	**Plant part**	**Reference**
4,5-Dihydroxy-2,3-dimethoxy-9,10-dihydrophenanthrene [**133**]	*D. ellipsophyllum*	Whole plant	(Tanagornmeatar *et al.*, 2014)
	D. sinense	Whole plant	(Chen *et al.*, 2013)
	D. pachyglossum	Whole plant	(Warinhomhoun *et al.*, 2021)
4,5-Dihydroxy-2,6-dimethoxy-9,10-dihydrophenanthrene [**134**]	*D. chrysotoxum*	Stem	(Hu *et al.*, 2012)
4,5-Dihydroxy-3,7-dimethoxy-9,10-dihydrophenanthrene [**135**]	*D. nobile*	Stem	(Ye & Zhao, 2002)
4,5-Dihydroxy-2-methoxy-9,10-dihydrophenanthrene (Orchinol)* [**136**]	*D. nobile*	Stem	(Yang *et al.*, 2007a)
	D. devonianum	Stem	(Wu *et al.*, 2019)
	D. christyanum	Root	(San *et al.*, 2020)
9,10-Dihydromoscatin [**137**]	*D. polyanthum*	Stem	(Hu *et al.*, 2009)
9,10-Dihydrophenanthrene-2,4,7-triol [**138**]	*D. officinale*	Stem	(Zhao *et al.*, 2018)
	D. polyanthum	Stem	(Hu *et al.*, 2009)

Table 3 (continued)

Phenanthrene derivatives			
Phytochemical	**Plant**	**Plant part**	**Reference**
1,5-Dihydroxy-3,4,7-trimethoxy-9,10-dihydrophenanthrene [**139**]	*D. moniliforme*	Whole plant	(Zhao *et al.*, 2016)
Coelonin [**140**]	*D. formosum*	Whole plant	(Inthongkaew *et al.*, 2017)
	D. nobile	Stem	(Yang *et al.*, 2007a)
	D. scabrilingue	Whole plant	(Sarakulwattana *et al.*, 2020)
Dendroinfundin A [**141**]	*D. infundibulum*	Whole plant	(Na Ranong *et al.*, 2019)
Dendroinfundin B [**142**]	*D. infundibulum*	Whole plant	(Na Ranong *et al.*, 2019)
Ephemeranthol A [**143**]	*D. infundibulum*	Whole plant	(Na Ranong *et al.*, 2019)
	D. nobile	Stem	(Hwang *et al.*, 2010; Yang *et al.*, 2007a)
	D. officinale	Stem	(Zhao *et al.*, 2018)
	D. gibsonii	Whole plant	(Thant *et al.*, 2020)
Ephemeranthol C [**144**]	*D. nobile*	Stem	(Hwang *et al.*, 2010; Yang *et al.*, 2007a)
Erianthridin [**145**]	*D. nobile*	Stem	(Hwang *et al.*, 2010)

Table 3 (continued)

Phenanthrene derivatives			
Phytochemical	**Plant**	**Plant part**	**Reference**
Erianthridin [**145**] (continued)	*D. formosum*	Whole plant	(Inthongkaew *et al.*, 2017)
	D. plicatile	Stem	(Yamaki & Honda, 1996)
Flavanthridin [**146**]	*D. nobile*	Stem	(Hwang *et al.*, 2010)
Hircinol [**147**]	*D. aphyllum*	Stem	(Yang *et al.*, 2015a)
	D. draconis	Stem	(Sritularak *et al.*, 2011a)
	D. formosum	Whole plant	(Inthongkaew *et al.*, 2017)
Lusianthridin [**148**]	*D. plicatile*	Stem	(Yamaki & Honda, 1996)
	D. scabrilingue	Whole plant	(Sarakulwattana *et al.*, 2020)
	D. venustum	Whole plant	(Sukphan *et al.*, 2014)
	D. gibsonii	Whole plant	(Thant *et al.*, 2020)
3-Hydroxy-2,4,7-trimethoxy-9,10-dihydrophenanthrene [**149**]	*D. nobile*	Stem	(Yang *et al.*, 2007a)

Table 3 (continued)

Phenanthrene derivatives			
Phytochemical	**Plant**	**Plant part**	**Reference**
7-Hydroxy-2,3,4-trimethoxy-9,10-dihydrophenanthrene [**150**]	*D. brymerianum*	Whole plant	(Klongkumnuankarn *et al.*, 2015)
	D. formosum	Whole plant	(Inthongkaew *et al.*, 2017)
	D. hainanense	Aerial part	(Zhang *et al.*, 2018)
	D. palpebrae	Whole plant	(Kyokong *et al.*, 2019)
2,7-Dihydroxy-3,4,6-trimethoxy-9,10-dihydrophenanthrene [**151**]	*D. densiflorum*	Stem	(Fan *et al.*, 2001)
2,8-Dihydroxy-3,4,7-trimethoxy-9,10-dihydrophenanthrene [**152**]	*D. nobile*	Stem	(Yang *et al.*, 2007a)
4,7-Dihydroxy-2,3,6-trimethoxy-9,10-dihydrophenanthrene [**153**]	*D. rotundatum*	Whole plant	(Majumder & Pal, 1992)
3,4-Dimethoxy-1-(methoxymethyl)-9,10-dihydrophenanthrene-2,7-diol [**154**]	*D. hainanense*	Aerial part	(Zhang *et al.*, 2018)

Table 3 (continued)

Phenanthrene derivatives			
Phytochemical	**Plant**	**Plant part**	**Reference**
Plicatol C [**155**]	*D. plicatile*	Stem	(Honda & Yamaki, 2000)
Rotundatin [**156**]	*D. rotundatum*	Whole plant	(Majumder & Pal, 1992)
(*S*)-2,4,5,9-Tetrahydroxy-9,10-dihydrophenanthrene [**157**]	*D. fimbriatum*	Stem	(Xu *et al.*, 2014)
2-Hydroxy-4,7-dimethoxy-9,10-dihydrophenanthrene [**158**]	*D. nobile*	Stem	(Yang *et al.*, 2007a)
7-Methoxy-9,10-dihydrophenanthrene-2,4,5-triol [**159**]	*D. draconis*	Stem	(Sritularak *et al.*, 2011a)
2,5,7-Trihydroxy-4-methoxy-9,10-dihydrophenanthrene [**160**]	*D. formosum*	Whole plant	(Inthongkaew *et al.*, 2017)
Dendrononе [**161**]	*D. cariniferum*	Stem	(Chen *et al.*, 2008d)
	D. longicornu	Stem	(Hu *et al.*, 2008a)
Ephemeranthoquinone [**162**]	*D. plicatile*	Stem	(Yamaki & Honda, 1996)

Table 3 (continued)

Phenanthrene derivatives			
Phytochemical	**Plant**	**Plant part**	**Reference**
5-Methoxy-7-hydroxy-9,10-dihydro-1,4-phenanthrenequinone [**163**]	*D. draconis*	Stem	(Sritularak *et al.*, 2011a)
	D. formosum	Whole plant	(Inthongkaew *et al.*, 2017)
Moniliformin [**164**]	*D. moniliforme*	Stem	(Lin *et al.*, 2001)
Cypripedin [**165**]	*D. densiflorum*	Stem	(Fan *et al.*, 2001)
	D. lindleyi	Whole plant	(Khoonrit *et al.*, 2020)
Denbinobin [**166**]	*D. moniliforme*	Stem	(Lin *et al.*, 2001)
	D. nobile	Stem	(Yang *et al.*, 2007a)
	D. wardianum	Stem	(Zhang *et al.*, 2017a)
Densiflorol B [**167**]	*D. densiflorum*	Stem	(Fan *et al.*, 2001)
	D. venustum	Whole plant	(Sukphan *et al.*, 2014)
Amoenumin [**168**]	*D. amoenum*	Whole plant	(Veerraju *et al.*, 1989)
Crystalltone [**169**]	*D. crystallinum*	Stem	(Wang *et al.*, 2009)
Chrysotoxol A [**170**]	*D. chrysotoxum*	Stem	(Hu *et al.*, 2012)
Chrysotoxol B [**171**]	*D. chrysotoxum*	Stem	(Hu *et al.*, 2012)
Fimbriatone [**172**]	*D. nobile*	Stem	(Zhang *et al.*, 2008b)
	D. pulchellum	Stem	(Chanvorachote *et al.*, 2013)
Loddigesiinol B [**173**]	*D. loddigesii*	Whole plant	(Ito *et al.*, 2010)
	D. polyanthum	Stem	(Hu *et al.*, 2009)

Table 3 (continued)

Phenanthrene derivatives			
Phytochemical	**Plant**	**Plant part**	**Reference**
Dendrochrysanene [**174**]	*D. chrysanthum*	Stem	(Yang *et al.*, 2006a)
Dendropalpebrone [**175**]	*D. palpebrae*	Whole plant	(Kyokong *et al.*, 2019)
2,2′-Dihydroxy-3,3′,4,4′,7,7′-hexamethoxy-9,9′,10,10′-tetrahydro-1,1′-biphenanthrene [**176**]	*D. nobile*	Stem	(Yang *et al.*, 2007a)
2,2′-Dimethoxy-4,4′,7,7′-tetrahydroxy-9,9′,10,10′-tetrahydro-1,1′-biphenanthrene [**177**]	*D. plicatile*	Stem	(Yamaki & Honda, 1996)
Flavanthrin [**178**]	*D. aphyllum*	Whole plant	(Chen *et al.*, 2008b)
Phoyunnanin C [**179**]	*D. venustum*	Whole plant	(Sukphan *et al.*, 2014)
Phoyunnanin E [**180**]	*D. venustum*	Whole plant	(Sukphan *et al.*, 2014)
Aphyllone A [**181**]	*D. aphyllum*	Stem	(Yang *et al.*, 2015a)
9,10-Dihydro-aphyllone A-5-*O*-β-D-glucopyranoside [**182**]	*D. fimbriatum*	Stem	(Xu *et al.*, 2017)

Table 3 (continued)

Phenanthrene derivatives			
Phytochemical	**Plant**	**Plant part**	**Reference**
2,4,5,9*S*-Tetrahydroxy-9,10-dihydrophenanthrene-4-*O*-β-D-glucopyranoside [**183**]	*D. primulinum*	Whole plant	(Ye *et al.*, 2016)
Dendrocandin P1 [**184**]	*D. officinale*	Stem	(Zhao *et al.*, 2018)
Dendrocandin P2 [**185**]	*D. officinale*	Stem	(Zhao *et al.*, 2018)
Loddigesiinol G [**186**]	*D. loddigesii*	Stem	(Lu *et al.*, 2014)
Loddigesiinol H [**187**]	*D. loddigesii*	Stem	(Lu *et al.*, 2014)
Loddigesiinol I [**188**]	*D. loddigesii*	Stem	(Lu *et al.*, 2014)
Loddigesiinol J [**189**]	*D. loddigesii*	Stem	(Lu *et al.*, 2014)
2,5,9*S*-Trihydroxy-9,10-dihydrophenanthrene-4-*O*-β-D-glucopyranoside [**190**]	*D. primulinum*	Whole plant	(Ye *et al.*, 2016)
4-Methoxy-5,9*R*-dihydroxy-9,10-dihydrophenanthrene-2-*O*-β-D-glucopyranoside [**191**]	*D. nobile*	Stem	(Zhou *et al.*, 2017)
(-)-Dendroparishiol [**192**]	*D. parishii*	Whole plant	(Kongkatitham *et al.*, 2018)
Dendrodevonin A [**193**]	*D. devonianum*	Stem	(Wu *et al.*, 2019)

Table 3 (continued)

Phenanthrene derivatives			
Phytochemical	**Plant**	**Plant part**	**Reference**
Dendrodevonin B [**194**]	*D. devonianum*	Stem	(Wu *et al.*, 2019)

*represent different names of the same compound

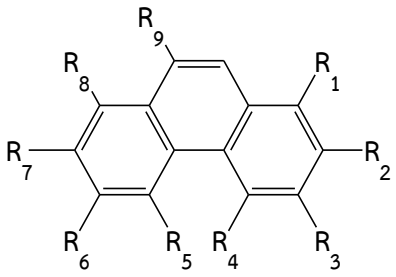

	R_1	R_2	R_3	R_4	R_5	R_6	R_7	R_8	R_9
Bulbophyllanthrin [**111**]	H	OMe	OH	OMe	OH	H	H	H	H
Confusarin [**112**]	OMe	OH	H	H	OMe	OMe	OH	H	H
Dendroscabrol A [**113**]	H	OH	OMe	OMe	H	H	OMe	H	H
Denthyrsinin [**115**]	H	OMe	OH	OMe	H	H	OH	OMe	H
3-Hydroxy-2,4,7-trimethoxy phenanthrene [**116**]	H	OMe	OH	OMe	H	OMe	H	H	H
5-Hydroxy-2,4-dimethoxy phenanthrene [**117**]	H	OMe	H	OMe	OH	OMe	H	H	H
Epheranthol B [**118**]	H	H	H	OMe	OH	H	OMe	H	H
Fimbriol B [**119**]	H	OH	OMe	OH	H	H	H	H	H
Flavanthrinin [**120**]	H	H	H	OMe	H	H	OH	H	H
Loddigesiinol A [**121**]	H	OH	H	OMe	OMe	H	H	H	OH
Moscatin [**122**]	H	H	H	OH	OMe	H	OH	H	H

Figure 3 Structures of phenanthrene derivatives of *Dendrobium* species

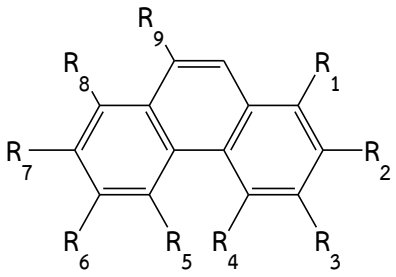

	R_1	R_2	R_3	R_4	R_5	R_6	R_7	R_8	R_9
Nudol [**123**]	H	OH	OMe	OMe	H	H	OH	H	H
Plicatol B [**125**]	H	OH	H	OMe	OH	H	H	H	H
2,5-Dihydroxy-3,4-dimethoxy phenanthrene [**126**]	H	OH	OMe	OMe	OH	H	H	H	H
2,5-Dihydroxy-4,9-dimethoxy phenanthrene [**127**]	H	OH	H	OMe	OH	H	H	H	OMe
2,6-Dihydroxy-1,5,7-trimethoxy phenanthrene [**128**]	OMe	OH	H	H	OMe	OH	OMe	H	H
2,8-Dihydroxy-3,4,7-trimethoxy phenanthrene [**129**]	H	OH	OMe	OMe	H	H	OMe	OH	H

Figure 3 (continued)

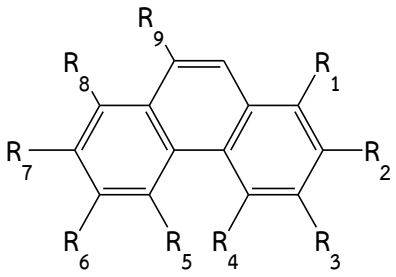

	R_1	R_2	R_3	R_4	R_5	R_6	R_7	R_8	R_9
1,5,7-Trimethoxy phenanthrene-2-ol [**130**]	OMe	OH	H	H	OMe	H	OMe	H	H
2,3,5-Trihydroxy-4,9-dimethoxy phenanthrene [**131**]	H	OH	OH	OMe	OH	H	H	H	OMe
3,4,8-Trimethoxy-phenanthrene-2,5-diol [**132**]	H	OH	OMe	OMe	OH	H	H	OMe	H

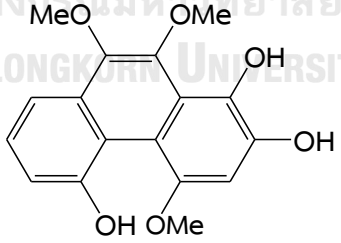

Plicatol A [**124**]

Figure 3 (continued)

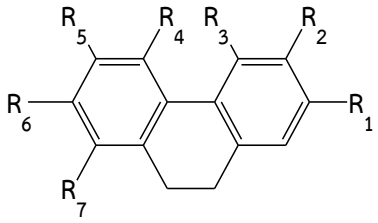

	R_1	R_2	R_3	R_4	R_5	R_6	R_7
4,5-Dihydroxy-2,3-dimethoxy-9,10-dihydrophenanthrene [**133**]	OMe	OMe	OH	OH	H	H	H
4,5-Dihydroxy-2,6-dimethoxy-9,10-dihydrophenanthrene [**134**]	OMe	H	OH	OH	OMe	H	H
4,5-Dihydroxy-3,7-dimethoxy-9,10-dihydrophenanthrene [**135**]	H	OMe	OH	OH	H	OMe	H
4,5-Dihydroxy-2-methoxy-9,10-dihydrophenanthrene (Orchinol)* [**136**]	OMe	H	OH	OH	H	H	H
9,10-Dihydromoscatin [**137**]	H	H	OH	OMe	H	OH	H
9,10-Dihydrophenanthrene-2,4,7-triol [**138**]	OH	H	OH	H	H	OH	H
1,5-Dihydroxy-3,4,7-trimethoxy-9,10- dihydrophenanthrene [**139**]	H	OMe	OMe	OH	H	OMe	H

Figure 3 (continued)

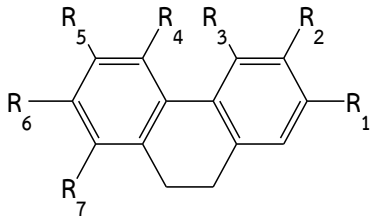

	R_1	R_2	R_3	R_4	R_5	R_6	R_7
Coelonin [**140**]	OH	H	OMe	H	H	OH	H
Dendroinfundin A [**141**]	OMe	OMe	OH	H	H	OMe	H
Dendroinfundin B [**142**]	OMe	OMe	OH	OH	H	H	OMe
Ephemeranthol A [**143**]	OH	H	H	OH	OMe	OMe	H
Ephemeranthol C [**144**]	OH	OH	OMe	OH	H	H	H
Erianthridin [**145**]	OH	OMe	OMe	H	H	OH	H
Flavanthridin [**146**]	OH	H	H	OMe	OH	OMe	H
Hircinol [**147**]	OH	H	OMe	OH	H	H	H
Lusianthridin [**148**]	OMe	H	OH	H	H	OH	H
3-Hydroxy-2,4,7-trimethoxy-9,10-dihydrophenanthrene [**149**]	OMe	OH	OMe	H	H	OMe	H
7-Hydroxy-2,3,4-trimethoxy-9,10-dihydrophenanthrene [**150**]	OMe	OMe	OMe	H	H	OH	H
2,7-Dihydroxy-3,4,6-trimethoxy-9,10-dihydrophenanthrene [**151**]	OH	OMe	OMe	H	OMe	OH	H

Figure 3 (continued)

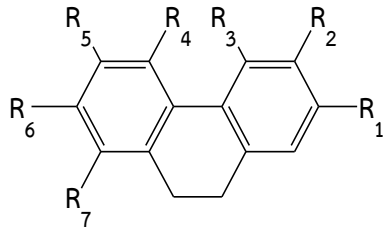

	R_1	R_2	R_3	R_4	R_5	R_6	R_7
2,8-Dihydroxy-3,4,7-trimethoxy-9,10-dihydrophenanthrene [**152**]	OH	OMe	OMe	H	H	OMe	OH
4,7-Dihydroxy-2,3,6-trimethoxy-9,10-dihydrophenanthrene [**153**]	OMe	OMe	OH	H	OMe	OH	H
3,4-Dimethoxy-1-(methoxymethyl)-9,10-dihydrophenanthrene-2,7-diol [**154**]	OH	H	H	OMe	OMe	OH	CH_2-OMe

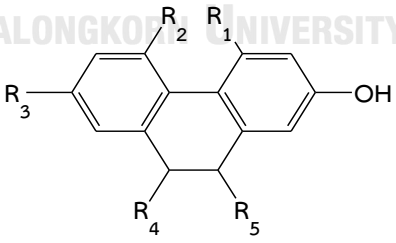

	R_1	R_2	R_3	R_4	R_5
Plicatol C [**155**]	OMe	OH	H	OMe	OMe
Rotundatin [**156**]	OMe	OH	H	OH	OH

Figure 3 (continued)

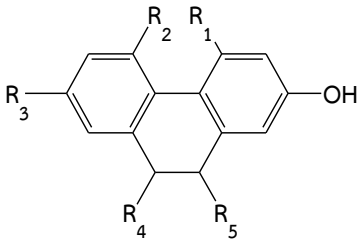

	R_1	R_2	R_3	R_4	R_5
(*S*)-2,4,5,9-Tetrahydroxy-9,10-dihydrophenanthrene [**157**]	OH	OH	H	OH	H
2-Hydroxy-4,7-dimethoxy-9,10-dihydrophenanthrene [**158**]	OMe	H	OMe	H	H
7-Methoxy-9,10-dihydrophenanthrene-2,4,5-triol [**159**]	OH	OH	OMe	H	H
2,5,7-Trihydroxy-4-methoxy-9,10-dihydrophenanthrene [**160**]	OMe	OH	OH	H	H

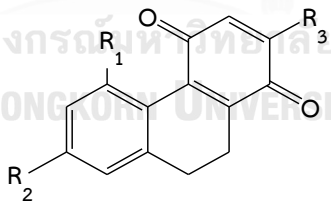

	R_1	R_2	R_3
Dendronone [**161**]	OH	OMe	H
Ephemeranthoquinone [**162**]	H	OH	OMe
5-Methoxy-7-hydroxy-9,10-dihydro-1,4-phenanthrenequinone [**163**]	OMe	OH	H

Figure 3 (continued)

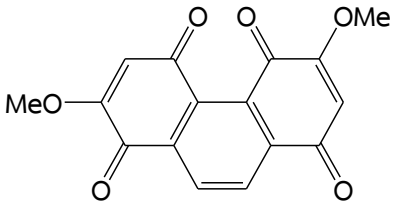

Moniliformin [**164**]

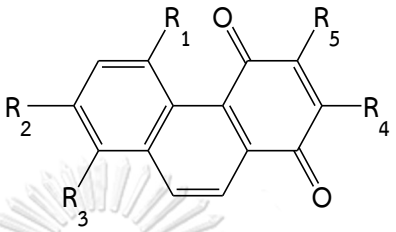

	R_1	R_2	R_3	R_4	R_5
Cypripedin [**165**]	H	OH	OMe	OMe	H
Denbinobin [**166**]	OH	OMe	H	H	OMe
Densiflorol B [**167**]	H	OH	H	OMe	H

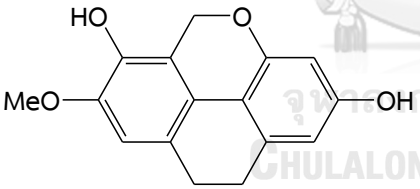

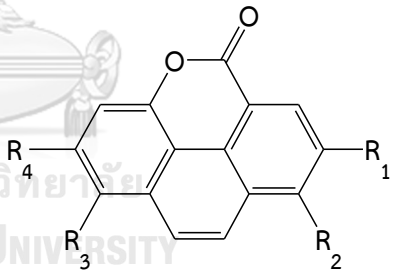

Amoenumin [**168**]

	R_1	R_2	R_3	R_4
Crystalltone [**169**]	OMe	H	OH	EtO
Fimbriatone [**172**]	OH	OMe	H	OH

Figure 3 (continued)

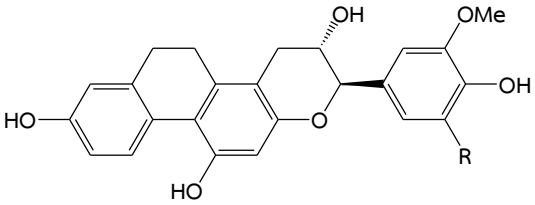

Chrysotoxol A [**170**] R = H

Chrysotoxol B [**171**] R = OMe

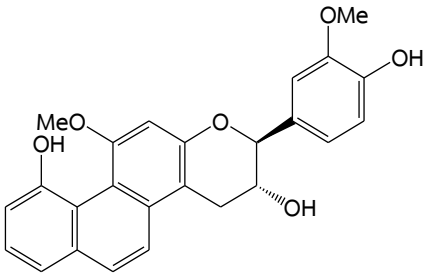

Loddigesiinol B [**173**]

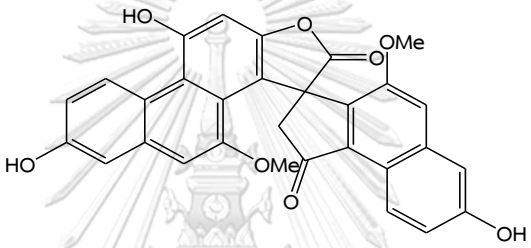

Dendrochrysanene [**174**]

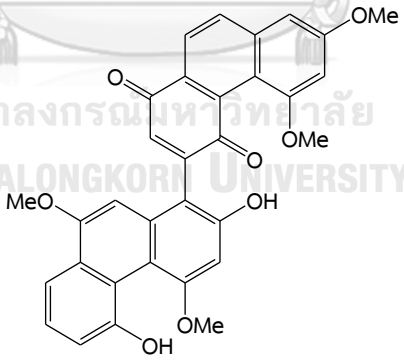

Dendropalpebrone [**175**]

Figure 3 (continued)

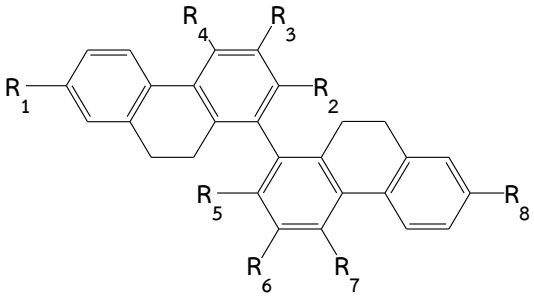

	R_1	R_2	R_3	R_4	R_5	R_6	R_7	R_8
2,2′-Dihydroxy-3,3′,4,4′,7,7′-hexamethoxy-9,9′,10,10′-tetrahydro-1,1′-biphenanthrene [**176**]	OMe	OH	OMe	OMe	OH	OMe	OMe	OMe
2,2′-Dimethoxy-4,4′,7,7′-tetrahydroxy-9,9′,10,10′-tetrahydro-1,1′-biphenanthrene [**177**]	OH	OMe	H	OH	OMe	H	OH	OH
Flavanthrin [**178**]	OH	OH	H	OMe	OH	H	OMe	OH

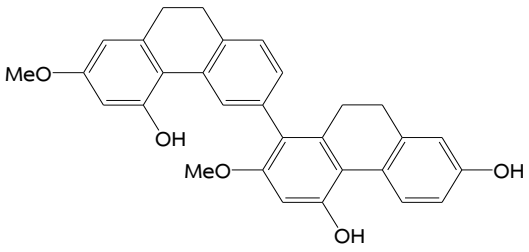

Phoyunnanin C [**179**]

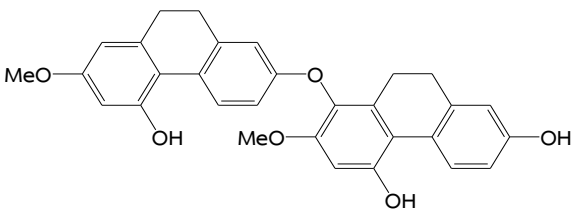

Phoyunnanin E [**180**]

Figure 3 (continued)

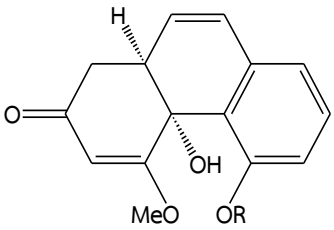

Aphyllone A [**181**] R = H

9,10-Dihydro-aphyllone A-

5-*O*-β-D-glucopyranoside [**182**] R = Glc

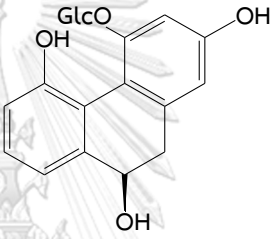

2,4,5,9*S*-Tetrahydroxy-9,10-dihydrophenanthrene-4-*O*-β-D-glucopyranoside [**183**]

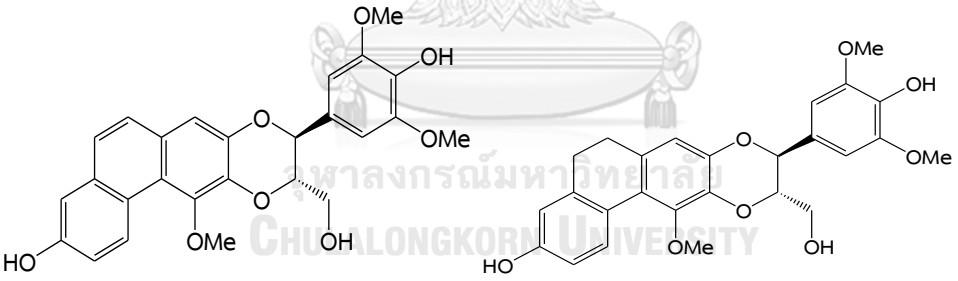

Dendrocandin P1 [**184**] Dendrocandin P2 [**185**]

Figure 3 (continued)

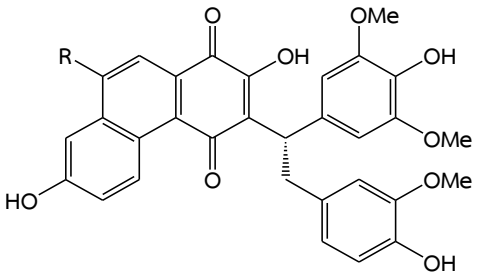

Loddigesiinol G [**186**] R = H

Loddigesiinol H [**187**] R = OH

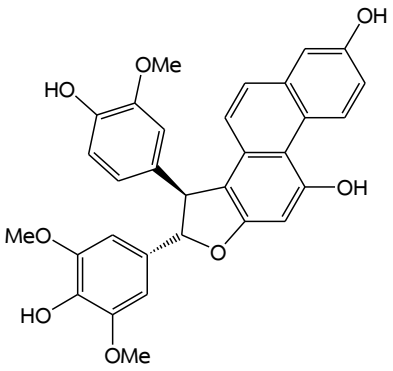

Loddigesiinol I [**188**]

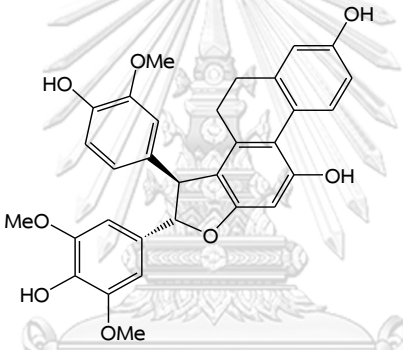

Loddigesiinol J [**189**]

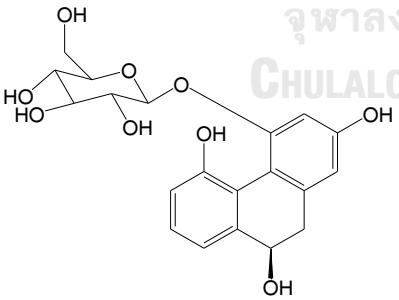

2,5,9*S*-Trihydroxy-9,10-dihydrophenanthrene-4-*O*-β-D-glucopyranoside [**190**]

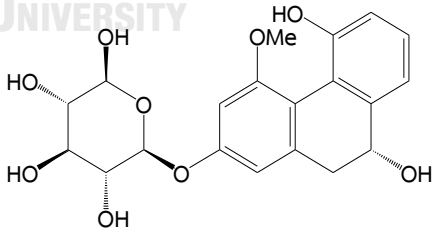

4-Methoxy-5,9*R*-dihydroxy-9,10-dihydrophenanthrene-2-*O*-β-D-glucopyranoside [**191**]

Figure 3 (continued)

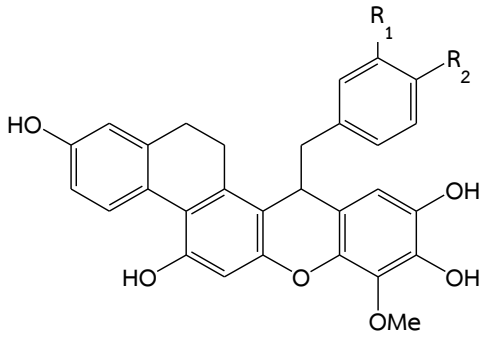

	R_1	R_2
Dendrosignatol [**114**]	H	OMe
(-)-Dendroparishiol [**192**]	OMe	OH

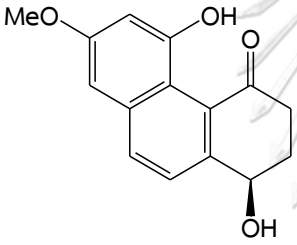

Dendrodevonin A [**193**]

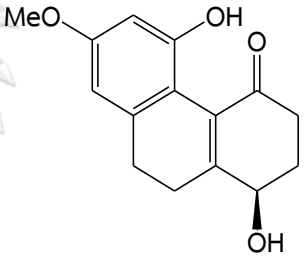

Dendrodevonin B [**194**]

Figure 3 (continued)

Table 4 Flavonoid derivatives of *Dendrobium* species

Flavonoid derivatives			
Phytochemical	**Plant**	**Plant part**	**Reference**
Apigenin [**195**]	*D. crystallinum*	Stem	(Wang *et al.*, 2009)
	D. williamsonii	Whole plant	(Rungwichaniwat *et al.*, 2014)
Apigenin 6-*C*-glucosyl-(1⟶2)-α-*L*-arabinoside [**196**]	*D. officinale*	Leaves	(Zhang *et al.*, 2017c)
6-*C*-(α-Arabinopyranosyl)-8-*C*-[(2-*O*-α-rhamnopyranosyl)-β-galactopyranosyl] apigenin [**197**]	*D. huoshanense*	Aerial part	(Chang *et al.*, 2010)
6-*C*-(α-Arabinopyranosyl)-8-*C*-[(2-*O*-α-rhamnopyranosyl)-β-glucopyranosyl] apigenin [**198**]	*D. huoshanense*	Aerial part	(Chang *et al.*, 2010)
6-*C*-[(2-*O*-α-Rhamnopyranosyl)-β-glucopyranosyl]-8-*C*-(α-arabinopyranosyl) apigenin [**199**]	*D. huoshanense*	Aerial part	(Chang *et al.*, 2010)
6-*C*-(β-Xylopyranosyl)-8-*C*-[(2-*O*-α-rhamnopyranosyl)-β-glucopyranosyl] apigenin [**200**]	*D. huoshanense*	Aerial part	(Chang *et al.*, 2010)

Table 4 (continued)

Flavonoid derivatives			
Phytochemical	**Plant**	**Plant part**	**Reference**
5-Hydroxy-3-methoxyflavone-7-*O*-[β-D-apiosyl-(1⟶6)]-β-D-glucoside [**201**]	*D. devonianum*	Whole plant	(Sun *et al.*, 2014)
5,6-Dihydroxy-4′-methoxyflavone [**202**]	*D. chrysotoxum*	Stem	(Hu *et al.*, 2012)
6‴-Glucosyl-vitexin [**203**]	*D. crystallinum*	Stem	(Wang *et al.*, 2009)
Chrysoeriol [**204**]	*D. ellipsophyllum*	Whole plant	(Tanagornmeatar *et al.*, 2014)
Isorhamnetin-3-*O*-β-D-rutinoside [**205**]	*D. nobile*	Stem	(Zhou *et al.*, 2017)
Isoschaftoside [**206**]	*D. huoshanense*	Aerial part	(Chang *et al.*, 2010)
Isoviolanthin [**207**]	*D. crystallinum*	Stem	(Wang *et al.*, 2009)
Kaempferol [**208**]	*D. aurantiacum var. denneanum*	Stem	(Yang *et al.*, 2006b)
Kaempferol-3-*O*-α-*L*-rhamnopyranoside [**209**]	*D. secundum*	Stem	(Phechrmeekha *et al.*, 2012)
Kaempferol-3,7-*O*-di-α-*L*-rhamnopyranoside [**210**]	*D. secundum*	Stem	(Phechrmeekha *et al.*, 2012)

Table 4 (continued)

Flavonoid derivatives			
Phytochemical	**Plant**	**Plant part**	**Reference**
Kaempferol-3-*O*-α-*L*-rhamnopyranosyl-(1⟶2)-β-D-glucopyranoside [**211**]	*D. capillipes*	Stem	(Phechrmeekha *et al.*, 2012)
Kaempferol-3-*O*-α-*L*-rhamnopyranosyl-(1⟶2)-β-D-xylopyranoside [**212**]	*D. capillipes*	Stem	(Phechrmeekha *et al.*, 2012)
Luteolin [**213**]	*D. aurantiacum var. denneanum*	Whole plant	(Ying *et al.*, 2009)
	D. ellipsophyllum	Whole plant	(Tanagornmeatar *et al.*, 2014)
Vicenin-2 [**214**]	*D. aurantiacum var. denneanum*	Stem	(Xiong *et al.*, 2013)
Quercetin-3-*O*-*L*-rhamnopyranoside [**215**]	*D. secundum*	Stem	(Phechrmeekha *et al.*, 2012)
Quercetin-3-*O*-α-*L*-rhamnopyranosyl-(1⟶2)-β-D-xylopyranoside [**216**]	*D. capillipes*	Stem	(Phechrmeekha *et al.*, 2012)

Table 4 (continued)

Flavonoid derivatives			
Phytochemical	**Plant**	**Plant part**	**Reference**
(*S*)-5,5′,7-Trihydroxy-3′,4′-Dimethoxyflavanone [**217**]	*D. loddigesii*	Stem	(Ma *et al.*, 2019b)
(2*S*)-Eriodictyol [**218**]	*D. ellipsophyllum*	Whole plant	(Tanagornmeatar *et al.*, 2014)
	D. tortile	Whole plant	(Limpanit *et al.*, 2016)
(2*S*)-Homoeriodictyol [**219**]	*D. densiflorum*	Stem	(Fan *et al.*, 2001)
	D. ellipsophyllum	Whole plant	(Tanagornmeatar *et al.*, 2014)
Naringenin [**220**]	*D. aurantiacum var. denneanum*	Stem	(Yang *et al.*, 2006b)
	D. densiflorum	Stem	(Fan *et al.*, 2001)
	D. longicornu	Stem	(Hu *et al.*, 2008a)

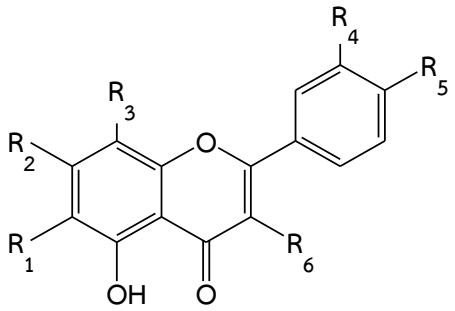

	R_1	R_2	R_3	R_4	R_5	R_6
Apigenin [**195**]	H	OH	H	H	OH	H
Apigenin 6-*C*-glucosyl-(1⟶2)-α-*L*-arabinoside [**196**]	[Ara-]$_2$	OH	H	H	OH	H
6-*C*-(α-Arabinopyranosyl)-8-*C*-[(2-*O*-α-rhamnopyranosyl)-β-galactopyranosyl] apigenin [**197**]	-Ara	OH	-Gal-Rha	H	OH	H
6-*C*-(α-Arabinopyranosyl)-8-*C*-[(2-*O*-α-rhamnopyranosyl)-β-glucopyranosyl] apigenin [**198**]	-Ara	OH	-Glc-Rha	H	OH	H
6-*C*-[(2-*O*-α-Rhamnopyranosyl)-β-glucopyranosyl]-8-*C*-(α-arabinopyranosyl) apigenin [**199**]	-Glc-Rha	OH	-Ara	H	OH	H

Figure 4 Structures of flavonoid derivatives of *Dendrobium* species

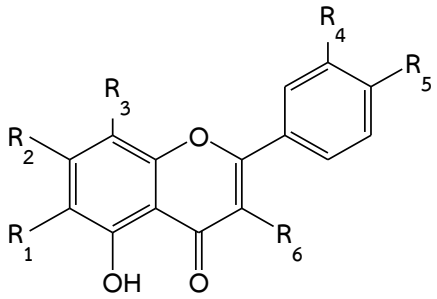

	R_1	R_2	R_3	R_4	R_5	R_6
6-*C*-(β-Xylopyranosyl)-8-*C*-[(2-*O*-α-rhamnopyranosyl)-β-glucopyranosyl] apigenin [**200**]	-Xyl	OH	-Glc-Rha	H	OH	H
5-Hydroxy-3-methoxyflavone-7-*O*-[β-D-apiosyl-(1⟶6)]-β-D-glucoside [**201**]	H	-Glc-Api	H	H	H	OMe
5,6-Dihydroxy-4′-methoxyflavone [**202**]	OH	H	H	H	OMe	H
6‴-Glucosyl-vitexin [**203**]	H	OH	-$(Glc)_2$	H	OH	H
Chrysoeriol [**204**]	H	OH	H	OMe	OH	H
Isoschaftoside [**206**]	-Ara	OH	-Glc	H	OH	H
Isoviolanthin [**207**]	-Rha	OH	-Glc	H	OH	H
Kaempferol [**208**]	H	OH	H	H	OH	OH
Kaempferol-3-*O*-α-*L*-rhamnopyranoside [**209**]	H	OH	H	H	OH	O-Rha

Figure 4 (continued)

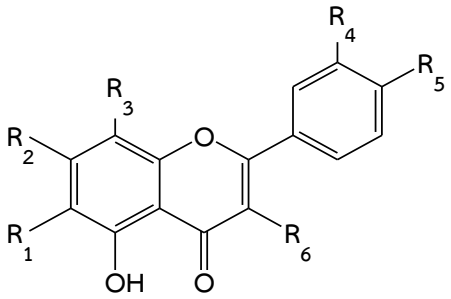

	R_1	R_2	R_3	R_4	R_5	R_6
Kaempferol-3,7-*O*-di-α-*L*-rhamnopyranoside [**210**]	H	O-Rha	H	H	OH	O-Rha
Kaempferol-3-*O*-α-*L*-rhamnopyranosyl-(1⟶2)-β-D-glucopyranoside [**211**]	H	OH	H	H	OH	O-Glc-Rha
Kaempferol-3-*O*-α-*L*-rhamnopyranosyl-(1⟶2)-β-D-xylopyranoside [**212**]	H	OH	H	H	OH	O-Xyl-Rha
Luteolin [**213**]	H	OH	H	OH	OH	H
Vicenin-2 [**214**]	-Glc	OH	-Glc	H	OH	H
Quercetin-3-*O*-*L*-rhamnopyranoside [**215**]	H	OH	H	OH	OH	-O-Rha

Figure 4 (continued)

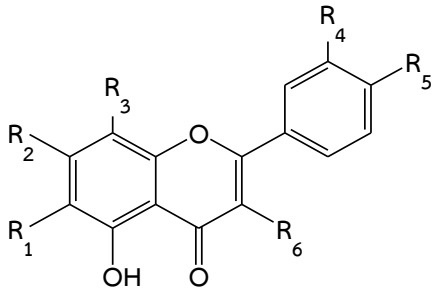

	R_1	R_2	R_3	R_4	R_5	R_6
Quercetin-3-*O*-α-*L*-rhamnopyranosyl-(1⟶2)-β-D-xylopyranoside [**216**]	H	OH	H	OH	OH	-O-Xyl-Rha

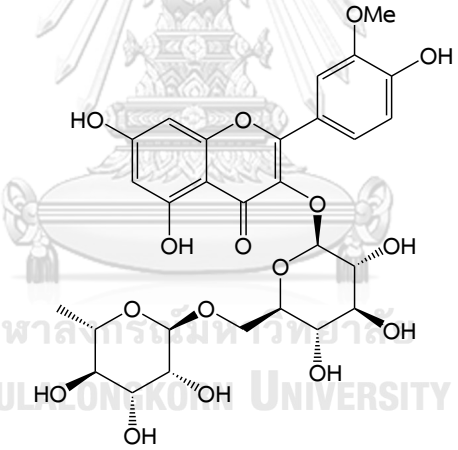

Isorhamnetin-3-*O*-β-D-rutinoside [**205**]

Figure 4 (continued)

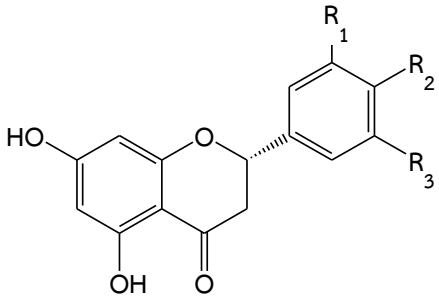

	R_1	R_2	R_3
(*S*)-5,5′,7-Trihydroxy-3′,4′-dimethoxyflavanone [**217**]	OH	OMe	OMe
(2*S*)-Eriodictyol [**218**]	OH	OH	H
(2*S*)-Homoeriodictyol [**219**]	OMe	OH	H
Naringenin [**220**]	H	OH	H

Figure 4 (continued)

Table 5 Terpenoid derivatives of *Dendrobium* species

Terpenoid derivatives			
Phytochemical	**Plant**	**Plant part**	**Reference**
Aduncin [**221**]	*D. aduncum*	Whole plant	(Gawell & Leander, 1976)
Amoenin [**222**]	*D. amoenum*	Whole plant	(Dahmén & Leander, 1978)
	D. williamsonii	Whole plant	(Yang *et al.*, 2019)
Amotin [**223**]	*D. amoenum*	Whole plant	(Majumder *et al.*, 1999)
Asiatic acid [**224**]	*D. parishii*	Whole plant	(Kongkatitham *et al.*, 2018)
Betulin [**225**]	*D. williamsonii*	Whole plant	(Yang *et al.*, 2018b)
Botrydiol-15-*O*-β-D-glucopyranoside [**226**]	*D. fimbriatum*	Stem	(Xu *et al.*, 2017)
Corchoionoside C [**227**]	*D. wardianum*	Stem	(Fan *et al.*, 2013)
	D. polyanthum	Stem	(Hu *et al.*, 2009)
Crystallinin [**228**]	*D. wardianum*	Stem	(Fan *et al.*, 2013)
	D. findlayanum	Whole plant	(Qin *et al.*, 2011)
Dendramine [**229**]	*D. nobile*	Stem	(Okamoto *et al.*, 1966a; Wang *et al.*, 2016)
	D. hildebrandii	Whole plant	(Elander & Leander, 1971)
Dendrine [**230**]	*D. nobile*	Stem	(Meng *et al.*, 2017)
Dendrobane A [**231**]	*D. nobile*	Stem	(Ye & Zhao, 2002)

Table 5 (continued)

Terpenoid derivatives			
Phytochemical	**Plant**	**Plant part**	**Reference**
Dendrobane A [**231**] (continued)	*D. wardianum*	Stem	(Fan *et al.*, 2013)
Dendrobine [**232**]	*D. crepidatum*	Stem	(Zhen-jian *et al.*, 2020)
	D. nobile	Stem	(Meng *et al.*, 2017; Wang *et al.*, 1985)
	D. findlayanum	Stem	(Yang *et al.*, 2018a)
Dendrobine-*N*-oxide [**233**]	*D. nobile*	Whole plant	(Huang *et al.*, 2019)
2-Hydroxydendrobine [**234**]	*D. findlayanum*	Stem	(Yang *et al.*, 2018a)
(-)-(1*R*,2*S*,3*R*,4*S*,5*R*,6*S*,9*S*, 11*R*)-11-Carboxymethyldendrobine [**235**]	*D. nobile*	Stem	(Meng *et al.*, 2017)
3-Hydroxy-2-oxodendrobine [**236**]	*D. findlayanum*	Whole plant	(Qin *et al.*, 2011)
	D. nobile	Stem	(Wang *et al.*, 1985)
	D. nobile	Whole plant	(Huang *et al.*, 2019)
N-Methyldendrobinium [**237**]	*D. nobile*	Stem	(Wang *et al.*, 2016)

Table 5 (continued)

Terpenoid derivatives			
Phytochemical	**Plant**	**Plant part**	**Reference**
N-Isopentenyldendrobinium [**238**]	*D. crepidatum*	Stem	(Zhen-jian *et al.*, 2020)
	D. nobile	Stem	(Wang *et al.*, 2016)
Dendroxine [**239**]	*D. nobile*	Stem	(Okamoto *et al.*, 1966b)
4-Hydroxy-dendroxine [**240**]	*D. nobile*	Stem	(Tang & Eisenbrand, 1992)
6-Hydroxy-dendroxine [**241**]	*D. findlayanum*	Stem	(Yang *et al.*, 2020)
N-Isopentenyldendroxinium [**242**]	*D. nobile*	Stem	(Okamoto *et al.*, 1966a)
	D. friedricksianum	Whole plant	(Hedman *et al.*, 1971)
	D. hilderbrandii	Whole plant	(Hedman *et al.*, 1971)
	D. nobile	Stem	(Wang *et al.*, 2016)
N-Isopentenyl-6-hydroxydendroxinium [**243**]	*D. friedricksianum*	Whole plant	(Hedman *et al.*, 1971)
	D. hilderbrandii	Whole plant	(Hedman *et al.*, 1971)
	D. nobile	Stem	(Wang *et al.*, 2016)
Dendrofindline A [**244**]	*D. findlayanum*	Stem	(Liu *et al.*, 2020a)
Dendrofindline B [**245**]	*D. findlayanum*	Stem	(Liu *et al.*, 2020a)

Table 5 (continued)

Terpenoid derivatives			
Phytochemical	**Plant**	**Plant part**	**Reference**
Dendrofindlayanoside A [**246**]	*D. findlayanum*	Stem	(Dan *et al.*, 2019)
Dendrofindlayanoside B [**247**]	*D. findlayanum*	Stem	(Dan *et al.*, 2019)
Dendrofindlayanoside C [**248**]	*D. findlayanum*	Stem	(Dan *et al.*, 2019)
Dendrofindlayanobilin [**249**]	*D. findlayanum*	Stem	(Dan *et al.*, 2019)
10β,12,14-Trihydroxyaromadendrane [**250**]	*D. findlayanum*	Stem	(Dan *et al.*, 2019)
10β,13,14-Trihydroxyaromadendrane [**251**]	*D. findlayanum*	Stem	(Dan *et al.*, 2019)
	D. moniliforme	Stem	(Zhao *et al.*, 2003b)
Dendronobilin A [**252**]	*D. nobile*	Stem	(Zhang *et al.*, 2007a)
Dendronobilin B [**253**]	*D. crystallinum*	Stem	(Wang *et al.*, 2009)
	D. nobile	Stem	(Zhang *et al.*, 2007a)
Dendronobilin C [**254**]	*D. nobile*	Stem	(Zhang *et al.*, 2007a)
Dendronobilin D [**255**]	*D. nobile*	Stem	(Zhang *et al.*, 2007a)

Table 5 (continued)

Terpenoid derivatives			
Phytochemical	**Plant**	**Plant part**	**Reference**
Dendronobilin E [**256**]	*D. nobile*	Stem	(Zhang *et al.*, 2007a)
Dendronobilin F [**257**]	*D. nobile*	Stem	(Zhang *et al.*, 2007a)
Dendronobilin G [**258**]	*D. nobile*	Stem	(Zhang *et al.*, 2007a)
Dendronobilin H [**259**]	*D. nobile*	Stem	(Zhang *et al.*, 2007a)
Dendronobilin I [**260**]	*D. findlayanum*	Stem	(Dan *et al.*, 2019)
	D. nobile	Stem	(Zhang *et al.*, 2007a)
	D. wardianum	Stem	(Fan *et al.*, 2013)
Dendronobilin J [**261**]	*D. nobile*	Stem	(Zhang *et al.*, 2007a)
Dendronobilin K [**262**]	*D. wardianum*	Stem	(Fan *et al.*, 2013)
	D. nobile	Stem	(Zhang *et al.*, 2008b)
Dendronobilin L [**263**]	*D. nobile*	Stem	(Zhang *et al.*, 2008b)
Dendronobilin M [**264**]	*D. nobile*	Stem	(Meng *et al.*, 2017; Zhang *et al.*, 2008b);

Table 5 (continued)

Terpenoid derivatives			
Phytochemical	**Plant**	**Plant part**	**Reference**
Dendronobilin N [**265**]	*D. nobile*	Stem	(Zhang *et al.*, 2008b)
Dendronobiline A [**266**]	*D. nobile*	Stem	(Qun Fang & Zhao, 2003; Xu *et al.*, 2010)
Dihydronobilonine [**267**]	*D. findlayanum*	Stem	(Yang *et al.*, 2020)
Nobiline (Nobilonine)* [**268**]	*D. nobile*	Stem	(Wang *et al.*, 2016)
	D. findlayanum	Stem	(Yang *et al.*, 2020)
	D. hilderbrandii	Whole plant	(Elander & Leander, 1971)
	D. friedricksianum	Whole plant	(Hedman *et al.*, 1971)
6-Hydroxy-nobiline (6-Hydroxy-nobilonine)* [**269**]	*D. friedricksianum*	Whole plant	(Hedman *et al.*, 1971)
	D. hilderbrandii	Whole plant	(Elander & Leander, 1971)
	D. nobile	Stem	(Nie *et al.*, 2016)
	D. moniliforme	Stem and leave	(Liu *et al.*, 2007)
Nobilomethylene [**270**]	*D. nobile*	Stem	(Okamoto *et al.*, 1972)
Dendrowardine [**271**]	*D. wardianum*	Whole plant	(Glomqvist *et al.*, 1973)

Table 5 (continued)

Terpenoid derivatives			
Phytochemical	**Plant**	**Plant part**	**Reference**
Dendromoniliside A [**272**]	*D. moniliforme*	Stem	(Zhao *et al.*, 2003a)
Dendromoniliside B [**273**]	*D. moniliforme*	Stem	(Zhao *et al.*, 2003a)
Dendromoniliside C [**274**]	*D. moniliforme*	Stem	(Zhao *et al.*, 2003a)
Dendromoniliside D [**275**]	*D. moniliforme*	Stem	(Zhao *et al.*, 2003a)
	D. nobile	Stem	(Nguyen *et al.*, 2017)
Dendronobiloside A [**276**]	*D. moniliforme*	Stem	(Zhao *et al.*, 2003a)
	D. nobile	Stem	(Ye & Zhao, 2002; Zhao *et al.*, 2001)
Dendronobiloside B [**277**]	*D. nobile*	Stem	(Ye & Zhao, 2002; Zhao *et al.*, 2001)
Dendronobiloside C [**278**]	*D. nobile*	Stem	(Ye & Zhao, 2002; Zhao *et al.*, 2001)
Dendronobiloside D [**279**]	*D. nobile*	Stem	(Ye & Zhao, 2002; Zhao *et al.*, 2001)
Dendronobiloside E [**280**]	*D. nobile*	Stem	(Ye & Zhao, 2002; Zhao *et al.*, 2001)
Dendroside A [**281**]	*D. moniliforme*	Stem	(Zhao *et al.*, 2003a)
	D. nobile	Stem	(Ye & Zhao, 2002; Zhao *et al.*, 2001)

Table 5 (continued)

Terpenoid derivatives			
Phytochemical	**Plant**	**Plant part**	**Reference**
Dendroside B [**282**]	*D. nobile*	Stem	(Ye & Zhao, 2002)
	D. williamsonii	Whole plant	(Yang *et al.*, 2019)
Dendroside C [**283**]	*D. nobile*	Stem	(Ye & Zhao, 2002)
	D. moniliforme	Stem	(Zhao *et al.*, 2003a)
Dendroside D [**284**]	*D. nobile*	Stem	(Ye & Zhao, 2002)
Dendroside E [**285**]	*D. nobile*	Stem	(Ye & Zhao, 2002)
Dendroside F [**286**]	*D. moniliforme*	Stem	(Zhao *et al.*, 2003a)
Dendroside G [**287**]	*D. nobile*	Stem	(Ye *et al.*, 2002)
Dendroterpene A [**288**]	*D. nobile*	Stem	(Wang *et al.*, 2019)
Dendroterpene B [**289**]	*D. nobile*	Stem	(Wang *et al.*, 2019)
Dendroterpene C [**290**]	*D. nobile*	Stem	(Wang *et al.*, 2019)
Dendroterpene D [**291**]	*D. nobile*	Stem	(Wang *et al.*, 2019)
Dendroterpene E [**292**]	*D. nobile*	Stem	(Wang *et al.*, 2020)
Dendrowardol A [**293**]	*D. wardianum*	Stem	(Fan *et al.*, 2013)
Dendrowardol B [**294**]	*D. wardianum*	Stem	(Fan *et al.*, 2013)
Dendrowardol C [**295**]	*D. wardianum*	Stem	(Fan *et al.*, 2013)
Dendrowillin A [**296**]	*D. williamsonii*	Whole plant	(Yang *et al.*, 2019)
Dendrowillin B [**297**]	*D. williamsonii*	Whole plant	(Yang *et al.*, 2019)
Findlayanin [**298**]	*D. nobile*	Stem	(Meng *et al.*, 2017)
	D. polyanthum	Stem	(Hu *et al.*, 2009)
	D. findlayanum	Whole plant	(Qin *et al.*, 2011)
Findlayine A [**299**]	*D. findlayanum*	Stem	(Yang *et al.*, 2018a)
Findlayine B [**300**]	*D. findlayanum*	Stem	(Yang *et al.*, 2018a)

Table 5 (continued)

Terpenoid derivatives			
Phytochemical	**Plant**	**Plant part**	**Reference**
Findlayine C [**301**]	*D. findlayanum*	Stem	(Yang *et al.*, 2018a)
Findlayine D [**302**]	*D. findlayanum*	Stem	(Yang *et al.*, 2018a)
Findlayine E [**303**]	*D. findlayanum*	Stem	(Yang *et al.*, 2020)
Findlayine F [**304**]	*D. findlayanum*	Stem	(Yang *et al.*, 2020)
Moniline [**305**]	*D. moniliforme*	Stem and leave	(Liu *et al.*, 2007)
(-)-Picrotin [**306**]	*D. williamsonii*	Whole plant	(Yang *et al.*, 2019)
α-Dihydropicrotoxinin [**307**]	*D. amoenum*	Whole plant	(Majumder *et al.*, 1999)
	D. williamsonii	Whole plant	(Yang *et al.*, 2019)
	D. moniliforme	Stem	(Zhao *et al.*, 2003a)
(+)-(1*R*,2*S*,3*R*,4*S*,5*R*,6*S*,9*R*)-3,11,12-Trihydroxypicrotoxane-2(15)-lactone [**308**]	*D. nobile*	Stem	(Ma *et al.*, 2019a)
(-)-(1*S*,2*R*,3*S*,4*R*,5*S*,6*R*,9*S*,12*R*)-3,11,13-Trihydroxypicrotoxane-2(15)-lactone [**309**]	*D. nobile*	Stem	(Ma *et al.*, 2019a)

Table 5 (continued)

Terpenoid derivatives			
Phytochemical	**Plant**	**Plant part**	**Reference**
(+)-(1*R*,5*R*,6*S*,8*R*,9*R*)-8,12-Dihydroxycopacamphan-3-en-2-one [**310**]	*D. nobile*	Stem	(Ma *et al.*, 2019a)
Flakinin A [**311**]	*D. snowflake*	Whole plant	(Fraga, 2001; Morita *et al.*, 2000)
Flakinin B [**312**]	*D. snowflake*	Whole plant	(Fraga, 2001; Morita *et al.*, 2000)
Mubironine A [**313**]	*D. snowflake*	Whole plant	(Fraga, 2001; Morita *et al.*, 2000)
Mubironine B [**314**]	*D. snowflake*	Whole plant	(Fraga, 2001; Morita *et al.*, 2000)
	D. findlayanum	Stem	(Yang *et al.*, 2020)
	D. nobile	Stem	(Wang *et al.*, 2016)
Mubironine C [**315**]	*D. snowflake*	Whole plant	(Fraga, 2001; Morita *et al.*, 2000)
Wardianumine A [**316**]	*D. wardianum*	Stem	(Zhang *et al.*, 2017a)
Dendrobiumane A [**317**]	*D. moniliforme*	Stem	(Zhao *et al.*, 2003a)
Dendrobiumane B [**318**]	*D. moniliforme*	Stem	(Zhao *et al.*, 2003a)
Dendrobiumane C [**319**]	*D. moniliforme*	Stem	(Zhao *et al.*, 2003a)

Table 5 (continued)

Terpenoid derivatives			
Phytochemical	**Plant**	**Plant part**	**Reference**
Dendrobiumane D [**320**]	*D. moniliforme*	Stem	(Zhao *et al.*, 2003a)
Dendrobiumane E [**321**]	*D. moniliforme*	Stem	(Zhao *et al.*, 2003a)

*represent different names of the same compound

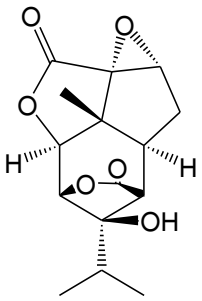

Aduncin [**221**]

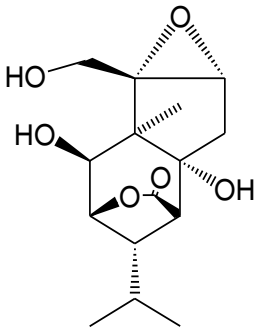

Amoenin [**222**]

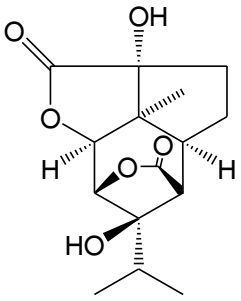

Amotin [**223**]

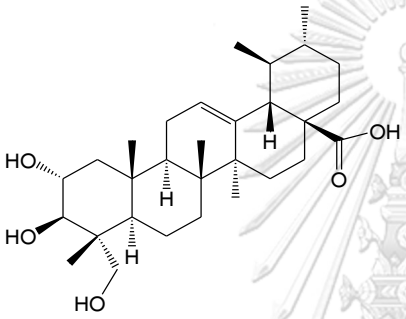

Asiatic acid [**224**]

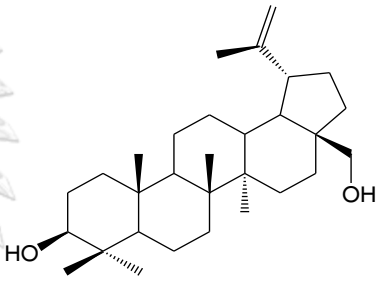

Betulin [**225**]

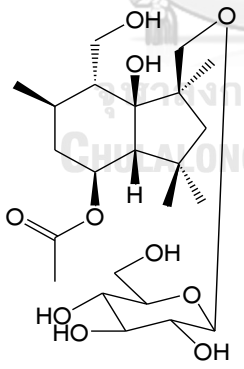

Botrydiol-15-*O*-β-D-glucopyranoside [**226**]

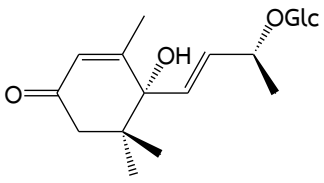

Corchoionoside C [**227**]

Figure 5 Structures of terpenoid derivatives of *Dendrobium* species

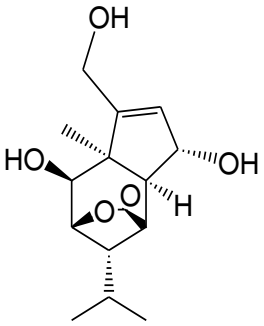

Crystallinin [**228**]

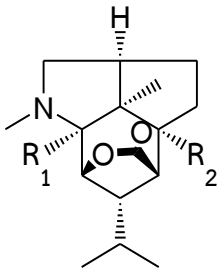

	R_1	R_2
Dendramine [**229**]	H	OH
Dendrobine [**232**]	H	H
2-Hydroxydendrobine [**234**]	OH	H

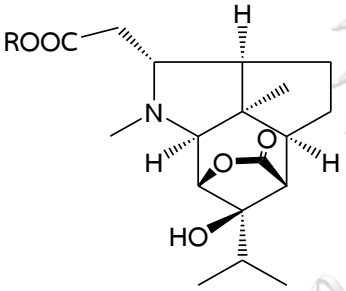

	R
Dendrine [**230**]	Me
(-)-(1*R*,2*S*,3*R*,4*S*,5*R*,6*S*,9*S*,11*R*)-11-Carboxymethyl dendrobine [**235**]	H

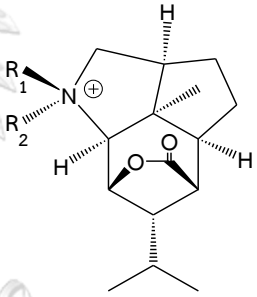

	R_1	R_2
Dendrobine-*N*-oxide [**233**]	O^-	Me
N-Methyldendrobinium [**237**]	Me	Me

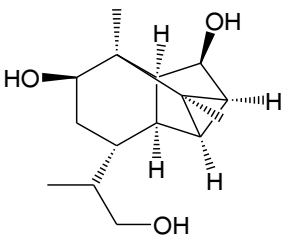

Dendrobane A [**231**]

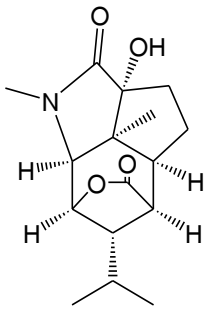

3-Hydroxy-2-oxodendrobine [**236**]

Figure 5 (continued)

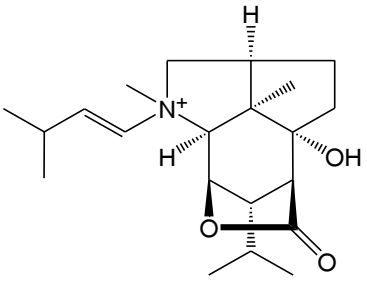

N-Isopentenyldendrobinium [**238**]

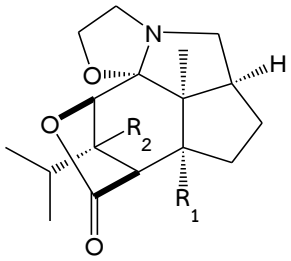

	R_1	R_2
Dendroxine [**239**]	H	H
4-Hydroxy-dendroxine [**240**]	H	OH
6-Hydroxy-dendroxine [**241**]	OH	H

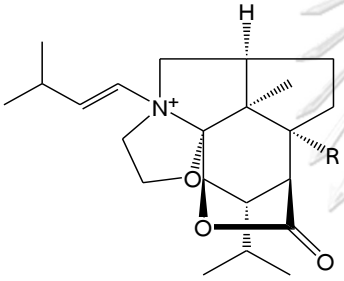

	R
N-Isopentenyldendroxinium [**242**]	H
N-Isopentenyl-6-hydroxydendroxinium [**243**]	OH

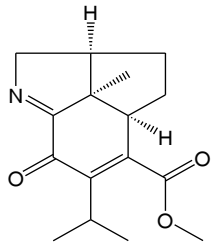

Dendrofindline A [**244**]

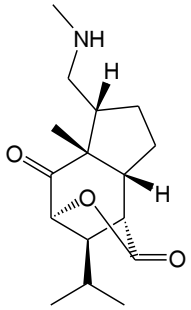

Dendrofindline B [**245**]

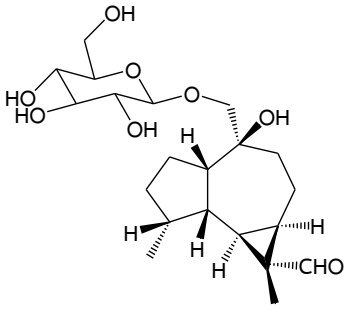

Dendrofindlayanoside A [**246**]

Figure 5 (continued)

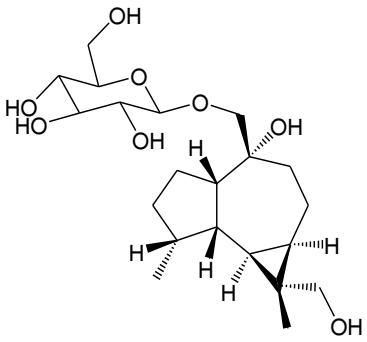

Dendrofindlayanoside B [**247**]

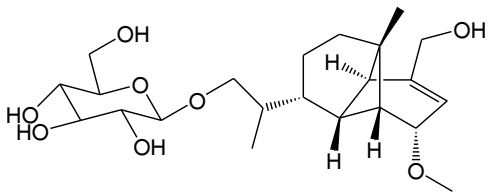

Dendrofindlayanoside C [**248**]

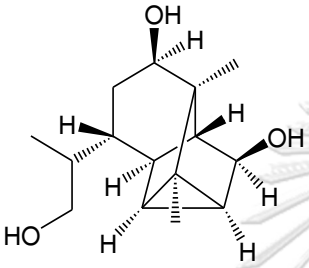

Dendrofindlayanobilin [**249**]

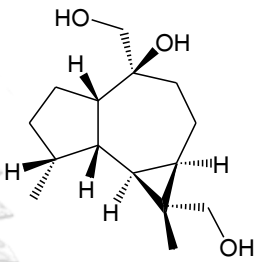

10β,12,14-Trihydroxyaromadendrane [**250**]

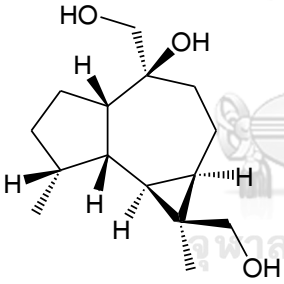

10β,13,14-Trihydroxyaromadendrane [**251**]

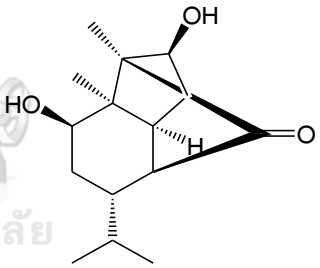

Dendronobilin A [**252**]

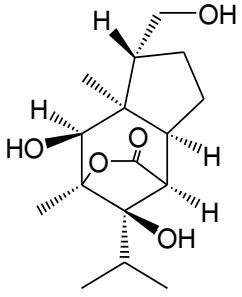

Dendronobilin B [**253**]

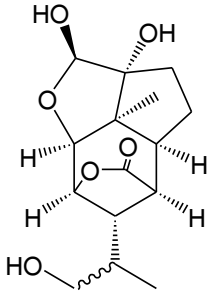

Dendronobilin C [**254**]

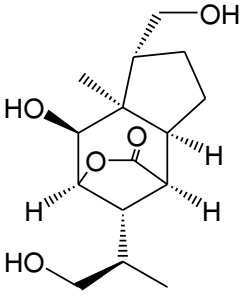

Dendronobilin D [**255**]

Figure 5 (continued)

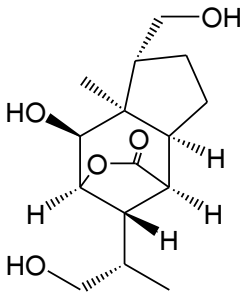

Dendronobilin E [**256**]

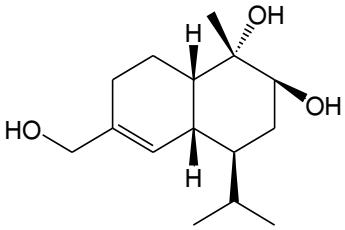

Dendronobilin F [**257**]

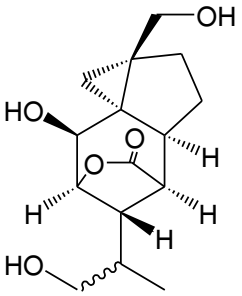

Dendronobilin G [**258**]

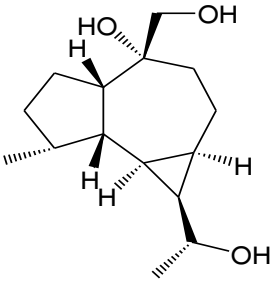

Dendronobilin H [**259**]

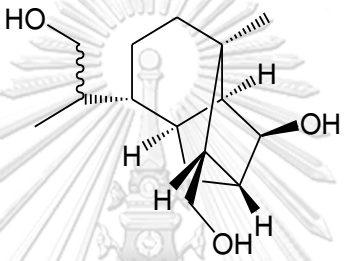

Dendronobilin I [**260**]

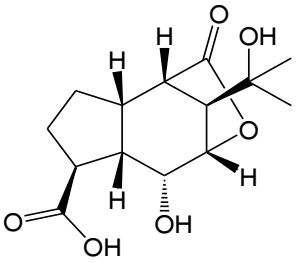

Dendronobilin J [**261**]

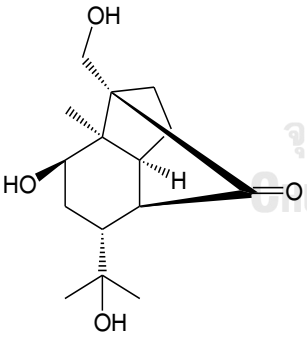

Dendronobilin K [**262**]

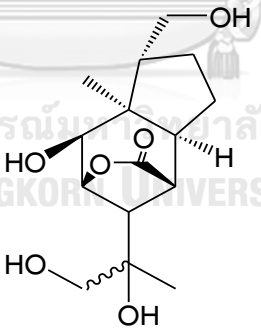

Dendronobilin L [**263**]

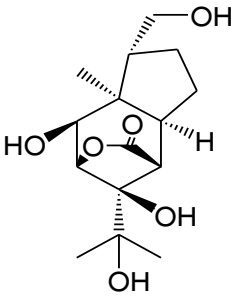

Dendronobilin M [**264**]

Figure 5 (continued)

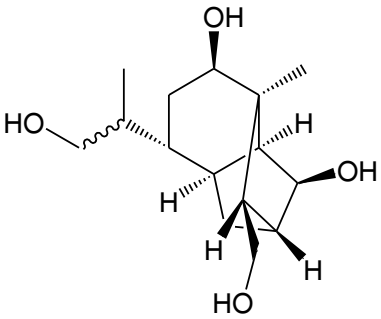

Dendronobilin N [**265**]

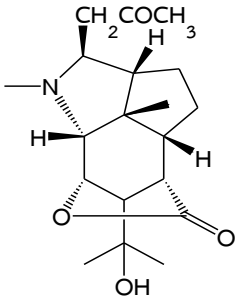

Dendronobiline A [**266**]

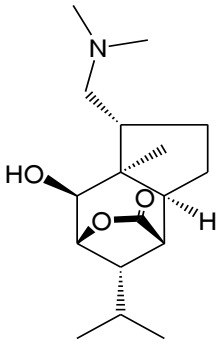

Dihydronobilonine [**267**]

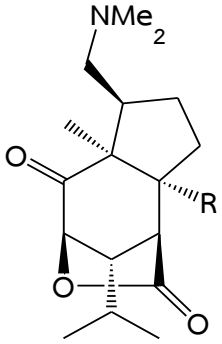

Nobiline

(Nobilonine)* [**268**] R = H

6-Hydroxy-nobiline

(6-Hydroxy-nobilonine)* [**269**] R = OH

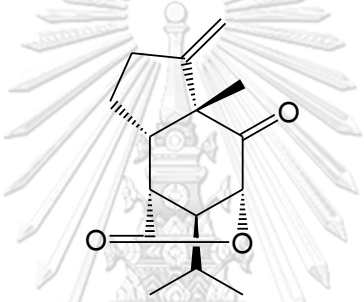

Nobilomethylene [**270**]

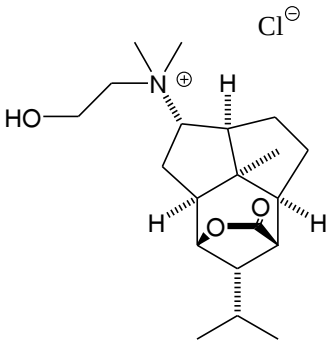

Dendrowardine [**271**]

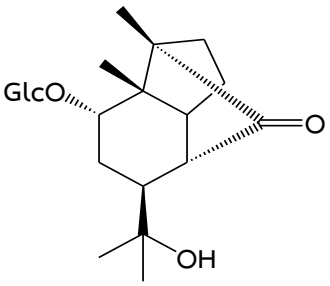

Dendromoniliside A [**272**]

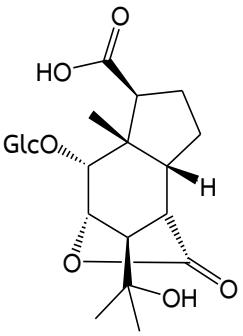

Dendromoniliside B [**273**]

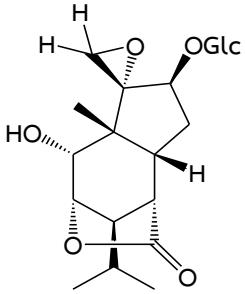

Dendromoniliside C [**274**]

Figure 5 (continued)

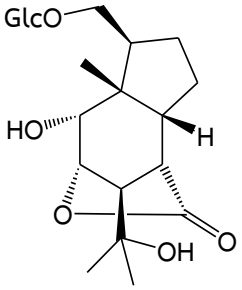

Dendromoniliside D [**275**]

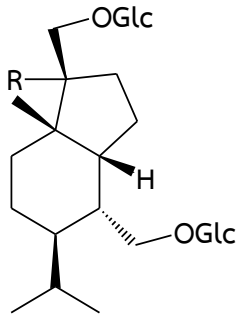

Dendronobiloside A [**276**] R = H

Dendronobiloside B [**277**] R = OH

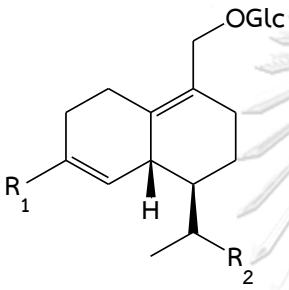

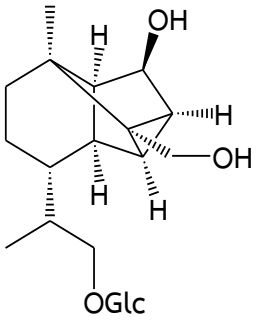

	R_1	R_2
Dendronobiloside C [**278**]	$-CH_2OGlc$	H
Dendronobiloside D [**279**]	H	$-CH_2OGlc$

Dendronobiloside E [**280**]

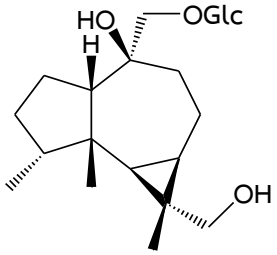

Dendroside A [**281**]

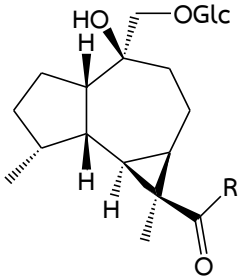

Dendroside B [**282**] R = OGlc

Dendroside C [**283**] R = OH

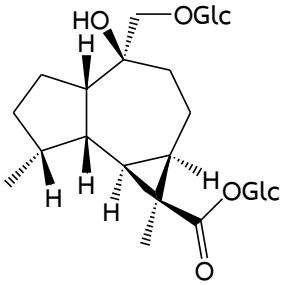

Dendroside D [**284**]

Figure 5 (continued)

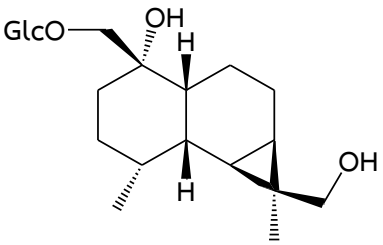

Dendroside E [**285**]

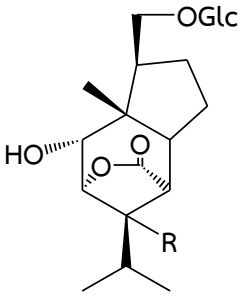

Dendroside F [**286**] R = H

Dendroside G [**287**] R = OH

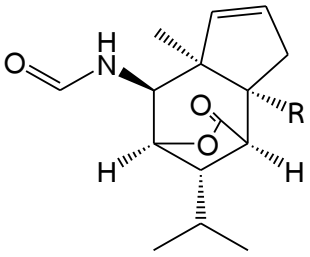

Dendroterpene A [**288**] R = H

Dendroterpene B [**289**] R = OH

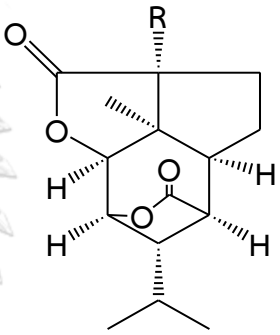

Dendroterpene C [**290**] R = H

Dendroterpene D [**291**] R = OH

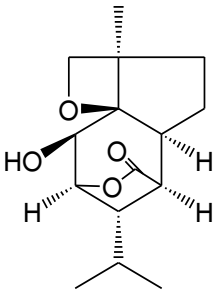

Dendroterpene E [**292**]

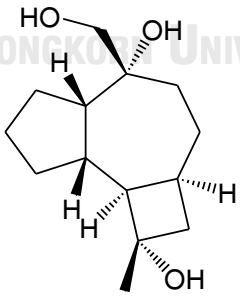

Dendrowardol A [**293**]

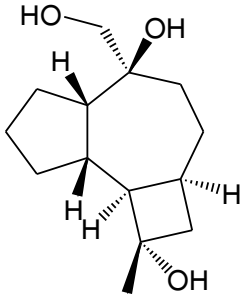

Dendrowardol B [**294**]

Figure 5 (continued)

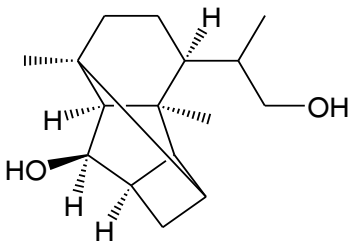

Dendrowardol C [**295**]

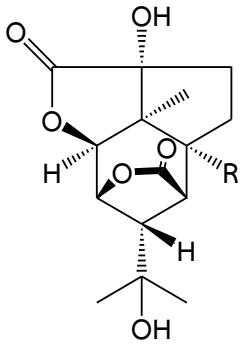

Dendrowillin A [**296**] R = OH

Dendrowillin B [**297**] R = H

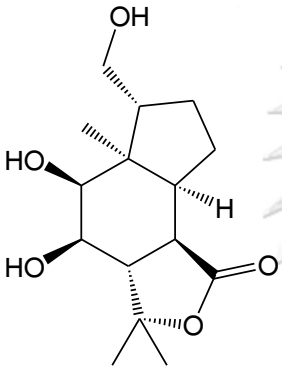

Findlayanin [**298**]

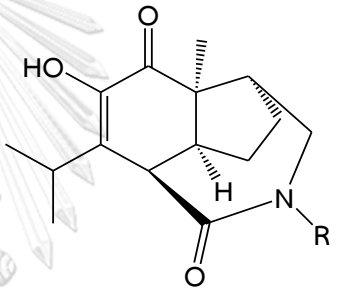

Findlayine A [**299**] R = Me

Findlayine B [**300**] R = H

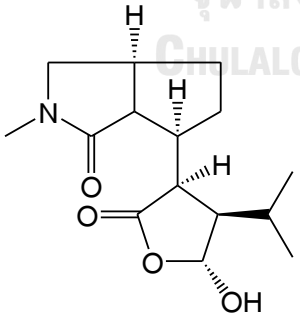

Findlayine C [**301**]

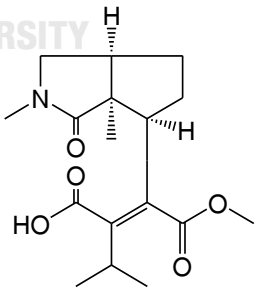

Findlayine D [**302**]

Figure 5 (continued)

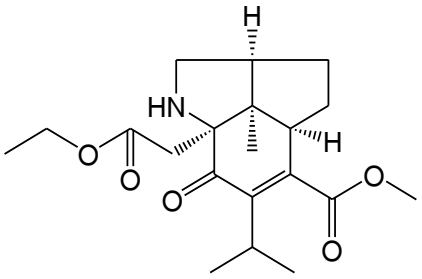

Findlayine E [**303**]

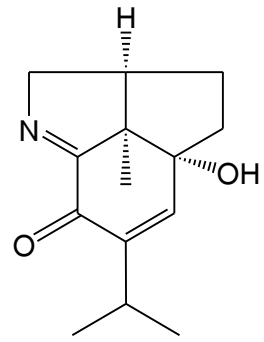

Findlayine F [**304**]

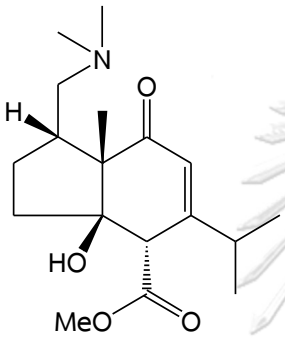

Moniline [**305**]

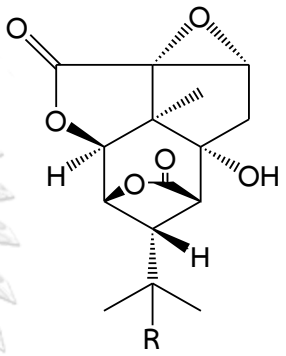

(-)-Picrotin [**306**] R = OH

α-Dihydropicrotoxinin [**307**] R = H

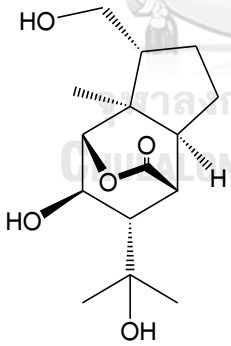

(+)-(1*R*,2*S*,3*R*,4*S*,5*R*,6*S*,9*R*)-3,11,12-Trihydroxypicrotoxane-2(15)-lactone [**308**]

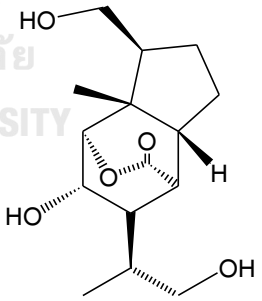

(-)-(1*S*,2*R*,3*S*,4*R*,5*S*,6*R*,9*S*,12*R*)-3,11,13-Trihydroxypicrotoxane-2(15)-lactone [**309**]

Figure 5 (continued)

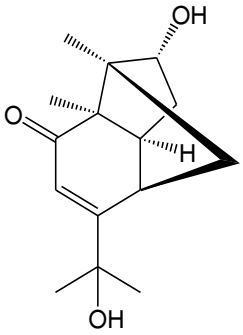

(+)-(1*R*,5*R*,6*S*,8*R*,9*R*)-8,12-Dihydroxycopacamphan-3-en-2-one [**310**]

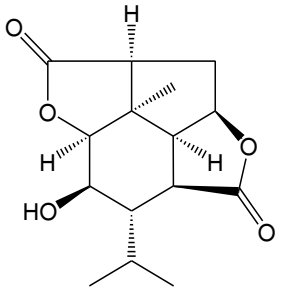

Flakinin A [**311**]

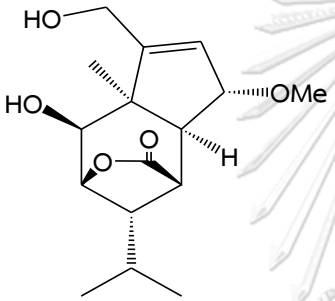

Flakinin B [**312**]

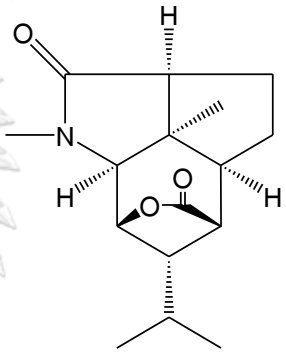

Mubironine A [**313**]

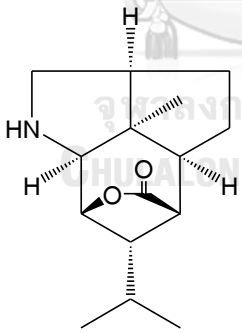

Mubironine B [**314**]

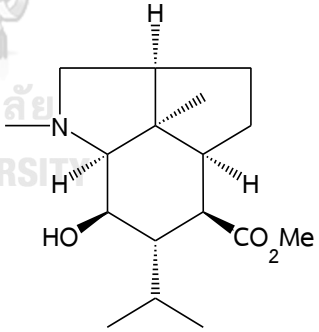

Mubironine C [**315**]

Figure 5 (continued)

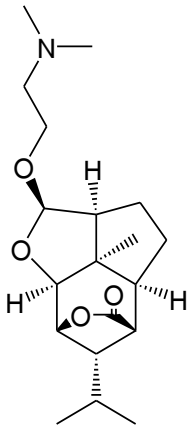

Wardianumine A [**316**]

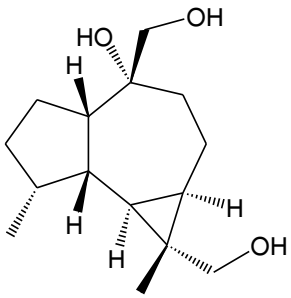

Dendrobiumane A [**317**]

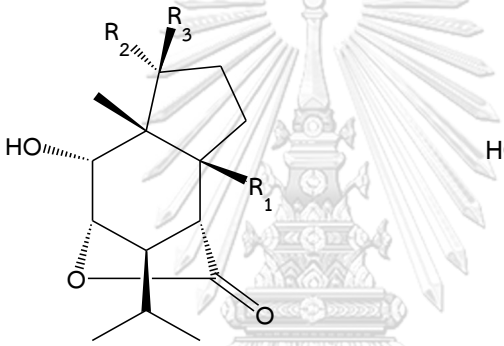

	R_1	R_2	R_3
Dendrobiumane B [**318**]	H	H	CH_2OH
Dendrobiumane D [**320**]	OH	CH_3	OH

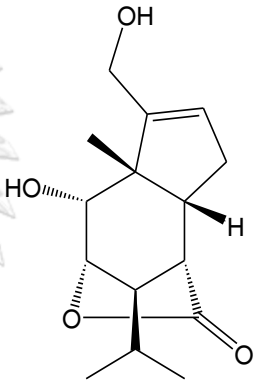

Dendrobiumane C [**319**]

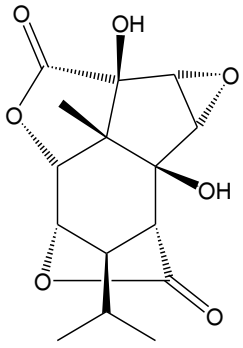

Dendrobiumane E [**321**]

Figure 5 (continued)

Table 6 Alkaloid derivatives of *Dendrobium* species

Alkaloid derivatives			
Phytochemical	**Plant**	**Plant part**	**Reference**
Crepidine [**322**]	*D. crepidatum*	Stem	(Xu *et al.*, 2019)
(+)-Homocrepidine A [**323**]	*D. crepidatum*	Stem	(Hu *et al.*, 2016)
(-)-Homocrepidine A [**324**]	*D. crepidatum*	Stem	(Hu *et al.*, 2016)
Homocrepidine B [**325**]	*D. crepidatum*	Stem	(Hu *et al.*, 2016)
Crepidamine [**326**]	*D. crepidatum*	Stem	(Xu *et al.*, 2019)
Crepidatumine A [**327**]	*D. crepidatum*	Stem	(Xu *et al.*, 2020)
Crepidatumine B [**328**]	*D. crepidatum*	Stem	(Xu *et al.*, 2020)
Crepidatumine C [**329**]	*D. crepidatum*	Stem	(Xu *et al.*, 2019)
Crepidatumine D [**330**]	*D. crepidatum*	Stem	(Xu *et al.*, 2019)
(+)-Dendrocrepidamine A [**331**]	*D. crepidatum*	Stem	(Hu *et al.*, 2020)
(-)-Dendrocrepidamine A [**332**]	*D. crepidatum*	Stem	(Hu *et al.*, 2020)
Dendrocrepine [**333**]	*D. crepidatum*	Stem	(Xu *et al.*, 2020)
(+)-Isocrepidamine [**334**]	*D. crepidatum*	Stem	(Hu *et al.*, 2020)
(-)-Isocrepidamine [**335**]	*D. crepidatum*	Stem	(Hu *et al.*, 2020)
Dendrocrepidine A [**336**]	*D. crepidatum*	Stem	(Hu *et al.*, 2018)
Dendrocrepidine B [**337**]	*D. crepidatum*	Stem	(Hu *et al.*, 2018)
Dendrocrepidine C [**338**]	*D. crepidatum*	Stem	(Hu *et al.*, 2018)
Dendrocrepidine D [**339**]	*D. crepidatum*	Stem	(Hu *et al.*, 2018)
Dendrocrepidine E [**340**]	*D. crepidatum*	Stem	(Hu *et al.*, 2018)

Table 6 (continued)

Alkaloid derivatives			
Phytochemical	**Plant**	**Plant part**	**Reference**
(+)-Dendrocrepidine F [**341**]	*D. crepidatum*	Stem	(Hu *et al.*, 2018)
(-)-Dendrocrepidine F [**342**]	*D. crepidatum*	Stem	(Hu *et al.*, 2018)
Dendroparine (Anosmine)* [**343**]	*D. anosmum*	Whole plant	(Leander & Lüning, 1968)
	D. parishii	Whole plant	(Hemscheidt & Spenser, 1991; Leander & Lüning, 1968)
	D. nobile	Stem	(Chen *et al.*, 2018)
5,7-Dimethyl-octahydroindolizine (Dendroprimine)* [**344**]	*D. primulinum*	Whole plant	(Lüning & Leander, 1965; Mou *et al.*, 2021)
Cis-dendrochrysine [**345**]	*D. chrysanthum*	Whole plant	(Ekevåg *et al.*, 1973)
Trans-dendrochrysine [**346**]	*D. chrysanthum*	Whole plant	(Ekevåg *et al.*, 1973)
Cis-dendrochrysanine [**347**]	*D. chrysanthum*	Stem	(Yang *et al.*, 2005)
Trans-dendrochrysanine [**348**]	*D. chrysanthum*	Stem	(Yang *et al.*, 2005)

Table 6 (continued)

Alkaloid derivatives			
Phytochemical	**Plant**	**Plant part**	**Reference**
Hygrine [**349**]	*D. primulinum*	Whole plant	(Lüning & Leander, 1965; Mou *et al.*, 2021)
Shihunidine [**350**]	*D. loddigesii*	Stem	(Li *et al.*, 1991; Mou *et al.*, 2021)
Shihunine [**351**]	*D. loddigesii*	Stem	(Li *et al.*, 1991; Mou *et al.*, 2021)
	D. lohohense	Whole plant	(Inubushi *et al.*, 1968)
	D. pierardii	Whole plant	(Elander *et al.*, 1971)
Dihydroshihunine [**352**]	*D. wardianum*	Stem	(Zhang *et al.*, 2017a)
N-cis-p-coumaroyltyramine [**353**]	*D. devonianum*	Stem	(Mou *et al.*, 2021)
N-cis-feruloyltyramine [**354**]	*D. devonianum*	Stem	(Mou *et al.*, 2021)
2,3,4,9-Tetrahydro-1*H*-pyrido[3,4-b]indole-3-carboxylic acid [**355**]	*D. devonianum*	Stem	(Mou *et al.*, 2021)
Pierardine [**356**]	*D. pierardii*	Whole plant	(Elander *et al.*, 1969; Mou *et al.*, 2021)

*represent different names of the same compound

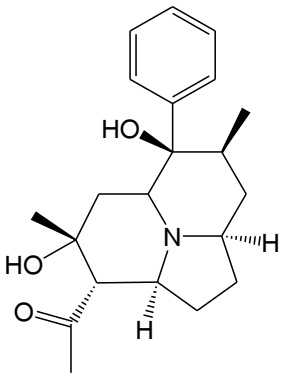

Crepidine [**322**]

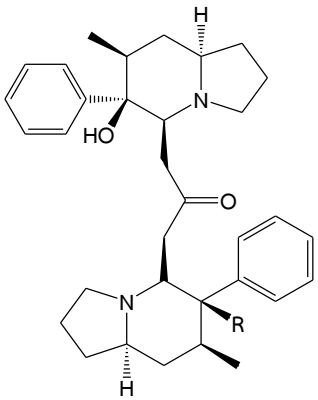

(+)-Homocrepidine A [**323**] R = OH

(+)-Dendrocrepidamine A [**331**] R = H

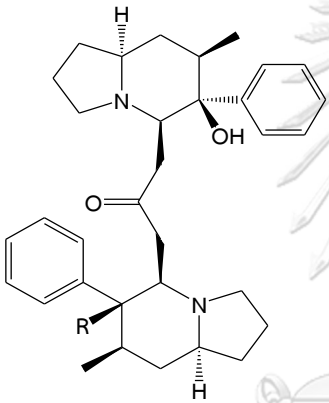

(-)-Homocrepidine A [**324**] R = OH

(-)-Dendrocrepidamine A [**332**] R = H

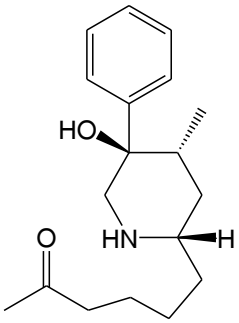

Homocrepidine B [**325**]

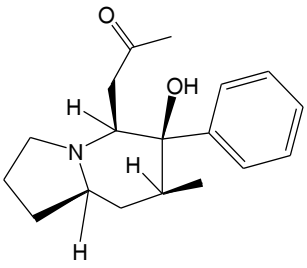

Crepidamine [**326**]

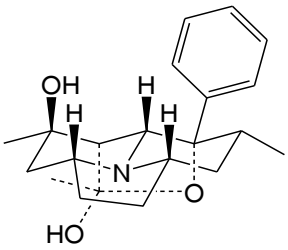

Crepidatumine A [**327**]

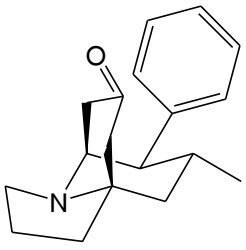

Crepidatumine B [**328**]

Figure 6 Structures of alkaloid derivatives of *Dendrobium* species

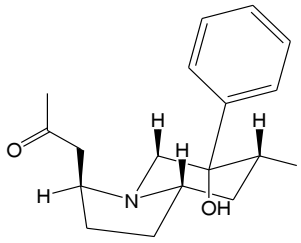

Crepidatumine C [**329**]

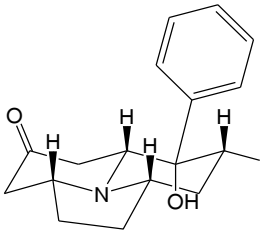

Crepidatumine D [**330**]

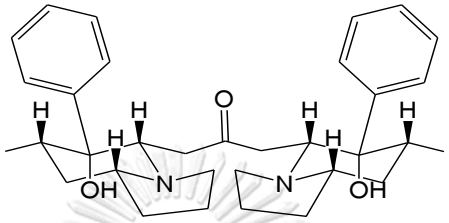

Dendrocrepine [**333**]

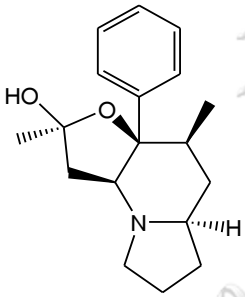

(+)-Isocrepidamine [**334**]

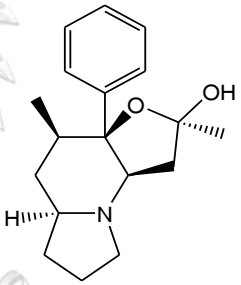

(-)-Isocrepidamine [**335**]

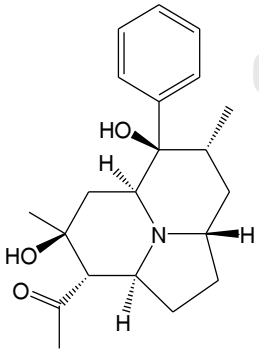

Dendrocrepidine A [**336**]

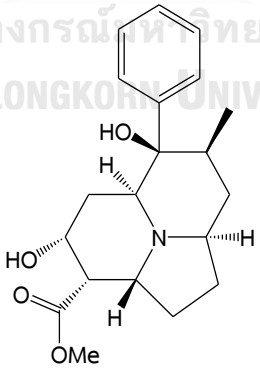

Dendrocrepidine B [**337**]

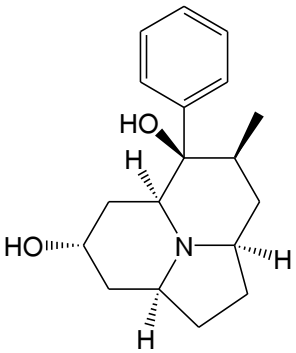

Dendrocrepidine C [**338**]

Figure 6 (continued)

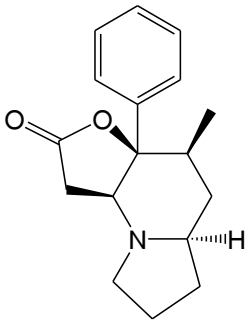

Dendrocrepidine D [**339**]

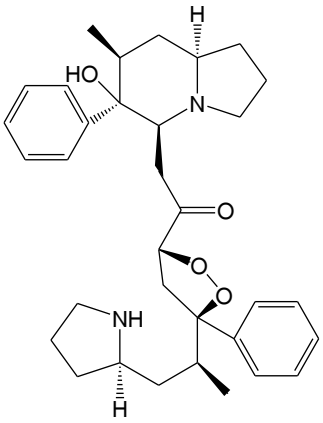

Dendrocrepidine E [**340**]

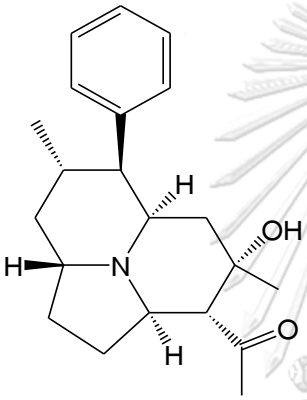

(+)-Dendrocrepidine F [**341**]

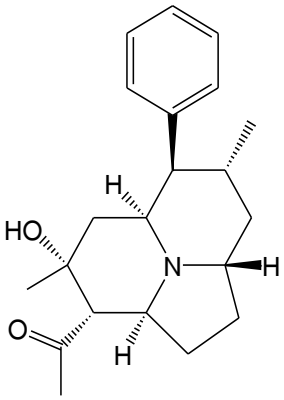

(-)-Dendrocrepidine F [**342**]

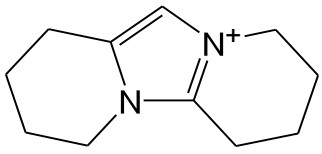

Dendroparine (Anosmine)* [**343**]

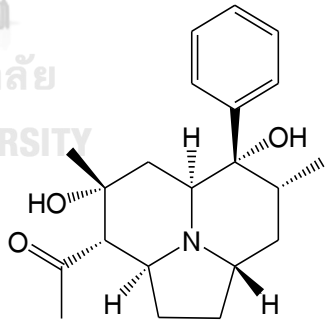

5,7-Dimethyl-octahydroindolizine

(Dendroprimine)* [**344**]

Figure 6 (continued)

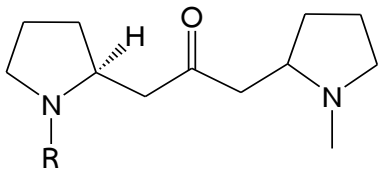

Cis-dendrochrysine [**345**]**:** R = *cis*-cinnmamoyl

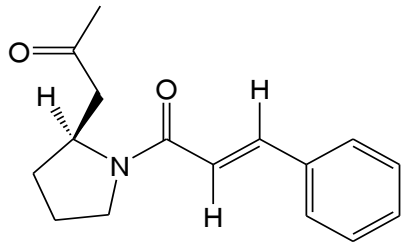

Cis-dendrochrysanine [**347**]

Trans-dendrochrysine [**346**]: R = *trans*-cinnmamoyl

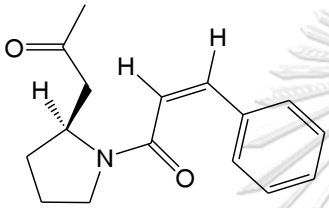

Trans-dendrochrysanine [**348**]

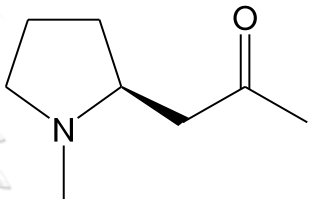

Hygrine [**349**]

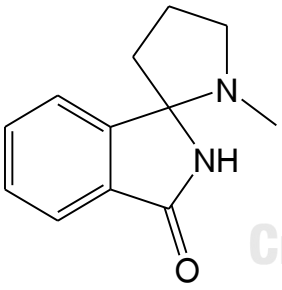

Shihunidine [**350**]

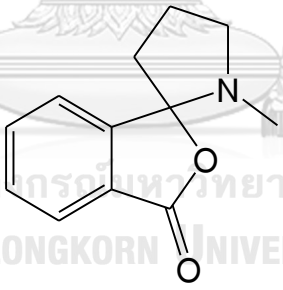

Shihunine [**351**]

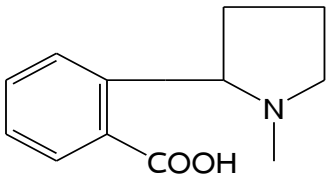

Dihydroshihunine [**352**]

Figure 6 (continued)

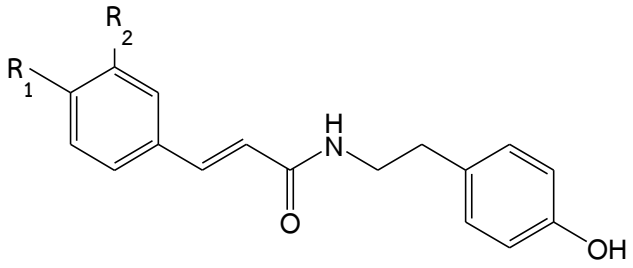

	R_1	R_2
N-cis-p-coumaroyltyramine [**353**]	OH	H
N-cis-feruloyltyramine [**354**]	OH	OMe

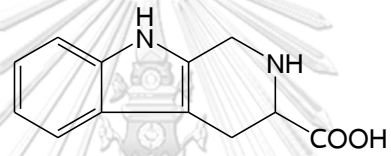

2,3,4,9-Tetrahydro-1*H*-pyrido[3,4-b]indole-3-carboxylic acid [**355**]

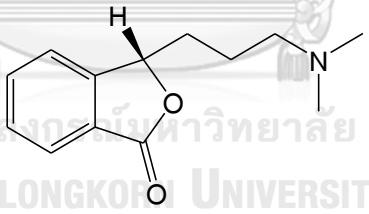

Pierardine [**356**]

Figure 6 (continued)

Table 7 Coumarin derivatives of *Dendrobium* species

Coumarin derivatives			
Phytochemical	**Plant**	**Plant part**	**Reference**
Ayapin [**357**]	*D. densiflorum*	Stem	(Fan *et al.*, 2001)
Coumarin [**358**]	*D. aurantiacum var. denneanum*	Stem	(Yang *et al.*, 2006b)
	D. clavatum var. aurantiacum	Stem	(Chang *et al.*, 2001)
Denthyrsin [**359**]	*D. thyrsiflorum*	Stem	(Zhang *et al.*, 2005)
Dendrocoumarin [**360**]	*D. nobile*	Stem	(Zhou *et al.*, 2018)
Itolide A [**361**]	*D. nobile*	Stem	(Zhou *et al.*, 2018)
Scoparone [**362**]	*D. densiflorum*	Stem	(Fan *et al.*, 2001)
	D. palpebrae	Whole plant	(Kyokong *et al.*, 2019)
	D. thyrsiflorum	Stem	(Zhang *et al.*, 2005)
	D. williamsonii	Whole plant	(Yang *et al.*, 2018b)
Scopoletin [**363**]	*D. densiflorum*	Stem	(Fan *et al.*, 2001)

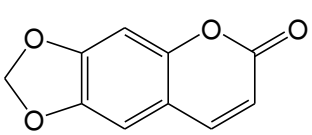

Ayapin [**357**]

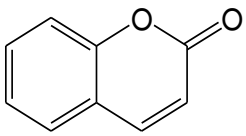

Coumarin [**358**]

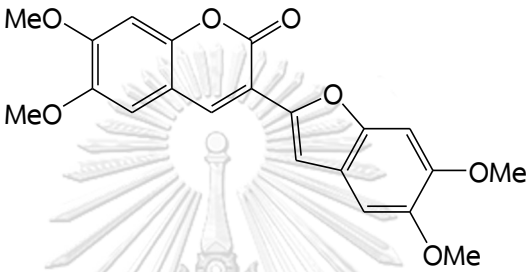

Denthyrsin [**359**]

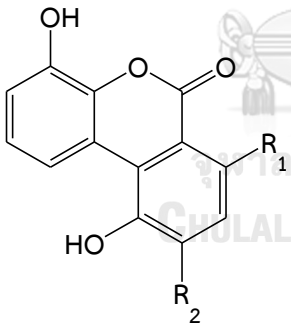

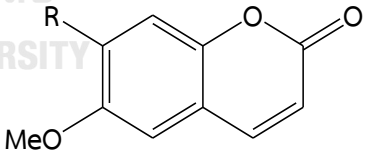

	R_1	R_2		
Dendrocoumarin [**360**]	H	OH	Scoparone [**362**]	R = OMe
Itolide A [**361**]	OH	H	Scopoletin [**363**]	R = OH

Figure 7 Structures of coumarin derivatives of *Dendrobium* species

Table 8 Lignans and neo-lignans of *Dendrobium* species

Lignans and neo-lignans			
Phytochemical	**Plant**	**Plant part**	**Reference**
Acanthoside B [**364**]	*D. chrysanthum*	Stem	(Ye *et al.*, 2004)
Balanophonin [**365**]	*D. williamsonii*	Whole plant	(Yang *et al.*, 2018b)
Balanophonin-4-*O*-β-D-glucopyranoside [**366**]	*D. fimbriatum*	Stem	(Xu *et al.*, 2017)
Ceurusin-4-*O*-β-D-glucopyranoside [**367**]	*D. fimbriatum*	Stem	(Xu *et al.*, 2017)
Denchryside B [**368**]	*D. chrysanthum*	Whole plant	(Ye *et al.*, 2003)
Dehydrodiconiferyl alcohol-4-*O*-β-D-glucoside [**369**]	*D. chrysanthum*	Stem	(Ye *et al.*, 2004)
	D. nobile	Stem	(Zhou *et al.*, 2017)
	D. fimbriatum	Stem	(Xu *et al.*, 2017)
(7*S*,8*R*)-Dehydrodiconiferyl alcohol-9′-β-D-glucopyranoside [**370**]	*D. nobile*	Stem	(Zhou *et al.*, 2017)
(+)-Dendrolactone [**371**]	*D. nobile*	Stem	(Zhou *et al.*, 2016)
Episyringaresinol [**372**]	*D. chrysotoxum*	Stem	(Hu *et al.*, 2012)
	D. longicornu	Stem	(Hu *et al.*, 2008a)
	D. nobile	Stem	(Zhang *et al.*, 2008b)

Table 8 (continued)

Lignans and neo-lignans			
Phytochemical	**Plant**	**Plant part**	**Reference**
Episyringaresinol 4″-*O*-β-D-glucopyranoside [**373**]	*D. moniliforme*	Stem	(Zhao *et al.*, 2003a)
Ficusal-4-*O*-β-D-glucopyranoside [**374**]	*D. fimbriatum*	Stem	(Xu *et al.*, 2017)
Erythro-1-(4-*O*-β-D-glucopyranosyl-3-methoxyphenyl)-2-[4-(3-hydroxypropyl)-2,6-dimethoxyphenoxy]-1,3-propanediol [**375**]	*D. longicornu*	Stem	(Hu *et al.*, 2008a)
7,7′-Bis-(4-hydroxy-3,5-dimethoxyphenyl)-8,8′-dihydroxymethyl-tetrahydrofuran-4-β-D-glucoside [**376**]	*D. chrysanthum*	Whole plant	(Ye *et al.*, 2003)
(-)-(7*S*,8*R*,7′*E*)-4-Hydroxy-3,3′,5,5′-tetramethoxy-8,4′-oxyneolign-7′-ene-7,9,9′-triol-7,9′-bis-*O*-β-D-glucopyranoside [**377**]	*D. aurantiacum var. denneanum*	Stem	(Xiong *et al.*, 2013)

Table 8 (continued)

Lignans and neo-lignans			
Phytochemical	**Plant**	**Plant part**	**Reference**
(-)-(8*R*,7′*E*)-4-Hydroxy-3,3′,5,5′-tetramethoxy-8,4′-oxyneolign-7′-ene-9,9′-diol-4,9-bis-*O*-β-D-glucopyranoside [**378**]	*D. auranticum*	Stem	(Li *et al.*, 2014a)
(-)-(8*S*,7′*E*)-4-Hydroxy-3,3′,5,5′-tetramethoxy-8,4′-oxyneolign-7′-ene-9,9′-diol-4,9-bis-*O*-β-D-glucopyranoside [**379**]	*D. auranticum*	Stem	(Li *et al.*, 2014a)
(-)-(8*R*,7′*E*)-4-Hydroxy-3,3′,5,5′,9′-pentamethoxy-8,4′-oxyneolign-7′-ene-9-ol-4,9-bis-*O*-β-D-glucopyranoside [**380**]	*D. auranticum*	Stem	(Li *et al.*, 2014a)
Liriodendrin [**381**]	*D. aurantiacum var. denneanum*	Stem	(Xiong *et al.*, 2013)
	D. pulchellum	Stem	(Chanvorachote *et al.*, 2013)
Lyoniresinol [**382**]	*D. chrysanthum*	Stem	(Ye *et al.*, 2004)
(-)-Medioresinol [**383**]	*D. loddigesii*	Whole plant	(Ito *et al.*, 2010)

Table 8 (continued)

Lignans and neolignans			
Phytochemical	**Plant**	**Plant part**	**Reference**
(-)-Pinoresinol [**384**]	*D. loddigesii*	Whole plant	(Ito *et al.*, 2010)
(+)-Pinoresinol [**385**]	*D. devonianum*	Stem	(Wu *et al.*, 2019)
Syringaresinol [**386**]	*D. secundum*	Stem	(Sritularak *et al.*, 2011b)
	D. williamsonii	Whole plannt	(Yang *et al.*, 2018b)
Syringaresinol-4-*O*-D-monoglucopyranoside [**387**]	*D. aurantiacum var. denneanum*	Stem	(Xiong *et al.*, 2013)
(-)-Syringaresinol-4,4′-bis-*O*-β-D-glucopyranoside [**388**]	*D. aurantiacum var. denneanum*	Stem	(Xiong *et al.*, 2013)

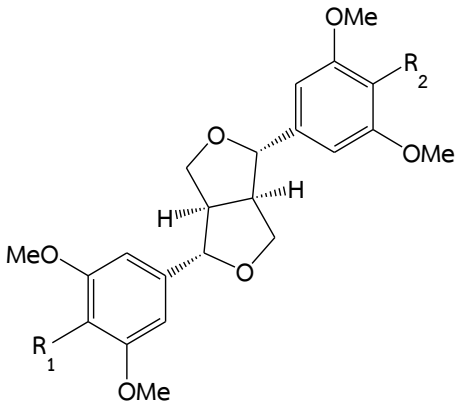

	R_1	R_2
Acanthoside B [**364**]	OGlc	OH
Liriodendrin [**381**]	OGlc	OGlc
Syringaresinol [**386**]	OH	OH

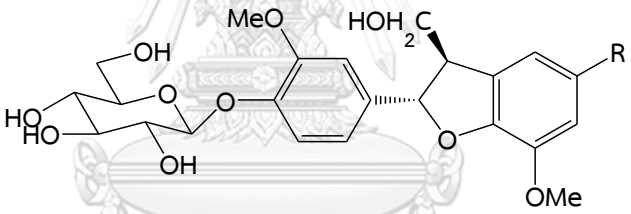

Balanophonin-4-*O*-β-D-glucopyranoside [**366**] R = 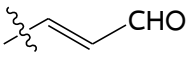

Ceurusin-4-*O*-β-D-glucopyranoside [**367**] R = 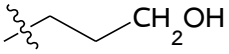

Dehydrodiconiferyl alcohol-4-*O*-β-D-glucoside [**369**] R = 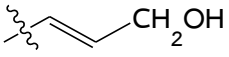

Ficusal-4-*O*-β-D-glucopyranoside [**374**] R = CHO

Figure 8 Structures of lignans and neolignans of *Dendrobium* species

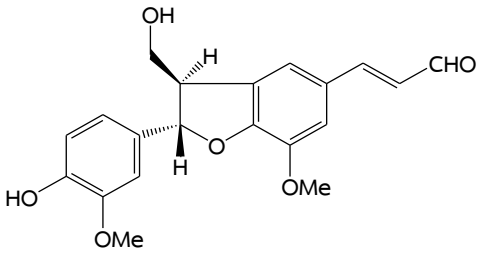

Balanophonin [**365**]

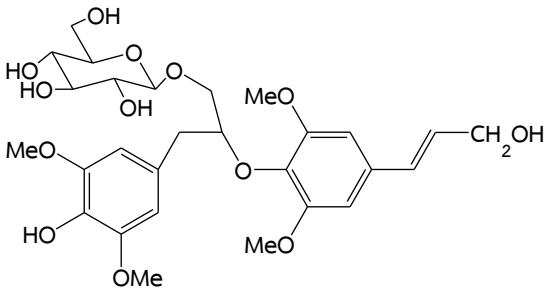

Denchryside B [**368**]

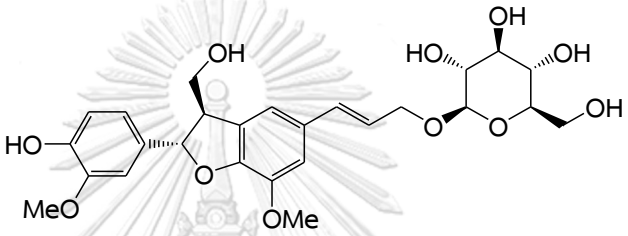

(7*S*,8*R*)-Dehydrodiconiferyl alcohol-9′-β-D-glucopyranoside [**370**]

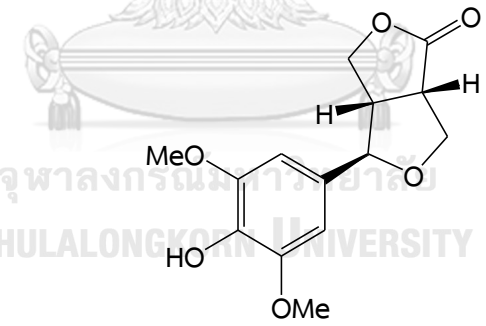

(+)-Dendrolactone [**371**]

Figure 8 (continued)

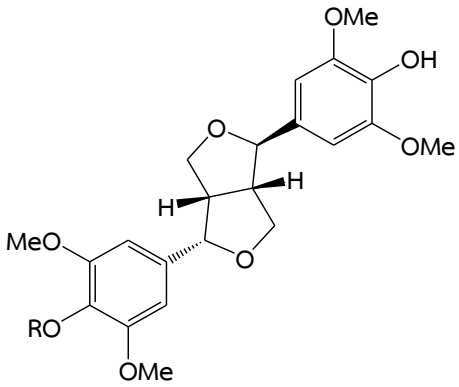

Episyringaresinol [**372**] R = H

Episyringaresinol 4″-*O*-β-D-glucopyranoside [**373**] R = Glc

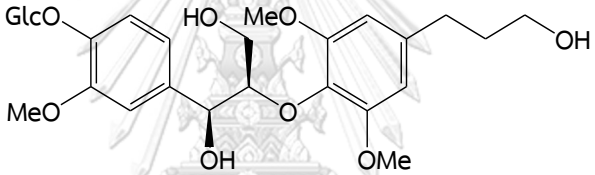

Erythro-1-(4-*O*-β-D-glucopyranosyl-3-methoxyphenyl)-2-[4-(3-hydroxypropyl)-2,6-dimethoxyphenoxy]-1,3-propanediol [**375**]

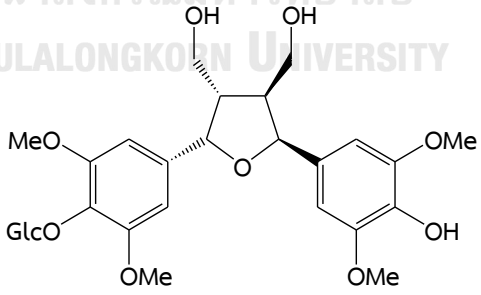

7,7′-Bis-(4-hydroxy-3,5-dimethoxyphenyl)-8,8′-dihydroxymethyl-tetrahydrofuran-4-β-D-glucoside [**376**]

Figure 8 (continued)

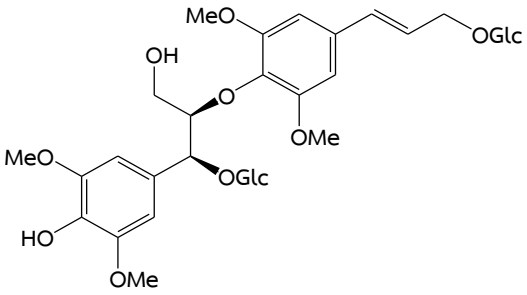

(-)-(7*S*,8*R*,7′*E*)-4-Hydroxy-3,3′,5,5′-tetramethoxy-8,4′-oxyneolign-7′-ene-7,9,9′-triol-7,9′-bis-*O*-β-D-glucopyranoside [**377**]

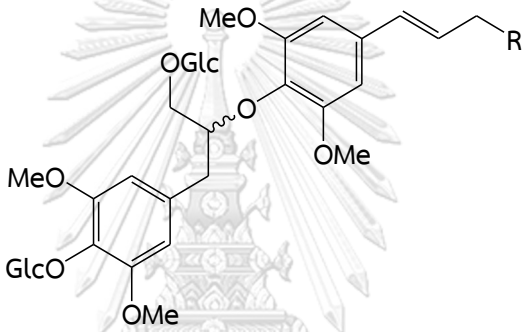

(-)-(8*R*,7′*E*)-4-Hydroxy-3,3′,5,5′-tetramethoxy-8,4′-oxyneolign-7′-ene-9,9′-diol-4,9-bis-*O*-β-D-glucopyranoside [**378**] R = OH; 8R

(-)-(8*S*,7′*E*)-4-Hydroxy-3,3′,5,5′-tetramethoxy-8,4′-oxyneolign-7′-ene-9,9′-diol-4,9-bis-*O*-β-D-glucopyranoside [**379**] R = OH; 8S

(-)-(8*R*,7′*E*)-4-Hydroxy-3,3′,5,5′,9′-pentamethoxy-8,4′-oxyneolign-7′-ene-9-ol-4,9-bis-*O*-β-D-glucopyranoside [**380**] R = OMe; 8R

Figure 8 (continued)

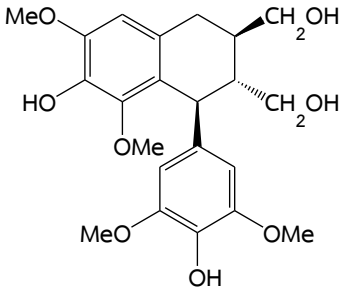

Lyoniresinol [**382**]

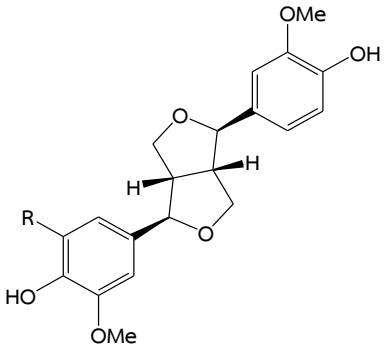

(-)-Medioresinol [**383**] R = OMe

(-)-Pinoresinol [**384**] R = H

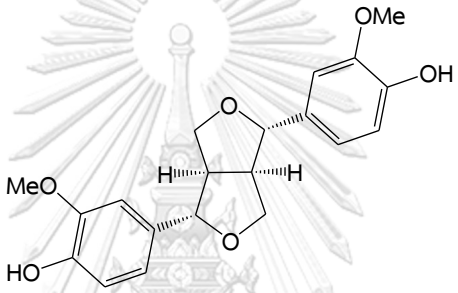

(+)-Pinoresinol [**385**]

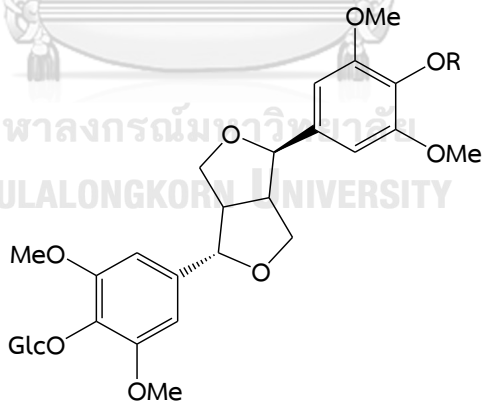

Syringaresinol-4-*O*-D-monoglucopyranoside [**387**] R = H

(-)-Syringaresinol-4,4′-bis-*O*-β-D-glucopyranoside [**388**] R = Glc

Figure 8 (continued)

Table 9 Fluorenone and fluorene derivatives of *Dendrobium* species

Fluorenone and fluorene derivatives			
Phytochemical	**Plant**	**Plant part**	**Reference**
Denchrysan A [**389**]	*D. chrysotoxum*	Whole plant	(Li *et al.*, 2009b)
	D. gibsonii	Whole plant	(Thant *et al.*, 2020)
Denchrysan B [**390**]	*D. brymerianum*	Whole plant	(Klongkumnuankarn *et al.*, 2015)
	D. chrysanthum	Whole plant	(Ye *et al.*, 2003)
Dendroflorin [**391**]	*D. aurantiacum var. denneanum*	Stem	(Yang *et al.*, 2006b)
	D. brymerianum	Whole plant	(Klongkumnuankarn *et al.*, 2015)
	D. palpebrae	Whole plant	(Kyokong *et al.*, 2019)
Dengibsin [**392**]	*D. aurantiacum var. denneanum*	Stem	(Yang *et al.*, 2006b)
	D. chrysanthum	Stem	(Yang *et al.*, 2006a)
	D. chrysanthum	Whole plant	(Li *et al.*, 2009b)
Dengibsinin [**393**]	*D. gibsonii*	Whole plant	(Thant *et al.*, 2020)
Nobilone [**394**]	*D. brymerianum*	Whole plant	(Klongkumnuankarn *et al.*, 2015)
	D. nobile	Stem	(Zhang *et al.*, 2007b)
	D. palpebrae	Whole plant	(Kyokong *et al.*, 2019)
	D. gibsonii	Whole plant	(Thant *et al.*, 2020)

Table 9 (continued)

Fluorenone and fluorene derivatives			
Phytochemical	**Plant**	**Plant part**	**Reference**
1,4,5-Trihydroxy-7-methoxy-9*H*-fluoren-9-one [**395**]	*D. chrysotoxum*	Whole plant	(Chen *et al.*, 2008c)
2,4,7-Trihydroxy-5-methoxy-9-fluorenone [**396**]	*D. chrysotoxum*	Stem	(Yang *et al.*, 2004)
2,4,7-Trihydroxy-1,5-dimethoxy-9-fluorenone [**397**]	*D. chrysotoxum*	Stem	(Yang *et al.*, 2004)
4-Methoxy-9*H*-fluorene-2,5,9-triol [**398**]	*D. chrysotoxum*	Stem	(Yang *et al.*, 2004)
	D. gibsonii	Whole plant	(Thant *et al.*, 2020)
Dihydrodengibsinin [**399**]	*D. gibsonii*	Whole plant	(Thant *et al.*, 2020)
Dendrogibsol [**400**]	*D. gibsonii*	Whole plant	(Thant *et al.*, 2020)

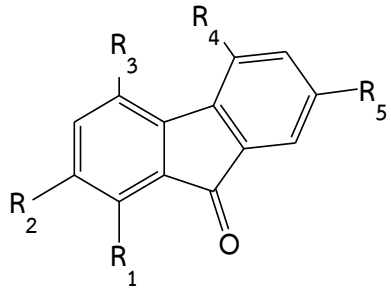

	R_1	R_2	R_3	R_4	R_5
Denchrysan A [**389**]	H	OH	OH	OMe	OH
Dendroflorin [**391**]	OH	H	OH	OMe	OH
Dengibsin [**392**]	H	OH	OMe	OH	H
Nobilone [**394**]	H	OH	H	OMe	OH
1,4,5-Trihydroxy-7-methoxy-9*H*-fluoren-9-one [**395**]	OH	H	OH	OH	OMe
2,4,7-Trihydroxy-5-methoxy-9-fluorenone [**396**]	OMe	OH	OH	H	OH
2,4,7-Trihydroxy-1,5-dimethoxy-9-fluorenone [**397**]	OMe	OH	OH	OMe	OH

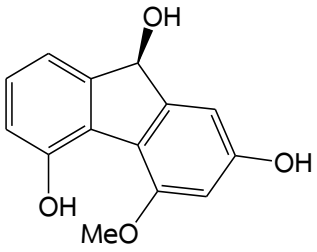

Denchrysan B [**390**]

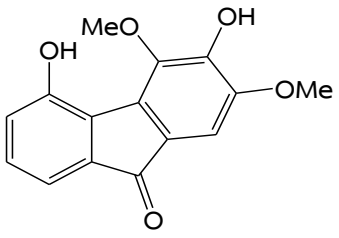

Dengibsinin [**393**]

Figure 9 Structures of fluorenone and fluorene derivatives of *Dendrobium* species

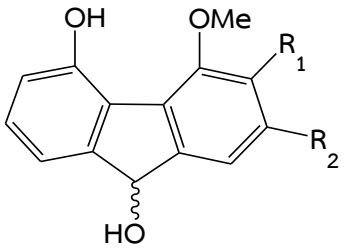

	R_1	R_2
4-Methoxy-9*H*-fluorene-2,5,9-triol [**398**]	H	OH
Dihydrodengibsinin [**399**]	OH	OMe

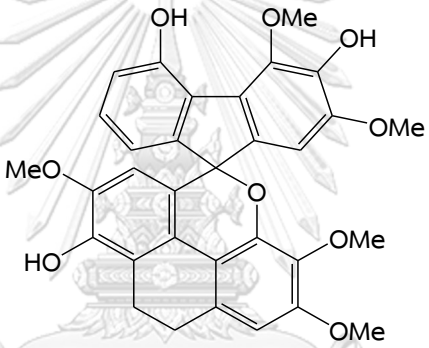

Dendrogibsol [**400**]

Figure 9 (continued)

Table 10 Aliphatic derivatives of *Dendrobium* species

Aliphatic derivatives			
Phytochemical	**Plant**	**Plant part**	**Reference**
Aliphatic acids [**401**]	*D. clavatum var. aurantiacum*	Stem	(Chang *et al.*, 2001)
Aliphatic alcohols [**402**]	*D. clavatum var. aurantiacum*	Stem	(Chang *et al.*, 2001)
Dimethyl malate [**403**]	*D. huoshanense*	Aerial part	(Chang *et al.*, 2010)
Malic acid [**404**]	*D. huoshanense*	Aerial part	(Chang *et al.*, 2010)
Isopentyl butyrate [**405**]	*D. huoshanense*	Aerial part	(Chang *et al.*, 2010)
Dendrodevonic acid A [**406**]	*D. devonianum*	Stem	(Wu *et al.*, 2019)
Dendrodevonic acid B [**407**]	*D. devonianum*	Stem	(Wu *et al.*, 2019)
Decumbic acid A [**408**]	*D. nobile*	Stem	(Zhou *et al.*, 2016)
Decumbic acid B [**409**]	*D. nobile*	Stem	(Zhou *et al.*, 2016)
(-)-Decumbic acid [**410**]	*D. nobile*	Stem	(Zhou *et al.*, 2016)
(-)-Shikimic acid [**411**]	*D. fuscescens*	Whole plant	(Talapatra *et al.*, 1989)
	D. huoshanense	Aerial part	(Chang *et al.*, 2010)
	D. pulchellum	Stem	(Chanvorachote *et al.*, 2013)

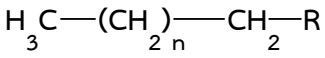

Aliphatic acids [**401**] R=COOH, n=19-31

Aliphatic alcohols [**402**] R=OH, n=22-32

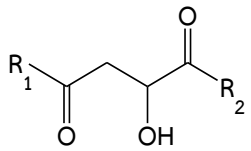

	R_1	R_2
Dimethyl malate [**403**]	OMe	OMe
Malic acid [**404**]	OH	OH

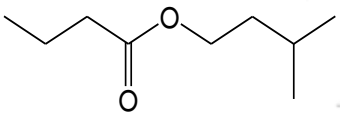

Isopentyl butyrate [**405**]

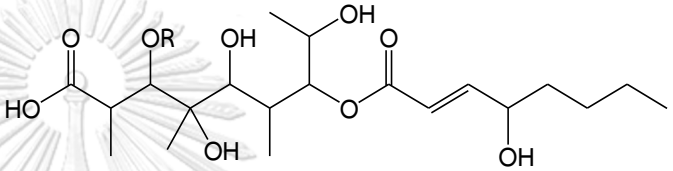

Dendrodevonic acid A [**406**] R = H

Dendrodevonic acid B [**407**] R = $COCH_3$

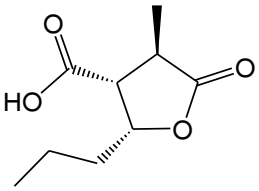

Decumbic acid A [**408**]

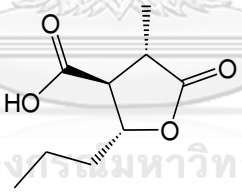

Decumbic acid B [**409**]

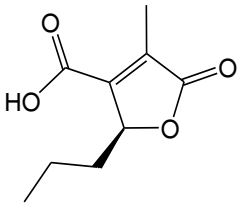

(-)-Decumbic acid [**410**]

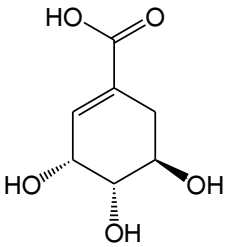

(-)-Shikimic acid [**411**]

Figure 10 Structures of aliphatic derivatives of *Dendrobium* species

Table 11 Phenylpropanoids and phenolic derivatives of *Dendrobium* species

Phenylpropanoids and phenolic derivatives			
Phytochemical	**Plant**	**Plant part**	**Reference**
p-Hydroxybenzoic acid [**412**]	*D. williamsonii*	Whole plant	(Yang *et al.*, 2018b)
3-Hydroxy-2-methoxy-5,6-dimethylbenzoic acid [**413**]	*D. crystallinum*	Stem	(Wang *et al.*, 2009)
Diorcinolic acid [**414**]	*D. christyanum*	Root	(San *et al.*, 2020)
Ferulic acid [**415**]	*D. secundum*	Stem	(Sritularak *et al.*, 2011b)
Gallic acid [**416**]	*D. longicornu*	Whole plant	(Li *et al.*, 2009a)
Phloretic acid [**417**]	*D. ellipsophyllum*	Whole plant	(Tanagornmeatar *et al.*, 2014)
Protocatechuic acid [**418**]	*D. nobile*	Stem	(Ye & Zhao, 2002)
Salicylic acid [**419**]	*D. huoshanense*	Aerial part	(Chang *et al.*, 2010)
	D. williamsonii	Whole plant	(Yang *et al.*, 2018b)
Syringic acid [**420**]	*D. crystallinum*	Stem	(Wang *et al.*, 2009)
Vanillic acid [**421**]	*D. chrysotoxum*	Stem	(Li *et al.*, 2009b)
	D. williamsonii	Whole plant	(Rungwichaniwat *et al.*, 2014)
	D. moniliforme	Whole plant	(Zhao *et al.*, 2016)
	D. devonianum	Whole plant	(Sun *et al.*, 2014)
	D. officinale	Stem	(Ye *et al.*, 2017)

Table 11 (continued)

Phenylpropanoids and phenolic derivatives			
Phytochemical	**Plant**	**Plant part**	**Reference**
Alatusol A [**422**]	*D. hainanense*	Aerial part	(Zhang *et al.*, 2018)
Antiarol [**423**]	*D. chrysotoxum*	Stem	(Hu *et al.*, 2012)
Coniferyl alcohol [**424**]	*D. officinale*	Stem	(Tang *et al.*, 2017)
	D. christyanum	Root	(San *et al.*, 2020)
Dihydroconiferyl alcohol [**425**]	*D. nobile*	Stem	(Wang, 2021; Zhang *et al.*, 2006b)
Salidrosol [**426**]	*D. chrysotoxum*	Stem	(Hu *et al.*, 2012)
(3*R*,3′*S*,4*R*,4′*S*)-3,3′,4,4′-Tetrahydro-6,6′-dimethoxy[3,3′-bi-2*H*-benzopyran]-4,4′-diol [**427**]	*D. williamsonii*	Whole plant	(Yang *et al.*, 2018b)
p-Hydroxybenzaldehyde [**428**]	*D. tortile*	Whole plant	(Limpanit *et al.*, 2016)
(*E*)-Coniferyl aldehyde [**429**]	*D. hainanense*	Aerial part	(Zhang *et al.*, 2018)
Coniferyl aldehyde [**430**]	*D. christyanum*	Root	(San *et al.*, 2020)
Ferulaldehyde [**431**]	*D. longicornu*	Whole plant	(Li *et al.*, 2009a)
Sinapicaldehyde [**432**]	*D. hainanense*	Aerial part	(Zhang *et al.*, 2018)
Methyl 4-hydroxybenzoate [**433**]	*D. williamsonii*	Whole plant	(Yang *et al.*, 2018b)

Table 11 (continued)

Phenylpropanoids and phenolic derivatives			
Phytochemical	**Plant**	**Plant part**	**Reference**
Methyl 2,4-dihydroxy-3,6-dimethylbenzoate [**434**]	*D. christyanum*	Root	(San *et al.*, 2020)
Methyl β-orsellinate [**435**]	*D. longicornu*	Stem	(Li *et al.*, 2009a)
3′,4′,5′-Trimethoxy cinnamyl acetate [**436**]	*D. nobile*	Stem	(Zhou *et al.*, 2016)
n-Triacontyl *p*-hydroxy-*cis*-cinnamate [**437**]	*D. moniliforme*	Stem	(Bi *et al.*, 2004)
Tetratriacontanyl-*trans*-*p*-coumarate [**438**]	*D. williamsonii*	Whole plant	(Rungwichaniwat *et al.*, 2014)
2-(*p*-Hydroxyphenyl) ethyl-*p*-coumarate [**439**]	*D. falconeri*	Stem	(Sritularak & Likhitwitayawuid, 2009)
Tetracosyl (*Z*)-*p*-coumarate [**440**]	*D. falconeri*	Whole plant	(Sritularak & Likhitwitayawuid, 2009)
Dihydroconiferyl dihydro-*p*-coumarate [**441**]	*D. formosum*	Whole plant	(Inthongkaew *et al.*, 2017)
	D. nobile	Stem	(Zhang *et al.*, 2006b)
	D. williamsonii	Whole plant	(Yang *et al.*, 2018b)

Table 11 (continued)

Phenylpropanoids and phenolic derivatives			
Phytochemical	**Plant**	**Plant part**	**Reference**
Alkyl 4′-hydroxy-*trans*-cinnamates [**442**]	*D. clavatum var. aurantiacum*	Stem	(Chang *et al.*, 2001)
n-Docosyl 4-hydroxy-*trans*-cinnamate [**443**]	*D. christyanum*	Root	(San *et al.*, 2020)
Ethyl haematommate [**444**]	*D. longicornu*	Whole plant	(Li *et al.*, 2009a)
Methyl haematommate [**445**]	*D. christyanum*	Root	(San *et al.*, 2020)
Alkyl *trans*-ferulates [**446**]	*D. clavatum var. aurantiacum*	Stem	(Chang *et al.*, 2001)
n-Octacosyl ferulate [**447**]	*D. aurantiacum var. denneanum*	Stem	(Yang *et al.*, 2006b)
	D. moniliforme	Stem	(Bi *et al.*, 2004)
n-Docosyl *trans*-ferulate [**448**]	*D. longicornu*	Whole plant	(Li *et al.*, 2009a)
n-Eicosyl *trans*-ferulate [**449**]	*D. christyanum*	Root	(San *et al.*, 2020)
trans-Tetracosyl ferulate [**450**]	*D. scabrilingue*	Whole plant	(Sarakulwattana *et al.*, 2020)
	D. tortile	Whole plant	(Limpanit *et al.*, 2016)

Table 11 (continued)

Phenylpropanoids and phenolic derivatives			
Phytochemical	**Plant**	**Plant part**	**Reference**
cis-Tetracosanoyl ferulate [**451**]	*D. scabrilingue*	Whole plant	(Sarakulwattana *et al.*, 2020)
cis-Hexacosanoyl ferulate [**452**]	*D. tortile*	Whole plant	(Limpanit *et al.*, 2016)
2-Hydroxy-3-(4-hydroxy-3-methoxyphenyl)-3-methoxypropyl-3-(4-hydroxylphenyl) propanoate [**453**]	*D. hainanense*	Aerial part	(Zhang *et al.*, 2018)
Dendroside [**454**]	*D. nobile*	Stem	(Zhou *et al.*, 2017)
Juniperoside [**455**]	*D. nobile*	Stem	(Zhou *et al.*, 2017)
Koaburaside [**456**]	*D. nobile*	Stem	(Zhou *et al.*, 2017)
cis-Melilotoside [**457**]	*D. aurantiacum var. denneanum*	Stem	(Yang *et al.*, 2007b)
trans-Melilotoside [**458**]	*D. aurantiacum var. denneanum*	Stem	(Yang *et al.*, 2007b)
Dihydromelilotoside [**459**]	*D. aurantiacum var. denneanum*	Stem	(Yang *et al.*, 2007b)
Shashenoside I [**460**]	*D. aurantiacum var. denneanum*	Stem	(Xiong *et al.*, 2013)
Tachioside [**461**]	*D. denneanum*	Stem	(Pan *et al.*, 2012)
Vanilloloside [**462**]	*D. denneanum*	Stem	(Pan *et al.*, 2012)

Table 11 (continued)

Phenylpropanoids and phenolic derivatives			
Phytochemical	**Plant**	**Plant part**	**Reference**
Eugenol-4-*O*-β-D-glucopyranoside [**463**]	*D. fimbriatum*	Stem	(Xu *et al.*, 2017)
threo-7-*O*-Ethyl-9-*O*-(4-hydroxyphenyl) propionyl-guaiacylglycerol [**464**]	*D. loddigesii*	Stem	(Ma *et al.*, 2019b)
Defuscin [**465**]	*D. aurantiacum var. denneanum*	Stem	(Yang *et al.*, 2006b)
Dihydroconiferin [**466**]	*D. fimbriatum*	Stem	(Xu *et al.*, 2017)
Syringin [**467**]	*D. aurantiacum var. denneanum*	Stem	(Xiong *et al.*, 2013)
Vanillin [**468**]	*D. williamsonii*	Whole plant	(Yang *et al.*, 2018b)
	D. christyanum	Root	(San *et al.*, 2020)
4-(3-Hydroxyphenyl)-2-butanone [**469**]	*D. nobile*	Stem	(Zhou *et al.*, 2016)
3-Hydroxy-1-(3-methoxy-4-hydroxyphenyl)-propan-1-one [**470**]	*D. nobile*	Stem	(Zhou *et al.*, 2016)
1-[4-(β-D-Glucopyranosyloxy)-3,5-dimethoxyphenyl]-1-propanone [**471**]	*D. aurantiacum var. denneanum*	Stem	(Xiong *et al.*, 2013)

Table 11 (continued)

Phenylpropanoids and phenolic derivatives			
Phytochemical	**Plant**	**Plant part**	**Reference**
p-Hydroxyphenyl propionic methyl ester [**472**]	*D. aphyllum*	Whole plant	(Chen *et al.*, 2008b)
Di-*p*-hydroxyphenylpropionic acidic-*p*-coumaric acid lactone [**473**]	*D. chrysanthum*	Whole plant	(Cai *et al.*, 2018)

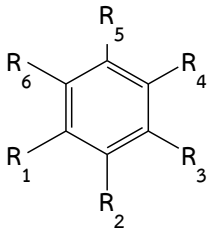

	R_1	R_2	R_3	R_4	R_5	R_6
p-Hydroxybenzoic acid [**412**]	H	OH	H	H	H	COOH
3-Hydroxy-2-methoxy-5,6-dimethylbenzoic acid [**413**]	COOH	CH_3	CH_3	H	OH	OMe
Gallic acid [**416**]	OH	OH	OH	H	COOH	H
Protocatechuic acid [**418**]	H	OH	OH	H	COOH	H
Salicylic acid [**419**]	H	H	H	COOH	OH	H
Syringic acid [**420**]	OMe	OH	OMe	H	COOH	H
Vanillic acid [**421**]	H	OH	OMe	H	COOH	H
Antiarol [**423**]	OMe	OMe	H	OH	H	OMe
p-Hydroxybenzaldehyde [**428**]	OH	H	H	CHO	H	H
Methyl 4-hydroxy benzoate [**433**]	H	H	COOMe	H	H	OH
Methyl-β-orsellinate [**435**]	H	OH	COOMe	CH3	H	OH
Ethyl haematommate [**444**]	H	CH_3	$COOC_2H_5$	OH	CHO	OH

Figure 11 Structures of phenylpropanoids and phenolic derivatives of *Dendrobium* species

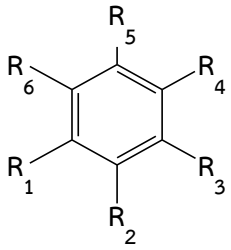

	R_1	R_2	R_3	R_4	R_5	R_6
Vanilloloside [**462**]	-OGlc	H	H	CHO	H	OMe
Vanillin [**468**]	OH	H	H	CHO	H	OMe

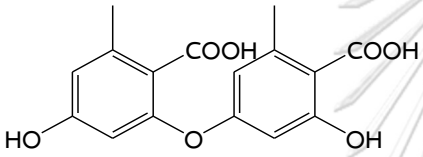

Diorcinolic acid [**414**]

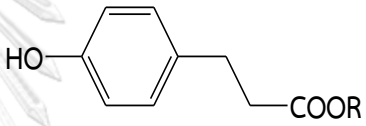

Phloretic acid [**417**] R = H

p-Hydroxyphenyl propionic methyl ester [**472**] R = CH_3

Figure 11 (continued)

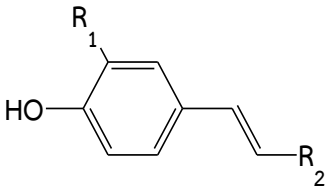

	R_1	R_2	
Ferulic acid [**415**]	OMe	COOH	
n-Triacontyl *p*-hydroxy-*cis*-cinnamate [**437**]	H	COO-$C_{30}H_{61}$	
Tetratriacontanyl-*trans*-*p*-coumarate [**438**]	H	COO-$(CH_2)_{33}CH_3$	
Alkyl 4′-hydroxy-*trans*-cinnamates [**442**]	H	COO-C_nH_{2n+1}	n=22-32
Alkyl *trans*-ferulates [**446**]	OMe	COO-C_nH_{2n+1}	n=18-28,30
n-Octacosyl ferulate [**447**]	OMe	COO-$(CH_2)_{27}CH_3$	
n-Docosyl *trans*-ferulate [**448**]	OMe	COO-$(CH_2)_{21}CH_3$	
trans-Tetracosyl ferulate [**450**]	OMe	COO-$(CH_2)_{23}CH_3$	
Defuscin [**465**]	H	COO-$(CH_2)_{29}CH_3$	

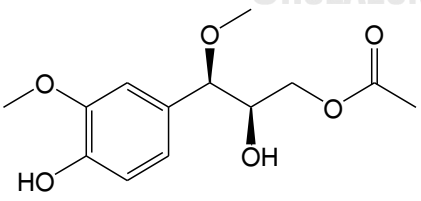

Alatusol A [**422**]

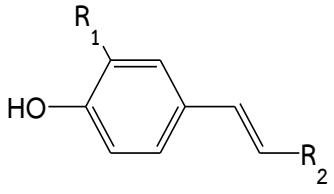

	R_1	R_2
Coniferyl alcohol [**424**]	OMe	OH
Ferulaldehyde [**431**]	OMe	CHO

Figure 11 (continued)

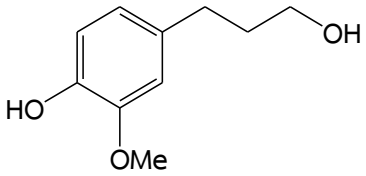

Dihydroconiferyl alcohol [**425**]

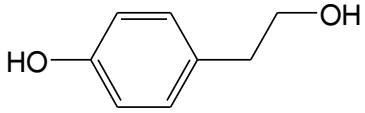

Salidrosol [**426**]

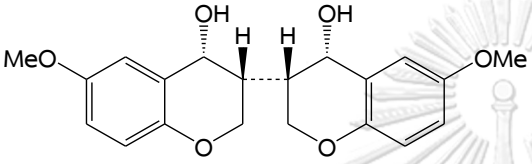

(3*R*,3′*S*,4*R*,4′*S*)-3,3′,4,4′-Tetrahydro-6,6′-dimethoxy[3,3′-bi-2*H*-benzopyran]-4,4′-diol [**427**]

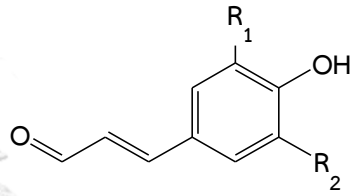

	R_1	R_2
(*E*)-Coniferyl aldehyde [**429**]	H	OMe
Sinapicaldehyde [**432**]	OMe	OMe

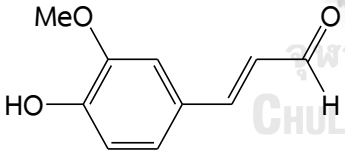

Coniferyl aldehyde [**430**]

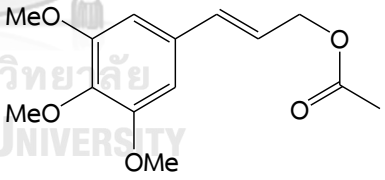

3′,4′,5′-Trimethoxy cinnamyl acetate [**436**]

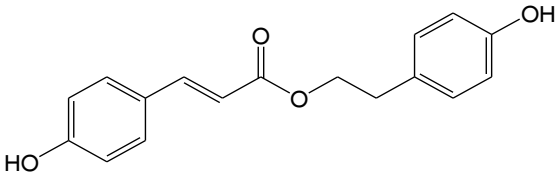

2-(*p*-Hydroxyphenyl) ethyl *p*-coumarate [**439**]

Figure 11 (continued)

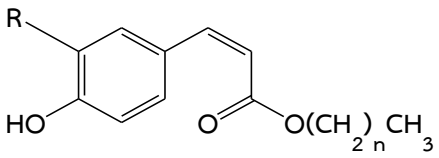

Tetracosyl (*Z*)-*p*-coumarate [**440**] R = H n = 23

cis-Tetracosanoyl ferulate [**451**] R = OMe n = 22

cis-Hexacosanoyl ferulate [**452**] R = OMe n = 25

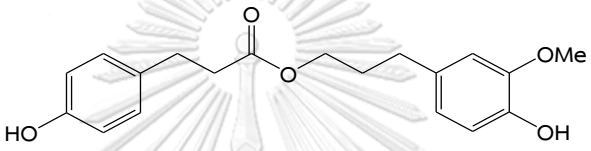

Dihydroconiferyl dihydro-*p*-coumarate [**441**]

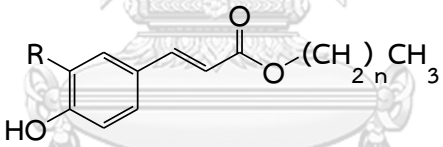

n-Docosyl 4-hydroxy-*trans*-cinnamate [**443**] R = H n = 21

n-Eicosyl *trans*-ferulate [**449**] R = OMe n = 19

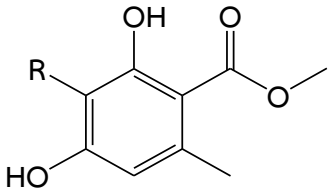

Methyl 2,4-dihydroxy-3,6-dimethylbenzoate [**434**] R = Me

Methyl haematommate [**445**] R = CHO

Figure 11 (continued)

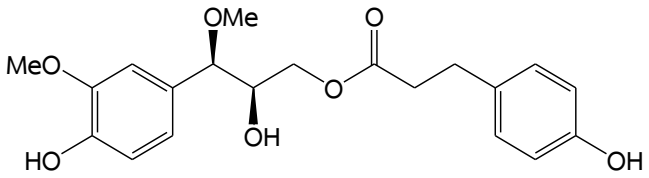

2-Hydroxy-3-(4-hydroxy-3-methoxyphenyl)-3-methoxypropyl-3-(4-hydroxylphenyl)

propanoate [**453**]

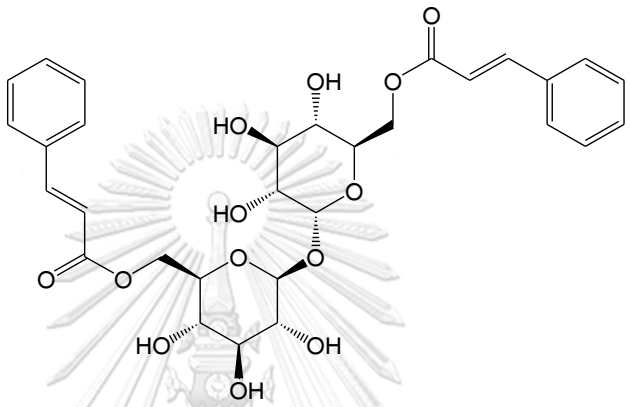

Dendroside [**454**]

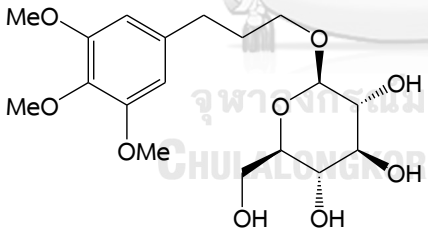

Juniperoside [**455**]

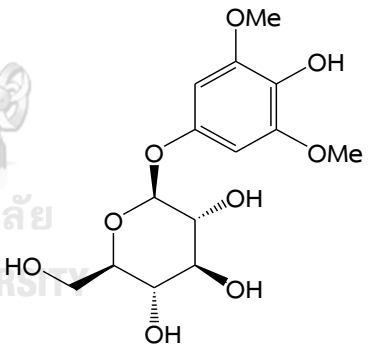

Koaburaside [**456**]

Figure 11 (continued)

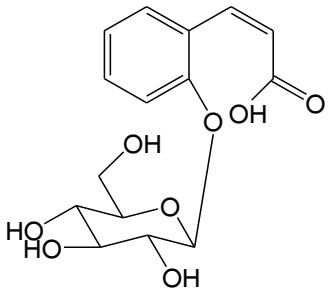

cis-Melilotoside [**457**]

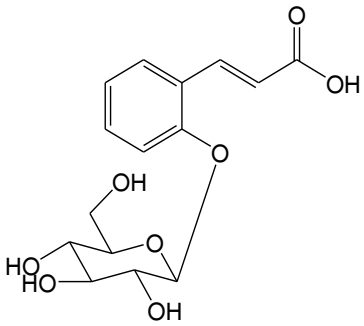

trans-Melilotoside [**458**]

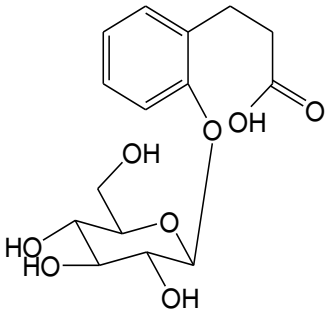

Dihydromelilotoside [**459**]

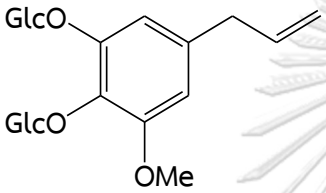

Shashenoside I [**460**]

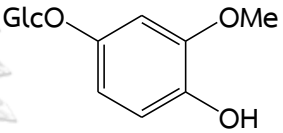

Tachioside [**461**]

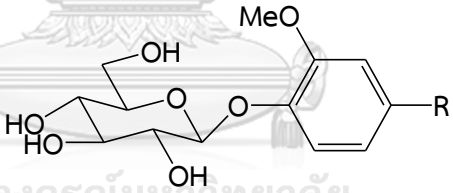

Eugenol-4-*O*-β-D-glucopyranoside [**463**]

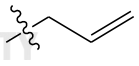

Dihydroconiferin [**466**]

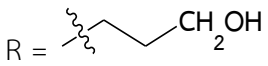

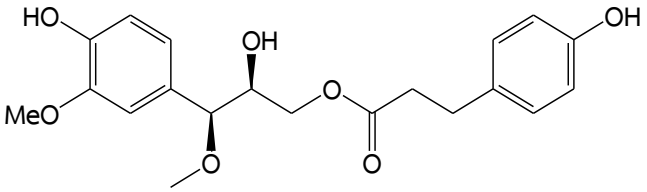

threo-7-*O*-Ethyl-9-*O*-(4-hydroxyphenyl) propionyl-guaiacylglycerol [**464**]

Figure 11 (continued)

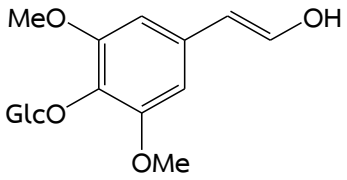

Syringin [**467**]

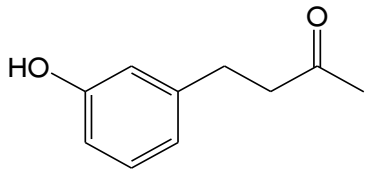

4-(3-Hydroxyphenyl)-2-butanone [**469**]

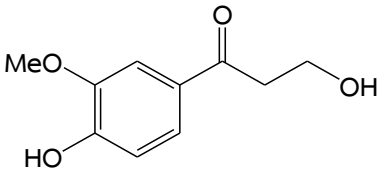

3-Hydroxy-1-(3-methoxy-4-hydroxyphenyl)-propan-1-one [**470**]

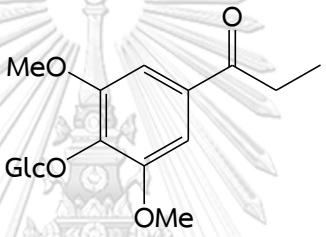

1-[4-(β-D-Glucopyranosyloxy)-3,5-dimethoxyphenyl]-1-propanone [**471**]

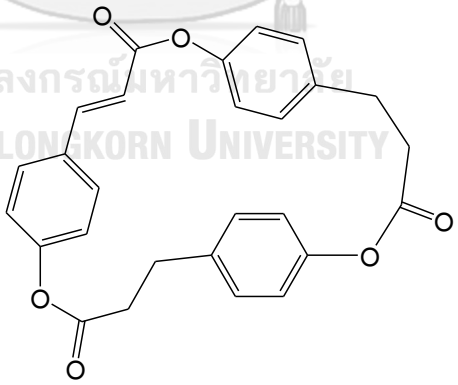

Di-*p*-hydroxyphenylpropionic acidic-*p*-coumaric acid lactone [**473**]

Figure 11 (continued)

Table 12 Miscellaneous compounds of *Dendrobium* species

Miscellaneous compounds			
Phytochemical	**Plant**	**Plant part**	**Reference**
β-Sitosterol [**474**]	*D. williamsonii*	Whole plant	(Yang *et al.*, 2018b)
Daucosterol [**475**]	*D. williamsonii*	Whole plant	(Yang *et al.*, 2018b)
Dehydrovomifoliol [**476**]	*D. loddigesii*	Whole plant	(Ito *et al.*, 2010)
Palmarumycin JC2 [**477**]	*D. crystallinum*	Stem	(Wang *et al.*, 2009)
RF-3192C [**478**]	*D. scabrilingue*	Whole plant	(Sarakulwattana *et al.*, 2020)
3,6,9-Trihydroxy-3,4-dihydroanthracen-1-(2*H*)-one [**479**]	*D. polyanthum*	Stem	(Hu *et al.*, 2009)
5,7-Dihydroxychromen-4-one [**480**]	*D. ellipsophyllum*	Whole plant	(Tanagornmeatar *et al.*, 2014)
4-(2-Hydroxypropyl)-2(5*H*)-furanone [**481**]	*D. tortile*	Whole plant	(Limpanit *et al.*, 2016)
2,6-Dimethoxybenzoquinone [**482**]	*D. chryseum*	Stem	(Ma *et al.*, 1998)
Ergosta-8(9),22-diene-3,5,6,7-tetraol [**483**]	*D. williamsonii*	Whole plant	(Yang *et al.*, 2018b)
3β-Hydroxy-5α,8α-epidioxyergosta-6,9,22-triene [**484**]	*D. williamsonii*	Whole plant	(Yang *et al.*, 2018b)
Stigmast-4-en-3α,6β-diol [**485**]	*D. williamsonii*	Whole plant	(Yang *et al.*, 2018b)

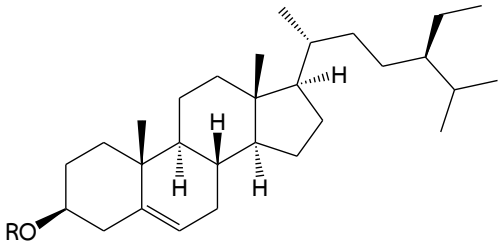

β-Sitosterol [**474**] R = H

Daucosterol [**475**] R = Glc

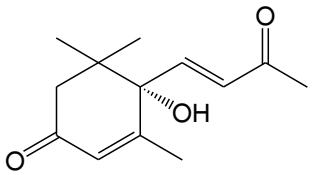

Dehydrovomifoliol [**476**]

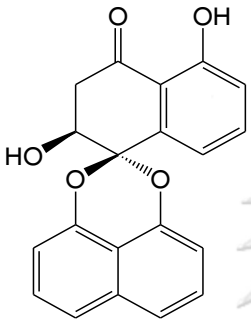

Palmarumycin JC2 [**477**]

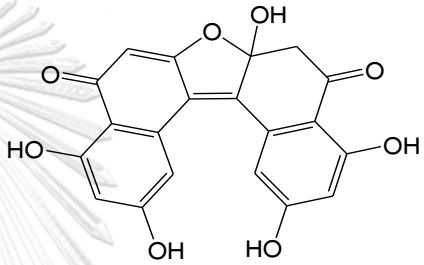

RF-3192C [**478**]

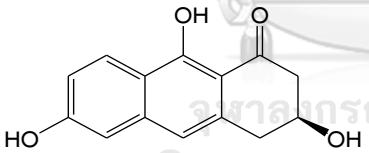

3,6,9-Trihydroxy-3,4-dihydroanthracen-1-(2*H*)-one [**479**]

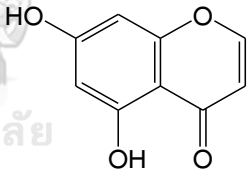

5,7-Dihydroxychromen-4-one [**480**]

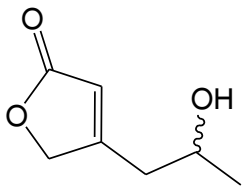

4-(2-Hydroxypropyl)-2(5*H*)-furanone [**481**]

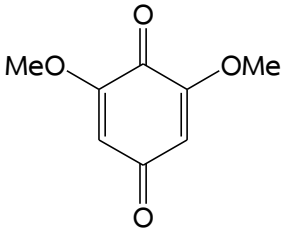

2,6-Dimethoxybenzoquinone [**482**]

Figure 12 Structures of miscellaneous compounds of *Dendrobium* species

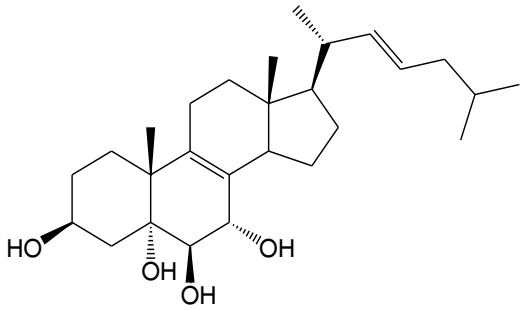

Ergosta-8(9),22-diene-3,5,6,7-tetraol [**483**]

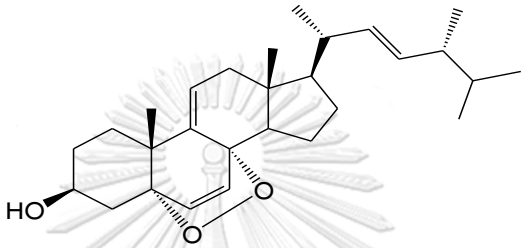

3β-Hydroxy-5α,8α- epidioxyergosta-6,9,22-triene [**484**]

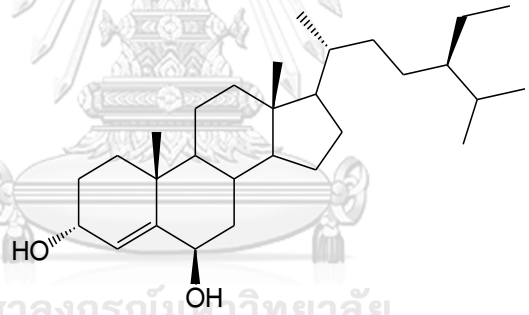

Stigmast-4-en-3α,6β-diol [**485**]

Figure 12 (continued)

1.4 *Dendrobium senile*

The name ‘senile’ of *Dendrobium senile* Parish & Rchb.f comes from the Latin word ‘senex’ which refers to old man due to the presence of its white haired pseudobulb (Covey, 1988). *D. senile* is also known as “Ueang Chanee” in Thailand (Vaddhanaphuti, 2005). It is an epiphytic plant commonly found at 900-1200 m elevated area and is distributed in Myanmar, Laos, Thailand and Vietnam. Long white hairs on the leaf sheaths and golden yellow flowers are also significant morphological characteristics of *D. senile* (Averyanov *et al.*, 2016). *D. senile* has never been investigated for its phytochemicals and biological activities prior to this study. Therefore, the phytochemical investigation of *D. senile* and evaluation for its pancreatic lipase inhibitory activity are the objectives of this research. The finding of 70% inhibition of the ethyl acetate extract of *D. senile* on pancreatic lipase in this study has prompted an attention to the active phytochemicals of *D. senile* as potentially new anti-obesity compounds of botanical origin.

Figure 13 *Dendrobium senile* Par. & Rchb.f.

CHAPTER III

EXPERIMENTAL

1. Source of plant materials

The whole plant of *D. senile* was purchased from Chatuchak market, Bangkok, in July 2017 and the plant identification was performed by Assoc. Prof. Boonchoo Sritularak through comparison with the database of the Botanical Garden Organization. A voucher specimen (BS-DSenile-072560) has been deposited at the Department of Pharmacognosy and Pharmaceutical Botany, Faculty of Pharmaceutical Sciences, Chulalongkorn University.

2. General techniques

2.1 Analytical thin-layer chromatography (TLC)

Silica gel 60 F_{254} precoated plates (E. Merck) were used in normal phase thin-layer chromatography (TLC) and RP C-18 precoated aluminum sheets (Anal Tech) were used in reverse-phase TLC. One-dimensional ascending technique was employed. The analysis was performed at room temperature, and the resulting spots on the TLC plate was visualized under UV light at the wavelengths of 254nm and 365nm.

2.2 Column chromatography

2.2.1 Adsorption column chromatography

Silica gel 60 (Merck, Kieselgel 60, 0.063-0.200 mm) was used as the adsorbent for normal phase vacuum liquid chromatography (VLC). In VLC, the sample was loaded using a dry-packing method. A small amount of adsorbent was added to the sample which was earlier dissolved in a small volume of an appropriate organic solvent. The mixture was then allowed to dry before loading into the column. For open column chromatography (OPC), silica gel 60 (Merck, Kieselgel 60, 0.040-0.063 mm) and C-18 (Merck, Kieselgel 60 RP-18, 40-63 μm) were used as the normal phase and reverse phase adsorbents, respectively. For OPC, a wet packing method was used. The sample was dissolved in a small volume of an

appropriate solvent and slowly applied on top of the column. To prepare a silica gel column, a slurry of silica gel in a suitable solvent was made and poured into a glass column to avoid the formation of air bubbles. For semi-preparative high-performance liquid chromatography (HPLC), the sample was prepared by dissolving in a solvent (mixture) and filtered through a Millipore filter paper before injection. HPLC grade solvents were used as the mobile phase. The maximum injection volume was 1 ml in each analysis and the flow rate was set at 3ml/min. A reverse phase COSMOSIL $5C_{18}$-AR-II (10ID x 250 mm) HPLC column was used with a step gradient of MeOH-H_2O as the mobile phase and a Shimadzu LC-20AD pump. The eluted components were detected using a Shimadzu SPD-20A UV detector. The chromatograms which show series of peaks with respect to the retention time were obtained via a Shimadzu C-R6A Chromatopac recorder. The obtained fractions were examined as described in section 2.1.

2.2.2 Size-exclusion chromatography

In size-exclusion chromatography, the column was packed in a manner similar to that of adsorption column chromatography. Sephadex LH-20 (25-100 μm, GE Healthcare) was used as gel medium. It was allowed to swell in an organic solvent such as methanol or acetone and then tightly packed into the column. The sample was dissolved in an appropriate solvent and loaded into the column as described in section 2.2.1. The resulting fractions were further examined as in section 2.1.

2.3 Spectroscopy

2.3.1 Nuclear Magnetic Resonance (NMR) spectroscopy

^{1}H NMR (300 MHz or 500 MHz) and ^{13}C NMR (75 MHz or 125 MHz) experiments, including and 2-D NMR such as COSY, NOESY, HSQC and HMBC experiments were performed on a Bruker Avance DPX-300 FT-NMR spectrometer (Faculty of Pharmaceutical Sciences, Chulalongkorn University) or a Bruker Avance III HD 500 NMR spectrometer (Scientific and Technology Research Equipment Center,

Chulalongkorn University). Deuterated acetone (acetone-d_6) was used as solvent and the chemical shifts were recorded in ppm.

2.3.2 Mass spectrometry (MS)

Mass spectra were recorded on a Bruker micro TOF mass spectrometer (ESI-MS) (Department of Chemistry, Faculty of Science, Mahidol University and Department of Chemistry, Faculty of Science, Chulalongkorn University).

2.3.3 Ultraviolet (UV) spectroscopy

UV spectra were measured with a Milton Roy Spectronic 3000 Array spectrophotometer (Pharmaceutical Research Instrument Center, Faculty of Pharmaceutical Sciences, Chulalongkorn University).

2.3.4 Infrared (IR) spectroscopy

IR spectra were recorded on a Perkin-Elmer FT-IR 1760X spectrophotometer (Scientific and Technology Research Equipment Center, Chulalongkorn University).

2.4 Solvents

Commercial grade organic solvents were used throughout the experiments and were purified by re-distillation before experiments.

3. Extraction and isolation

3.1 Extraction

The air-dried whole plant of *D. senile* (2.7 kg) was ground and macerated with methanol for a week to give a methanolic extract (212 g) after removal of the solvent by rotary evaporator. The resulting methanolic extract was dissolved in distilled water and then partitioned with ethyl acetate and n-butanol, respectively, in a separatory funnel resulting in an aqueous extract (50 g), an ethyl acetate extract (82 g) and a n-butanol extract (77 g), respectively (**Scheme 1**).

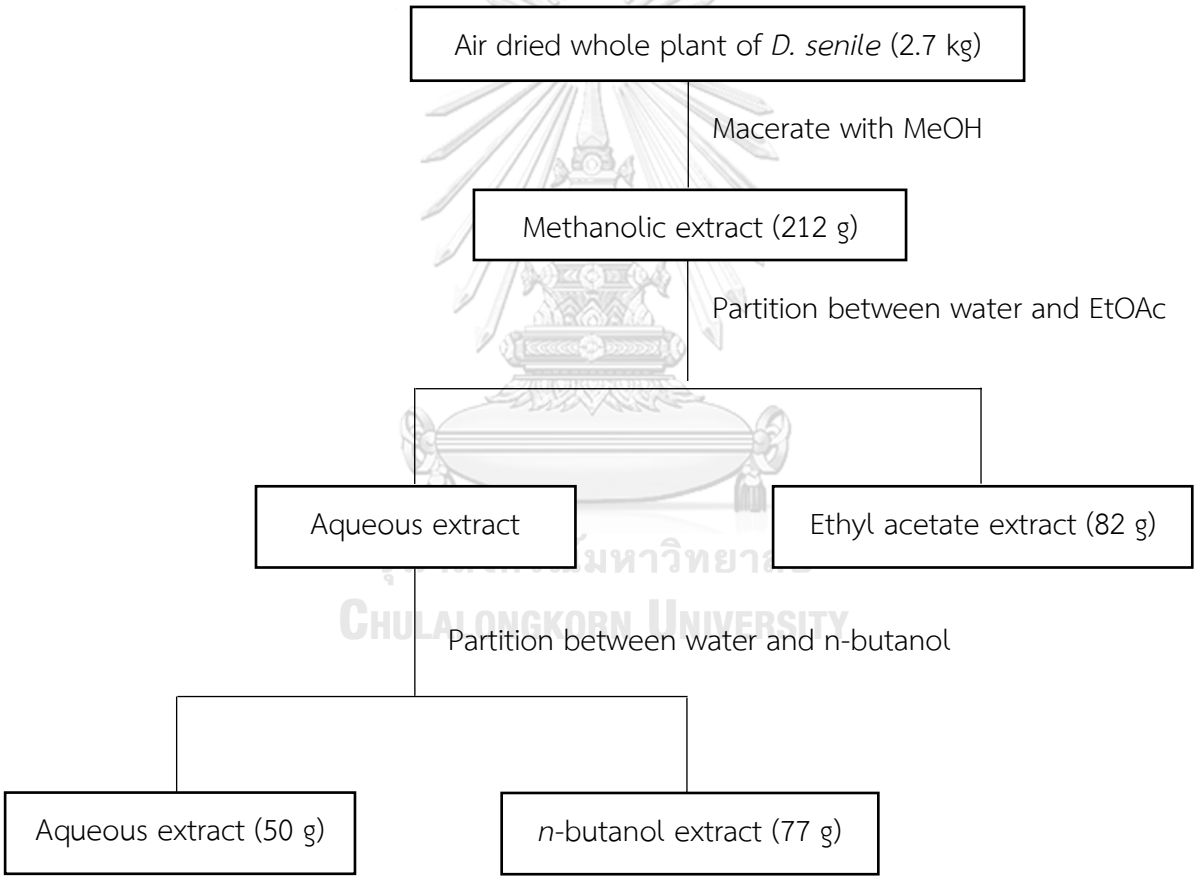

Scheme 1 Extraction of *Dendrobium senile*

3.2 Isolation

The ethyl acetate extract (82 g) was fractionated by vacuum liquid chromatography on silica gel (EtOAc-hexane, gradient) as described in section 2.2.1 to give 5 fractions (A-E) (**Scheme 2**).

3.2.1 Isolation of moscatin

Vacuum-liquid chromatography (see section 2.2.1) of fraction C (6.5 g) on silica gel (acetone-hexane, gradient) was performed to obtain 8 fractions (CI-CVIII). **Compound 2** (moscatin, 254mg) was purified from fraction CIV (193mg) on a Sephadex LH-20 column (acetone) (see section 2.2.2) (**Scheme 2**).

3.2.2 Isolation of 2,5-dihydroxy-4,9-dimethoxyphenanthrene

Separation of fraction CV (746 mg) on a Sephadex LH-20 column (acetone) (see section 2.2.2) resulted in 4 fractions (CV1-CV4). **Compound 3** (11 mg) was isolated after repeated column chromatography of fraction CV1 (307.9 mg) on silica gel (acetone-hexane, gradient and CH_2Cl_2, isocratic) (see section 2.2.1). **Compound 3** was identified as 2,5-dihydroxy-4,9-dimethoxyphenanthrene (**Scheme 2**).

3.2.3 Isolation of moscatilin and aloifol I

Fraction CVI (1.1 g) was separated by column chromatography on silica gel (EtOAc-CH_2Cl_2, gradient) and then on Sephadex LH-20 (acetone) to provide **compound 4** (moscatilin, 523 mg) and **compound 5** (aloifol I, 508 mg) (see section 2.2.2) (**Scheme 2**).

3.2.4 Isolation of 4,4′,8,8′-tetramethoxy[1,1′-biphenanthrene]-2,2′,7,7′-tetrol

Fraction D (15 g) was subjected to column chromatography on silica gel (EtOAc-CH_2Cl_2, gradient) (see section 2.2.1) to yield 8 fractions (DI-DVIII). Separation of fraction DV (1.2 g) on a Sephadex LH-20 column (acetone) (see section 2.2.1) yielded 6 subfractions (DV1-DV6). Fraction DV3 (285 mg) was further separated

by column chromatography on silica gel (acetone-hexane, gradient) (see section 2.2.1) to give 14 fractions (DV3a-DV3n). Through the separation of fraction DV3k (90 mg) on column chromatography (silica gel, acetone-CH_2Cl_2, gradient) and subsequent purification by semi-preparative HPLC (C-18, water-methanol, gradient) (see section 2.2.1), **compound 6** (4,4′,8,8′-tetramethoxy[1,1′-biphenanthrene]-2,2′,7,7′-tetrol, 2.3 mg) was isolated (**Scheme 3**).

3.2.5 Isolation of 2,5,7-trihydroxy-4-methoxyphenanthrene

Repeated column chromatography (silica gel, acetone-CH_2Cl_2, gradient) (see section 2.2.1) of fraction DV5 (130 mg) was performed to give 3 fractions (DV5a- DV5c). Fraction DV5b was further purified on a Sephadex LH-20 column (acetone) (see section 2.2.2) to furnish **compound 1** (14 mg). **Compound 1** was structurally characterized as a new phenanthrene derivative, 2,5,7-trihydroxy-4-methoxyphenanthrene (**Scheme 3**).

3.2.6 Isolation of 2,2′,7,7′-tetrahydroxy-4,4′-dimethoxy-1,1′-biphenanthrene and blefomin G

Fraction DV5c (34 mg) was chromatographed on a Sephadex LH-20 column (acetone) (see section 2.2.2) to give 6 fractions (DV5c1-DV5c6). **Compound 7** (2,2′,7,7′-tetrahydroxy-4,4′-dimethoxy-1,1′-biphenanthrene, 7 mg) was obtained from fraction DV5c5. **Compound 8** (5 mg) was purified from fraction DV5c4 (15 mg) by column chromatography (silica gel, MeOH-CH_2Cl_2, gradient) (see section 2.2.2). **Compound 8** was identified as blefomin G (**Scheme 3**).

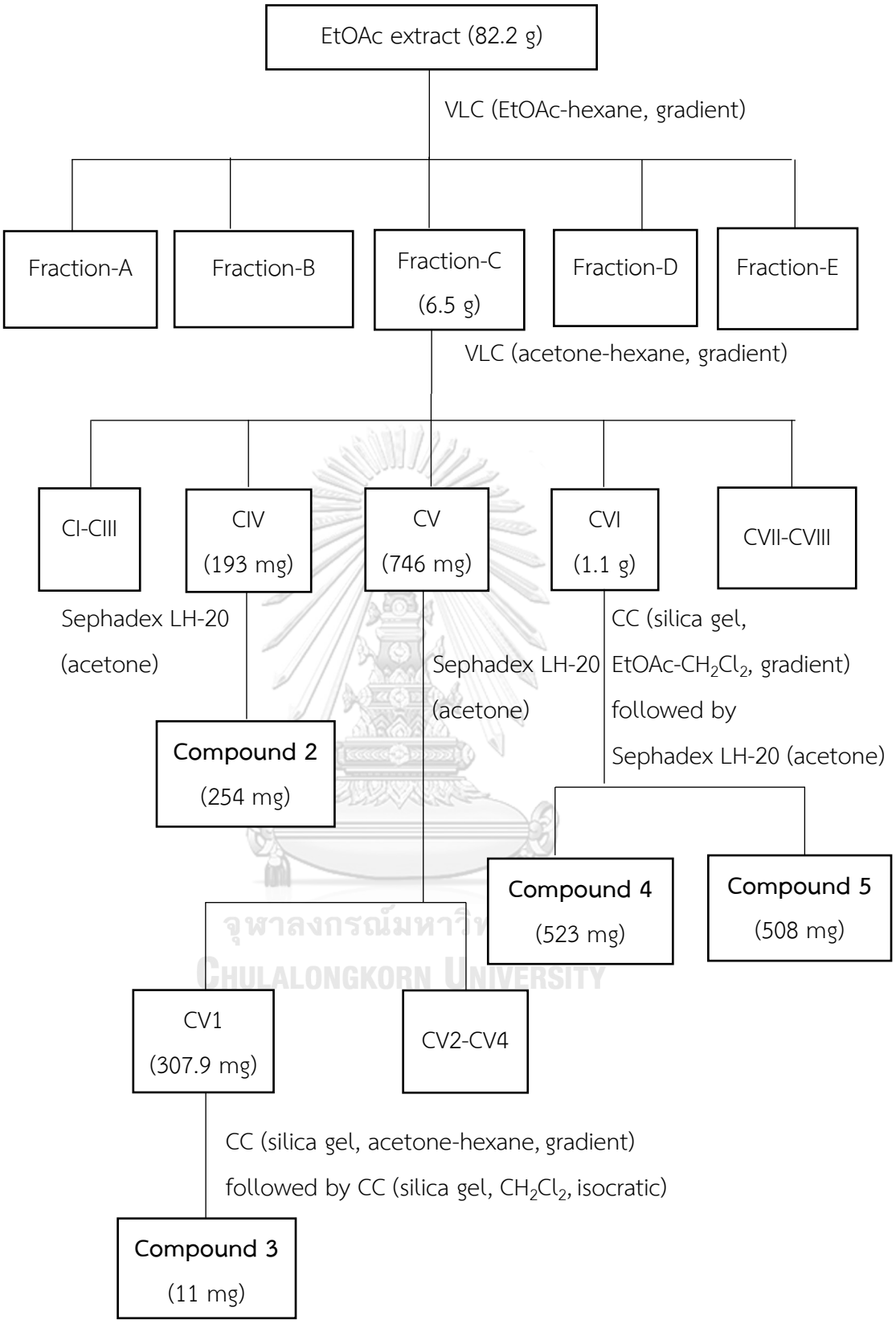

Scheme 2 Isolation of compounds from fraction C of *Dendrobium senile*

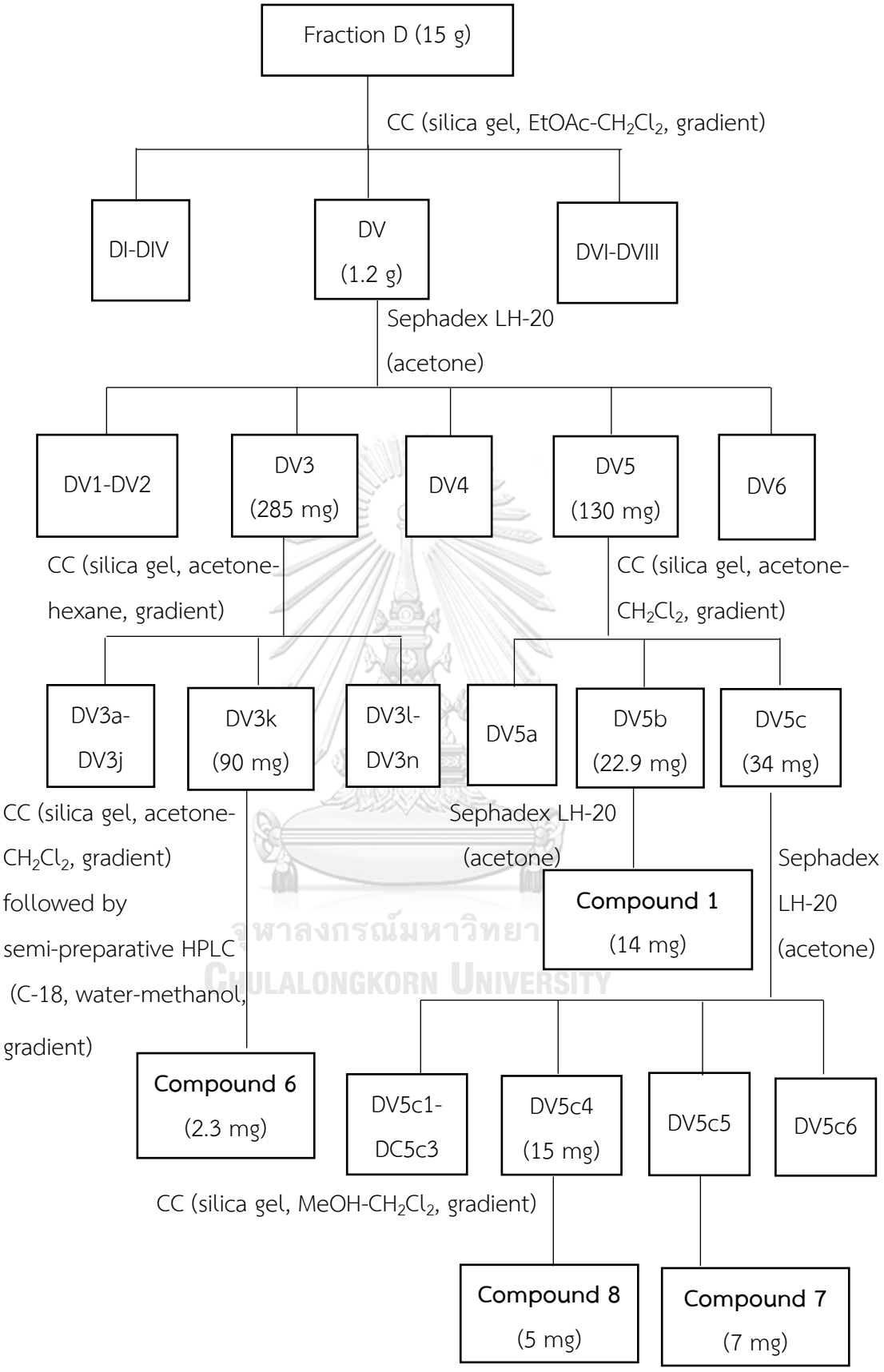

Scheme 3 Isolation of compounds from fraction D of *Dendrobium senile*

4. Physical and spectral data of isolated compounds

4.1 Compound 1 (2,5,7-trihydroxy-4-methoxyphenanthrene)

Compound 1 was obtained as a brown amorphous solid (14 mg, 0.0005 % based on dried weight of whole plant). It was soluble in acetone.

HR-ESI-MS [M-H]$^-$ at *m/z* 255.0663 (calcd. for 255.0657, $C_{15}H_{11}O_4$)

UV (MeOH) λ_{max} (log ε): 205 (4.85), 265 (4.25), 315 (3.52), 360 (3.19) nm

IR (film) ν_{max}: 3281, 2922, 2852, 1709, 1614, 1447, 1431, 1259, 1157 cm^{-1}

^{1}H NMR δ ppm, 300 MHz, acetone-d_6; **Table 13**

^{13}C NMR δ ppm, 75 MHz, acetone-d_6; **Table 13**

4.2 Compound 2 (moscatin)

Compound 2 was obtained as a yellowish-brown amorphous solid (254 mg, 0.0094 % based on dried weight of whole plant). It was soluble in acetone.

HR-ESI-MS [M+Na]$^+$ at *m/z* 263.0682 (calcd. for 263.0684, $C_{15}H_{12}O_3Na$)

^{1}H NMR δ ppm, 300 MHz, acetone-d_6; **Table 14**

^{13}C NMR δ ppm, 75 MHz, acetone-d_6; **Table 14**

4.3 Compound 3 (2,5-dihydroxy-4,9-dimethoxyphenanthrene)

Compound 3 was obtained as a brown amorphous solid (11 mg, 0.0004 % based on dried weight of whole plant). It was soluble in acetone.

HR-ESI-MS [M+Na]$^+$ at *m/z* 293.0758 (calcd. for 293.0789, $C_{16}H_{14}O_4Na$)

^{1}H NMR δ ppm, 300 MHz, acetone-d_6; **Table 15**

^{13}C NMR δ ppm, 75 MHz, acetone-d_6; **Table 15**

4.4 Compound 4 (moscatilin)

Compound 4 was obtained as a pale orange gum (523 mg, 0.0194 % based on dried weight of whole plant). It was soluble in acetone.

HR-ESI-MS $[M+Na]^+$ at *m/z* 327.1221 (calcd. for 327.1208, $C_{17}H_{20}O_5Na$)

^1H NMR δ ppm, 300 MHz, acetone-d_6; **Table 16**

^{13}C NMR δ ppm, 75 MHz, acetone-d_6; **Table 16**

4.5 Compound 5 (aloifol I)

Compound 5 was obtained as a pale-yellow gum (508 mg, 0.0188 % based on dried weight of whole plant). It was soluble in acetone.

HR-ESI-MS $[M+Na]^+$ at *m/z* 297.1113 (calcd. for 297.1103, $C_{16}H_{18}O_4Na$)

^1H NMR δ ppm, 300 MHz, acetone-d_6; **Table 17**

^{13}C NMR δ ppm, 75 MHz, acetone-d_6; **Table 17**

4.6 Compound 6 (4,4′,8,8′-tetramethoxy[1,1′-biphenanthrene]-2,2′,7,7′-tetrol)

Compound 6 was obtained as a red amorphous solid (2.3 mg, 0.0001 % based on dried weight of whole plant). It was soluble in acetone.

HR-ESI-MS $[M+Na]^+$ at *m/z* 561.1530 (calcd. for 561.1525, $C_{32}H_{26}O_8Na$)

^1H NMR δ ppm, 300 MHz, acetone-d_6; **Table 18**

^{13}C NMR δ ppm, 75 MHz, acetone-d_6; **Table 18**

4.7 Compound 7 (2,2′,7,7′-tetrahydroxy-4,4′-dimethoxy-1,1′-biphenanthrene)

Compound 7 was obtained as a brown amorphous solid (7 mg, 0.0003 % based on dried weight of whole plant). It was soluble in acetone.

HR-ESI-MS $[M+Na]^+$ at *m/z* 501.1317 (calcd. for 501.1314, $C_{30}H_{22}O_6Na$)

^{1}H NMR δ ppm, 500 MHz, acetone-d_6; **Table 19**

^{13}C NMR δ ppm, 125 MHz, acetone-d_6; **Table 19**

4.8 Compound 8 (bleformin G)

Compound 8 was obtained as a brown amorphous solid (5 mg, 0.0002 % based on dried weight of whole plant). It was soluble in acetone.

HR-ESI-MS $[M+Na]^+$ at *m/z* 531.1425 (calcd. for 531.1419, $C_{31}H_{24}O_7Na$)

^{1}H NMR δ ppm, 500 MHz, acetone-d_6; **Table 20**

^{13}C NMR δ ppm, 125 MHz, acetone-d_6; **Table 20**

5. Assay for *in vitro* pancreatic lipase inhibitory activity

5.1 Materials and instruments

- Porcine pancreatic lipase enzyme (Sigma-Aldrich)
- 4-Methylumbelliferyl oleate (4-MUO) (Sigma-Aldrich)
- Orlistat (Sigma-Aldrich)
- Calcium chloride (Riedel-De Haen)
- Sodium chloride (Merk)
- Sodium citrate (Merk)
- Tris-base (Sigma-Aldrich)
- Vortex Genie2 mixer (Scientific Industries)
- CLARIOstar Microplate Reader (BMG LABTECH)

5.2 Determination of *in vitro* pancreatic lipase inhibitory activity

This assay measures the fluorescence signal of 4-Methylumbelliferone (4-MU) released after the hydrolytic reaction of 4-Methylumbelliferlyl oleate (4-MUO) substrate by the lipase enzyme using a previously reported method (Inthongkaew *et al.*, 2017). Each test sample was evaluated at the initial concentration of 100 µg/ml. Tris-buffer (13 mM Tris-Base, 150 mM NaCl, 1.3 mM $CaCl_2$, pH 8.0) was used to freshly prepare 0.25 mM of 4-MUO and 0.125 mg/ml of porcine pancreatic lipase, respectively. 20 % DMSO was used to dissolve each test sample and the final concentration of DMSO had no effect on the pancreatic lipase as it did not exceed 5% in each well. Briefly, 25 µl of each test sample, 50 µl of 0.25 mM of 4-MUO and 0.125 mg/ml of porcine pancreatic lipase were added into each well of the 96 well plate, and the mixture was incubated at room temperature for 30 minutes. After incubation, the reaction was terminated by adding 100 µl of 0.1 M sodium citrate (pH 4.2), and the fluorescence signal of 4-MU was rapidly measured at the excitation and emission wavelengths of 355 nm and 460 nm, respectively using a microplate reader. The percentage of pancreatic lipase inhibition was calculated using the following equation:

$$\% \text{ inhibition} = \frac{(F_{control} - F_{control\ blank}) - (F_{sample} - F_{sample\ blank})}{(F_{control} - F_{control\ blank})} \times 100$$

Where $F_{control}$ and $F_{control\ blank}$ represent the fluorescence value of negative control with and without enzyme, and F_{sample} and $F_{sample\ blank}$ refer to the fluorescence value of each test sample with and without enzyme. Orlistat was used as the positive control and evaluated under the same condition as the test samples.

An IC_{50} determination was carried out for the test samples which were active at the concentration of 100 µg/ml. Each experiment was done in triplicate. A linear regression equation was used to analyze the IC_{50} values of active compounds, and the data analysis was done with mean ± SD (n=3).

CHAPTER IV

RESULTS AND DISCUSSION

As described earlier, the dried powder of *Dendrobium senile* was macerated to give a methanolic extract. Then, ethyl acetate, n-butanol and aqueous extracts were obtained after solvent partition of the methanol extract. The ethyl acetate extract was found to be active in the preliminary screening for pancreatic lipase inhibitory activity with more than 70% inhibition at 100 µg/ml and selected for further investigation. Through chromatographic separation, eight compounds were obtained, and their structures were structurally characterized using spectroscopic techniques. All the isolated compounds were then evaluated for *in vitro* pancreatic lipase inhibitory activity, and IC_{50} values were determined for the active compounds.

1. Chemical investigation of isolated compounds of *Dendrobium senile*

The phytochemical investigation of the extract of *D. senile* resulted in the isolation of a new phenanthrene derivative namely 2,5,7-trihydroxy-4-methoxyphenanthrene (**1**), together with seven known compounds including moscatin (**2**), 2,5-dihydroxy-4,9-dimethoxyphenanthrene (**3**), moscatilin (**4**), aloifol I (**5**), 4,4′,8,8′-tetramethoxy[1,1′-biphenanthrene]-2,2′,7,7′-tetrol (**6**), 2,2′,7,7′-tetrahydroxy-4,4′-dimethoxy-1,1′-biphenanthrene (**7**) and blefomin G (**8**) (**Figure 14**).

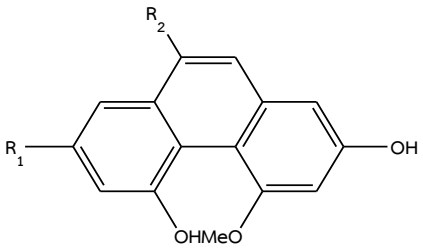

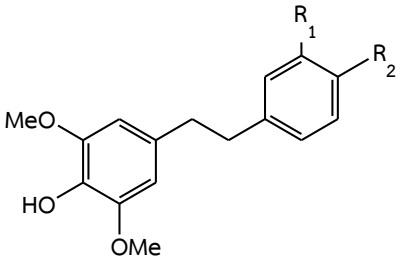

	R_1	R_2		R_1	R_2
2,5,7-trihydroxy-			Moscatilin (**4**)	OMe	OH
4-methoxyphenanthrene (**1**)	OH	H	Aloifol I (**5**)	OH	H
Moscatin (**2**)	H	H			
2,5-dihydroxy-					
4,9-dimethoxyphenanthrene (**3**)	H	OMe			

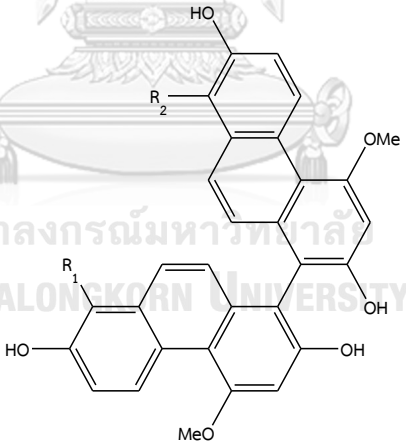

	R_1	R_2
4,4′,8,8′-tetramethoxy[1,1′-biphenanthrene]-2,2′,7,7′-tetrol (**6**)	OMe	OMe
2,2′,7,7′-tetrahydroxy-4,4′-dimethoxy-1,1′-biphenanthrene (**7**)	H	H
Bleformin G (**8**)	H	OMe

Figure 14 Chemical structures of compounds **1-8** of *Dendrobium senile*

1.1 Structural characterization of compound 1

Compound 1 was obtained as a brown amorphous solid. Its molecular formula of $C_{15}H_{12}O_4$ was established by HR-ESI-MS which showed a deprotonated molecular ion peak at *m/z* 255.0663 $[M-H]^-$ (calcd. for 255.0657, $C_{15}H_{11}O_4$) (**Figure 18**). The UV spectrum showed absorption maxima at 205, 265, 315 and 360 nm, indicative of a phenanthrene derivative (**Figure 19**) (Sarakulwattana *et al.*, 2020). The absorptions at 3281 cm^{-1} (OH) and 2922, 1614 cm^{-1} (aromatic rings) in IR spectrum suggested phenolic functional groups (**Figure 20**).

The ^1H NMR spectrum (**Figure 21**) exhibited four *meta*-coupled aromatic protons at δ 6.69 (1H, d, *J* = 2.4 Hz, H-6), δ 6.83 (1H, d, *J* = 2.4 Hz, H-8), δ 6.94 (1H, d, *J* = 2.4 Hz, H-3) and δ 7.01 (1H, d, *J* = 2.4 Hz, H-1), two *ortho*-coupled doublet protons at δ 7.41 (1H, d, *J* = 9.0 Hz, H-10) and δ 7.47 (1H, d, *J* = 9.0 Hz, H-9), a hydroxy proton at δ 9.73 (1H, s) and a methoxy proton signal at δ 4.11 (3H, s). The ^{13}C NMR spectrum of **1** (**Figure 22**) showed fourteen aromatic carbons at δ 102.9 (C-3), 105.6 (C-8), 106.3 (C-6), 108.1 (C-1), 113.5 (C-4b), 114.6 (C-4a), 127.4 (C-10), 129.4 (C-9), 135.9 (C-10a), 136.2 (C-8a), 155.5 (C-4), 156.2 (C-2), 156.7 (C-5), 157.1 (C-7) and a methoxy carbon at δ 58.7. The structure of **1** was further studied by analysis of the HSQC, HMBC and NOESY spectra.

The HSQC spectrum (**Figure 23**) provided single bond correlations between ^1H and ^{13}C atoms. The location of the methoxy group was deduced from the HMBC and NOESY correlations. On ring A, the singlet proton signal at δ 9.73 (s, 5-OH) was assigned from its 2- and 3-bond correlation with C-5 (δ 156.7) and C-6 (δ 106.3), respectively, in the HMBC spectrum (**Figure 24**). The signal for C-4a (δ 114.6) was assigned from its HMBC correlation with H-1, H-3 and H-10. The HMBC correlation of C-4b (δ 113.5) to H-6, H-8 and H-9 were also observed. The assignments of H-9 and H-10 were obtained from HMBC correlations with C-8a (δ 136.2) and C-10a (δ

135.9), respectively. The assignment of H-8 at δ 6.83 was confirmed by its NOESY interaction with H-9 and H-6. On ring B, the attachment of the methoxy group at C-4 was supported by its correlation with H-3 in the NOESY spectrum (**Figure 25**). H-3 and H-10 also showed NOESY correlations to H-1.

Based on the above spectral data, **compound 1** was characterized as a new phenanthrene derivative, 2,5,7-trihydroxy-4-methoxyphenanthrene.

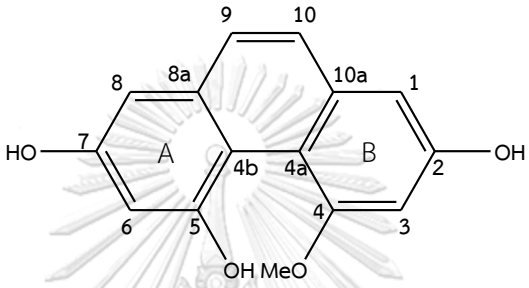

Figure 15 Chemical structure of **compound 1**

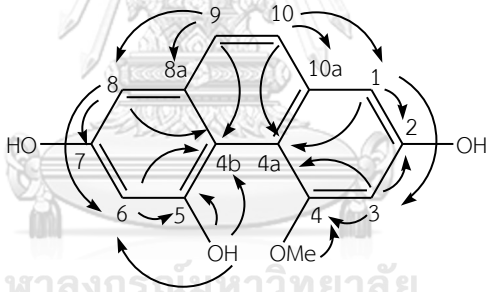

Figure 16 HMBC correlation of **compound 1**

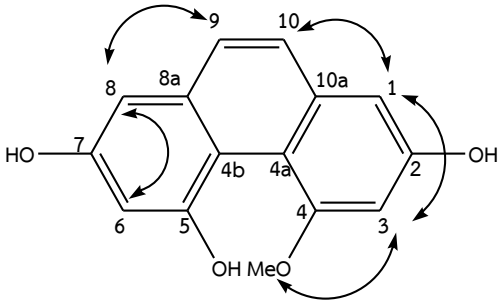

Figure 17 NOESY correlation of **compound 1**

Table 13 ^{1}H (300 MHz) and ^{13}C NMR (75 MHz) spectral data of **compound 1** in acetone-d_6

Position	δ_H in ppm (mult., *J* in Hz)	δ_C in ppm	HMBC (correlation with ^{1}H)
1	7.01 (d, *J* = 2.4 Hz)	108.1	3, 10
2	-	156.2	1*, 3*
3	6.94 (d, *J* = 2.4 Hz)	102.9	1
4	-	155.5	3*, 4-OMe
4a	-	114.6	1, 3, 10
4b	-	113.5	6, 8, 9, 5-OH
5	-	156.7	6*, 5-OH
6	6.69 (d, *J* = 2.4 Hz)	106.3	8, 5-OH
7	-	157.1	6*,8*
8	6.83 (d, *J* = 2.4 Hz)	105.6	6, 9
8a	-	136.2	10
9	7.47 (d, *J* = 9.0 Hz)	129.4	8
10	7.41 (d, *J* = 9.0 Hz)	127.4	1
10a	-	135.9	9
4-OMe	4.11 (s)	58.7	-
5-OH	9.73 (s)	-	-

* represent two-bond coupling

Mass Spectrum List Report

Analysis Info

Analysis Name	D:\Data\Data Service\201012\Chanee 13a_RA5_01_4712.d	Acquisition Date	10/19/2020 4:55:44 PM
Method	nv_neg_5min_profile_190214.m	Operator	CU.
Sample Name	Chanee 13a	Instrument / Ser#	micrOTOF-Q II 10335
Comment			

Acquisition Parameter

Source Type	ESI	Ion Polarity	Negative	Set Nebulizer	3.0 Bar
Focus	Not active	Set Capillary	2500 V	Set Dry Heater	200 ℃
Scan Begin	100 m/z	Set End Plate Offset	-500 V	Set Dry Gas	8.0 l/min
Scan End	1500 m/z	Set Collision Cell RF	250.0 Vpp	Set Divert Valve	Waste

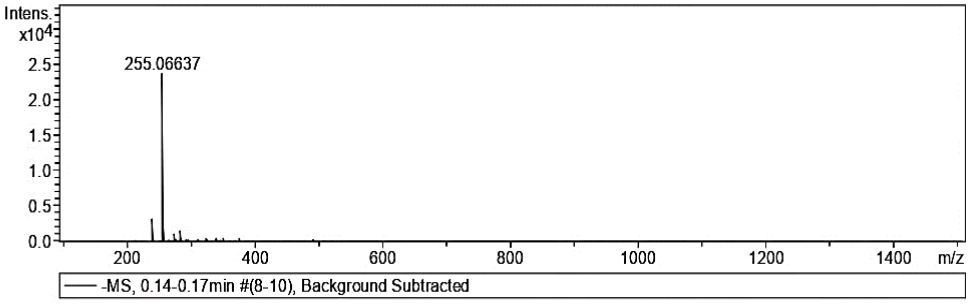

Figure 18 HR-ESI-MS spectrum of **compound 1**

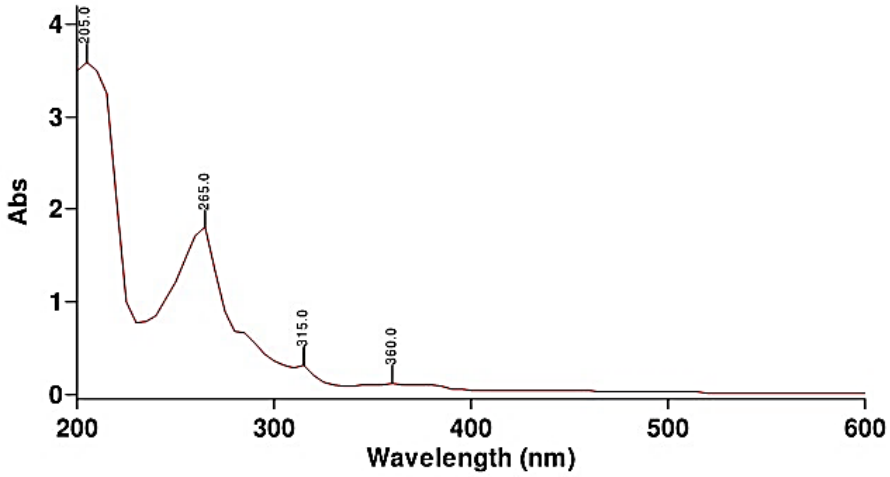

Figure 19 UV spectrum of **compound 1**

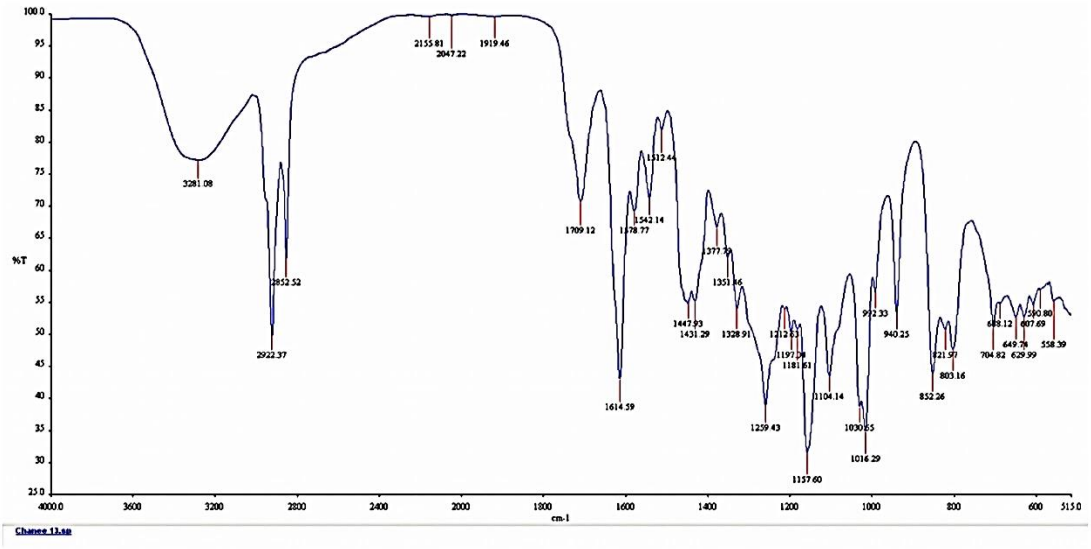

Figure 20 IR spectrum of **compound 1**

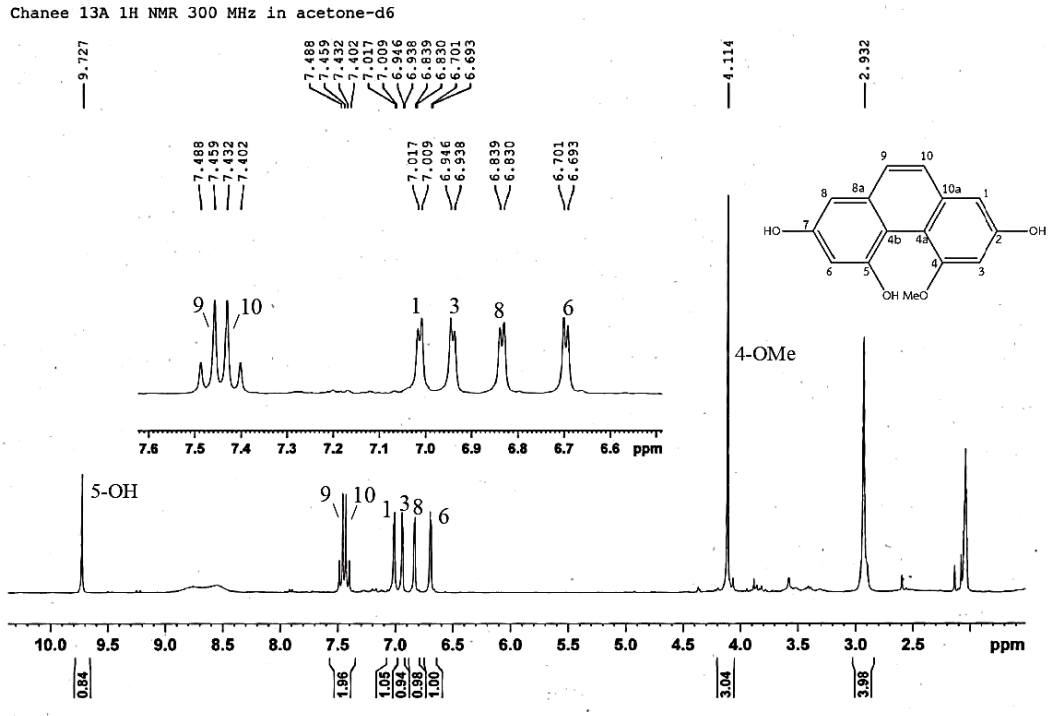

Figure 21 ^{1}H NMR spectrum of **compound 1** (300 MHz) in acetone-d_6

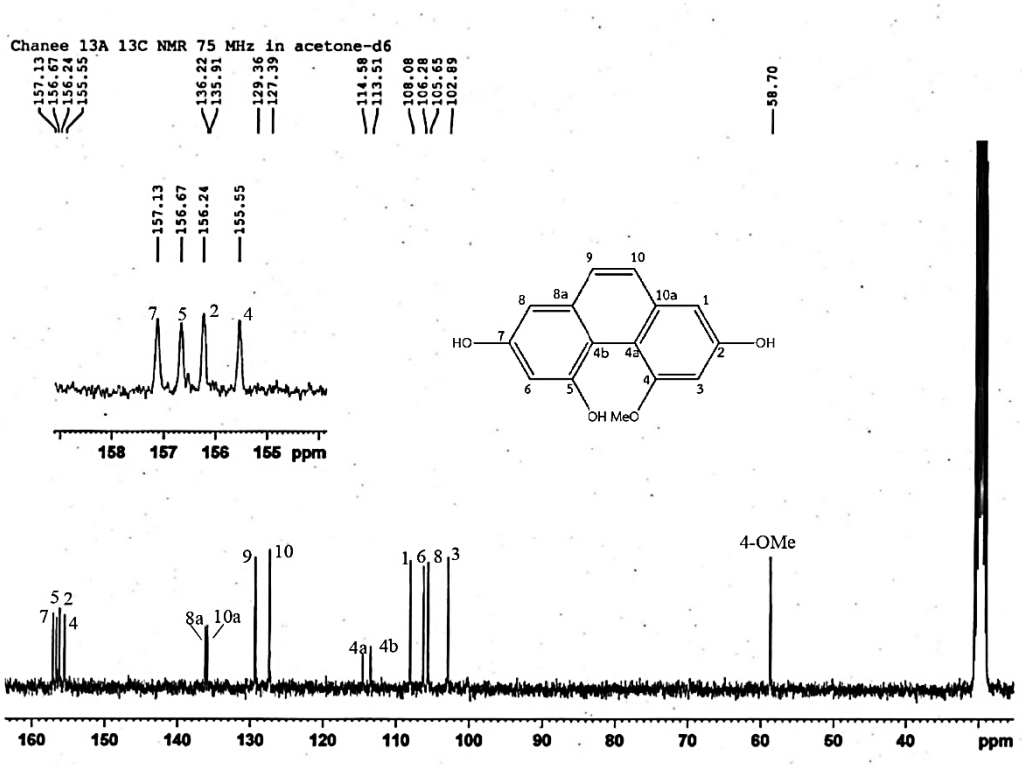

Figure 22 ^{13}C NMR spectrum **of compound 1** (75 MHz) in acetone-d_6

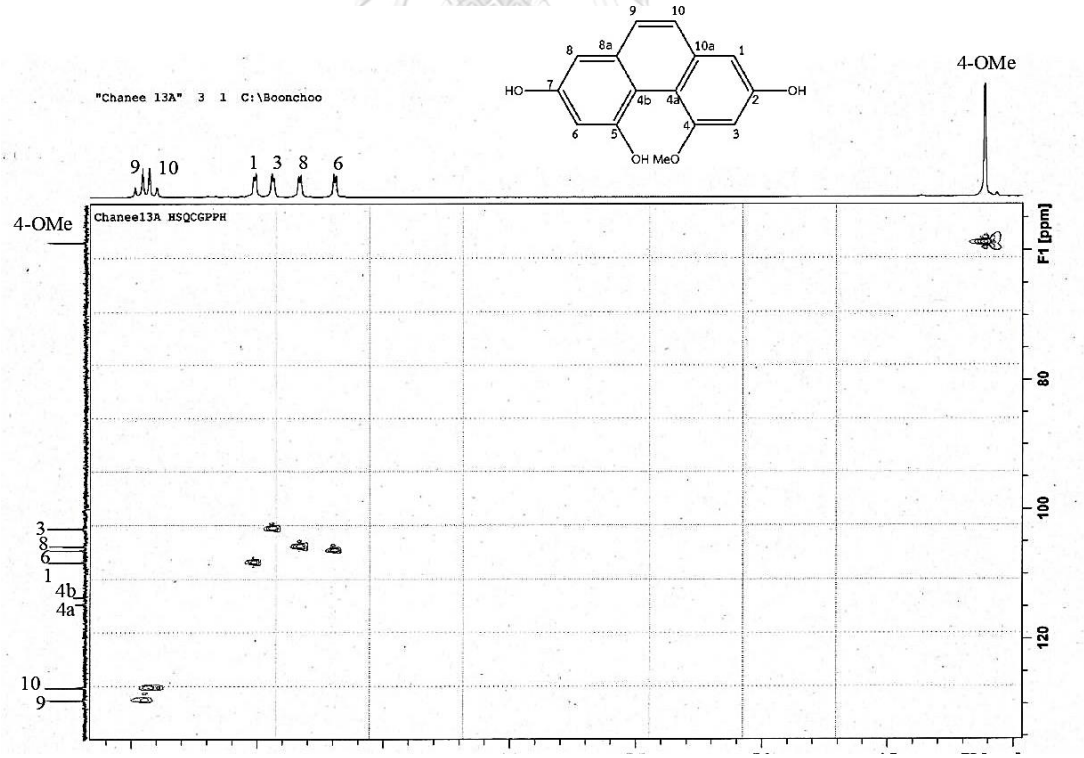

Figure 23 HSQC spectrum of **compound 1** in acetone-d_6

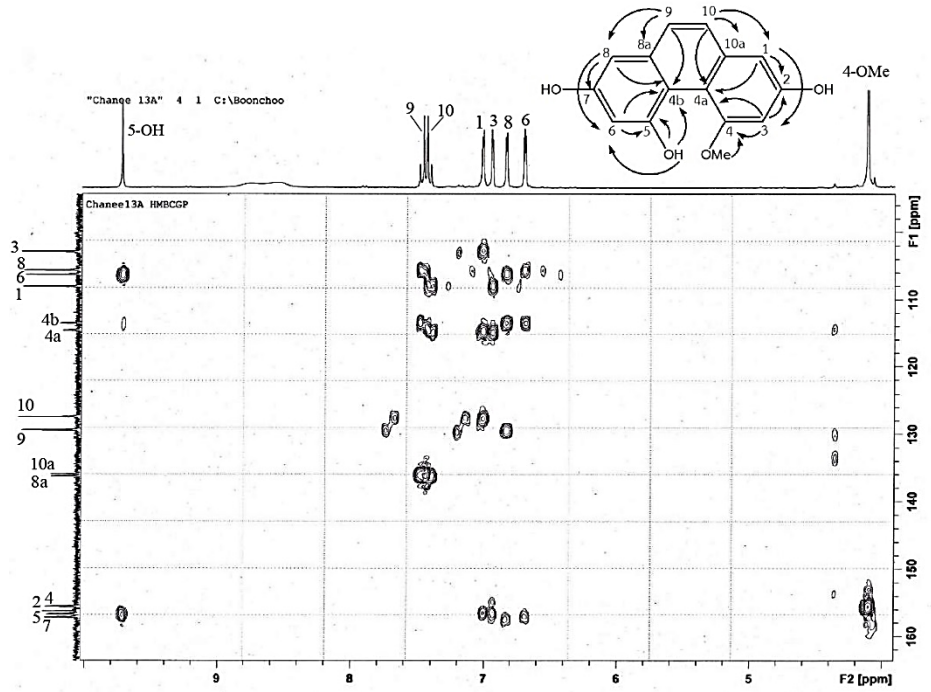

Figure 24 HMBC spectrum of **compound 1** in acetone-d_6

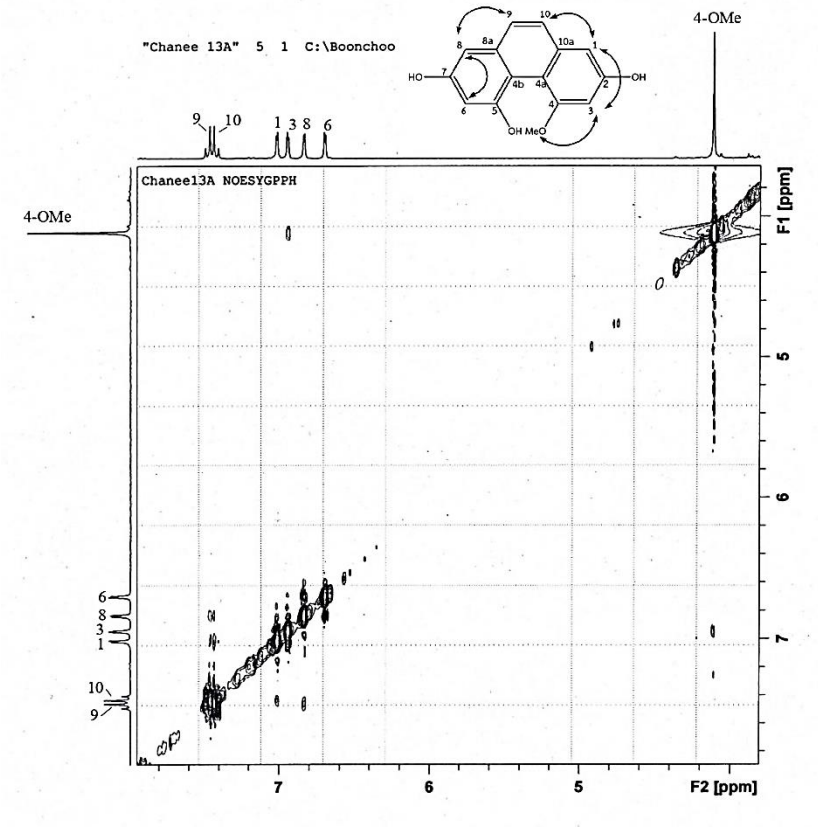

Figure 25 NOESY spectrum of **compound 1** in acetone-d_6

1.2 Structural characterization of compound 2

Compound 2 was purified as a yellowish-brown amorphous solid. The positive HR-ESI-MS spectral data showed a sodium-adduct molecular ion $[M+Na]^+$ peak at *m/z* 263.0682 (calcd. for 263.0684, $C_{15}H_{12}O_3Na$), implying a molecular formula of $C_{15}H_{12}O_3$ (**Figure 29**).

The ^1H NMR spectrum (**Figure 30**) displayed seven aromatic protons at δ 7.006-7.64, a hydroxy proton at δ 9.53 (1H, s) and a methoxy proton at δ 4.16 (3H, s). The ^{13}C NMR spectrum (**Figure 31**) exhibited fourteen aromatic carbons at δ 101.66-156.44 and a methoxy carbon at δ 57.7. The HSQC spectral data (**Figure 32**) suggested that **compound 2** was a phenanthrene derivative, showing correlation peaks for H-9 (δ 7.64, 1H, d, *J* = 9 Hz)/C-9 (δ 128.87) and H-10 (δ 7.51, 1H, d, *J* = 9 Hz)/C-10 (δ 126.12). The doublet proton signal at δ 7.64 was assigned as H-9 based on the HMBC (**Figure 33**) correlation of C-9 (δ 128.87) with H-8 (δ 7.43, 1H, d, *J* = 6.6 Hz) and the signal at 7.51 was assigned to H-10 from the HMBC correlation from C-10 (δ 126.12) to H-1 (δ 7.088,1H, d, *J* = 2.4 Hz). From the HMBC correlation with C-10a (δ 136.22), H-9 and H-10 were also assigned. The attachment of 5-OH (δ 9.53, 1H, s) at C-5 (δ 154.35) in **compound 2** was revealed by its HMBC correlation of the singlet proton of 5-OH with C-5 and C-4b. C-4b (δ 118.92) exhibited correlations with H-9, H-6, H-8 and 5-OH in the HMBC spectrum. The assignment of C-4a at δ 113.05 was obtained from its HMBC correlations to H-1, H-3 and H-10. On ring B, the attachment of methoxy group at C-4 (δ 155.5) was observed through its NOESY correlation (**Figure 34**) with the *meta*-coupled aromatic proton at δ 7.006 (1H, d, *J* = 2.4 Hz, H-3). The assignment of C-4 at δ 155.5 was also confirmed by its HMBC correlation to H-3.

By comparison to the above evidence and the previously reported spectral data (Ono *et al.*, 1995), **compound 2** was identified as moscatin.

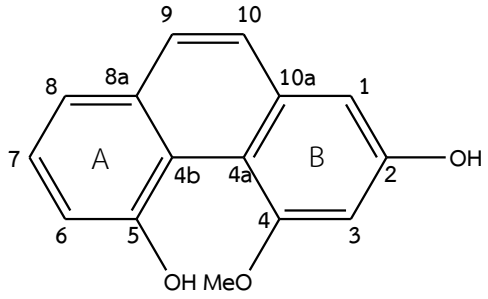

Figure 26 Chemical structure of **compound 2**

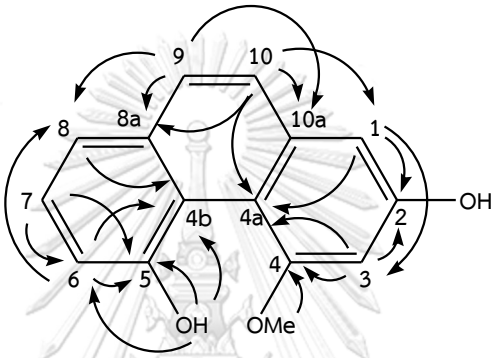

Figure 27 HMBC correlation of **compound 2**

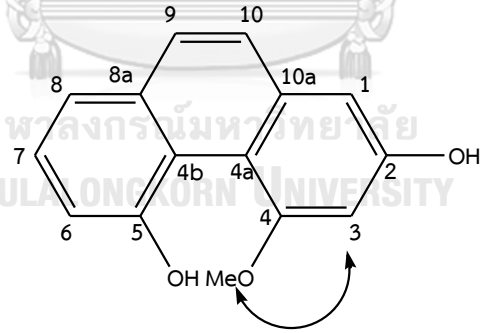

Figure 28 NOESY correlation of **compound 2**

Table 14 NMR spectral data of **compound 2** (300 MHz in acetone-d_6) and moscatin (500 MHz in $CDCl_3$)

Position	Compound 2		Moscatin*	
	δ_H in ppm (mult., *J* in Hz)	**δ_C in ppm**	**δ_H in ppm (mult., *J* in Hz)**	**δ_C in ppm**
1	7.09 (d, *J* = 2.4 Hz)	106.9	6.96 (d, *J* = 2.5 Hz)	107.4
2	-	156.4	-	154.4
3	7.01 (d, *J* = 2.4 Hz)	101.7	6.82 (d, *J* = 2.5 Hz)	101.7
4	-	155.5	-	155.4
4a	-	113.1	-	114.2
4b	-	118.9	-	118.8
5	-	154.3	-	153.8
6	7.12 (dd, *J* = 6.6,2.4 Hz)	116.1	7.23 (dd, *J* = 8.0, 1.2 Hz)	116.6
7	7.43 (d, *J* = 6.6 Hz)	126.6	7.48 (dd, *J* = 8.0, 8.0 Hz)	129.4
8	7.43 (d, *J* = 6.6 Hz)	120.2	7.41 (dd, *J* = 8.0, 1.2 Hz)	120.8
8a	-	134.1	-	134.1
9	7.64 (d, *J* = 9 Hz)	128.9	7.61 (d, *J* = 9.2 Hz)	127.0
10	7.51 (d, *J* = 9 Hz)	126.1	7.41 (d, *J* = 9.2 Hz)	125.9
10a	-	136.2	-	136.1
4-OMe	4.16 (s)	57.7	4.04 (s)	58.4
5-OH	9.5 (s)	-	-	-

*(Ono *et al.*, 1995)

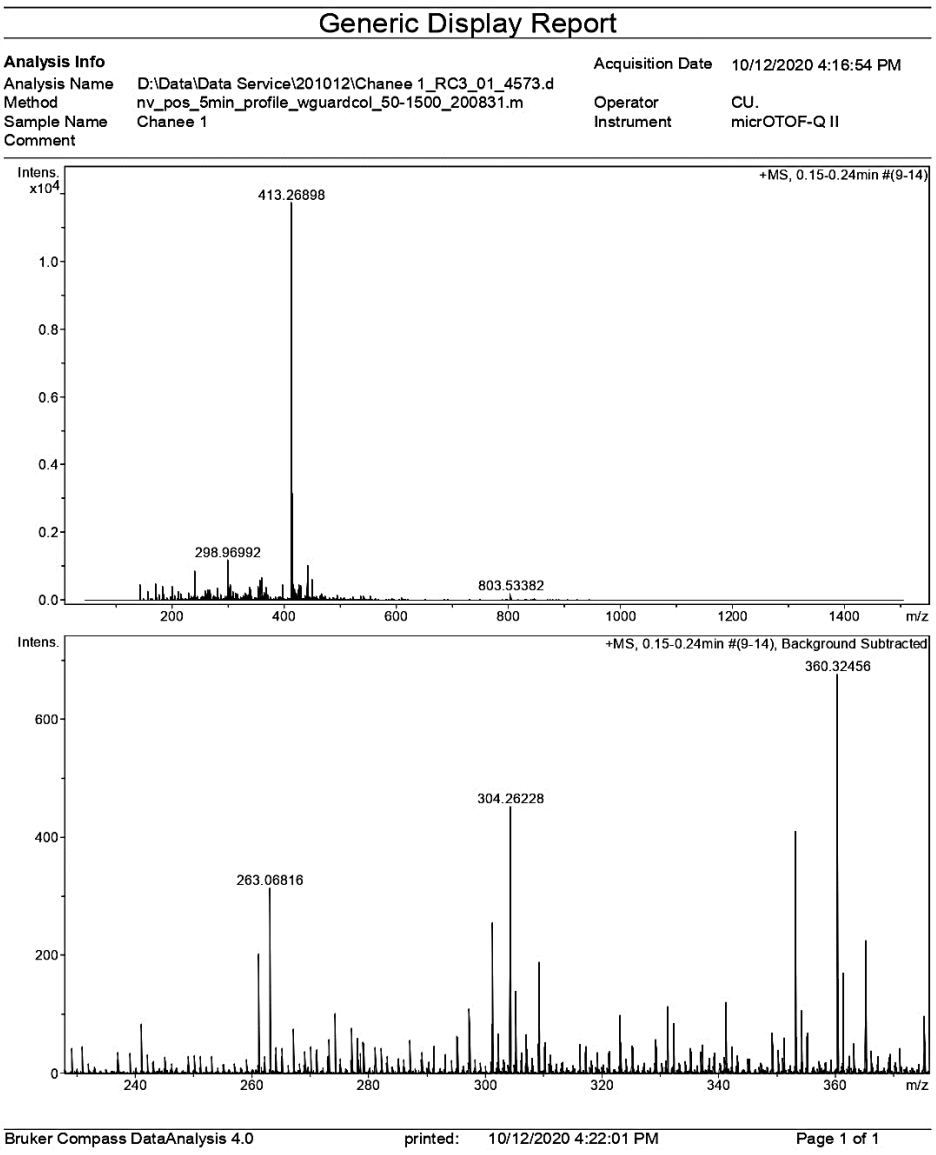

Figure 29 HR-ESI-MS spectrum of **compound 2**

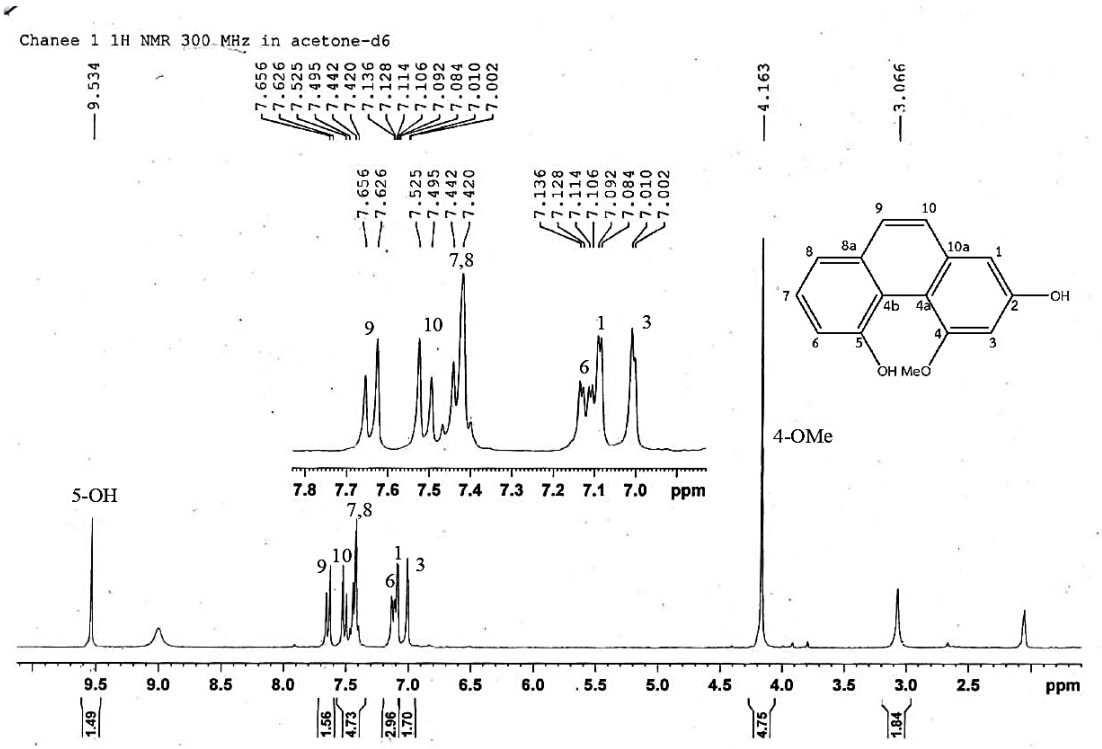

Figure 30 ^{1}H NMR spectrum of **compound 2** (300 MHz) in acetone-d_6

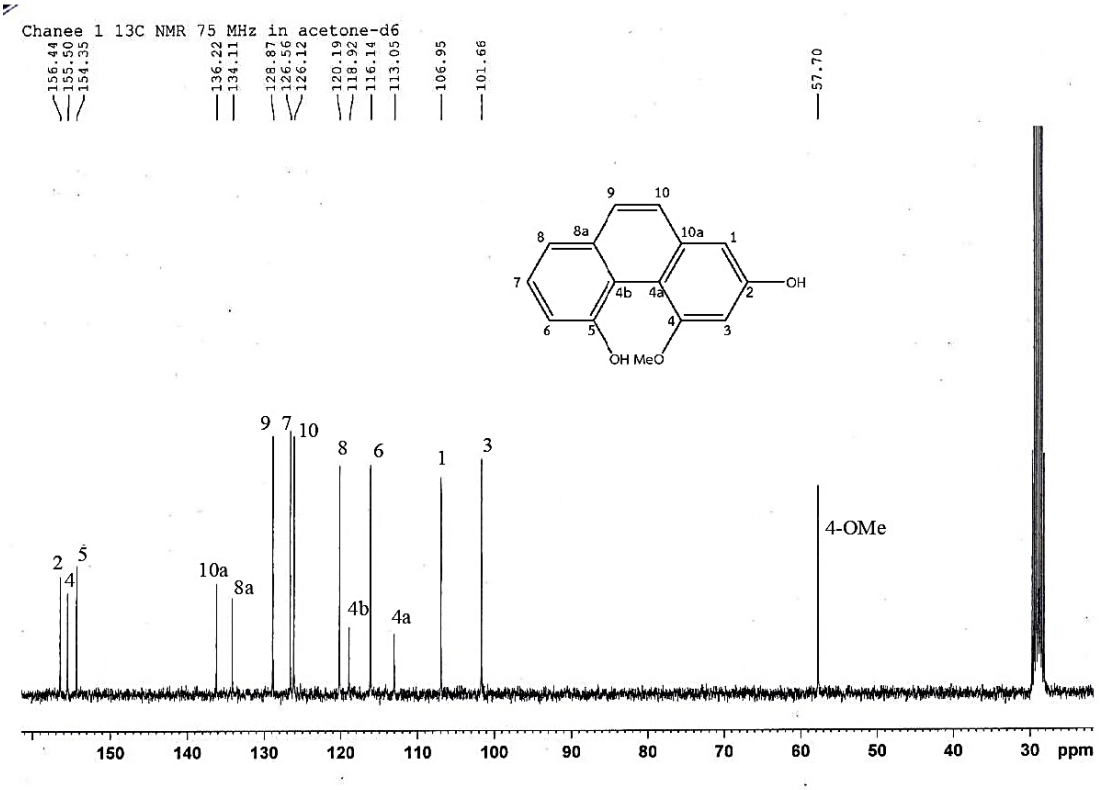

Figure 31 ^{13}C NMR spectrum of **compound 2** (75 MHz) in acetone-d_6

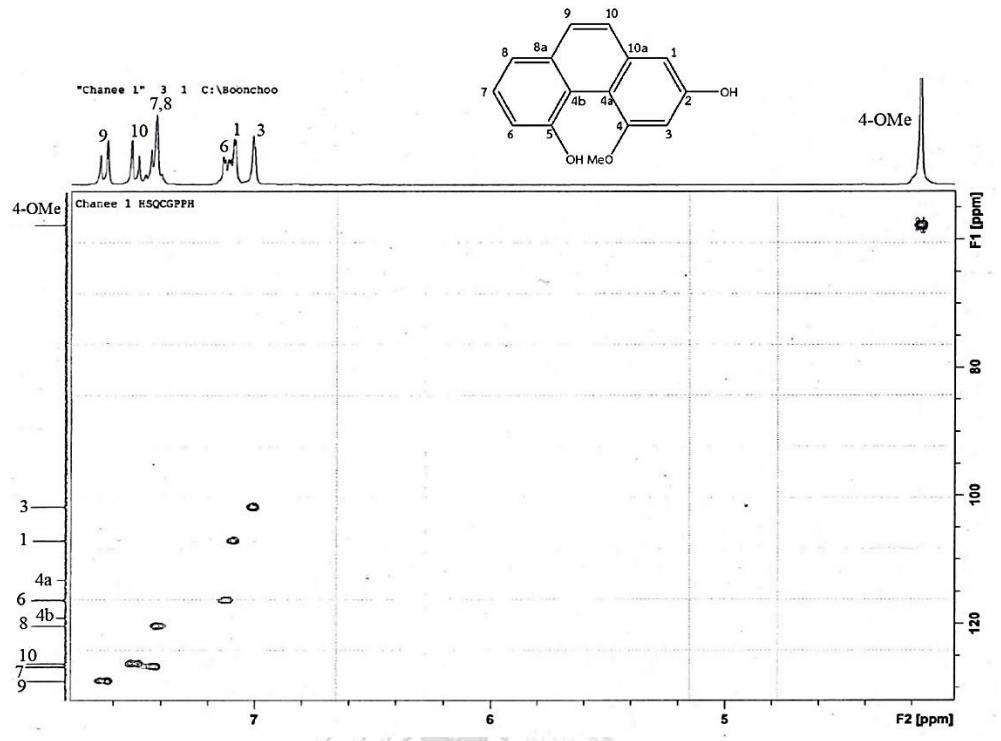

Figure 32 HSQC spectrum of **compound 2** in acetone-d_6

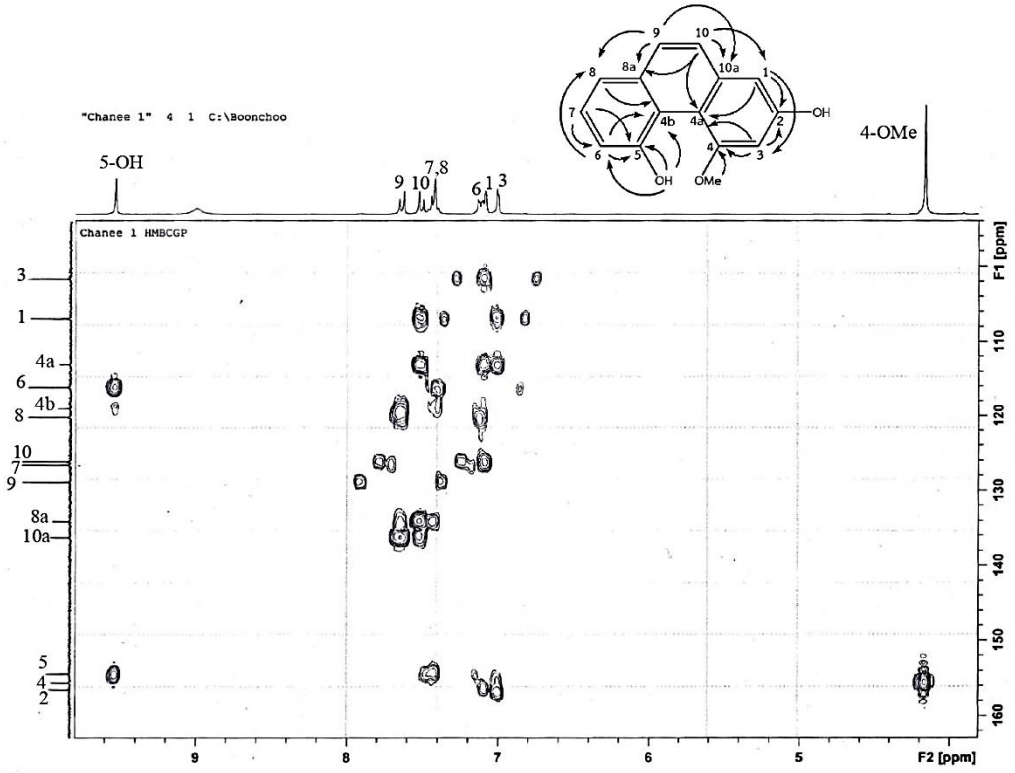

Figure 33 HMBC spectrum of **compound 2** in acetone-d_6

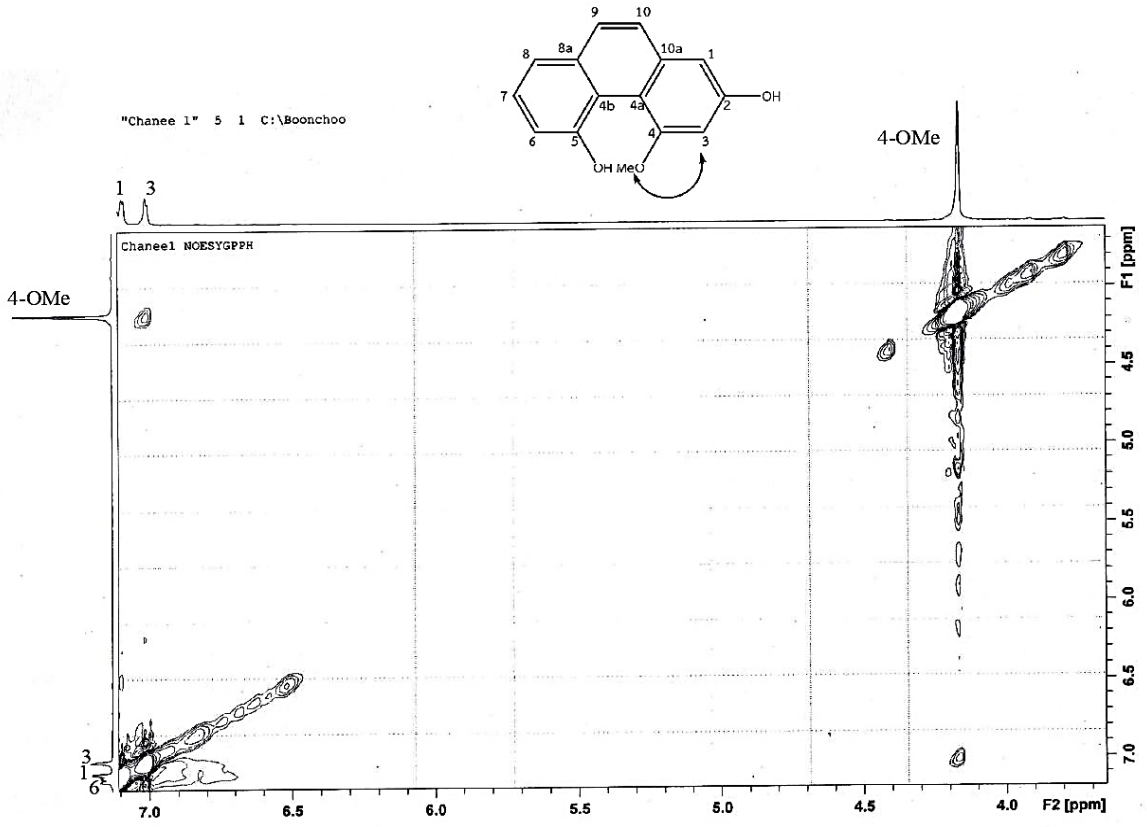

Figure 34 NOESY spectrum of **compound 2** in acetone-d_6

1.3 Structural characterization of compound 3

Compound 3 was isolated as a brown amorphous solid. The HR-ESI-MS presented the sodium-adduct molecular ion peak $[M+Na]^+$ at *m/z* 293.0758 (calcd. for 293.0789, $C_{16}H_{14}O_4Na$), suggesting the molecular formula $C_{16}H_{14}O_4$ (**Figure 38**).

The ^1H NMR spectrum (**Figure 39**) suggested six aromatic protons at δ 6.83-7.87, two methoxy protons at δ 4.13 (3H, s) and δ 4.04 (3H, s) and a hydroxy proton at δ 9.45 (1H, s). The locations of the methoxy and hydroxy groups were confirmed by analysis of the HMBC and NOESY spectral data. The first methoxy group was placed at C-4 of ring B as suggested from the HMBC (**Figure 42**) correlation between C-4 (δ 155.4) and 4-OMe proton (δ 4.13, 3H, s) and from the NOESY (**Figure 43**) interaction between 4-OMe protons and H-3 (δ 6.83, 1H, d, *J* = 2.1 Hz). The assignment of H-3 was based on the HMBC correlation with C-1 (δ 106.1), C-4a (δ 109.1) and C-4 (δ 155.4). The second methoxy group was placed at C-9, as supported by the HMBC correlation between C-9 (δ 154.3) and 9-OMe protons (δ 4.04, 3H, s). This was confirmed by the NOESY interaction of 9-OMe protons with H-10 (δ 6.94, 1H, s). The ^1H NMR signal at δ 6.94 (1H, s) was assigned as H-10 from its HMBC correlations to C-9 (δ 154.3) and C-8a (δ 128.3). On ring A, one hydroxy group was attached at C-5, based on the HMBC correlation peaks of 5-OH proton (δ 9.45, 1H, s) and C-6 (δ 116.7). On ring B, the position of the second hydroxy group at C-2 (δ 156.6) was suggested from the presence of two *meta*-coupled doublet protons at δ 7.01 (1H, d, *J* = 2.1 Hz, H-1) and δ 6.83 (1H, d, *J* = 2.1 Hz, H-3). The assignment of C-2 was based on its HMBC correlation with H-1 and H-3. NOESY interactions of H-1 with H-3 and H-10 were observed. H-1 was assigned at δ 7.01 because of its HMBC correlations to C-3 (δ 99.4), C-10 (δ 101.9) and C-4a (δ 109.1). On ring C, C-4a at δ

109.1 was assigned from its HMBC correlation with H-1, H-3 and H-10. From the 3-bond correlation from C-4b to H-6 and H-8, the signal at δ 120 was assigned to C-4b.

Based on the above spectroscopic evidence and through comparison with the previously reported ^{1}H and ^{13}C spectral data (Zhang *et al.*, 2008c), **compound 3** was identified as 2,5-dihydroxy-4,9-dimethoxyphenanthrene.

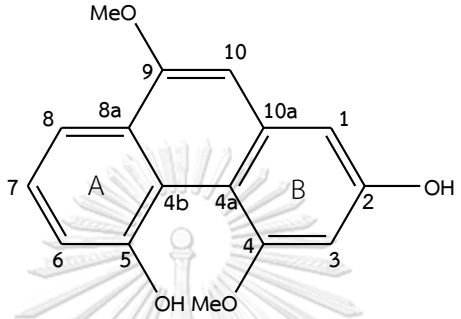

Figure 35 Chemical structure of **compound 3**

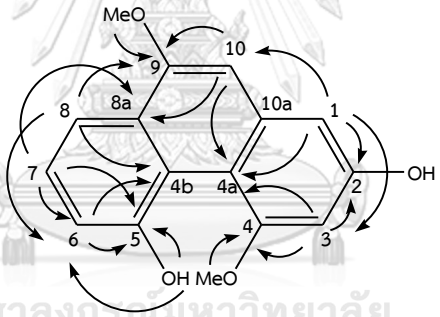

Figure 36 HMBC correlation of **compound 3**

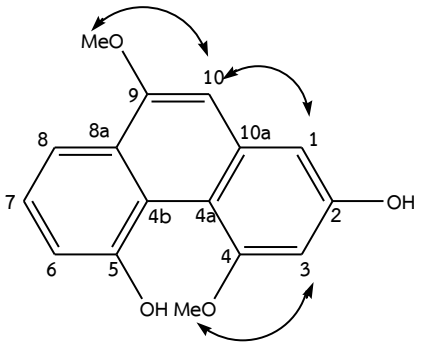

Figure 37 NOESY correlation of **compound 3**

Table 15 NMR spectral data of **compound 3** (300 MHz in acetone-d_6) and 2,5-dihydroxy-4,9-dimethoxyphenanthrene (400 MHz in $CDCl_3$)

Position	Compound 3		2,5-dihydroxy-4,9-dimethoxyphenanthrene*	
	δ_H in ppm (mult., *J* in Hz)	**δ_C in ppm**	**δ_H in ppm (mult., *J* in Hz)**	**δ_C in ppm**
1	7.01 (d, *J* = 2.1 Hz)	106.1	6.87 (d, *J* = 2.5 Hz)	106.3
2	-	156.6	-	154.5
3	6.83 (d, *J* = 2.1 Hz)	99.4	6.68 (d, *J* = 2.5 Hz)	99.4
4	-	155.4	-	155.4
4a	-	109.1	-	110.6
4b	-	120.0	-	119.9
5	-	154.1	-	153.8
6	7.13 (d, *J* = 8.1 Hz)	116.7	7.25 (dd, *J* = 7.8, 1.4 Hz)	117.3
7	7.45 (t, *J* = 8.1 Hz)	126.2	7.50 (t, *J* = 7.8 Hz)	126.9
8	7.87 (d, *J* = 8.1 Hz)	113.5	7.94 (dd, *J* = 7.8, 1.4 Hz)	114.1
8a	-	128.3	-	128.5
9	-	154.3	-	154.6
10	6.94 (s)	101.9	6.71 (s)	101.6
10a	-	136.9	-	136.8
4-OMe	4.13 (s)	57.6	4.04 (s)	58.3
9-OMe	4.04(s)	55.1	4.03 (s)	55.5
5-OH	9.45(s)	-	9.50 (s)	-

*(Zhang *et al.*, 2008c)

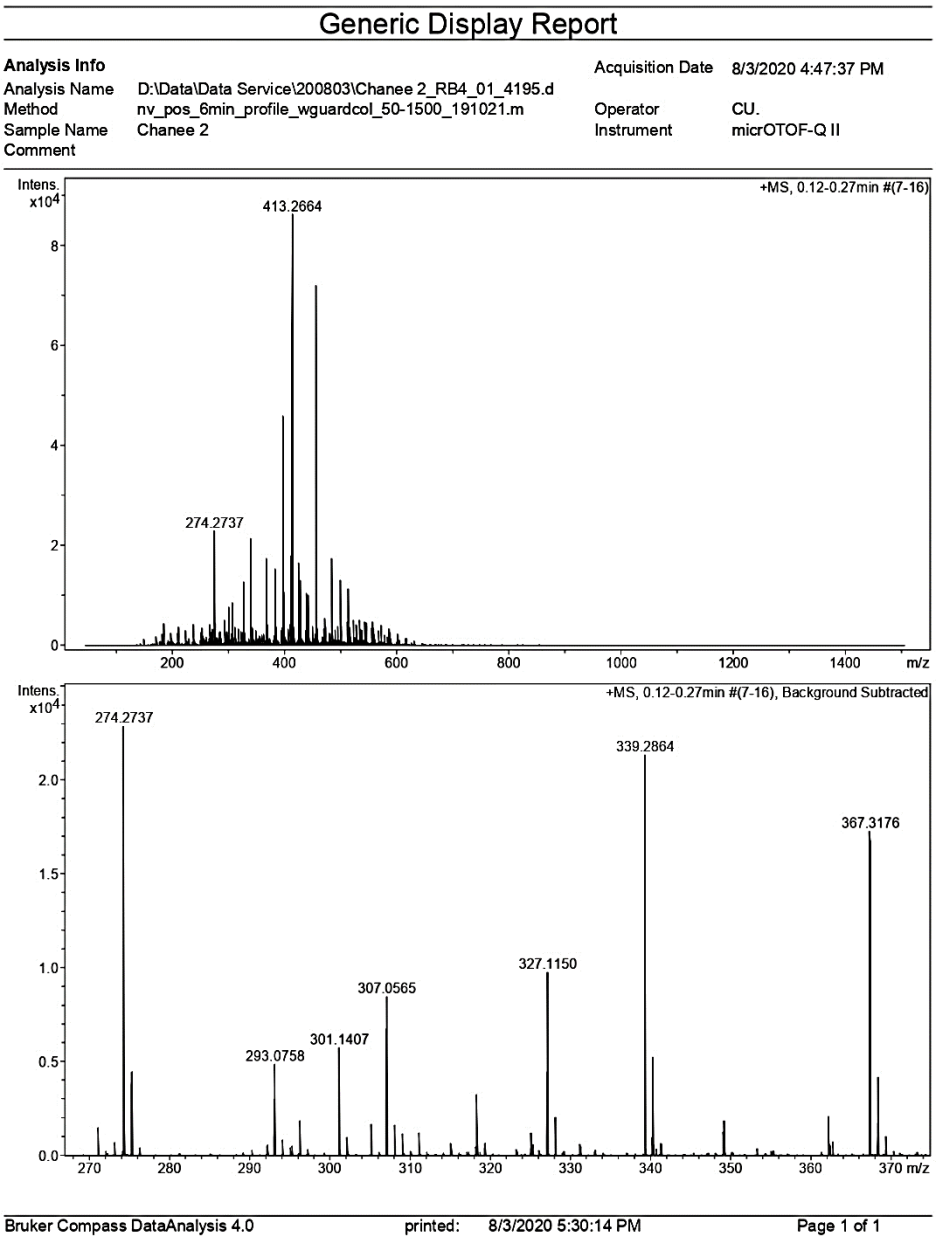

Figure 38 HR-ESI-MS spectrum of **compound 3**

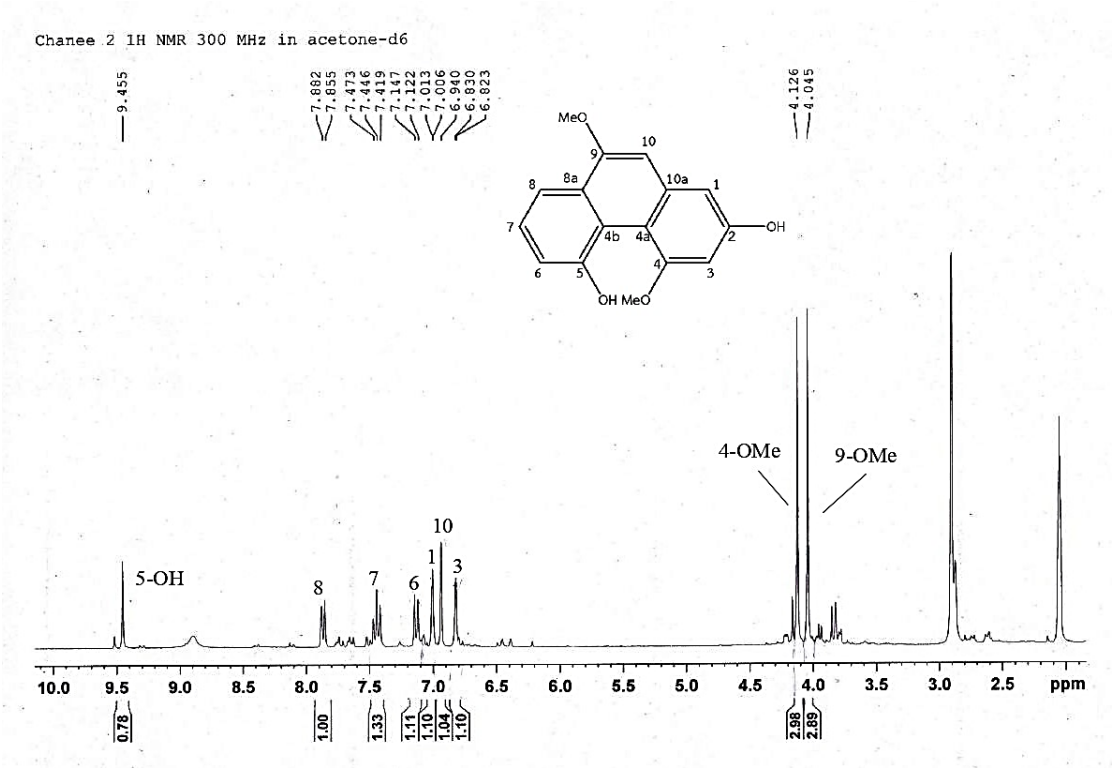

Figure 39 ^{1}H NMR spectrum of **compound 3** (300 MHz) in acetone-d_6

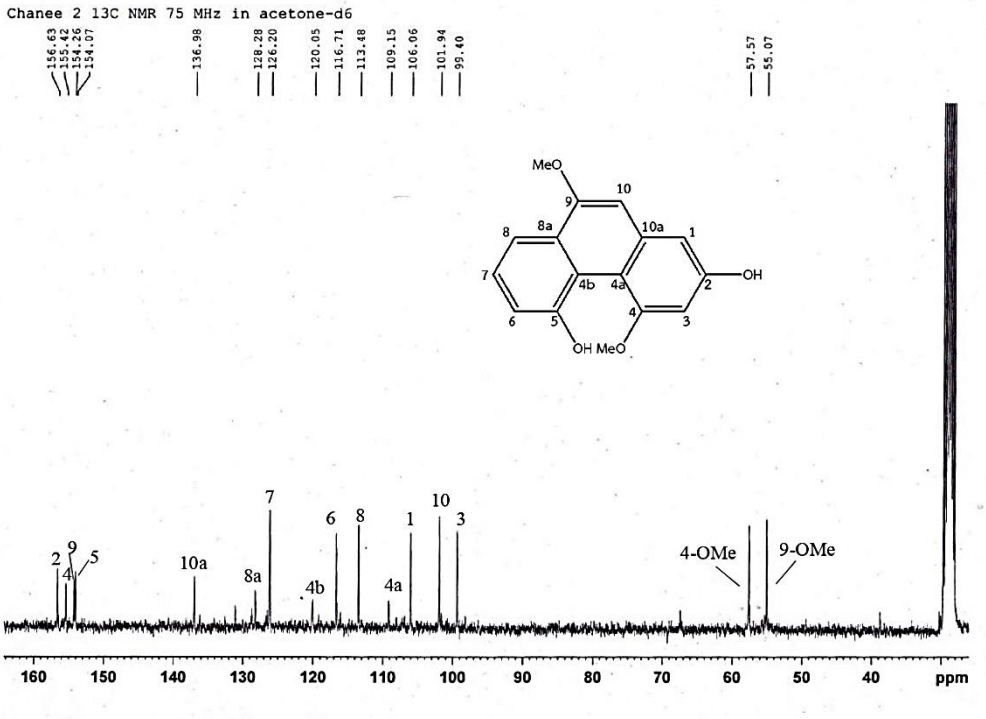

Figure 40 ^{13}C NMR spectrum of **compound 3** (75 MHz) in acetone-d_6

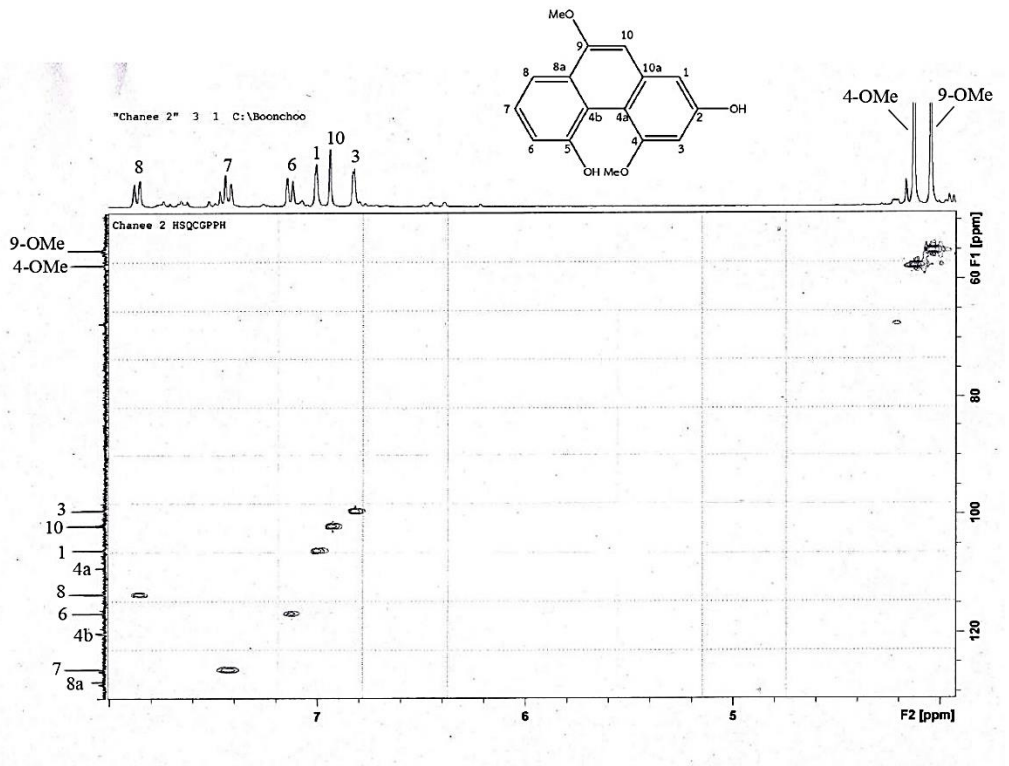

Figure 41 HSQC spectrum of **compound 3** in acetone-d_6

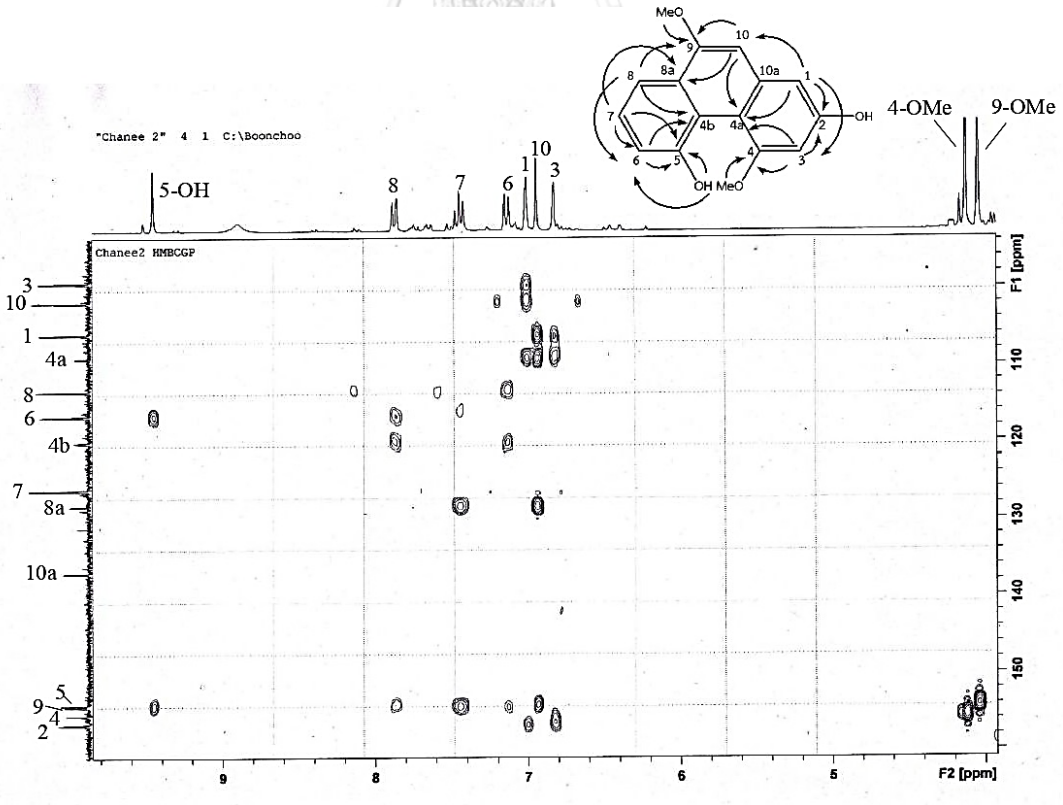

Figure 42 HMBC spectrum of **compound 3** in acetone-d_6

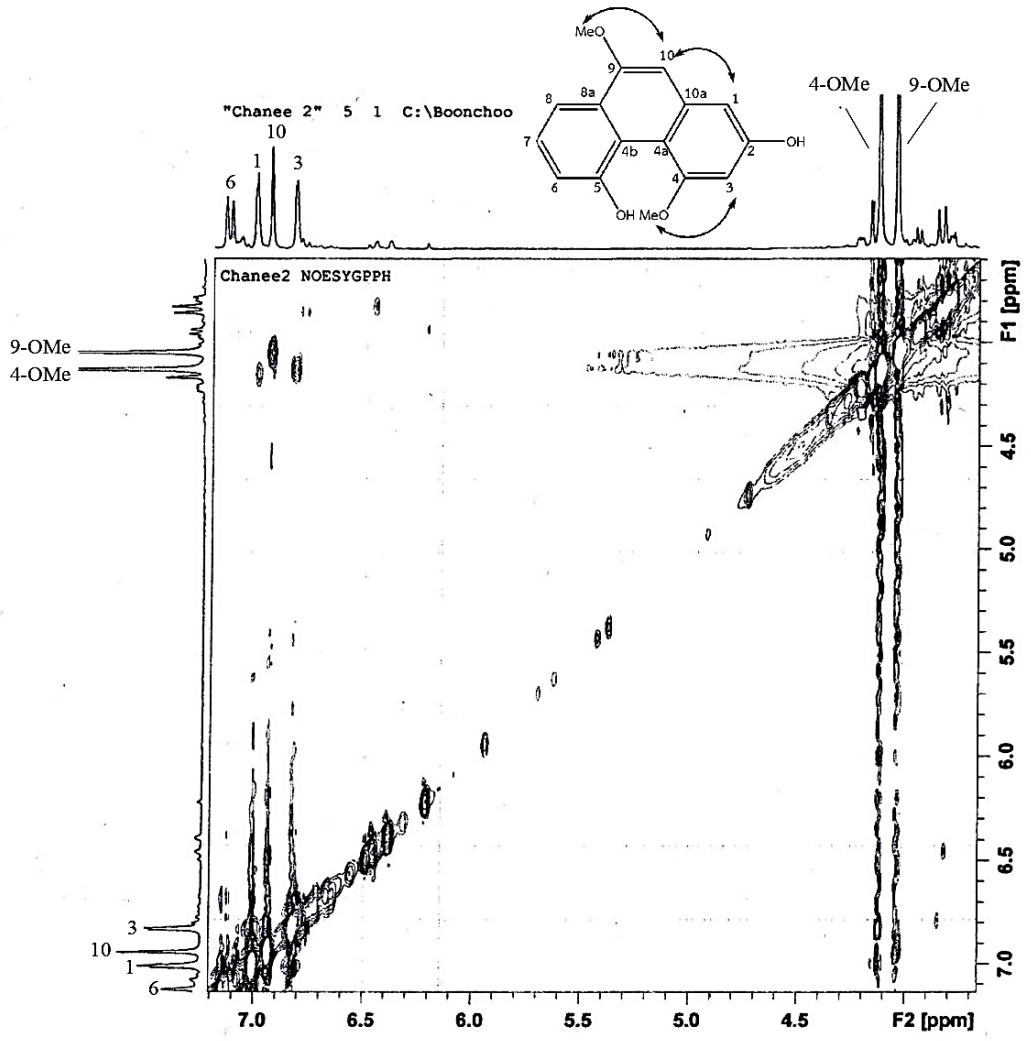

Figure 43 NOESY spectrum of **compound 3** in acetone-d_6

1.4 Structural characterization of compound 4

Compound 4 was obtained as a pale orange gum. The molecular formula of $C_{17}H_{20}O_5$ was indicated by the $[M+Na]^+$ peak at *m/z* 327.1221 (calcd. for 327.1208, $C_{17}H_{20}O_5Na$) in the HR-ESI mass spectrum (**Figure 45**).

The ^{1}H NMR spectrum (**Figure 46**) presented two aromatic singlet protons at δ 6.49 (2H, s, H-2 and H-6), indicating symmetrical substitutions on C-3 and C-5 (δ147.6) and also the position of a hydroxy group on C-4 (δ 132.4). On ring B, the *meta*-coupled aromatic proton at δ 6.79 (1H, d, *J* = 1.5 Hz) was assigned to H-2′ and the *ortho*-coupled doublet proton at δ 6.75 to H-5′, and this deduction was supported by the ^{1}H NMR signal of an *ortho* and *meta*-coupled H-6′ δ 6.66 (1H, dd, *J* = 7.8, 1.5 Hz). The presence of a hydroxy group at C-4′ (δ 144.7) was suggested by an *ortho*-coupled H-5′ and an *ortho* and *meta*-coupling H-6′ in the ^{1}H NMR spectrum. **Compound 4** should be bibenzyl, as suggested from the ^{1}H NMR signals of two methylene groups at δ 2.80 (4H, s, α and α'). Further comparison of the NMR data of **Compound 4** with previously reported values of moscatilin (Majumder & Sen, 1987a) indicated that they were identical.

Compound 4 was characterized as moscatilin through comparison between the above evidence and the reported spectral data (Majumder & Sen, 1987a).

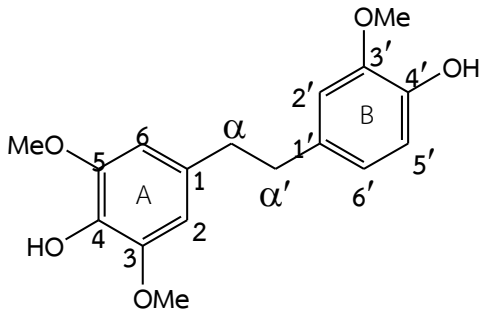

Figure 44 Chemical structure of **compound 4**

Table 16 NMR spectral data of **compound 4** (300 MHz in acetone-d_6) and moscatilin (100 MHz in $CDCl_3$)

Position	Compound 4		Moscatilin*	
	δ_H (mult., *J* in Hz)	**δ_C**	**δ_H (mult., *J* in Hz)**	**δ_C**
1	-	132.4	-	132.8
2	6.49 (s)	105.9	6.30 (s)	105.2
3	-	147.6	-	146.8
4	-	134.1	-	133.5
5	-	147.6	-	146.8
6	6.49 (s)	105.9	6.30 (s)	105.2
α	2.80 (s)	38.1	2.79 (s)	38.3
α′	2.80 (s)	37.6	2.79 (s)	37.8
1′	-	133.4	-	132.8
2′	6.79 (d, *J* = 1.5 Hz)	112.1	6.60 (d, *J* = 2 Hz)	111.2
3′	-	147.2	-	146.1
4′	-	144.7	-	143.7
5′	6.75 (d, *J* = 7.8 Hz)	114.7	6.77 (d, *J* = 8 Hz)	114.1
6′	6.66 (dd, *J* = 7.8, 1.5 Hz)	120.8	6.74 (dd, *J* = 8, 2 Hz)	121.0
3-OMe	3.77(s)	55.7	3.81 (s)	56.2
5-OMe	3.77(s)	55.7	3.81 (s)	56.2
3′-OMe	3.79(s)	55.3	3.81 (s)	55.8

* (Majumder & Sen, 1987a)

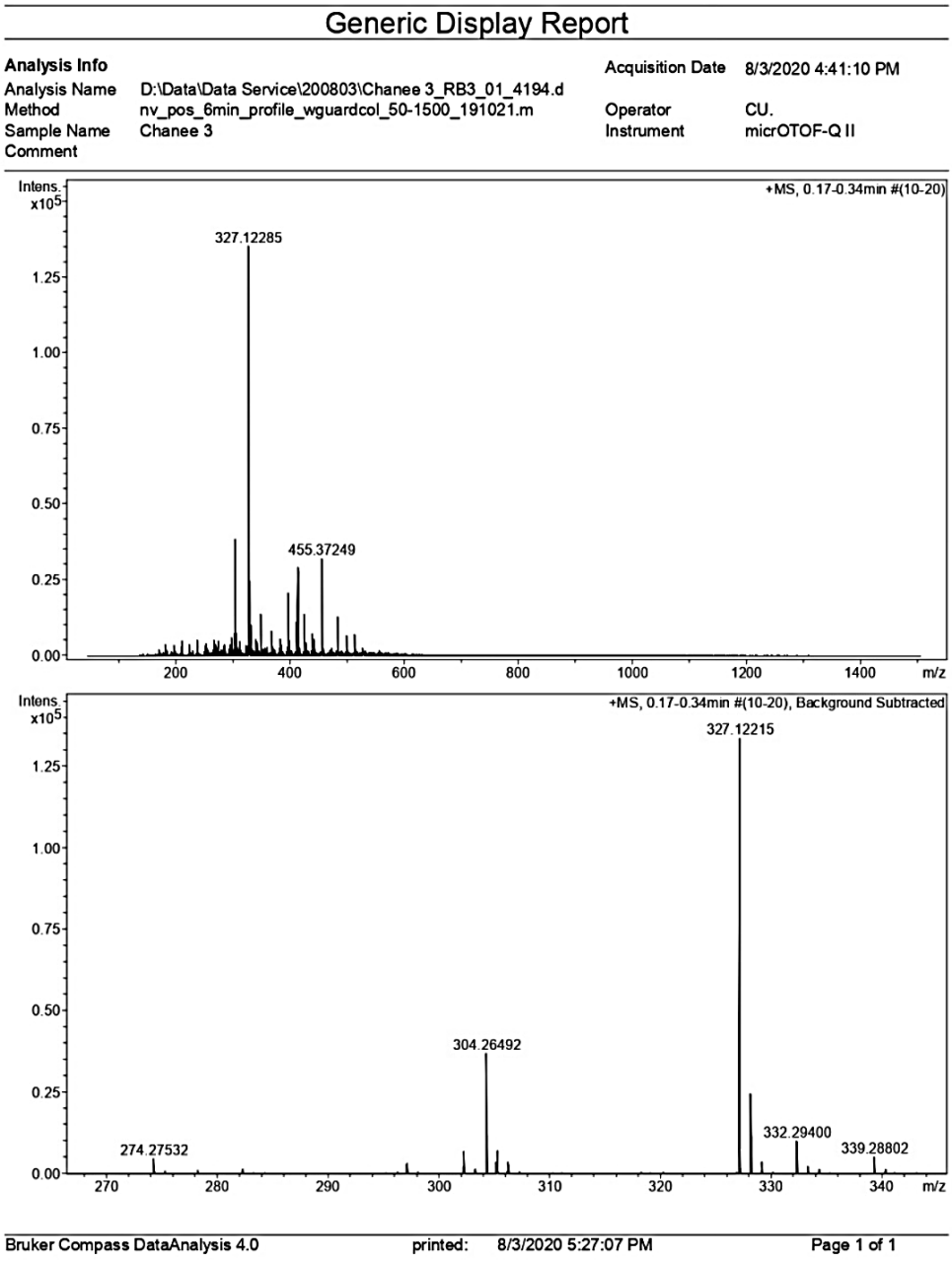

Figure 45 HR-ESI-MS spectrum of **compound 4**

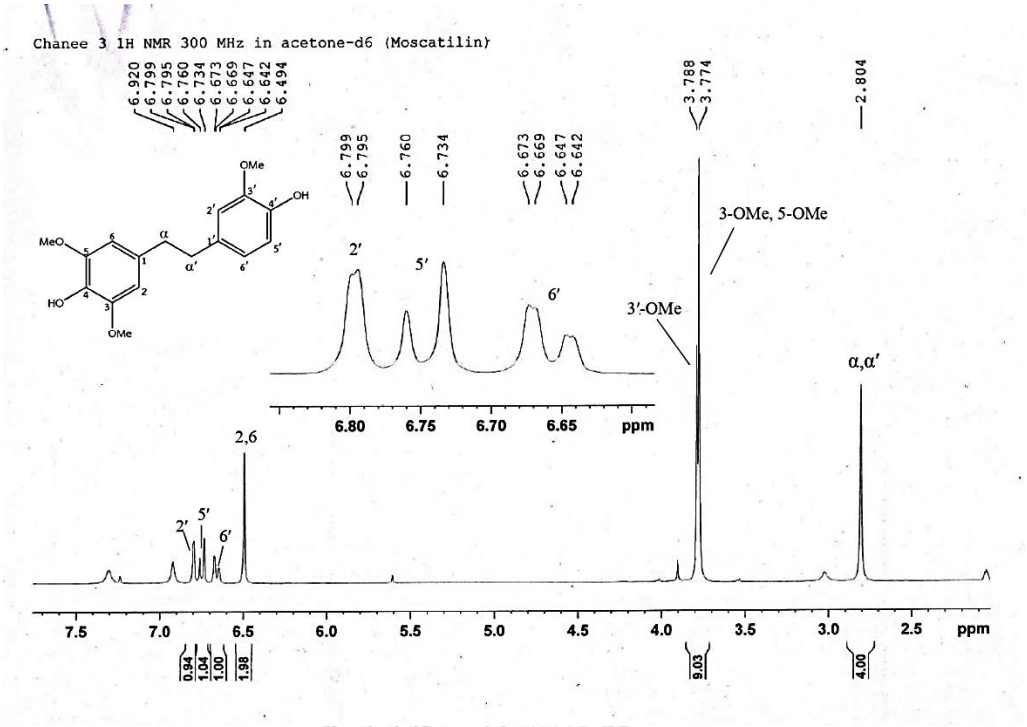

Figure 46 ^{1}H NMR spectrum of **compound 4** (300 MHz) in acetone-d_6

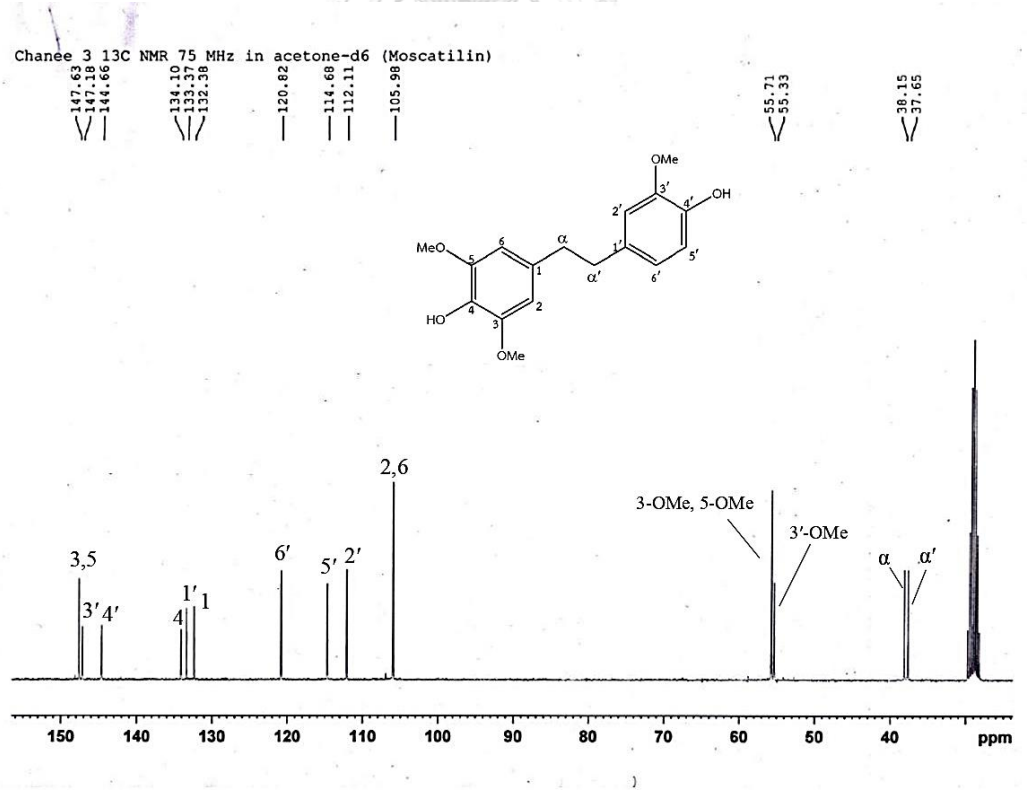

Figure 47 ^{13}C NMR spectrum of **compound 4** (75 MHz) in acetone-d_6

1.5 Structural characterization of compound 5

Compound 5 was obtained as a pale-yellow gum. The HR-ESI-MS data showed the sodium-adduct molecular ion $[M+Na]^+$ peak at *m/z* 297.1113 (calcd. for 297.1103, $C_{16}H_{18}O_4Na$) and thus indicated a molecular formula of $C_{16}H_{18}O_4$ (**Figure 50**).

The ^1H NMR spectrum (**Figure 51**) exhibited two singlet aromatic protons at δ 6.49 (2H, s, H-2 and H-6), a *meta*-coupled aromatic proton at δ 6.70 (1H, d, *J* = 2.1 Hz, H-2′), a triplet *ortho*-coupled aromatic proton at δ 7.09 (1H, t, *J* = 7.8 Hz, H-5′) and two *ortho* and *meta*-coupled doublet of doublet protons at δ 6.69 (2H, dd, *J* = 7.8, 2.1 Hz, H-4′ and H-6′). Two pairs of methylene protons at δ 2.82 (4H, s, H-α and H-α') and two methoxy protons at δ 3.77 (6H, s, 3-OMe and 5-OMe) and a hydroxy proton at δ 6.99 (1H, s, 4-OH) were also revealed in the ^1H NMR spectrum. There were thirteen carbon signals in ^{13}C NMR spectrum (**Figure 52**) including the carbon signals of two methoxy and two methylene groups. This was confirmed by analysis of the HSQC (**Figure 53**) and HMBC spectra (**Figure 54**). On ring A, the signals of C-3 and C-5 at δ 147.6 and C-2 and C-6 at δ 105.9 were assigned from the symmetry of substitution with methoxy groups on C-3 and C-5. The symmetrical substitution was also supported by the singlet proton peak of H-2 and H-6 at δ 6.49 in the ^1H NMR spectrum. This was also confirmed by the HMBC correlations from C-3 and C-5 (δ 147.6) to 3-OMe and 5-OMe protons (δ 3.77, 6H, s). The location of the first hydroxy group at C-4 was determined from the HMBC correlation peaks from 4-OH proton (δ 6.99, 1H, br s) to C-5 and C-3 (δ 147.6). The carbon C-α (δ 37.9) showed 3-bond correlations to H-2 and H-6, and the signal at δ 37.7 was assigned to C-α' from its HMBC correlation to H-2′ and H-6′. The presence of two methylene groups was suggested from the overlapping singlet proton signals of H-α and H-α' at δ 2.82 which were HSQC correlated to C-α (δ 37.9) and C-α' (δ 37.7),

respectively. HMBC cross-peaks were observed from C-1 (δ 132.3) to H-2 and H-6 and from C-1′ (δ 143.6) to H-5′. On ring B, the position of the second hydroxy group at C-3′ (δ 157.3) was indicated from the signals of a *meta*-coupled proton (H-2′), an *ortho*-coupled proton (H-5′) and two *ortho* and *meta*-coupled protons (H-4′ and H-6′). The assignment of C-3′ at δ 157.3 was confirmed by its HMBC correlations to H-2′, H-4′ and H-5′. The HMBC correlations from C-α' to H-2′ and H-6′ were also observed.

Based on the above evidence and the spectral data from the previous report (Juneja *et al.*, 1987), **compound 5** was identified as aloifol I.

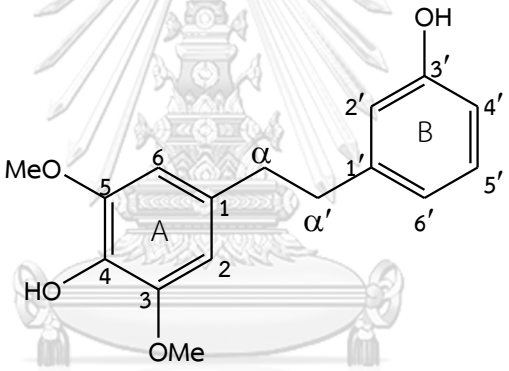

Figure 48 Chemical structure of **compound 5**

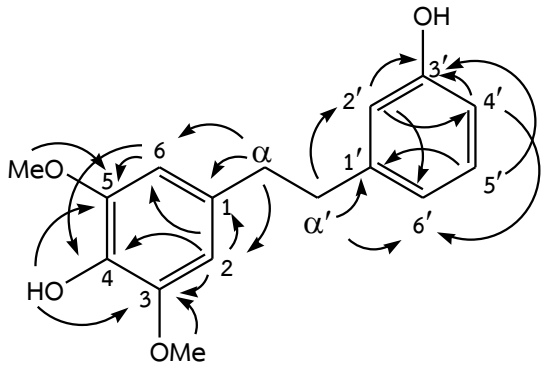

Figure 49 HMBC correlation of **compound 5**

Table 17 NMR spectral data of **compound 5** (300 MHz in acetone-d_6) and aloifol I (400 MHz in $CDCl_3$)

Position	Compound 5		Aloifol I*	
	δ_H in ppm (mult., *J* in Hz)	**δ_C in ppm**	**δ_H in ppm (mult., *J* in Hz)**	**δ_C in ppm**
1	-	132.3	-	132.8
2	6.49 (s)	105.9	6.27 (s)	105.4
3	-	147.6	-	146.8
4	-	134.0	-	132.9
5	-	147.6	-	146.8
6	6.49 (s)	105.9	6.27 (s)	105.4
α	2.82 (s)	37.9	2.75 (s)	36.7
α′	2.82 (s)	37.7	2.75 (s)	37.7
1′	-	143.6	-	143.3
2′	6.70 (d, *J* = 2.1 Hz)	115.5	6.62 (m)	115.2
3′	-	157.3	-	155.9
4′	6.69 (dd, *J* = 7.8, 2.1 Hz)	112.7	6.62 (dd, *J* = 9.0, 2.5 Hz)	112.9
5′	7.09 (t, *J* = 7.8 Hz)	129.2	7.03 (t, *J* = 9.0 Hz)	129.2
6′	6.69 (dd, *J* = 7.8, 2.1 Hz)	119.7	6.62 (dd, *J* = 9.0, 2.5 Hz)	120.5
3-OMe	3.77 (s)	55.7	3.72 (s)	56.2
5-OMe	3.77 (s)	55.7	3.76 (s)	56.2
4-OH	6.99 (br s)	-	-	-

*****(Juneja *et al.*, 1987)

Mass Spectrum List Report

Analysis Info

Analysis Name	D:\Data\Data Service\200803\Chanee 4_RB1_01_4192.d	Acquisition Date	8/3/2020 4:28:17 PM
Method	nv_pos_6min_profile_wguardcol_50-1500_191021.m	Operator	CU.
Sample Name	Chanee 4	Instrument / Ser#	micrOTOF-Q II 10335
Comment			

Acquisition Parameter

Source Type	ESI	Ion Polarity	Positive	Set Nebulizer	3.0 Bar
Focus	Not active	Set Capillary	4000 V	Set Dry Heater	200 ℃
Scan Begin	50 m/z	Set End Plate Offset	-500 V	Set Dry Gas	8.0 l/min
Scan End	1500 m/z	Set Collision Cell RF	250.0 Vpp	Set Divert Valve	Waste

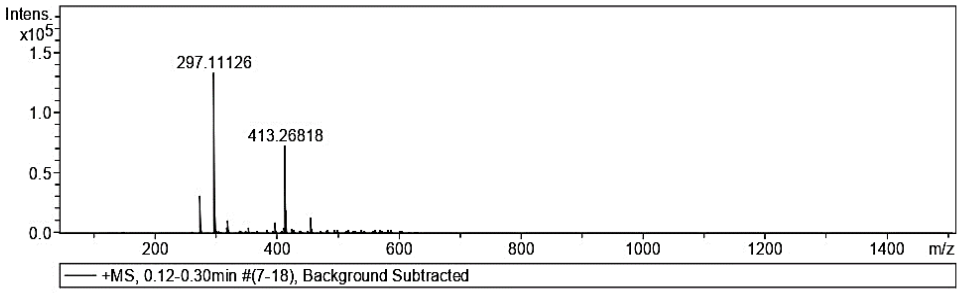

Figure 50 HR-ESI-MS spectrum of **compound 5**

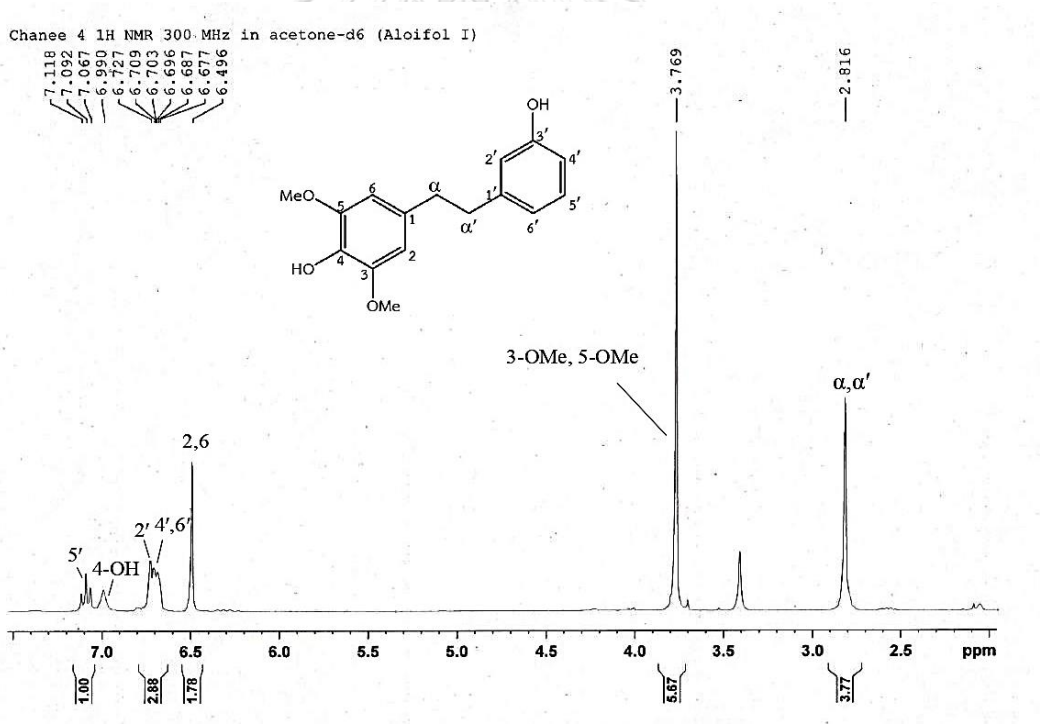

Figure 51 ^{1}H NMR spectrum of **compound 5** (300 MHz) in acetone-d_6

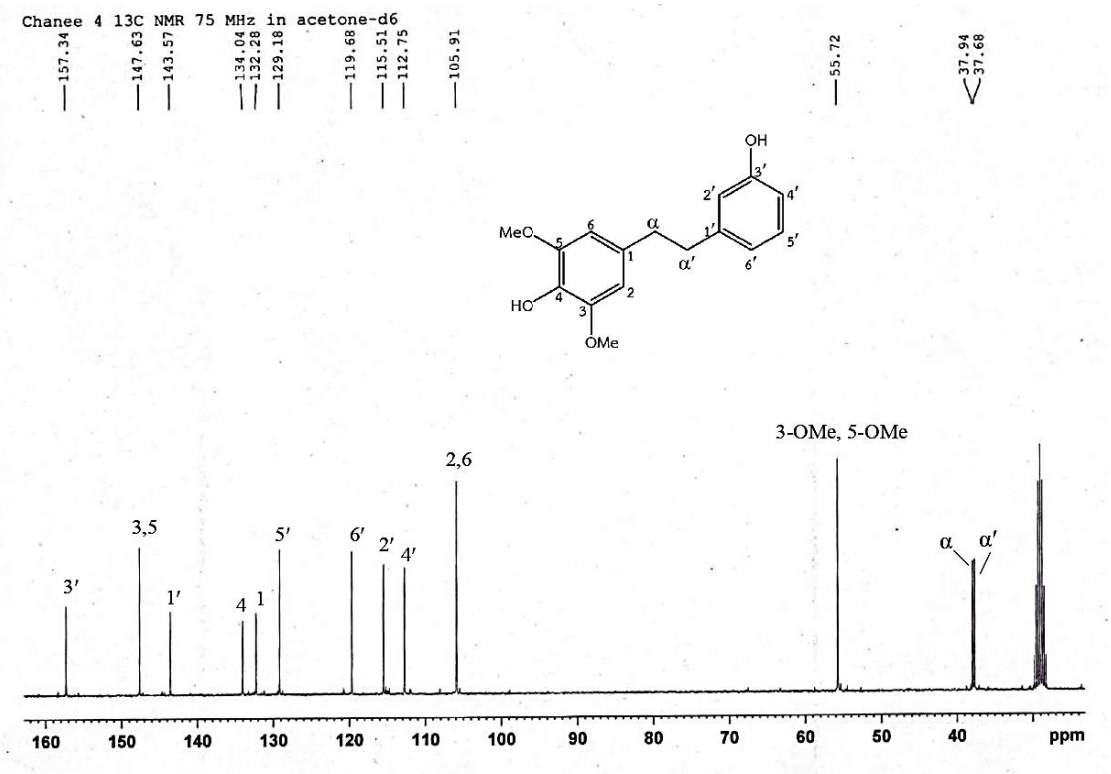

Figure 52 ^{13}C NMR spectrum of **compound 5** (75 MHz) in acetone-d_6

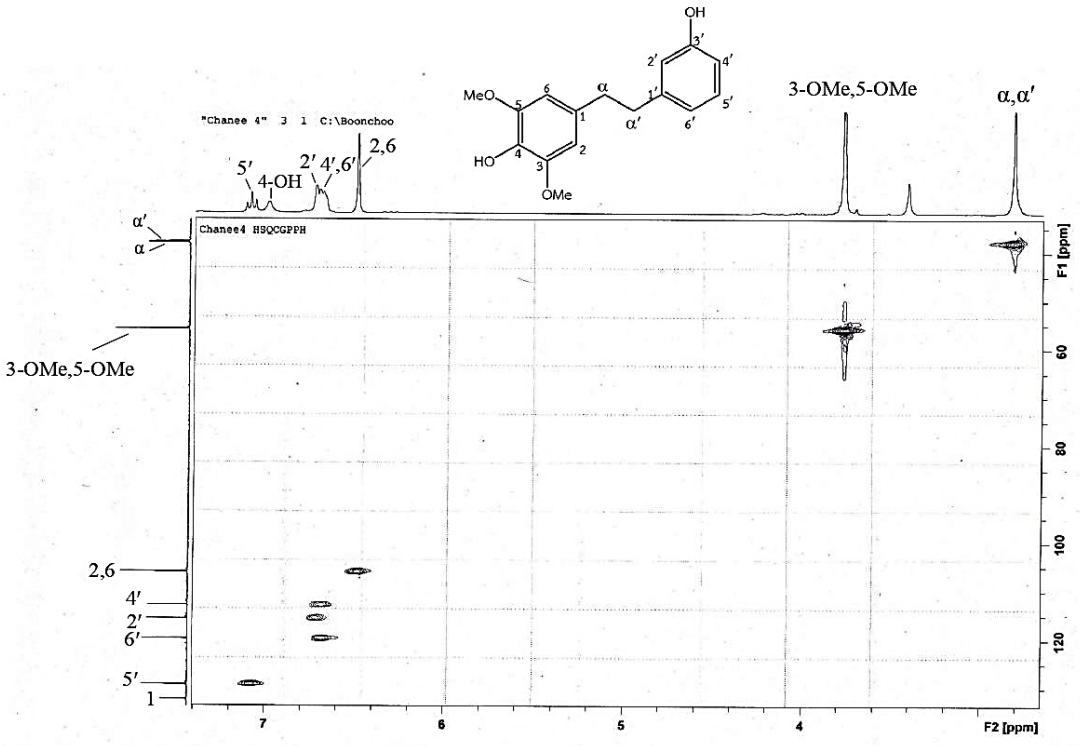

Figure 53 HSQC spectrum of **compound 5** in acetone-d_6

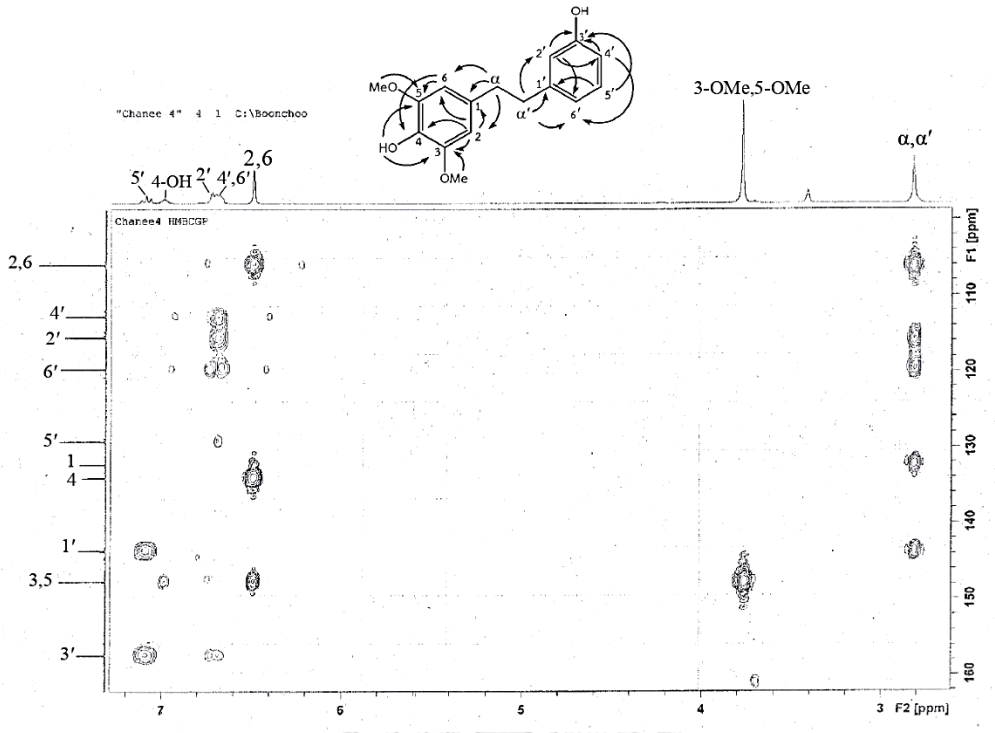

Figure 54 HMBC spectrum of **compound 5** in acetone-d_6

1.6 Structural characterization of compound 6

Compound 6 was isolated as a red amorphous solid. Its HR-ESI mass spectrum presented an $[M+Na]^+$ peak at *m/z* 561.1530 (calcd. for 561.1525, $C_{32}H_{26}O_8Na$), indicating a molecular formula of $C_{32}H_{26}O_8$ (**Figure 58**).

The ^{13}C NMR spectrum **(Figure 59)** showed only 16 signals, suggesting that **compound 6** might be a dimeric compound with two identical subunits. The ^{13}C NMR signals included 14 pairs of aromatic carbons at δ 99.6 (C-3 and C-3′), 109.1 (C-1 and C-1′), 115.8 (C-4a and C-4a′), 117.1 (C-6 and C-6′), 120.7 (C-9 and C-9′), 124.5 (C-5 and C-5′), 124.7 (C-10 and C-10′), 125.3 (C-10a and C-10a′), 126.7 (C-4b and C-4b′), 134.2 (C-8a and C-8a′), 141.1 (C-8 and C-8′), 145.8 (C-7 and C-7′), 159.5 (C-4 and C-4′) and 154.6 (C-2 and C-2′) and two pairs of methoxy carbons at δ 55.1 (4-OMe and 4′-OMe) and 60.5 (8-OMe and 8′-OMe). These NMR properties suggest two identical phenanthrene units for **compound 6**. In support of this, the ^1H NMR spectrum (**Figure 60**) showed a pair of singlet protons at δ 7.05 (2H, s, H-3/H-3′), four pairs of *ortho*-coupled doublet protons at δ 7.12 (2H, d, *J* = 9.6 Hz, H-10/H-10′), 7.27 (2H, d, *J* = 9.6 Hz, H-6/H-6′), 7.80 (2H, d, *J* = 9.6 Hz, H-9/H-9′) and 9.35 (2H, d, *J* = 9.6 Hz, H-5/H-5′) and two pairs of methoxy protons at δ 3.85 (6H, s, 8-OMe/8-OMe) and 4.22 (6H, s, 4-OMe/4′-OMe). The signal at δ 7.80 was assigned to H-9/H-9′, based on the HMBC correlations from H-9/H-9′ to C-4b/C-4b′, C-8/C-8′, C-8a/C-8a′, C-10a/C-10a′, and C-10/C-10′. The proton signal at δ 7.12 was assigned to H-10/H-10′ due to the HMBC correlations from H-10/H-10′ with C-1/C-1′, C-4a/C-4a′, C-8a/C-8a′, and C-10a/C-10a′. An HMBC cross peak was observed between C-4b/C-4b′ and H-5, H-5′ (**Figure 62**). The position of 4-OMe/4′-OMe at C-4/C-4′ was confirmed by the NOESY interaction (**Figure 63**) with H-3/H-3′ and H-5/H-5′. The carbon C-4/C-4′ were assigned at δ 159.5 from the HMBC correlation to the 4-OMe/4′-OMe protons. The NOESY

spectrum also showed interaction between 8-OMe/8′-OMe protons and H-9/H-9′. The assignment of C-8/C-8′ was confirmed from its HMBC correlation to H-6/H-6′ and H-9/H-9′. The quaternary carbon at δ 109.1 (C-1/C-1′) showed 3-bond correlations to H-10/H-10′ and H-3/H-3′. The HMBC correlations of C-2/C-2′, C-4a/C-4a′ with H-3/H-3′ were also observed.

Based on the comparison of the above spectral data and those from a previous report (Tuchinda *et al.*, 1988), **compound 6** was identified as 4,4′,8,8′-tetramethoxy[1,1′-biphenanthrene]-2,2′,7,7′-tetrol.

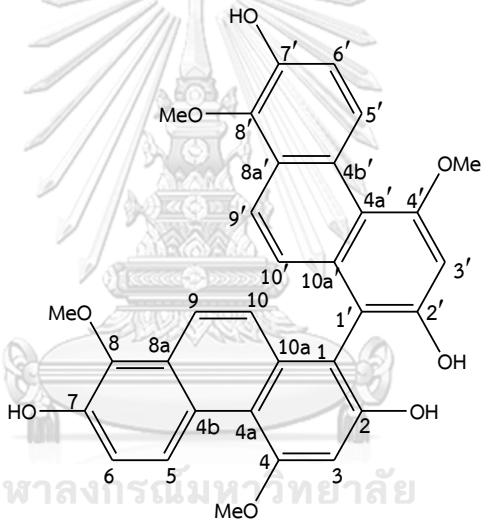

Figure 55 Chemical structure of **compound 6**

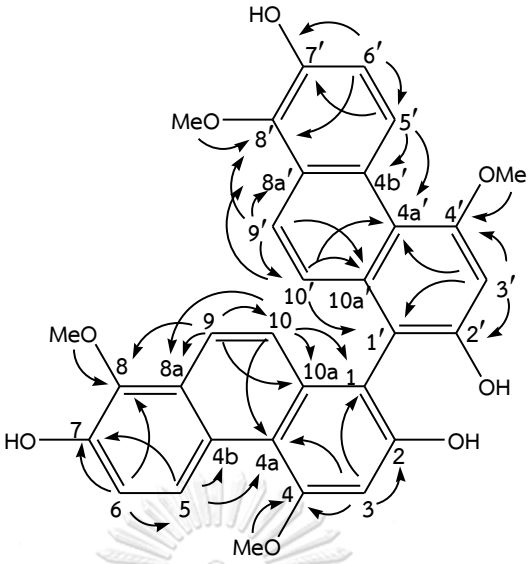

Figure 56 HMBC correlation of **compound 6**

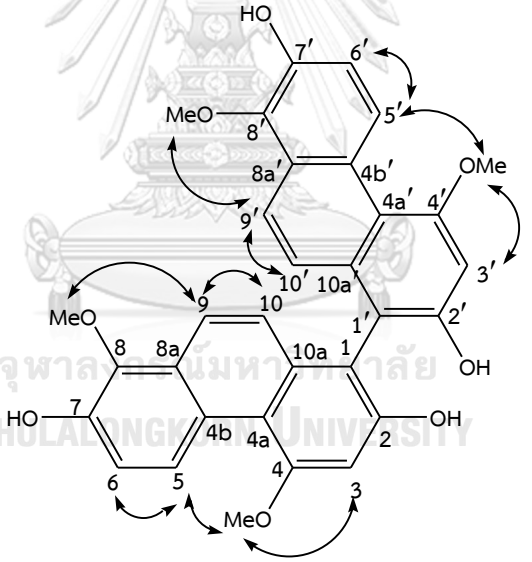

Figure 57 NOESY correlation of **compound 6**

Table 18 NMR spectral data of **compound 6** (300 MHz) and 4,4′,8,8′-tetramethoxy[1,1′-biphenanthrene]-2,2′,7,7′-tetrol (400 MHz) in acetone-d_6

Position	Compound 6		4,4′,8,8′-tetramethoxy[1,1′-biphenanthrene]-2,2′,7,7′-tetrol*
	δ_H in ppm (mult., *J* in Hz)	δ_C in ppm	δ_H in ppm (mult., *J* in Hz)
1	-	109.1	-
2	-	154.6	-
3	7.05 (s)	99.6	7.09 (s)
4	-	159.5	-
4a	-	115.8	-
4b	-	126.7	-
5	9.35 (d, *J* = 9.6 Hz)	124.5	9.39 (dd, *J* = 9.6, 0.7 Hz)
6	7.27 (d, *J* = 9.6 Hz)	117.1	7.31 (d, *J* = 9.6 Hz)
7	-	145.8	-
8	-	141.1	-
8a	-	134.2	-
9	7.80 (d, *J* = 9.6 Hz)	120.7	7.84 (dd, *J* = 9.6, 0.7 Hz)
10	7.12 (d, *J* = 9.6 Hz)	124.7	7.16 (d, *J* = 9.6 Hz)
10a	-	125.3	-
1′	-	109.1	-
2′	-	154.6	-
3′	7.05 (s)	99.6	7.09 (s)
4′	-	159.5	-

Table 18 (continued)

Position	Compound 6		4,4′,8,8′-tetramethoxy[1,1′-biphenanthrene]-2,2′,7,7′-tetrol*
	δ_H in ppm (mult., *J* in Hz)	δ_C in ppm	δ_H in ppm (mult., *J* in Hz)
4a′	-	115.8	-
4b′	-	126.7	-
5′	9.35 (d, *J* = 9.6 Hz)	124.5	9.39 (dd, *J* = 9.6, 0.7 Hz)
6′	7.27 (d, *J* = 9.6 Hz)	117.1	7.31 (d, *J* = 9.6 Hz)
7′	-	145.8	-
8′	-	141.1	-
8a′	-	134.2	-
9′	7.80 (d, *J* = 9.6 Hz)	120.7	7.84 (dd, *J* = 9.6, 0.7 Hz)
10′	7.12 (d, *J* = 9.6 Hz)	124.7	7.16 (d, *J* = 9.6 Hz)
10a′	-	125.3	-
4-OMe	4.22 (s)	55.1	4.26 (s)
4′-OMe	4.22 (s)	55.1	4.26 (s)
8-OMe	3.85 (s)	60.5	3.89 (s)
8′-OMe	3.85 (s)	60.5	3.89 (s)

* (Tuchinda *et al.*, 1988)

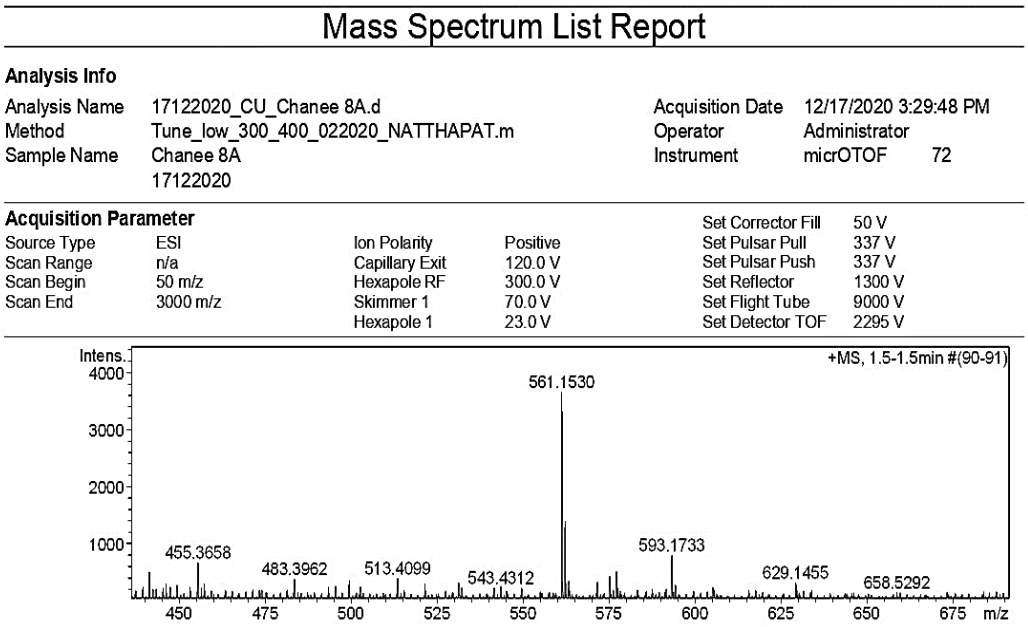

Figure 58 HR-ESI-MS spectrum of **compound 6**

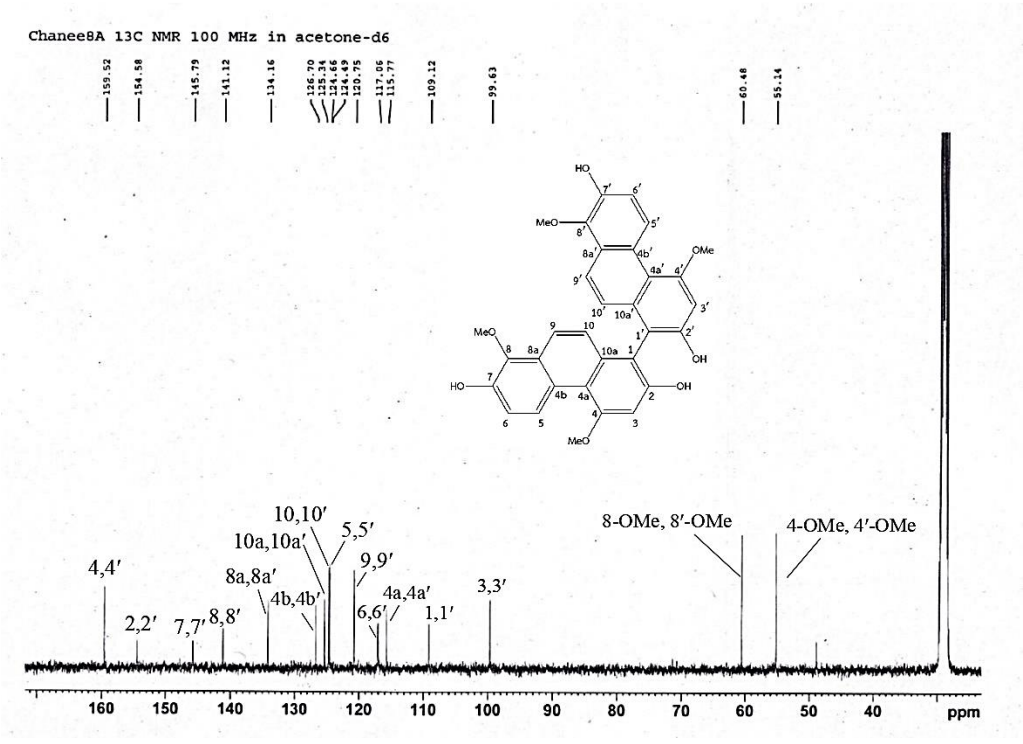

Figure 59 ^{13}C NMR spectrum of **compound 6** (75 MHz) in acetone-d_6

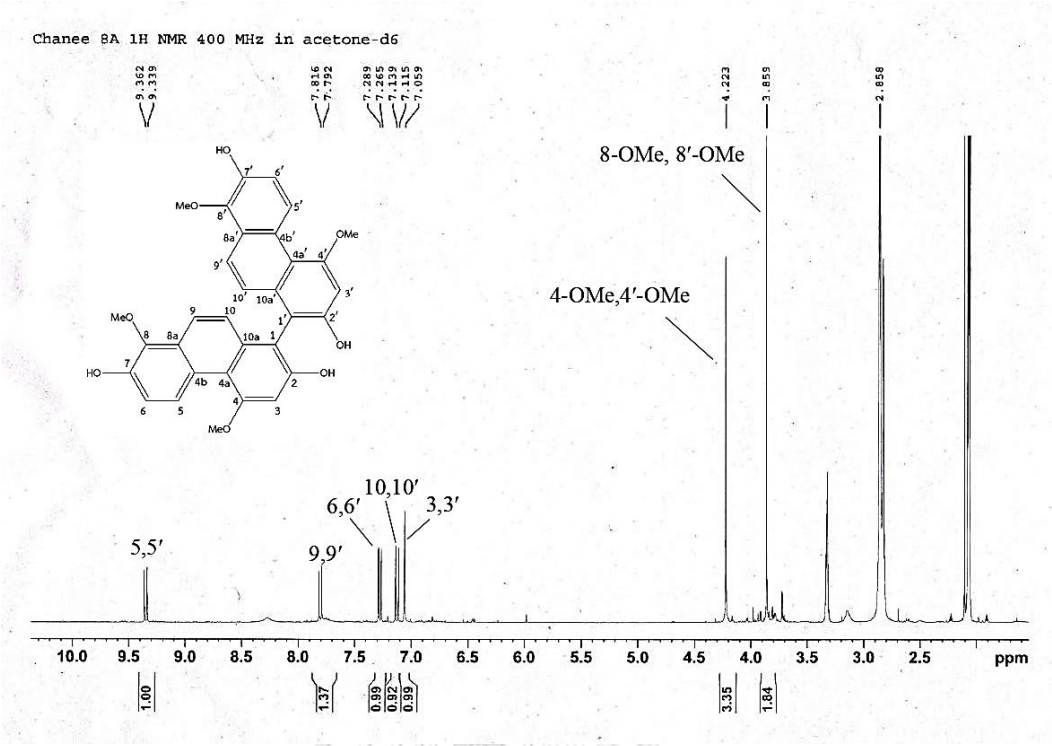

Figure 60 ^{1}H NMR spectrum of **compound 6** (300 MHz) in acetone-d_6

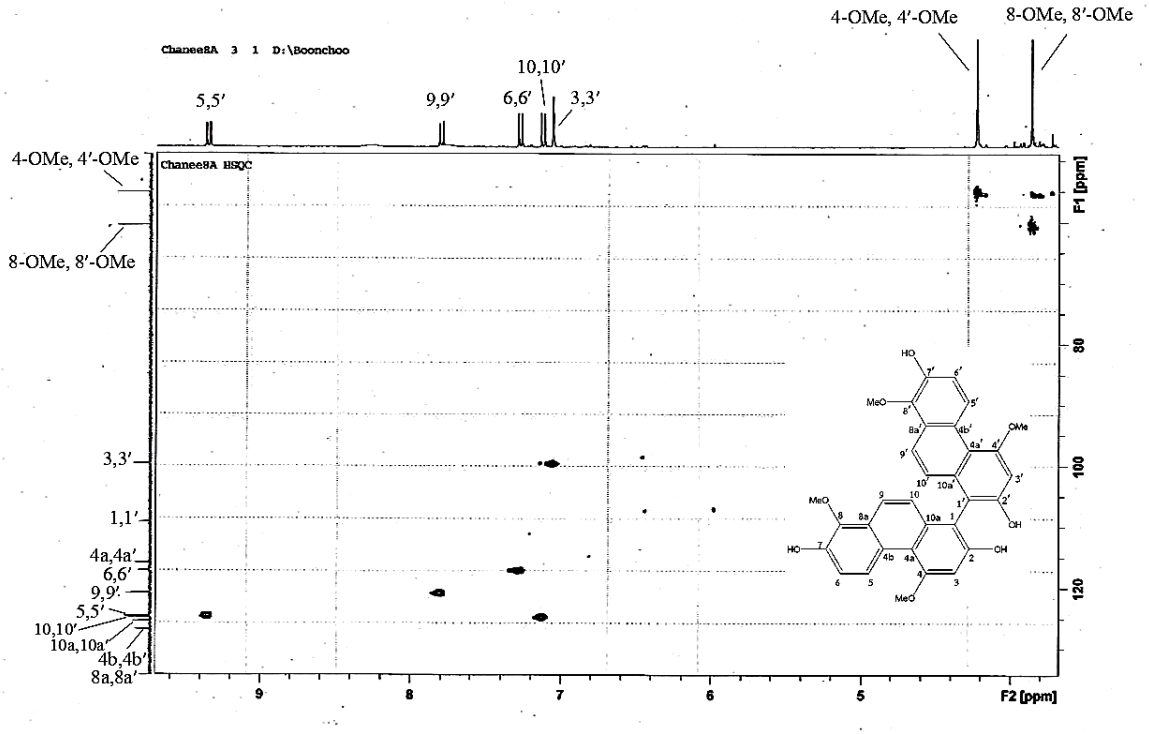

Figure 61 HSQC spectrum of **compound 6** in acetone-d_6

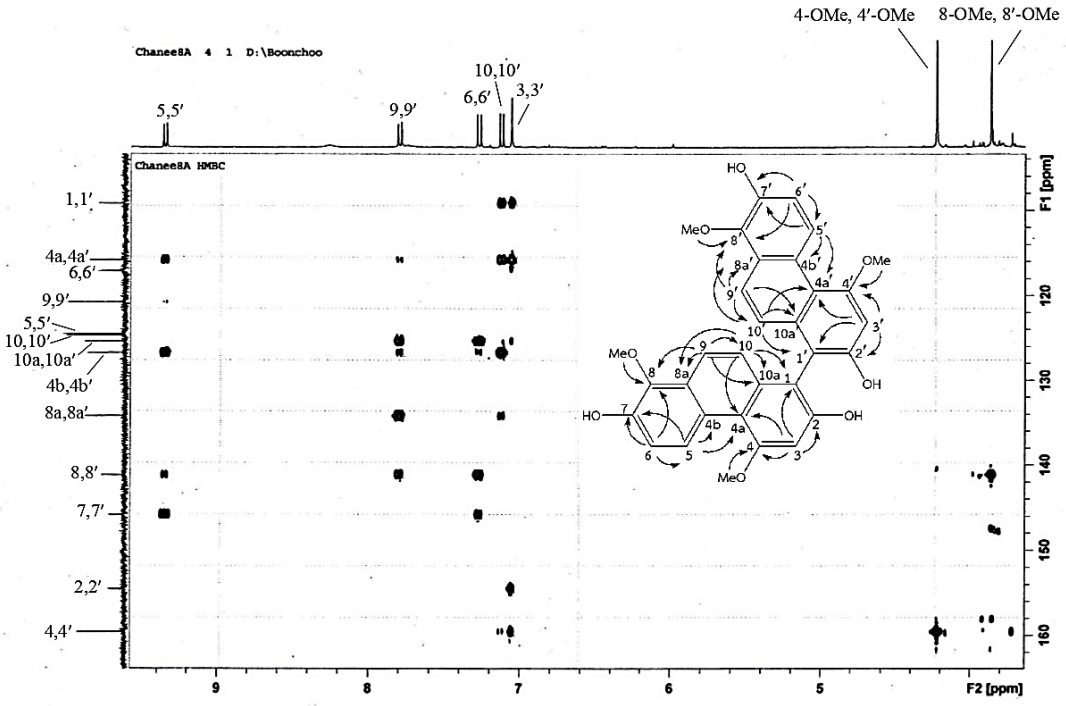

Figure 62 HMBC spectrum of **compound 6** in acetone-d_6

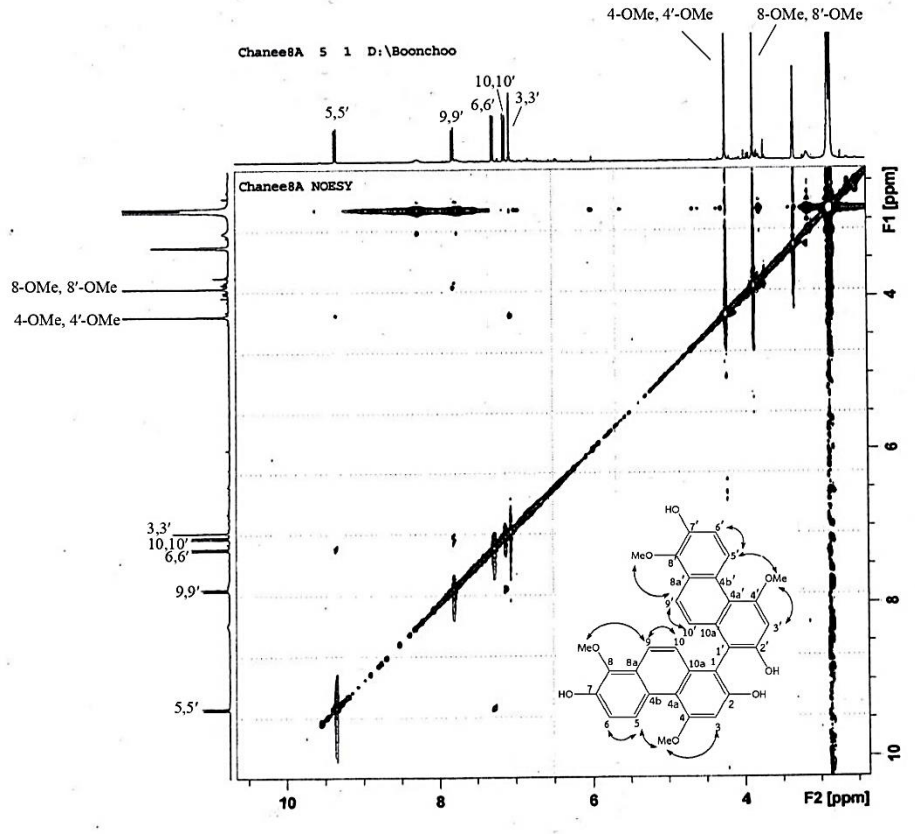

Figure 63 NOESY spectrum of **compound 6** in acetone-d_6

1.7 Structural characterization of compound 7

Compound 7 was purified as a brown amorphous solid. The sodium-adduct molecular ion $[M+Na]^+$ peak at *m/z* 501.1317 (calcd. for 501.1314, $C_{30}H_{22}O_6Na$) in the HR-ESI-MS suggested a molecular formula of $C_{30}H_{22}O_6$ (**Figure 67**).

The ^1H NMR (**Figure 68**) and ^{13}C NMR (**Figure 69**) spectra of **compound 7** showed a close resemblance to those of **compound 6**, suggesting a symmetrical dimeric phenanthrene structure. The only difference was the absence of signals for the two methoxy groups on C-8/C-8′ in **compound 7**. This was supported by the presence of a pair of *meta*-coupled aromatic doublet protons at δ 7.03 (2H, d, *J* = 3.0 Hz, H-8 and H-8′) on ring A/A′ of this biphenanthrene. The ^1H NMR signals of δ 7.02 (2H, d, *J* = 9.0 Hz, H-10/H-10′) and 7.38 (2H, d, *J* = 9.0 Hz, H-9/H-9′) further confirmed compound **7** as a dimeric phenanthrene. The assignment of H-9/H-9′ was based on the 2-bond correlations with the carbons at δ 125.5 (C-10/C-10′) and 134.1 (C-8a/C-8a′) and 3-bond correlations with the carbons at δ 111.9 (C-8/C-8′), 125.3 (C-4b/C-4b′) and 135.1 (C-10a/C-10a′). From the HMBC (**Figure 71**) correlation with the carbons at δ 134.1 (C-8a/C-8a′) and 109.9 (C-1/C-1′), H-10 and H-10′ were assigned at δ 7.02. The assignments of C-4b/C-4b′ at δ 125.3 was supported by the HMBC correlations with H-6/H-6′, H-8/H-8′ and H-9/H-9′.

By comparison of the above spectral evidence with literature values (Xue *et al.*, 2006), **compound 7** was identified as 2,2′,7,7′-tetrahydroxy-4,4′-dimethoxy-1,1′-biphenanthrene and its trivial name is cirrhopetalanthin.

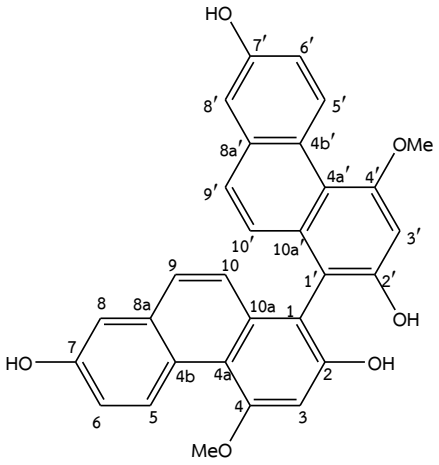

Figure 64 Chemical structure of **compound 7**

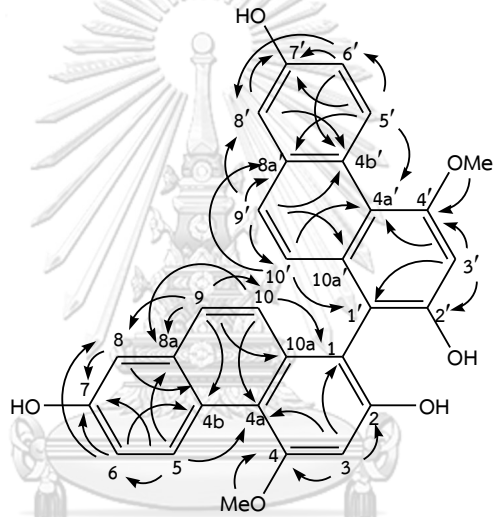

Figure 65 HMBC correlation of **compound 7**

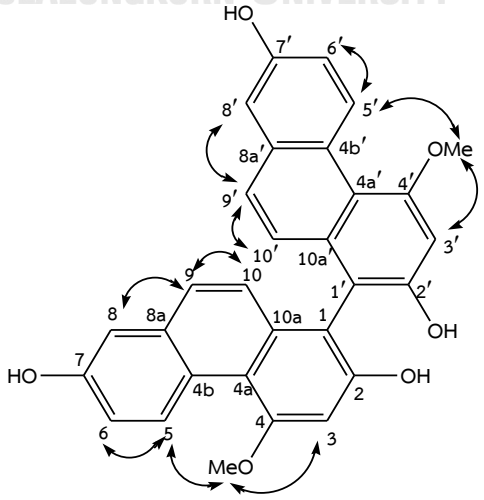

Figure 66 NOESY correlation of **compound 7**

Table 19 NMR spectral data of **compound 7** (500 MHz in acetone-d_6) and 2,2′,7,7′-tetrahydroxy-4,4′-dimethoxy-1,1′-biphenanthrene (500 MHz in methanol-d_4)

Position	Compound 7		2,2′,7,7′-tetrahydroxy-4,4′-dimethoxy-1,1′-biphenanthrene*	
	δ_H in ppm (mult., *J* in Hz)	δ_C in ppm	δ_H in ppm (mult., *J* in Hz)	δ_C in ppm
1	-	109.9	-	111.5
2	-	155.1	-	154.6
3	7.02 (s)	100.3	6.94 (s)	100.3
4	-	160.2	-	160.5
4a	-	116.5	-	117
4b	-	125.3	-	125.8
5	9.51 (d, *J* = 10 Hz)	130.2	9.42 (d, *J* = 9.0 Hz)	130.5
6	7.19 (dd, *J* = 10, 3.0 Hz)	117.4	7.05 (dd, *J* = 9.0, 3.0 Hz)	117.3
7	-	155.3	-	155.4
8	7.03 (d, *J* = 3.0 Hz)	111.9	7.01 (d, *J* = 3.0 Hz)	112
8a	-	134.1	-	134.6
9	7.38 (d, *J* = 9.0 Hz)	128.3	7.25 (d, *J* = 9.5 Hz)	128.4
10	7.02 (d, *J* = 9.0 Hz)	125.5	6.94 (d, *J* = 9.5 Hz)	125.9
10a	-	135.1	-	135.5
1′	-	109.9	-	111.5
2′	-	155.1	-	154.6
3′	7.02 (s)	100.3	6.94 (s)	100.3
4′	-	160.2	-	160.5
4a′	-	116.5	-	117

Table 19 (continued)

Position	Compound 7		2,2′,7,7′-tetrahydroxy-4,4′-dimethoxy-1,1′-biphenanthrene*	
	δ_H in ppm (mult., *J* in Hz)	δ_C in ppm	δ_H in ppm (mult., *J* in Hz)	δ_C in ppm
4b′	-	125.3	-	125.8
5′	9.51 (d, *J* = 10 Hz)	130.2	9.42 (d, *J* = 9.0 Hz)	130.5
6′	7.19 (dd, *J* = 10, 3.0 Hz)	117.4	7.05 (dd, *J* = 9.0, 3.0 Hz)	117.3
7′	-	155.3	-	155.4
8′	7.03 (d, *J* = 3.0 Hz)	111.9	7.01 (d, *J* = 3.0 Hz)	112
8a′	-	134.1	-	134.6
9′	7.38 (d, *J* = 9.0 Hz)	128.3	7.25 (d, *J* = 9.5 Hz)	128.4
10′	7.02 (d, *J* = 9.0 Hz)	125.5	6.94 (d, *J* = 9.5 Hz)	125.9
10a′	-	135.1	-	135.5
4-OMe	4.19 (s)	55.9	4.12 (s)	56.1
4′-OMe	4.19 (s)	55.9	4.12 (s)	56.1

* (Xue *et al.*, 2006)

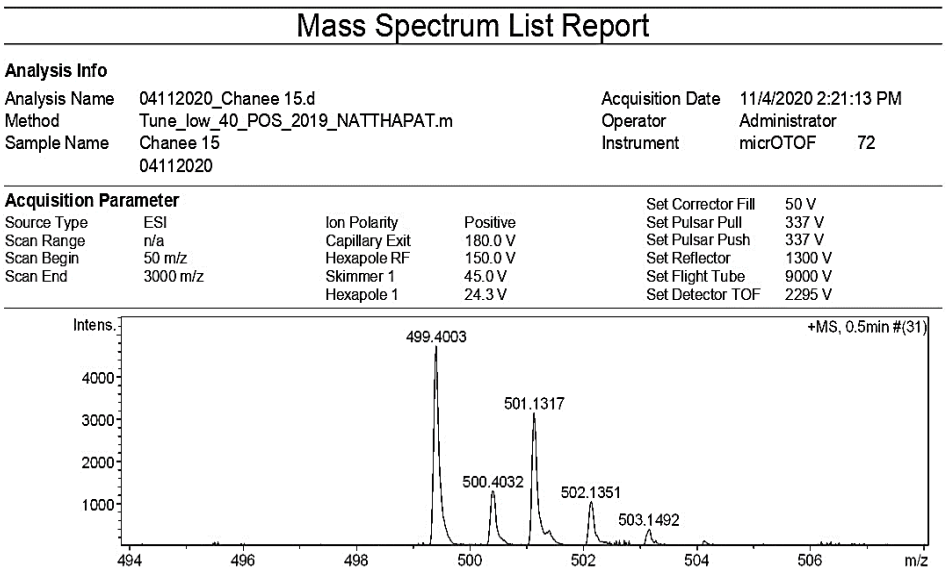

Figure 67 HR-ESI-MS spectrum of **compound 7**

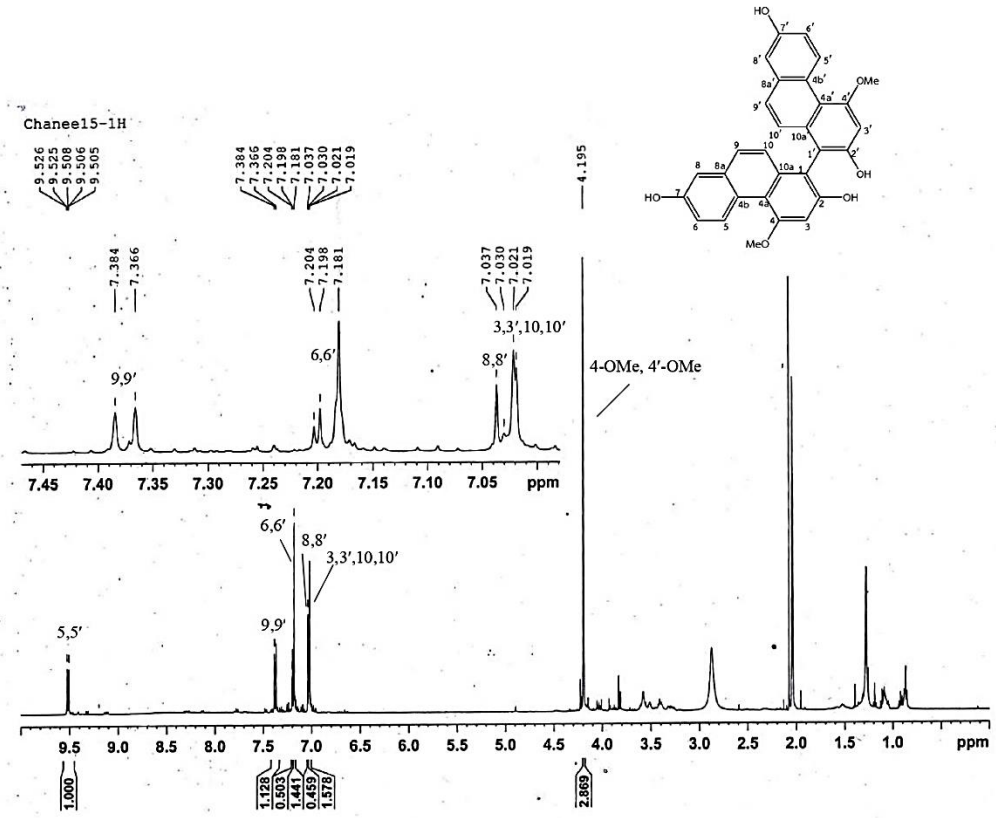

Figure 68 ^{1}H NMR spectrum of **compound 7** (500 MHz) in acetone-d_6

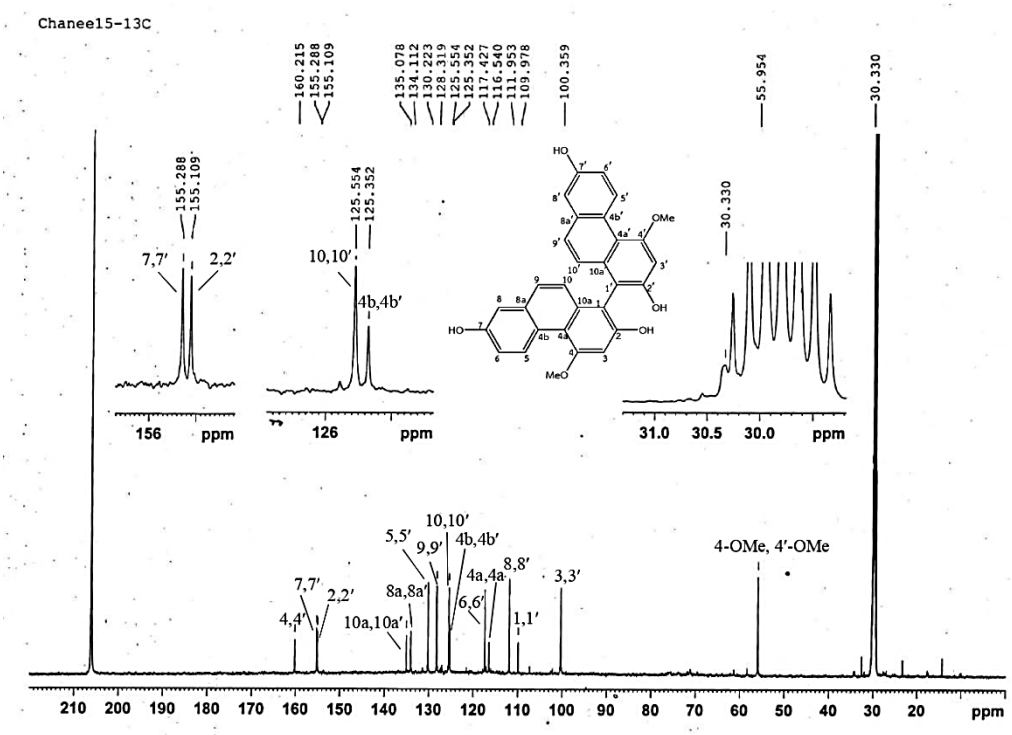

Figure 69 ^{13}C NMR spectrum of **compound 7** (125 MHz) in acetone-d_6

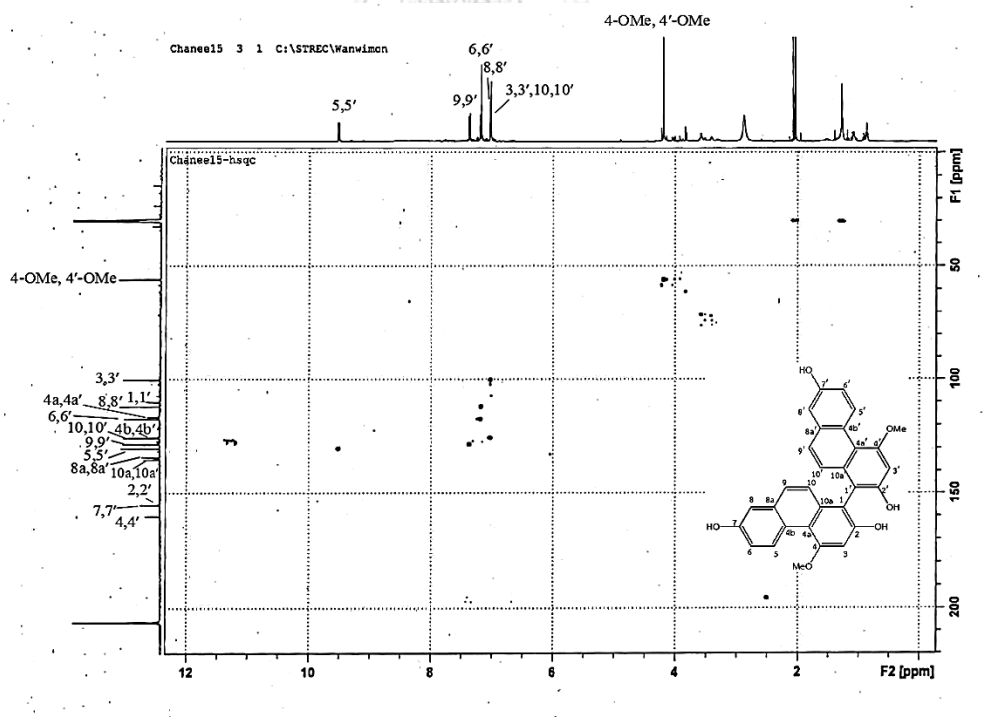

Figure 70 HSQC spectrum of **compound 7** in acetone-d_6

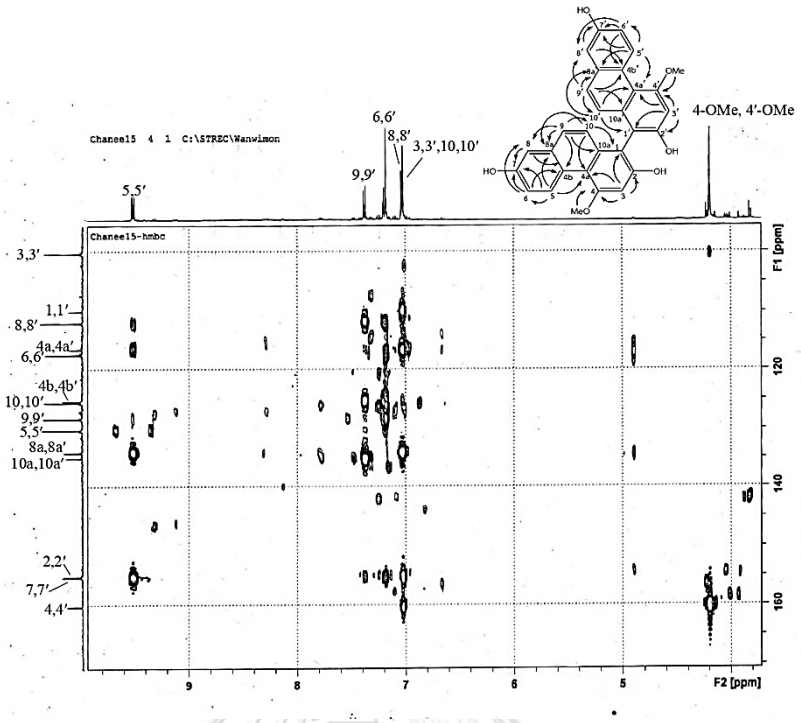

Figure 71 HMBC spectrum of **compound 7** in acetone-d_6

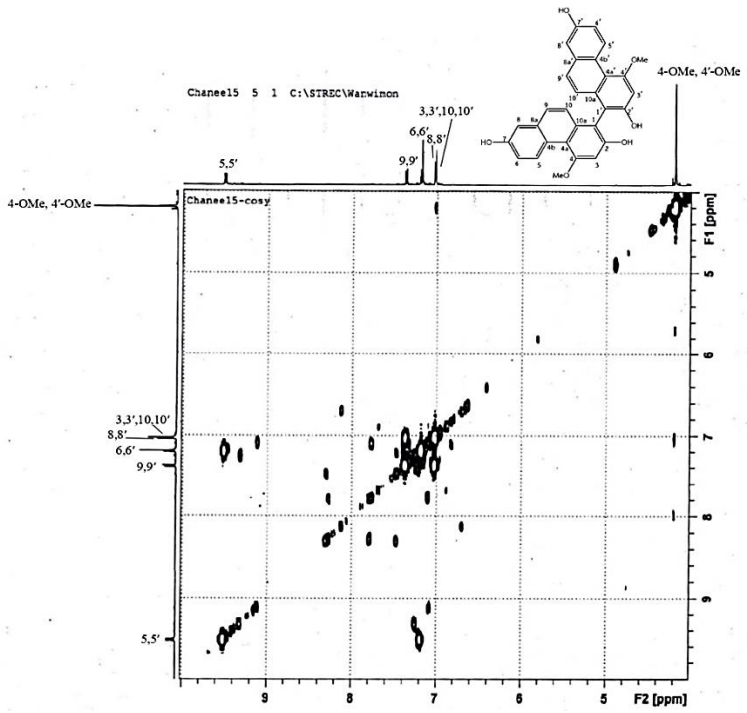

Figure 72 COSY spectrum of **compound 7** in acetone-d_6

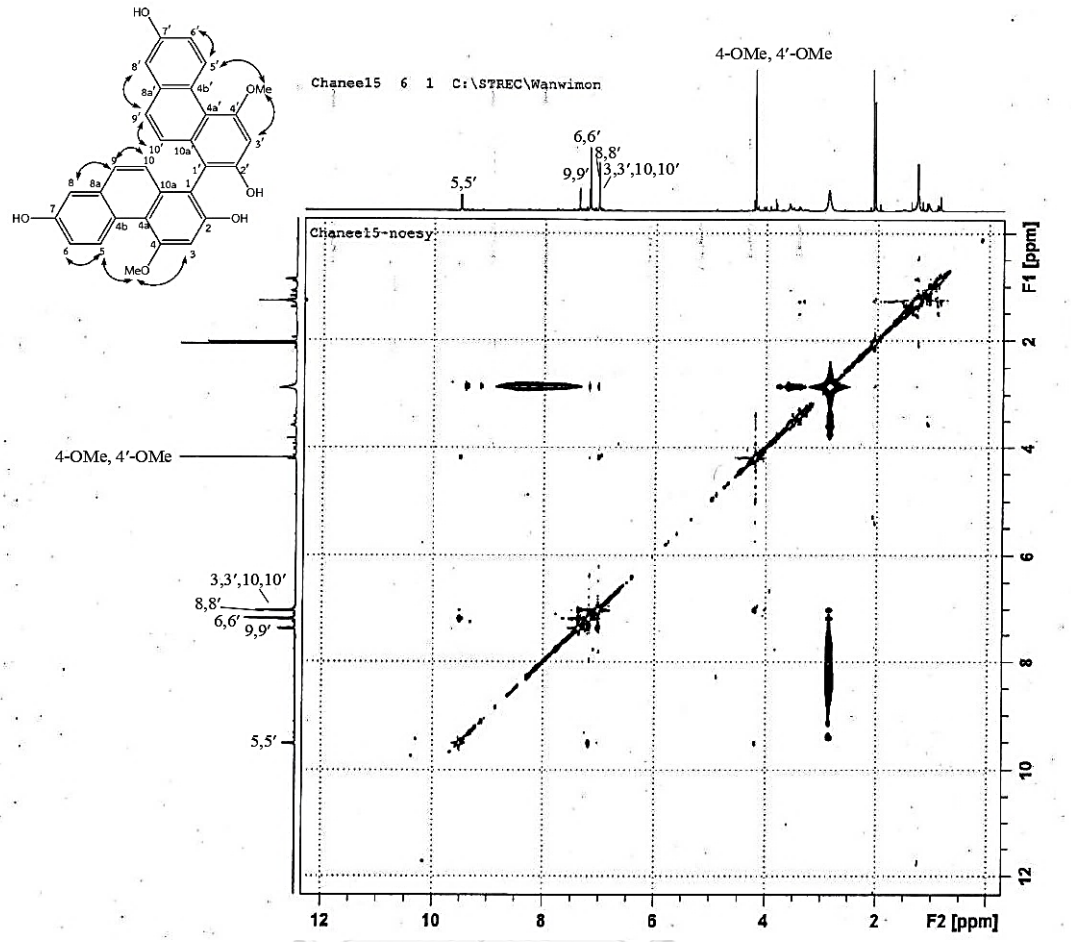

Figure 73 NOESY spectrum of **compound 7** in acetone-d_6

1.8 Structural characterization of compound 8

Compound 8 was obtained as a brown amorphous solid. The $[M+Na]^+$ peak at *m/z* 531.1425 (calcd. for 531.1419, $C_{31}H_{24}O_7Na$) in the HR-ESI-MS indicated a molecular formula of $C_{31}H_{24}O_7$ (**Figure 77**).

^1H NMR (**Figure 78**) and ^{13}C NMR signals (**Figure 79**) of **compound 8** resembled those of **compound 6** (4,4′,8,8′-tetramethoxy[1,1′-biphenanthrene]-2,2′,7,7′-tetrol) and **compound 7** (2,2′,7,7′-tetrahydroxy-4,4′-dimethoxy-1,1′-biphenanthrene), two biphenanthrenes isolated from this orchid. The ^1H NMR signals at δ 7.38 (1H, d, *J* = 9.0 Hz, H-9), 7.03 (1H, d, *J* = 9.0 Hz, H-10), 7.77 (1H, d, *J* = 9.5 Hz, H-9′) and 7.09 (1H, d, *J* = 9.5 Hz, H-10′) suggest **compound 8** as a dimeric phenanthrene. The assignment of H-9 was based on its HMBC (**Figure 81**) correlation with C-8 (δ 112.0), C-4b (δ 125.5) and C-10a (δ 135.1). On the second phenanthrene unit, H-10′ was assigned to δ 7.09 from the 3-bond correlations of H-10′ to C-1′ (109.9), C-4a′ (116.6) and C-8a′ (127.6). The substitution of 8′-OMe at C-8′ (δ 142.0) was supported by the NOESY (**Figure 83**) interaction with H-9′ and 7′-OH.

Based on the above spectral evidence and ^1H and the ^{13}C spectral data described in a previous study (Lin *et al.*, 2016), **compound 8** was determined to be bleformin G.

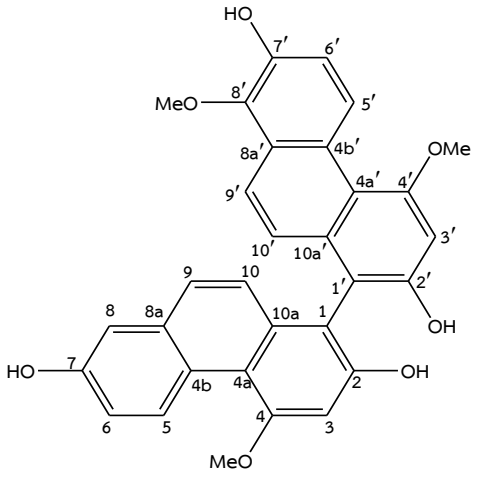

Figure 74 Chemical structure of **compound 8**

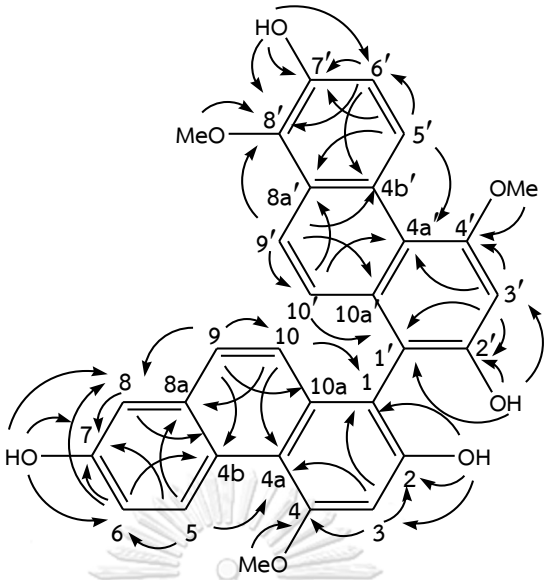

Figure 75 HMBC correlation of **compound 8**

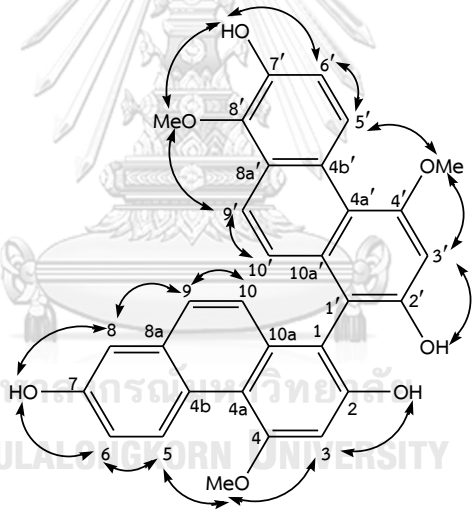

Figure 76 NOESY correlation of **compound 8**

Table 20 NMR spectral data of **compound 8** (500 MHz) and bleformin G (700 MHz) in acetone-d_6

Position	Compound 8		Bleformin G*	
	δ_H in ppm (mult., *J* in Hz)	**δ_C in ppm**	**δ_H in ppm (mult., *J* in Hz)**	**δ_C in ppm**
1	-	110.0	-	110.0
2	-	155.2	-	155.1
3	7.02 (s)	100.5	7.01 (s)	100.4
4	-	160.4	-	160.3
4a	-	116.7	-	116.4
4b	-	125.5	-	125.3
5	9.51 (d, *J* = 8.5 Hz)	130.2	9.51 (d, *J* = 7.0 Hz)	130.2
6	7.19 (dd, *J* = 8.5, 3.0 Hz)	117.5	7.19 (dd, *J* = 7.0, 2.8 Hz)	117.4
7	-	155.3	-	155.3
8	7.18 (s)	112.0	7.18 (d, *J* = 2.8 Hz)	111.9
8a	-	134.1	-	134.1
9	7.38 (d, *J* = 9.0 Hz)	128.4	7.38 (d, *J* = 7.0 Hz)	128.3
10	7.03 (d, *J* = 9.0 Hz)	125.5	7.02 (d, *J* = 7.0Hz)	125.5
10a	-	135.1	-	135.0
1′	-	109.9	-	110.1
2′	-	155.1	-	155.4
3′	7.02 (s)	100.4	7.03 (s)	100.3
4′	-	160.3	-	160.1
4a′	-	116.6	-	116.5

Table 20 (continued)

Position	Compound 8		Bleformin G*	
	δ_H in ppm (mult., *J* in Hz)	δ_C in ppm	δ_H in ppm (mult., *J* in Hz)	δ_C in ppm
4b′	-	126.2	-	126.1
5′	9.31 (d, *J* = 9.0 Hz)	125.4	9.32 (d, *J* = 7.0 Hz)	125.4
6′	7.24 (d, *J* = 9.0 Hz)	117.9	7.25 (d, *J* = 7.0 Hz)	117.9
7′	-	146.6	-	146.6
8′	-	142.0	-	141.9
8a′	-	127.6	-	127.5
9′	7.77 (d, *J* = 9.5 Hz)	121.6	7.77 (d, *J* = 7.0 Hz)	121.5
10′	7.09 (d, *J* = 9.5 Hz)	125.5	7.09 (d, *J* = 7.0 Hz)	125.5
10a′	-	135.0	-	135.1
4-OMe	4.20 (s)	56.0	4.20 (s)	56.0
4′-OMe	4.19 (s)	56.0	4.19 (s)	55.9
8′-OMe	3.83 (s)	61.3	3.82 (s)	61.3
2-OH	7.68 (s)	-	-	-
7-OH	8.50 (s)	-	-	-
2′-OH	7.65 (s)	-	-	-
7′-OH	8.21 (s)	-	-	-

*(Lin *et al.*, 2016)

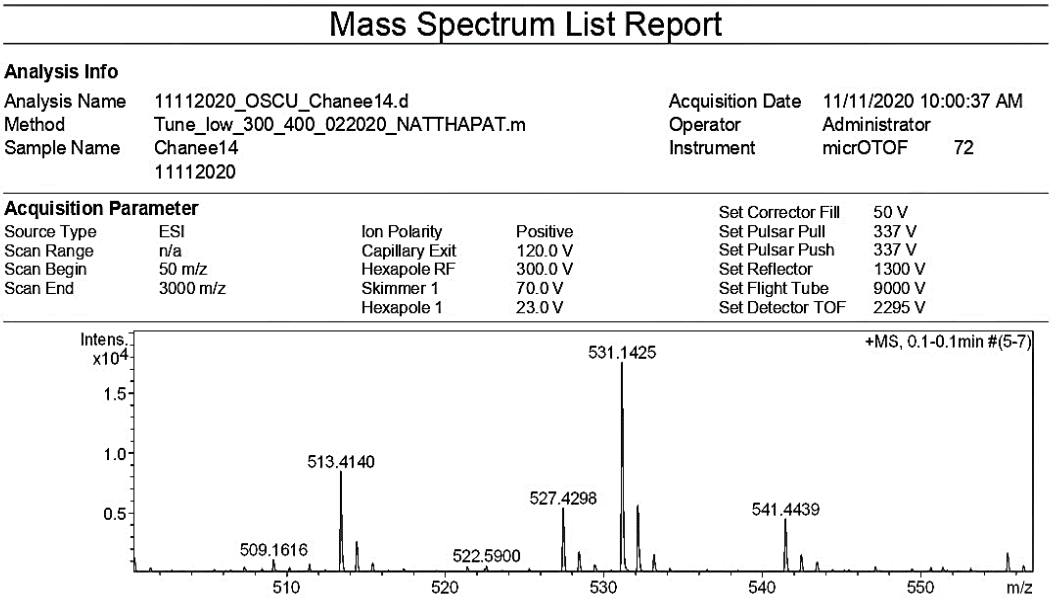

Mass Spectrum List Report

Analysis Info

Analysis Name	11112020_OSCU_Chanee14.d	Acquisition Date	11/11/2020 10:00:37 AM
Method	Tune_low_300_400_022020_NATTHAPAT.m	Operator	Administrator
Sample Name	Chanee14 11112020	Instrument	micrOTOF 72

Acquisition Parameter

Source Type	ESI	Ion Polarity	Positive	Set Corrector Fill	50 V
Scan Range	n/a	Capillary Exit	120.0 V	Set Pulsar Pull	337 V
Scan Begin	50 m/z	Hexapole RF	300.0 V	Set Pulsar Push	337 V
Scan End	3000 m/z	Skimmer 1	70.0 V	Set Reflector	1300 V
		Hexapole 1	23.0 V	Set Flight Tube	9000 V
				Set Detector TOF	2295 V

Figure 77 HR-ESI-MS spectrum of **compound 8**

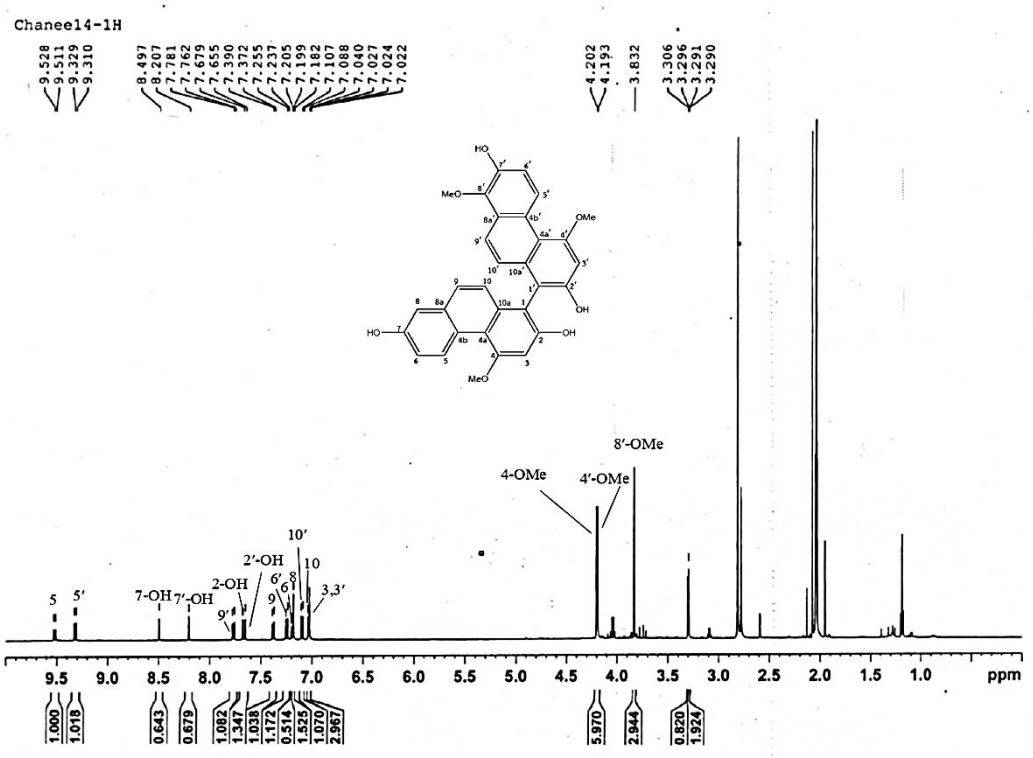

Figure 78 ^{1}H NMR spectrum of **compound 8** (500 MHz) in acetone-d_6

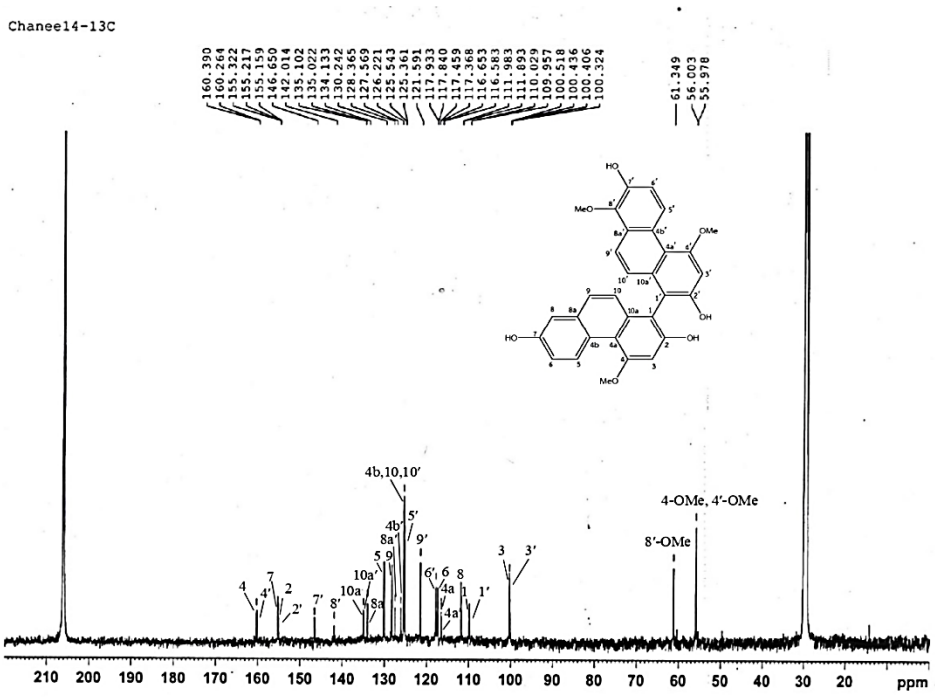

Figure 79 ^{13}C NMR spectrum of **compound 8** (125 MHz) in acetone-d_6

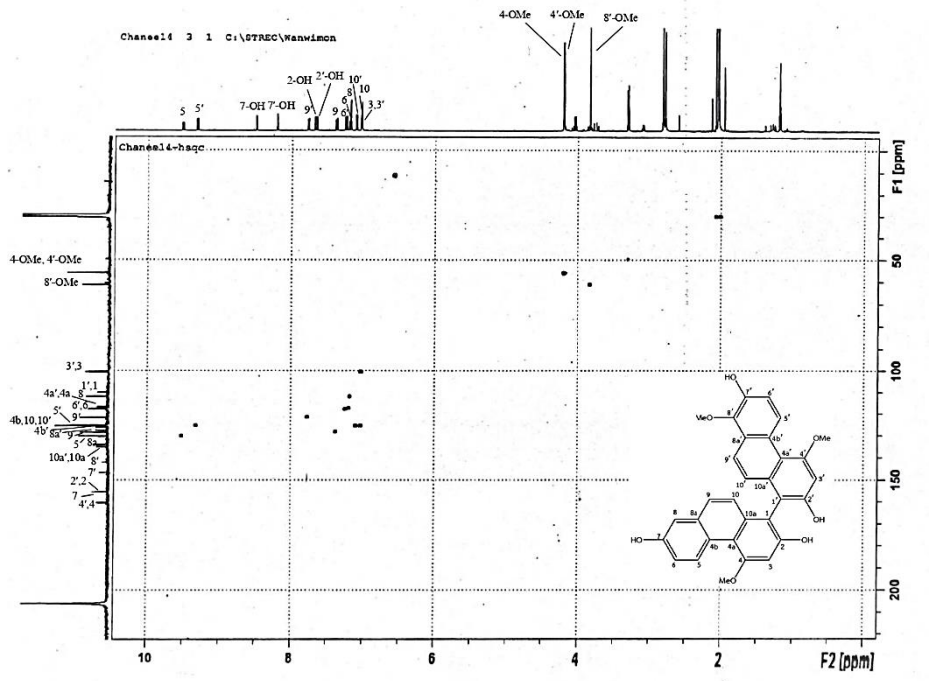

Figure 80 HSQC spectrum of **compound 8** in acetone-d_6

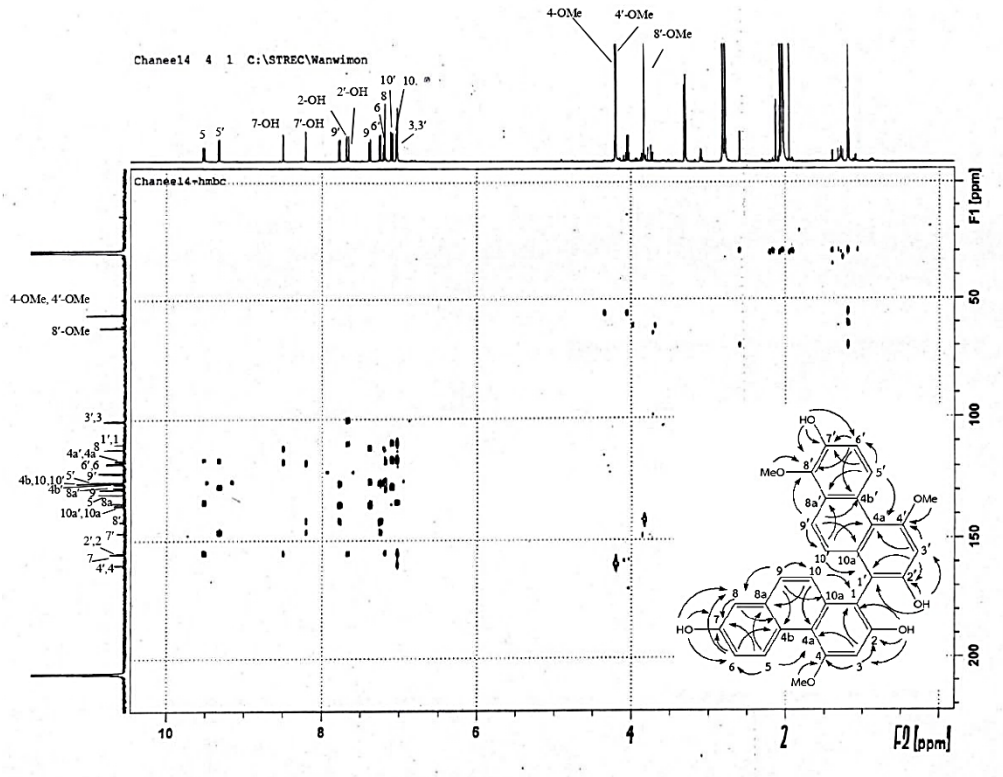

Figure 81 HMBC spectrum of **compound 8** in acetone-d_6

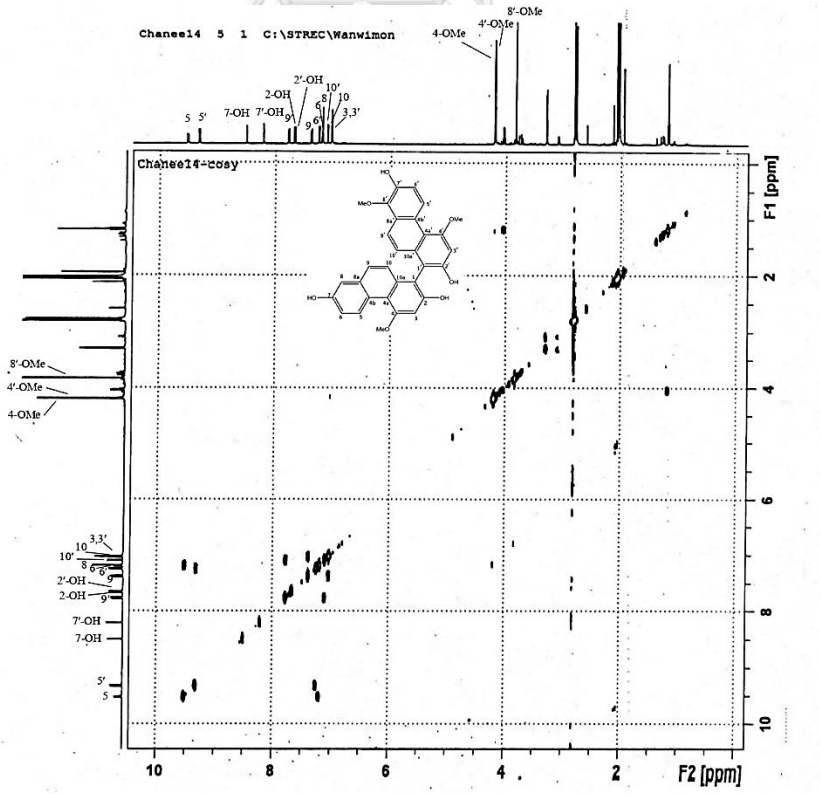

Figure 82 COSY spectrum of **compound 8** in acetone-d_6

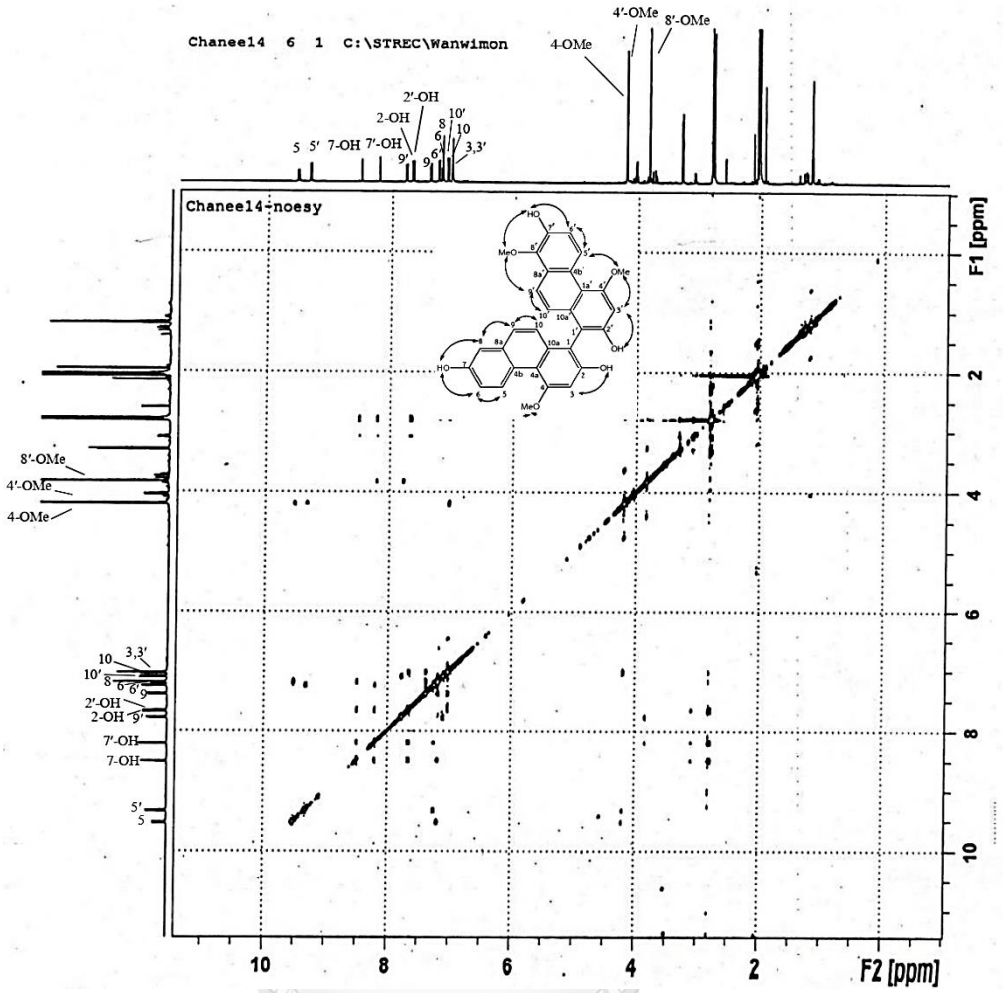

Figure 83 NOESY spectrum of **compound 8** in acetone-d_6

2. Evaluation of *in vitro* pancreatic lipase inhibitory activity

The methanol, ethyl acetate and n-butanol extracts (see section 3.1) were evaluated for *in vitro* pancreatic lipase inhibitory activity (**Table 21**). The ethyl acetate extract showed 70% inhibitory activity at 100 µg/ml and was considered as active, while the methanol and n-butanol extracts were inactive. Therefore, the ethyl acetate extract was further investigated. Through chromatographic separation, eight compounds were isolated and evaluated for PL inhibitory activity. Moscatin (**2**), 2,5-dihydroxy-4,9-dimethoxyphenanthrene (**3**) and 4,4′,8,8′-tetramethoxy[1,1′-biphenanthrene]-2,2′,7,7′-tetrol (**6**) showed more than 70% pancreatic lipase inhibitory activity *in vitro* assay. Using two-fold serial dilution, the IC_{50} values of compounds **2** and **3** were determined in comparison to that of orlistat (**Table 22**). However, the IC_{50} value of compound **6** was not determined due to its limited amount.

Table 21 Preliminary screening result of extracts from *Dendrobium senile* in lipase inhibition assay

Extracts	% Lipase inhibition (at 100 µg/ml)
Methanol	No activity
Ethyl acetate	70.00
n-butanol	No activity
Aqueous	Not determined
Orlistat (Positive control)	96.88

Table 22 IC_{50} values of **compounds 1-8** isolated from *Dendrobium senile* in lipase inhibition assay

Compounds	Pancreatic lipase inhibition IC_{50} (μM)
2,5,7-trihydroxy-4-methoxyphenanthrene (**1**)	No activity
Moscatin (**2**)	57.6 ± 3.3
2,5-dihydroxy-4,9-dimethoxyphenanthrene (**3**)	58.6 ± 3.4
Moscatilin (**4**)	No activity
Aloifol I (**5**)	No activity
4,4′,8,8′-tetramethoxy[1,1′-biphenanthrene]-2,2′,7,7′-tetrol (**6**)	Not determined
2,2′,7,7′-tetrahydroxy-4,4′-dimethoxy-1,1′-biphenanthrene (**7**)	No activity
Bleformin G (**8**)	No activity
Orlistat	0.031 ± 0.004

As described in **Table 22**, the two phenanthrenes namely moscatin (**2**) and 2,5-dihydroxy-4,9-dimethoxyphenanthrene (**3**) showed noticeable pancreatic lipase inhibition with IC_{50} values of 57.6 ± 3.3 and 58.6 ± 3.4 μM, respectively. The relatively similar IC_{50} values of both compounds suggest that an additional methoxy substitution on C-9 of 2,5-dihydroxy-4,9-dimethoxyphenanthrene (**3**) has no effect on the potency of the compound by comparing to moscatin (**2**) which does not include a methoxy group on C-9. As reported on the influence of the number and position of phenolic hydroxy groups in the lipase inhibition (Buchholz & Melzig, 2015), it was observed that 2,5,7-trihydroxy-4-methoxyphenanthrene (1) was devoid of activity due to the position of a hydroxy group on C-7 through comparison to the two active

phenanthrenes although the number of hydroxy groups of a compound positively influences on the potency of the lipase inhibition.

A principle of the impact of hydroxy groups for the greater lipase inhibition and methoxy groups for the reduction of potency as reported by Buchholz & Melzig, 2015 was significantly seen in the two inactive bibenzyls based on the previous report for the positive effect of a bibenzyl derivative namely dendrosinen B from *Dendrobium infundibulum* on the lipase inhibition by Na Ranong et al., 2019. The chemical structure of the reported dendrosinen B consists of three hydroxy substitutions on C-3, C-4 and C-3′ and a methoxy group on C-5. However, from this study, there were no inhibitory activities of both moscatilin (**4**) and aloifol I (**5**) on the lipase. This may be due to the fact that moscatilin (**4**) comprises of three methoxy substitutions on C-3, C-5 and C-3′ with only two hydroxy groups on both C-4 and C-4′**.** As for aloifol I (**5**), it may be due to the attachment of a methoxy group on C-3 which is different to the reported dendrosinen B that includes a hydroxy group on C-3 although the remaining substitutions are similar in both compounds.

Moreover, the IC_{50} of 4,4′,8,8′-tetramethoxy[1,1′-biphenanthrene]-2,2′,7,7′-tetrol (**6**) was not determined due to its limited amount, however, it showed 75 % at 100 µg/ml in the evaluation of lipase inhibition assay. On the other hand, the remaining two dimeric phenanthrenes including 2,2′,7,7′-tetrahydroxy-4,4′-dimethoxy-1,1′-biphenanthrene (**7**) and bleformin G (**8**) did not exhibit the lipase inhibitory activity. Therefore, in order to determine the structure-activity relationship (SAR) of these dimeric phenanthrenes on their lipase inhibition, it was expected that the inhibitory effect of 4,4′,8,8′-tetramethoxy[1,1′-biphenanthrene]-2,2′,7,7′-tetrol (**6**) was due to the number and position of its two additional methoxy groups on C-8 and C-8′, both of which are excluded in 2,2′,7,7′-tetrahydroxy-4,4′-dimethoxy-1,1′-biphenanthrene (**7**) and only one additional methoxy group is substituted on C-8′ of

bleformin G (**8**). This finding is similar to a previous report on the effect of one or more hydrophobic methoxy groups on the potency of the lipase inhibition by enhancing the compound's binding to the hydrophobic region of the lipase (Huang *et al.*, 2020). In this fact, **compound 6** exhibited the lipase inhibition which may also be affected by the position of the methoxy substituents. To summarize the SAR of all of the isolated compounds, both the number and position of hydroxy and methoxy groups of a compound greatly impact on the lipase inhibitory activity.

Until now, there have been several biological investigations for all of these 7 known compounds. It has been observed that moscatin (**2**) and moscatilin (**4**) possess both anti-platelet aggregation and anti-oxidant activities (Chen *et al.*, 1994; Ono *et al.*, 1995). Additionally, moscatilin (**4**) manifests for its apoptosis in melanoma and pancreatic cancer cells, anti-metastasis on human hepatocellular carcinoma, anti-migratory activity on breast cancer cells, anti-angiogenesis against non-small cell lung cancer cells, anti-mutagenic property on human colorectal cancer cells and then neuroprotective effect (Cardile *et al.*, 2020; Chen *et al.*, 2008a; Lai *et al.*, 2020a; Pai *et al.*, 2013; Tsai *et al.*, 2010; Yu *et al.*, 2021; Zhang *et al.*, 2017b). Also, the cytotoxic effects of all of these compounds except 4,4′,8,8′-tetramethoxy[1,1′-biphenanthrene]-2,2′,7,7′-tetrol (**6**) have been reported (Chen *et al.*, 2014; Chen *et al.*, 2008e; Lai *et al.*, 2020a; Lee *et al.*, 2020; Liu *et al.*, 2016). **Compounds 3, 6, 7 and 8** show anti-inflammatory properties (Bae *et al.*, 2017; Lin *et al.*, 2016; Sun *et al.*, 2021; Suzuki *et al.*, 2012). Besides, the anti-bacterial activity against gram-positive bacteria have been investigated for **compounds 6 and 7** (Qian *et al.*, 2015). Moreover, the anti-oxidant and glucose-uptake stimulatory activities have been studied for 2,5-dihydroxy-4,9-dimethoxyphenanthrene (**3**) and aloifol I (**5**), respectively (San *et al.*, 2020; Zhang *et al.*, 2008c).

CHAPTER V

CONCLUSION

Before this study, *Dendrobium senile* had no reports of chemical constituents and biological activities. In the present investigation, the dried materials of *Dendrobium senile* were macerated with methanol. The dried methanol extract was partitioned by solvent extraction to provide ethyl acetate, n-butanol and aqueous extracts. All the extracts were screened for pancreatic lipase inhibitory activity at 100 µg/ml, but only the ethyl acetate extract was active showing 70% inhibitory effect and therefore was further investigated to identify the active principles. Eight pure compounds were isolated and structurally characterized through analysis of the NMR, UV, IR and MS spectral data. The isolated compounds were a new phenanthrene namely 2,5,7-trihydroxy-4-methoxyphenanthrene (**1**), and seven known compounds including moscatin (**2**), 2,5-dihydroxy-4,9-dimethoxyphenanthrene (**3**), moscatilin (**4**), aloifol I (**5**), 4,4′,8,8′-tetramethoxy[1,1′-biphenanthrene]-2,2′,7,7′-tetrol (**6**), 2,2′,7,7′-tetrahydroxy-4,4′-dimethoxy-1,1′-biphenanthrene (**7**) and bleformin G (**8**). All these isolated compounds were evaluated for pancreatic lipase inhibitory activity. Moscatin (**2**) and 2,5-dihydroxy-4,9-dimethoxyphenanthrene (**3**) possessed recognizable lipase inhibition with IC_{50} values of 57.6 ± 3.3 µM and 58.6 ± 3.4 µM, respectively. The data on the phytochemicals from *D. senile* as well as their lipase inhibitory effects should provide useful information for developing new potent anti-obesity molecules from plant sources.

REFERENCES

Adejobi, O. I. I., Guan, J., Yang, L., Hu, J.-M., Yu, A., Muraguri, S., & Liu, A. (2021). Transcriptomic analyses shed light on critical genes associated with bibenzyl biosynthesis in *Dendrobium officinale*. *Plants, 10*(4), 1-18.

Al-Omar, M. A., Al-Suwailem, A., Al-Tamimi, A., & Al-Suhibani, M. (2006). Safety and mechanism of action of orlistat (tetrahydrolipstatin) as the first local antiobesity drug. *Journal of Applied Sciences Research, 2*(4), 205-208.

Alruwaili, H., Dehestani, B., & le Roux, C. W. (2021). Clinical Impact of liraglutide as a treatment of obesity. *Clinical Pharmacology: Advances and Applications, 13*, 53-60.

Aronne, L. J. (2002). Classification of obesity and assessment of obesity-related health risks. *Obesity Research, 10*(S12), 105S-115S.

Averyanov, L. V., Ponert, J., Nguyen, P. T., Van Duy, N., & Khang, N. S. (2016). A survey of *Dendrobium* Sw. sect. Formosae (Benth. & Hook. f.) Hook. f. in Cambodia, Laos and Vietnam. *Adansonia, 38*(2), 199-217.

Bacha, A. B., Karray, A., Daoud, L., Bouchaala, E., Ali, M. B., Gargouri, Y., & Ali, Y. B. (2011). Biochemical properties of pancreatic colipase from the common stingray *Dasyatis pastinaca*. *Lipids in Health and Disease, 10*(1), 1-7.

Bae, J. Y., Lee, J. W., Jin, Q., Jang, H., Lee, D., Kim, Y., Hong, J. T., Lee, M. K., Lee, M. S., & Hwang, B. Y. (2017). Chemical constituents isolated from *Bletilla striata* and their inhibitory effects on nitric oxide production in RAW 264.7 Cells. *Chemistry & Biodiversity, 14*(2), 1-5.

Bajes, H. R., Almasri, I., & Bustanji, Y. (2020). Plant products and their inhibitory activity against pancreatic lipase. *Revista Brasileira de Farmacognosia, 30*(3), 321-330.

Baretić, M. (2012). Targets for medical therapy in obesity. *Digestive Diseases, 30*(2), 168-172.

Bénarouche, A., Point, V., Carrière, F., & Cavalier, J.-F. (2014). Using the reversible inhibition of gastric lipase by orlistat for investigating simultaneously lipase adsorption and substrate hydrolysis at the lipid–water interface. *Biochimie, 101*, 221-231.

Bergman, M. E., Davis, B., & Phillips, M. A. (2019). Medically useful plant terpenoids: biosynthesis, occurrence, and mechanism of action. *Molecules, 24*(21), 1-23.

Bi, Z.-M., Wang, Z.-T., & Xu, L.-S. (2004). Chemical constituents of *Dendrobium moniliforme*. *Acta Botanica Sinica, 46*(1), 124-126.

Birari, R. B., & Bhutani, K. K. (2007). Pancreatic lipase inhibitors from natural sources: unexplored potential. *Drug Discovery Today, 12*(19-20), 879-889.

Birari, R. B., Gupta, S., Mohan, C. G., & Bhutani, K. K. (2011). Antiobesity and lipid lowering effects of *Glycyrrhiza* chalcones: experimental and computational studies. *Phytomedicine, 18*(8-9), 795-801.

Bourgaud, F., Hehn, A., Larbat, R., Doerper, S., Gontier, E., Kellner, S., & Matern, U. (2006). Biosynthesis of coumarins in plants: a major pathway still to be unravelled for cytochrome P450 enzymes. *Phytochemistry Reviews, 5*(2), 293-308.

Buchholz, T., & Melzig, M. F. (2015). Polyphenolic compounds as pancreatic lipase inhibitors. *Planta Medica, 81*(10), 771-783.

Bús, C., Kulmány, Á., Kúsz, N., Gonda, T., Zupkó, I., Mándi, A., Kurtán, T., Tóth, B., Hohmann, J., & Hunyadi, A. (2020). Oxidized juncuenin B analogues with increased antiproliferative activity on human adherent cell lines: semisynthesis and biological evaluation. *Journal of Natural Products, 83*(11), 3250-3261.

Cai, J., Yang, C., Chen, T., & Zhao, L. (2018). Detection of new phenylpropanoids from *Dendrobium chrysanthum*. *Natural Product Research, 32*(13), 1600-1604.

Cakova, V., Bonte, F., & Lobstein, A. (2017). *Dendrobium*: sources of active ingredients to treat age-related pathologies. *Aging and Disease, 8*(6), 827-849.

Cardile, V., Avola, R., Graziano, A. C., & Russo, A. (2020). Moscatilin, a bibenzyl derivative from the orchid *Dendrobium loddigesii*, induces apoptosis in melanoma cells. *Chemico-biological Interactions, 323*, 1-9.

Casas-Godoy, L., Gasteazoro, F., Duquesne, S., Bordes, F., Marty, A., & Sandoval, G. (2018). Lipases: an overview. *Methods in Molecular Biology (Clifton, NJ), 1835*, 3-38.

Chang, C.-C., Ku, A. F., Tseng, Y.-Y., Yang, W.-B., Fang, J.-M., & Wong, C.-H. (2010). 6,8-Di-*C*-glycosyl flavonoids from *Dendrobium huoshanense*. *Journal of Natural Products, 73*(2), 229-232.

Chang, S.-J., Lin, T.-H., & Chen, C.-C. (2001). Constituents from the stems of *Dendrobium clavatum var. aurantiacum*. *Journal of Chinese Medicine, 12*(3), 211-218.

Chanvorachote, P., Kowitdamrong, A., Ruanghirun, T., Sritularak, B., Mungmee, C., & Likhitwitayawuid, K. (2013). Anti-metastatic activities of bibenzyls from *Dendrobium pulchellum*. *Natural Product Communications, 8*(1), 115-118.

Chapus, C., Sari, H., Semeriva, M., & Desnuelle, P. (1975). Role of colipase in the interfacial adsorption of pancreatic lipase at hydrophilic interfaces. *Federation of European Biochemical Societies Letters, 58*(1-2), 155-158.

Chedda, U., Kaikini, A., Bagle, S., Seervi, M., & Sathaye, S. (2016). *In vitro* pancreatic lipase inhibition potential of commonly used Indian spices. *The International Organization of Scientific Research Journal of Pharmacy, 6*(10), 10-13.

Chen, C.-C., Wu, L.-G., Ko, F.-N., & Teng, C.-M. (1994). Antiplatelet aggregation principles of *Dendrobium loddigesii*. *Journal of Natural Products, 57*(9), 1271-1274.

Chen, H., Li, X., Xu, Y., Lo, K., Zheng, H., Hu, H., Wang, J., & Lin, Y. (2018). Study on the polar extracts of *Dendrobium nobile*, *D. officinale*, *D. loddigesii,* and *Flickingeria fimbriata*: metabolite identification, content evaluation, and bioactivity assay. *Molecules, 23*(5), 1-10.

Chen, T.-H., Pan, S.-L., Guh, J.-H., Liao, C.-H., Huang, D.-Y., Chen, C.-C., & Teng, C.-M. (2008a). Moscatilin induces apoptosis in human colorectal cancer cells: a crucial role of c-Jun NH_2-terminal protein kinase activation caused by tubulin depolymerization and DNA damage. *Clinical Cancer Research, 14*(13), 4250-4258.

Chen, X.-J., Mei, W.-L., Cai, C.-H., Guo, Z.-K., Song, X.-Q., & Dai, H.-F. (2014). Four new bibenzyl derivatives from *Dendrobium sinense*. *Phytochemistry Letters, 9*, 107-112.

Chen, X.-J., Mei, W.-L., Zuo, W.-J., Zeng, Y.-B., Guo, Z.-K., Song, X.-Q., & Dai, H.-F. (2013). A new antibacterial phenanthrenequinone from *Dendrobium sinense*. *Journal of Asian Natural Products Research, 15*(1), 67-70.

Chen, Y., Li, J., Wang, L., & Liu, Y. (2008b). Aromatic compounds from *Dendrobium aphyllum*. *Biochemical Systematics and Ecology, 5*(36), 458-460.

Chen, Y., Li, Y., Qing, C., Zhang, Y., Wang, L., & Liu, Y. (2008c). 1,4,5-Trihydroxy-7-methoxy-9*H*-fluoren-9-one, a new cytotoxic compound from *Dendrobium chrysotoxum*. *Food Chemistry, 108*(3), 973-976.

Chen, Y., Liu, Y., Jiang, J., Zhang, Y., & Yin, B. (2008d). Dendronone, a new phenanthrenequinone from *Dendrobium cariniferum*. *Food Chemistry, 111*(1), 11-12.

Chen, Y., Xu, J., Yu, H., Qing, C., Zhang, Y., Wang, L., Liu, Y., & Wang, J. (2008e). Cytotoxic phenolics from *Bulbophyllum odoratissimum*. *Food Chemistry, 107*(1), 169-173.

Chen, Y., Yu, H., & Lian, X. (2015). Isolation of stilbenoids and lignans from *Dendrobium hongdie*. *Tropical Journal of Pharmaceutical Research, 14*(11), 2055-2059.

Covey, H. C. (1988). Historical terminology used to represent older people. *The Gerontologist, 28*(3), 291-297.

Da Silva, J. A. T., & Ng, T. B. (2017). The medicinal and pharmaceutical importance of *Dendrobium* species. *Applied Microbiology and Biotechnology, 101*(6), 2227-2239.

Da Silva, J. A. T., Tsavkelova, E. A., Zeng, S., Ng, T. B., Parthibhan, S., Dobránszki, J., Cardoso, J. C., & Rao, M. (2015). Symbiotic *in vitro* seed propagation of *Dendrobium*: fungal and bacterial partners and their influence on plant growth and development. *Planta, 242*, 1-22.

Dahmén, J., & Leander, K. (1978). Amotin and amoenin, two sesquiterpenes of the picrotoxane group from *Dendrobium amoenum*. *Phytochemistry, 17*(11), 1949-1952.

Dan, Y., Cheng, Z.-Q., Cheng-Ting, Z., Liu, Y., Fa-Wu, D., Jiang-Miao, H., & Jun, Z. (2019). Four new sesquiterpene derivatives from *Dendrobium findlayanum*. *Chinese Journal of Natural Medicines, 17*(12), 900-905.

Dey, P., Kundu, A., Kumar, A., Gupta, M., Lee, B. M., Bhakta, T., Dash, S., & Kim, H. S. (2020). Analysis of alkaloids (indole alkaloids, isoquinoline alkaloids, tropane alkaloids). *Recent Advances in Natural Products Analysis*, 505-567.

Dubrovina, A., & Kiselev, K. (2017). Regulation of stilbene biosynthesis in plants. *Planta, 246*(4), 597-623.

Ekevåg, U., Elander, M., Gawell, L., Leander, K., & Lüning, B. (1973). Studies on Orchidaceae alkaloids. xXXIII. Two new alkaloids, *N-cis*-and *N-trans*-cinnamoyl-norcuskhygrine from *Dendrobium chrysanthum* Wall. *Acta Chemica Scandinavica, 27*(6), 1982-1986.

Elander, M., Gawell, L., & Leander, K. (1971). Studies on Orchidaceae alkaloids. XXII. Synthesis and absolute configuration of pierardine, lactone-betaine isomerization of shihunine. *Acta Chemica Scandinavica, 25*(2), 721-724.

Elander, M., & Leander, K. (1971). Studies on Orchidaceae alkaloids. XXI. 6-hydroxynobiline, a new alkaloid from *Dendrobium hildebrandii* Rolfe. *Acta Chemica Scandinavica, 25*(2), 717-720.

Elander, M., Leander, K., & Luning, B. (1969). Studies on Orchidaceae alkaloids. 14. A phthalide alkaloid from *Dendrobium Pierardii* Roxb. Acta Chemica Scandinavica, *23*(6), 2177.

Eom, S. H., Lee, M. S., Lee, E. W., Kim, Y. M., & Kim, T. H. (2013). Pancreatic lipase inhibitory activity of phlorotannins isolated from *Eisenia bicyclis*. *Phytotherapy Research, 27*(1), 148-151.

Fan, C., Wang, W., Wang, Y., Qin, G., & Zhao, W. (2001). Chemical constituents from *Dendrobium densiflorum*. *Phytochemistry, 57*(8), 1255-1258.

Fan, W.-W., Xu, F.-Q., Dong, F.-W., Li, X.-N., Li, Y., Liu, Y.-Q., Zhou, J., & Hu, J.-M. (2013). Dendrowardol C, a novel sesquiterpenoid from *Dendrobium wardianum* Warner. *Natural Products and Bioprospecting, 3*(3), 89-92.

Filippatos, T. D., Derdemezis, C. S., Gazi, I. F., Nakou, E. S., Mikhailidis, D. P., & Elisaf, M. S. (2008). Orlistat-associated adverse effects and drug interactions. *Drug Safety, 31*(1), 53-65.

Fraga, B. M. (2001). Natural sesquiterpenoids. *Natural Product Reports, 18*(6), 650-673.

Garza, A. L. d. l., Milagro-Yoldi, F. I., Boque, N., Campión-Zabalza, J., & Martinez, J. A. (2011). Natural inhibitors of pancreatic lipase as new players in obesity treatment. *Planta Medica, 77*(08), 773-785.

Gawell, L., & Leander, K. (1976). The constitution of aduncin, a sesquiterpene related to picrotoxinin, found in *Dendrobium aduncum*. *Phytochemistry, 15*(12), 1991-1992.

Glomqvist, L., Brandänge, S., Gawell, L., Leander, K., & Lüning, B. (1973). Studies on Orchidaceae alkaloids. XXXVII. Dendrowardine, a quaternary alkaloid from *Dendrobium Wardianum* Wr. *Acta Chemica Scandinavica, 27*(4), 1439-1441.

González-Castejón, M., & Rodriguez-Casado, A. (2011). Dietary phytochemicals and their potential effects on obesity: a review. *Pharmacological Research, 64*(5), 438-455.

Gorham, J. (1989). Stilbenes and phenanthrenes. In *Methods in Plant Biochemistry* (Vol. 1, pp. 159-196): Academic Press.

Goyal, A., Sharma, A., Sharma, D., Behl, T., Kamboj, A., & Babu, A. (2020). Ameliorative effect of selegiline in high fat diet induced obesity rat model: possible role of dopaminergic pathway. *Obesity Medicine, 20*, 1-5.

GuyáDodson, G. (1992). Structural and evolutionary relationships in lipase mechanism and activation. *Faraday Discussions, 93*, 95-105.

Habtemariam, S. (2012). The anti-obesity potential of sigmoidin A. *Pharmaceutical Biology, 50*(12), 1519-1522.

Habtemariam, S. (2013). Antihyperlipidemic components of *Cassia auriculata* aerial parts: identification through *in vitro* studies. *Phytotherapy Research, 27*(1), 152-155.

Hamosh, M. (1990). Lingual and gastric lipases. *Nutrition (Burbank, Los Angeles County, Calif.), 6*(6), 421-428.

He, L., Su, Q., Bai, L., Li, M., Liu, J., Liu, X., Zhang, C., Jiang, Z., He, J., & Shi, J. (2020). Recent research progress on natural small molecule bibenzyls and its derivatives in *Dendrobium* species. *European Journal of Medicinal Chemistry, 204*, 1-17.

Hedman, K., Leander, K., & Lüning, B. (1971). Studies on Orchidaceae alkaloids. XXV. *N*-isopentenyl derivatives of dendroxine and 6-hydroxydendroxine from *Dendrobium friedricksianum* Lindl. and *Dendrobium hildebrandii* Rolfe. *Acta Chemica Scandinavica, 25*(3), 1142-1144.

Hemscheidt, T., & Spenser, I. D. (1991). Biosynthesis of anosmine, an imidazole alkaloid of the orchid *Dendrobium parishii*. *Journal of the Chemical Society, Chemical Communications,* (7), 494-497.

Honda, C., & Yamaki, M. (2000). Phenanthrenes from *Dendrobium plicatile*. *Phytochemistry, 53*(8), 987-990.

Hu, J.-M., Chen, J.-J., Yu, H., Zhao, Y.-X., & Zhou, J. (2008a). Five new compounds from *Dendrobium longicornu*. *Planta Medica, 74*(05), 535-539.

Hu, J.-M., Chen, J.-J., Yu, H., Zhao, Y.-X., & Zhou, J. (2008b). Two novel bibenzyls from *Dendrobium trigonopus*. *Journal of Asian Natural Products Research, 10*(7), 647-651.

Hu, J.-M., Zhao, Y.-X., Miao, Z.-H., & Zhou, J. (2009). Chemical components of *Dendrobium polyanthum*. *Bulletin of the Korean Chemical Society, 30*(9), 2098-2100.

Hu, J., Fan, W., Dong, F., Miao, Z., & Zhou, J. (2012). Chemical components of *Dendrobium chrysotoxum*. *Chinese Journal of Chemistry, 30*(6), 1327-1330.

Hu, Y., Ren, J., Wang, L., Zhao, X., Zhang, M., Shimizu, K., & Zhang, C. (2018). Protective effects of total alkaloids from *Dendrobium crepidatum* against LPS-induced acute lung injury in mice and its chemical components. *Phytochemistry, 149*, 12-23.

Hu, Y., Yang, H., Ding, X., Liu, J., Wang, X., Hu, L., Liu, M., & Zhang, C. (2020). Anti-inflammatory octahydroindolizine alkaloid enantiomers from *Dendrobium crepidatum*. *Bioorganic Chemistry, 100*, 1-7.

Hu, Y., Zhang, C., Zhao, X., Wang, Y., Feng, D., Zhang, M., & Xie, H. (2016). (±)-Homocrepidine A, a pair of anti-inflammatory enantiomeric octahydroindolizine alkaloid dimers from *Dendrobium crepidatum*. *Journal of Natural Products, 79*(1), 252-256.

Huang, J., Huang, N., Zhang, M., Nie, J., Xu, Y., Wu, Q., & Shi, J. (2019). *Dendrobium* alkaloids decrease Aβ by regulating α-and β-secretases in hippocampal neurons of SD rats. *PeerJ, 7*, 1-15.

Huang, X., Zhu, J., Wang, L., Jing, H., Ma, C., Kou, X., & Wang, H. (2020). Inhibitory mechanisms and interaction of tangeretin, 5-demethyltangeretin, nobiletin, and 5-demethylnobiletin from citrus peels on pancreatic lipase: kinetics, spectroscopies, and molecular dynamics simulation. *International Journal of Biological Macromolecules, 164*, 1927-1938.

Hwang, J. S., Lee, S. A., Hong, S. S., Han, X. H., Lee, C., Kang, S. J., Lee, D., Kim, Y., Hong, J. T., & Lee, M. K. (2010). Phenanthrenes from *Dendrobium nobile* and their inhibition of the LPS-induced production of nitric oxide in macrophage RAW 264.7 cells. *Bioorganic & Medicinal Chemistry Letters, 20*(12), 3785-3787.

Inthongkaew, P., Chatsumpun, N., Supasuteekul, C., Kitisripanya, T., Putalun, W., Likhitwitayawuid, K., & Sritularak, B. (2017). α-Glucosidase and pancreatic lipase inhibitory activities and glucose uptake stimulatory effect of phenolic compounds from *Dendrobium formosum*. *Revista Brasileira de Farmacognosia, 27*(4), 480-487.

Inubushi, Y., Tsuda, Y., Konita, T., & Matsumoto, S. (1968). The structure of shihunine, a new phthalide-pyrrolidine alkaloid. *Chemical and Pharmaceutical Bulletin, 16*(6), 1014-1018.

Iqbal, J., & Hussain, M. M. (2009). Intestinal lipid absorption. *American Journal of Physiology-Endocrinology and Metabolism, 296*(6), E1183-E1194.

Isoda, H., Motojima, H., Onaga, S., Samet, I., Villareal, M. O., & Han, J. (2014). Analysis of the erythroid differentiation effect of flavonoid apigenin on K562 human chronic leukemia cells. *Chemico-biological Interactions, 220*, 269-277.

Ito, M., Matsuzaki, K., Wang, J., Daikonya, A., Wang, N.-L., Yao, X.-S., & Kitanaka, S. (2010). New phenanthrenes and stilbenes from *Dendrobium loddigesii*. *Chemical and Pharmaceutical Bulletin, 58*(5), 628-633.

Jang, D. S., Lee, G. Y., Kim, J., Lee, Y. M., Kim, J. M., Kim, Y. S., & Kim, J. S. (2008). A new pancreatic lipase inhibitor isolated from the roots of *Actinidia arguta*. *Archives of Pharmacal Research, 31*(5), 666-670.

Juneja, R., Sharma, S., & Tandon, J. (1987). Two substituted bibenzyls and a dihydrophenanthrene from *Cymbidium aloifolium*. *Phytochemistry, 26*(4), 1123-1125.

Jung, U. J., & Choi, M.-S. (2014). Obesity and its metabolic complications: The role of adipokines and the relationship between obesity, inflammation, insulin resistance, dyslipidemia and nonalcoholic fatty liver disease. *International Journal of Molecular Sciences, 15*(4), 6184-6223.

Kato, E., Yama, M., Nakagomi, R., Shibata, T., Hosokawa, K., & Kawabata, J. (2012). Substrate-like water soluble lipase inhibitors from *Filipendula kamtschatica*. *Bioorganic & Medicinal Chemistry Letters, 22*(20), 6410-6412.

Khoonrit, P., Mirdogan, A., Dehlinger, A., Mekboonsonglarp, W., Likhitwitayawuid, K., Priller, J., Böttcher, C., & Sritularak, B. (2020). Immune modulatory effect of a novel 4,5-dihydroxy-3,3′,4′-trimethoxybibenzyl from *Dendrobium lindleyi*. *PloS One, 15*(9), 1-15.

Kim, B.-Y., Kang, S. M., Kang, J.-H., Kim, K. K., Kim, B., Kim, S. J., Kim, Y.-H., Kim, J.-H., Kim, J. H., & Nam, G. E. (2020). Current long-term pharmacotherapies for the management of obesity. *Journal of Obesity & Metabolic Syndrome, 29*(2), 99-109.

Kim, D. H., Kim, J. Y., Kim, R. M., Maharjan, P., Ji, Y.-G., Jang, D.-J., Min, K. A., Koo, T.-S., & Cho, K. H. (2018). Orlistat-loaded solid SNEDDS for the enhanced solubility, dissolution, and *in vivo* performance. *International Journal of Nanomedicine, 13*, 7095–7106.

Kim, G.-N., Shin, M.-R., Shin, S. H., Lee, A. R., Lee, J. Y., Seo, B.-I., Kim, M. Y., Kim, T. H., Noh, J. S., & Rhee, M. H. (2016). Study of antiobesity effect through inhibition of pancreatic lipase activity of *Diospyros kaki* fruit and *Citrus unshiu* peel. *BioMed Research International, 2016*, 1-7.

Kim, J. H., Oh, S.-Y., Han, S.-B., Uddin, G. M., Kim, C. Y., & Lee, J. K. (2015). Anti-inflammatory effects of *Dendrobium nobile* derived phenanthrenes in LPS-stimulated murine macrophages. *Archives of Pharmacal Research, 38*(6), 1117-1126.

Klongkumnuankarn, P., Busaranon, K., Chanvorachote, P., Sritularak, B., Jongbunprasert, V., & Likhitwitayawuid, K. (2015). Cytotoxic and antimigratory activities of phenolic compounds From *Dendrobium Brymerianum*. *Evidence-Based Complementary and Alternative Medicine, 2015*, 1-9.

Kojta, I., Chacińska, M., & Błachnio-Zabielska, A. (2020). Obesity, bioactive lipids, and adipose tissue inflammation in insulin resistance. *Nutrients, 12*(5), 1-19.

Kongkatitham, V., Muangnoi, C., Kyokong, N., Thaweesest, W., Likhitwitayawuid, K., Rojsitthisak, P., & Sritularak, B. (2018). Anti-oxidant and anti-inflammatory effects of new bibenzyl derivatives from *Dendrobium parishii* in hydrogen peroxide and lipopolysaccharide treated RAW264.7 cells. *Phytochemistry Letters, 24*, 31-38.

Kopelman, P. G. (2000). Obesity as a medical problem. *Nature, 404*(6778), 635-643.

Kulkarni, B. V., & Mattes, R. D. (2014). Lingual lipase activity in the orosensory detection of fat by humans. *American Journal of Physiology-Regulatory, Integrative and Comparative Physiology, 306*(12), R879-R885.

Kumar, A., & Chauhan, S. (2021). Pancreatic lipase inhibitors: the road voyaged and successes. *Life Sciences, 271*, 1-23.

Kuzuyama, T., & Seto, H. (2012). Two distinct pathways for essential metabolic precursors for isoprenoid biosynthesis. *Japan Academy Proceedings Series B: Physical and Biological Sciences, 88*(3), 41-53.

Kwon, C.-S., Sohn, H. Y., Kim, S. H., Kim, J. H., Son, K. H., Lee, J. S., Lim, J. K., & Kim, J.-S. (2003). Anti-obesity effect of *Dioscorea nipponica* Makino with lipase-inhibitory activity in rodents. *Bioscience, Biotechnology, and Biochemistry, 67*(7), 1451-1456.

Kyokong, N., Muangnoi, C., Thaweesest, W., Kongkatitham, V., Likhitwitayawuid, K., Rojsitthisak, P., & Sritularak, B. (2019). A new phenanthrene dimer from *Dendrobium palpebrae*. *Journal of Asian Natural Products Research, 21*(4), 391-397.

Lai, M. C., Liu, W. Y., Liou, S.-S., & Liu, I.-M. (2020a). The protective effects of moscatilin against methylglyoxal-induced neurotoxicity via the regulation of p38/JNK MAPK pathways in PC12 neuron-like cells. *Food and Chemical Toxicology, 140*, 1-10.

Lai, W. W., Galer, B. S., Wong, P. C., Farfel, G., Pringsheim, M., Keane, M. G., & Agarwal, A. (2020b). Cardiovascular safety of fenfluramine in the treatment of Dravet syndrome: Analysis of an ongoing long‐term open‐label safety extension study. *Epilepsia, 61*(11), 2386-2395.

Lam, Y., Ng, T. B., Yao, R. M., Shi, J., Xu, K., Sze, S. C. W., & Zhang, K. Y. (2015). Evaluation of chemical constituents and important mechanism of pharmacological biology in *Dendrobium* plants. *Evidence-Based Complementary and Alternative Medicine, 2015*, 1-25.

Leander, K., & Lüning, B. (1968). Studies on Orchidaceae alkaloids VIII: an imidazolium salt from *Dendrobium anosmum* lindl. and *Dendrobium parishii* Rchb. f. *Tetrahedron Letters, 9*(8), 905-908.

Lee, E., Han, A.-R., Nam, B., Kim, Y.-R., Jin, C. H., Kim, J.-B., Eun, Y.-G., & Jung, C.-H. (2020). Moscatilin induces apoptosis in human head and neck squamous cell carcinoma cells via JNK signaling pathway. *Molecules, 25*(4), 1-12.

Lee, E. M., Lee, S. S., Chung, B. Y., Cho, J.-Y., Lee, I. C., Ahn, S. R., Jang, S. J., & Kim, T. H. (2010). Pancreatic lipase inhibition by *C*-glycosidic flavones isolated from *Eremochloa ophiuroides*. *Molecules, 15*(11), 8251-8259.

Li, C.-B., Wang, C., Fan, W.-W., Dong, F.-W., Xu, F.-Q., Wan, Q.-L., Luo, H.-R., Liu, Y.-Q., Hu, J.-M., & Zhou, J. (2013). Chemical components of *Dendrobium crepidatum* and their neurite outgrowth enhancing activities. *Natural Products and Bioprospecting, 3*(2), 70-73.

Li, J.-T., Yin, B.-L., Liu, Y., Wang, L.-Q., & Chen, Y.-G. (2009a). Mono-aromatic constituents of *Dendrobium longicornu*. *Chemistry of Natural Compounds, 45*(2), 234-236.

Li, M., Hirata, Y., Xu, G., Niwa, M., & Wu, H. (1991). Studies on the chemical constituents of *Dendrobium loddigesii* rolfe. *Yao Xue Xue Bao = Acta Pharmaceutica Sinica, 26*(4), 307-310.

Li, X.-h., Guo, L., Yang, L., Peng, C., He, C.-j., Zhou, Q.-m., Xiong, L., Liu, J., & Zhang, T.-m. (2014a). Three new neolignan glucosides from the stems of *Dendrobium aurantiacum var. denneanum*. *Phytochemistry Letters, 9*, 37-40.

Li, Y.-P., Qing, C., Fang, T.-T., Liu, Y., & Chen, Y.-G. (2009b). Chemical constituents of *Dendrobium chrysotoxum*. *Chemistry of Natural Compounds, 45*(3), 414-416.

Li, Y., Wang, C.-L., Guo, S.-X., Yang, J.-S., & Xiao, P.-G. (2008). Two new compounds from *Dendrobium candidum*. *Chemical and Pharmaceutical Bulletin, 56*(10), 1477-1479.

Li, Y., Wang, C.-L., Wang, Y.-J., Wang, F.-F., Guo, S.-X., Yang, J.-S., & Xiao, P.-G. (2009c). Four new bibenzyl derivatives from *Dendrobium candidum*. *Chemical and Pharmaceutical Bulletin, 57*(9), 997-999.

Li, Y., Wang, C.-L., Zhao, H.-J., & Guo, S.-X. (2014b). Eight new bibenzyl derivatives from *Dendrobium candidum*. *Journal of Asian Natural Products Research, 16*(11), 1035-1043.

Lim, H. J., Xue, H., & Wang, Y. (2020). Global trends in obesity. *Handbook of Eating and Drinking: Interdisciplinary Perspectives*, 1217-1235.

Limpanit, R., Chuanasa, T., Likhitwitayawuid, K., Jongbunprasert, V., & Sritularak, B. (2016). α-glucosidase Inhibitors from *Dendrobium tortile*. *Records of Natural Products, 10*(5), 609-616.

Lin, C.-W., Hwang, T.-L., Chen, F.-A., Huang, C.-H., Hung, H.-Y., & Wu, T.-S. (2016). Chemical constituents of the rhizomes of *Bletilla formosana* and their potential anti-inflammatory activity. *Journal of Natural Products, 79*(8), 1911-1921.

Lin, T.-H., Chang, S.-J., Chen, C.-C., Wang, J.-P., & Tsao, L.-T. (2001). Two Phenanthraquinones from *Dendrobium moniliforme*. *Journal of Natural Products, 64*(8), 1084-1086.

Liu, G.-Y., Tan, L., Cheng, L., Ding, L.-S., Zhou, Y., Deng, Y., He, Y.-Q., Guo, D.-L., & Xiao, S.-J. (2020a). Dendrobine-type alkaloids and bibenzyl derivatives from *Dendrobium findlayanum*. *Fitoterapia, 142*, 1-6.

Liu, T.-T., Liu, X.-T., Chen, Q.-X., & Shi, Y. (2020b). Lipase inhibitors for obesity: a review. *Biomedicine & Pharmacotherapy, 128*, 1-9.

Liu, W.-H., Hua, Y.-F., & Zhan, Z.-J. (2007). Moniline, a new alkaloid from *Dendrobium moniliforme*. *Journal of Chemical Research, 2007*(6), 317-318.

Liu, X.-Q., Li, X.-P., & Yuan, Q.-Y. (2016). Two new phenanthrene glucosides from *Cremastra appendiculata*. *Chemistry of Natural Compounds, 52*(1), 23-25.

Lowe, M. E. (1997). Structure and function of pancreatic lipase and colipase. *Annual Review of Nutrition, 17*(1), 141-158.

Lu, Y., Kuang, M., Hu, G.-P., Wu, R.-B., Wang, J., Liu, L., & Lin, Y.-C. (2014). Loddigesiinols G–J: **α**-glucosidase inhibitors from *Dendrobium loddigesii*. *Molecules, 19*(6), 8544-8555.

Lunagariya, N. A., Patel, N. K., Jagtap, S. C., & Bhutani, K. K. (2014). Inhibitors of pancreatic lipase: state of the art and clinical perspectives. *Experimental and Clinical Sciences Journal, 13*, 897-921.

Lüning, B., & Leander, K. (1965). Studies on Orchidaceae alkaloids III. The alkaloids in *Dendrobium primulinum* and *Dendrobium chrysanthum*. *Acta Chemica Scandinavica, 19*, 1607-1611.

Ma, C., Meng, C.-W., Zhou, Q.-M., Peng, C., Liu, F., Zhang, J.-W., Zhou, F., & Xiong, L. (2019a). New sesquiterpenoids from the stems of *Dendrobium nobile* and their neuroprotective activities. *Fitoterapia, 138*, 1-6.

Ma, D., Sun, D., Wang, C., Li, Y., & Guo, T. (2014). Expression of flavonoid biosynthesis genes and accumulation of flavonoid in wheat leaves in response to drought stress. *Plant Physiology and Biochemistry, 80*, 60-66.

Ma, G.-X., Wang, T.-S., Yin, L., Pan, Y., Xu, G.-J., & Xu, L.-S. (1998). Studies on chemical constituents of *Dendrobium chryseum*. *Journal of Chinese Pharmaceutical Sciences, 7*(1), 52-54.

Ma, R.-J., Yang, L., Bai, X., Li, J.-Y., Yuan, M.-Y., Wang, Y.-Q., Xie, Y., Hu, J.-M., & Zhou, J. (2019b). Phenolic constituents with antioxidative, tyrosinase inhibitory and anti-aging activities from *Dendrobium loddigesii* Rolfe. *Natural Products and Bioprospecting, 9*(5), 329-336.

Majumder, P., & Chatterjee, S. (1989). Crepidatin, a bibenzyl derivative from the orchid *Dendrobium crepidatum*. *Phytochemistry, 28*(7), 1986-1988.

Majumder, P., Guha, S., & Sen, S. (1999). Bibenzyl derivatives from the orchid *Dendrobium amoenum*. *Phytochemistry, 52*(7), 1365-1369.

Majumder, P., & Pal, S. (1992). Rotundatin, a new 9,10-dihydrophenanthrene derivative from *Dendrobium rotundatum*. *Phytochemistry, 31*(9), 3225-3228.

Majumder, P., & Pal, S. (1993). Cumulatin and tristin, two bibenzyl derivatives from the orchids *Dendrobium cumulatum* and *Bulbophyllum triste*. *Phytochemistry, 32*(6), 1561-1565.

Majumder, P., & Sen, R. (1987a). Moscatilin, a bibenzyl derivative from the orchid *Dendrobium moscatum*. *Phytochemistry, 26*(7), 2121-2124.

Majumder, P., & Sen, R. (1987b). Structure of moscatin-a new phenanthrene derivative from the orchid *Dendrobium moscatum*. *Indian Journal of Chemistry - Section B Organic and Medicinal Chemistry, 26*, 18-20.

Marmouzi, I., Ezzat, S. M., Mostafa, E. S., El Jemli, M., Radwan, R. A., Faouzi, M. E. A., Tamsouri, N., & Kharbach, M. (2021). Isolation of secondary metabolites from the mediterranean sponge species; *Hemimycale columella* and its biological properties. *SN Applied Sciences, 3*(2), 1-13.

Marti, A., Moreno-Aliaga, M., Hebebrand, J., & Martinez, J. (2004). Genes, lifestyles and obesity. *International Journal of Obesity, 28*(3), S29-S36.

Matsumoto, M., Hosokawa, M., Matsukawa, N., Hagio, M., Shinoki, A., Nishimukai, M., Miyashita, K., Yajima, T., & Hara, H. (2010). Suppressive effects of the marine carotenoids, fucoxanthin and fucoxanthinol on triglyceride absorption in lymph duct-cannulated rats. *European Journal of Nutrition, 49*(4), 243-249.

McClendon, K. S., Riche, D. M., & Uwaifo, G. I. (2009). Orlistat: current status in clinical therapeutics. *Expert Opinion on Drug Safety, 8*(6), 727-744.

Meng, C.-W., He, Y.-L., Peng, C., Ding, X.-J., Guo, L., & Xiong, L. (2017). Picrotoxane sesquiterpenoids from the stems of *Dendrobium nobile* and their absolute configurations and angiogenesis effect. *Fitoterapia, 121*, 206-211.

Miled, N., Canaan, S., Dupuis, L., Roussel, A., Rivière, M., Carrière, F., de Caro, A., Cambillau, C., & Verger, R. (2000). Digestive lipases: from three-dimensional structure to physiology. *Biochimie, 82*(11), 973-986.

Mittraphab, A., Muangnoi, C., Likhitwitayawuid, K., Rojsitthisak, P., & Sritularak, B. (2016). A New bibenzyl-phenanthrene derivative from *Dendrobium Signatum* and Its cytotoxic activity. *Natural Product Communications, 11*(5), 657-659.

Miyazawa, M., Shimamura, H., Nakamura, S.-i., Sugiura, W., Kosaka, H., & Kameoka, H. (1999). Moscatilin from *Dendrobium nobile*, a naturally occurring bibenzyl compound with potential antimutagenic activity. *Journal of Agricultural and Food Chemistry, 47*(5), 2163-2167.

Morita, H., Fujiwara, M., Yoshida, N., & Kobayashi, J. i. (2000). New picrotoxinin-type and dendrobine-type sesquiterpenoids from *Dendrobium snowflake* 'Red Star'. *Tetrahedron, 56*(32), 5801-5805.

Mou, Z., Zhao, Y., Ye, F., Shi, Y., Kennelly, E. J., Chen, S., & Zhao, D. (2021). Identification, biological activities and biosynthetic pathway of *Dendrobium* alkaloids. *Frontiers in Pharmacology, 12*, 1-14.

Mukherjee, A. K. (2014). Hydrophobic-hydrophilic interaction in lipase catalytic triad and possibility of a cofactor mediated catalysis. *International Journal of Agricultural and Food Science, 4*(3), 84-89.

Na Ranong, S., Likhitwitayawuid, K., Mekboonsonglarp, W., & Sritularak, B. (2019). New dihydrophenanthrenes from *Dendrobium infundibulum*. *Natural Product Research, 33*(3), 420-426.

Nakai, M., Fukui, Y., Asami, S., Toyoda-Ono, Y., Iwashita, T., Shibata, H., Mitsunaga, T., Hashimoto, F., & Kiso, Y. (2005). Inhibitory effects of oolong tea polyphenols on pancreatic lipase *in vitro*. *Journal of Agricultural and Food Chemistry, 53*(11), 4593-4598.

Nguyen, T. V. T., Giang, T. P. L., Le Huyen, T., Bui, H. T., Vu, Q. H., & Phan, V. K. (2017). A new picrotoxane sesquiterpene glucoside from *Dendrobium nobile*. *Natural Product Communications, 12*(12), 1825 - 1826.

Nie, J., Tian, Y., Zhang, Y., Lu, Y.-L., Li, L.-S., & Shi, J.-S. (2016). *Dendrobium* alkaloids prevent $A\beta_{25-35}$-induced neuronal and synaptic loss via promoting neurotrophic factors expression in mice. *PeerJ, 4*, 1-16.

Ninomiya, K., Matsuda, H., Shimoda, H., Nishida, N., Kasajima, N., Yoshino, T., Morikawa, T., & Yoshikawa, M. (2004). Carnosic acid, a new class of lipid absorption inhibitor from sage. *Bioorganic & Medicinal Chemistry Letters, 14*(8), 1943-1946.

Nyakudya, E., Jeong, J. H., Lee, N. K., & Jeong, Y.-S. (2014). Platycosides from the roots of *Platycodon grandiflorum* and their health benefits. *Preventive Nutrition and Food Science, 19*(2), 59-68.

Okamoto, T., Natsume, M., Onaka, T., Uchimaru, F., & Shimizu, M. (1966a). The structure of dendramine (6-oxydendrobine) and 6-oxydendroxine the fourth and fifth alkaloid from *Dendrobium nobile*. *Chemical and Pharmaceutical Bulletin, 14*(6), 676-680.

Okamoto, T., Natsume, M., Onaka, T., Uchimaru, F., & Shimizu, M. (1966b). The structure of dendroxine. The third alkaloid from *Dendrobium nobile*. *Chemical & Pharmaceutical Bulletin, 14*(6), 672-675.

Okamoto, T., Natsume, M., Onaka, T., Uchimaru, F., & Shimizu, M. (1972). Further studies on the alkaloidal constituents of *Dendrobium nobile* (Orchidaceae)-structure determination of 4-hydroxy-dendroxine and nobilomethylene. *Chemical and Pharmaceutical Bulletin, 20*(2), 418-421.

Onakpoya, I. J., Heneghan, C. J., & Aronson, J. K. (2016). Post-marketing withdrawal of anti-obesity medicinal products because of adverse drug reactions: a systematic review. *BioMed Central Medicine, 14*(1), 1-11.

Ono, M., Ito, Y., Masuoka, C., Koga, H., & Nohara, T. (1995). Antioxidative constituents from *Dendrobii Herba* (stems of Dendrobium spp.). *Food Science and Technology International, Tokyo, 1*(2), 115-120.

Pai, H.-C., Chang, L.-H., Peng, C.-Y., Chang, Y.-L., Chen, C.-C., Shen, C.-C., Teng, C.-M., & Pan, S.-L. (2013). Moscatilin inhibits migration and metastasis of human breast cancer MDA-MB-231 cells through inhibition of Akt and Twist signaling pathway. *Journal of Molecular Medicine, 91*(3), 347-356.

Pan, H., Chen, B., Li, F., & Wang, M. (2012). Chemical constituents of *Dendrobium denneanum*. *Chinese Journal of Applied and Environmental Biology, 18*(3), 378-380.

Panche, A., Diwan, A., & Chandra, S. (2016). Flavonoids: an overview. *Journal of Nutritional Science, 5*(47), 1-15.

Patel, D. (2015). Pharmacotherapy for the management of obesity. *Metabolism, 64*(11), 1376-1385.

Patel, D. K., & Stanford, F. C. (2018). Safety and tolerability of new-generation anti-obesity medications: a narrative review. *Postgraduate Medicine, 130*(2), 173-182.

Pereira, M. N., Justino, A. B., Martins, M. M., Peixoto, L. G., Vilela, D. D., Santos, P. S., Teixeira, T. L., da Silva, C. V., Goulart, L. R., & Pivatto, M. (2017). Stephalagine, an alkaloid with pancreatic lipase inhibitory activity isolated from the fruit peel of *Annona crassiflora* Mart. *Industrial Crops and Products, 97*, 324-329.

Peyachoknagul, S., Mongkolsiriwatana, C., Wannapinpong, S., Huehne, P. S., & Srikulnath, K. (2014). Identification of native *Dendrobium* species in Thailand by PCR-RFLP of rDNA-ITS and chloroplast DNA. *ScienceAsia, 40*(2), 113-120.

Phechrmeekha, T., Sritularak, B., & Likhitwitayawuid, K. (2012). New phenolic compounds from *Dendrobium capillipes* and *Dendrobium secundum*. *Journal of Asian Natural Products Research, 14*(8), 748-754.

Priyadharshini, A., Ahalya, S., Vaishnavi, P., Pavithra, S., & Rosario, A. R. (2019). A review on benefits and toxicity of orlistat therapy. *Drug Invention Today, 12*(3), 550-553.

Qi, X. (2018). Review of the clinical effect of orlistat. In *IOP Conference Series: Materials Science and Engineering, 301*(1), p. 012063. IOP publishing.

Qian, C.-D., Jiang, F.-S., Yu, H.-S., Shen, Y., Fu, Y.-H., Cheng, D.-Q., Gan, L.-S., & Ding, Z.-S. (2015). Antibacterial biphenanthrenes from the fibrous roots of *Bletilla striata*. *Journal of Natural Products, 78*(4), 939-943.

Qin, X.-D., Qu, Y., Ning, L., Liu, J.-K., & Fan, S.-K. (2011). A new picrotoxane-type sesquiterpene from *Dendrobium findlayanum*. *Journal of Asian Natural Products Research, 13*(11), 1047-1050.

Qun Fang, L., & Zhao, W. M. (2003). A new dendrobine-type alkaloid from *Dendrobium nobile*. *Chinese Chemical Letters, 14*(3), 278-279.

Rajan, L., Palaniswamy, D., & Mohankumar, S. K. (2020). Targeting obesity with plant-derived pancreatic lipase inhibitors: a comprehensive review. *Pharmacological Research, 155*, 1-34.

Reinecke, T., & Kindl, H. (1993). Characterization of bibenzyl synthase catalysing the biosynthesis of phytoalexins of orchids. *Phytochemistry, 35*(1), 63-66.

Rodgers, R. J., Tschöp, M. H., & Wilding, J. P. (2012). Anti-obesity drugs: past, present and future. *Disease Models & Mechanisms, 5*(5), 621-626.

Rungwichaniwat, P., Sritularak, B., & Likhitwitayawuid, K. (2014). Chemical constituents of *Dendrobium williamsonii*. *Pharmacognosy Journal 6*(3), 36-41.

San, H. T., Boonsnongcheep, P., Putalun, W., Mekboonsonglarp, W., Sritularak, B., & Likhitwitayawuid, K. (2020). **α**-Glucosidase inhibitory and glucose uptake stimulatory effects of phenolic compounds from *Dendrobium christyanum*. *Natural Product Communications, 15*(3), 1-8.

Sarakulwattana, C., Mekboonsonglarp, W., Likhitwitayawuid, K., Rojsitthisak, P., & Sritularak, B. (2020). New bisbibenzyl and phenanthrene derivatives from *Dendrobium scabrilingue* and their **α**-glucosidase inhibitory activity. *Natural Product Research, 34*(12), 1694-1701.

Sarmah, N., Revathi, D., Sheelu, G., Yamuna Rani, K., Sridhar, S., Mehtab, V., & Sumana, C. (2018). Recent advances on sources and industrial applications of lipases. *Biotechnology Progress, 34*(1), 5-28.

Schcolnik-Cabrera, A., Chávez-Blanco, A., Domínguez-Gómez, G., Taja-Chayeb, L., Morales-Barcenas, R., Trejo-Becerril, C., Perez-Cardenas, E., Gonzalez-Fierro, A., & Dueñas-González, A. (2018). Orlistat as a FASN inhibitor and multitargeted agent for cancer therapy. *Expert Opinion on Investigational Drugs, 27*(5), 475-489.

Seyedan, A., Alshawsh, M. A., Alshagga, M. A., Koosha, S., & Mohamed, Z. (2015). Medicinal plants and their inhibitory activities against pancreatic lipase: a review. *Evidence-Based Complementary and Alternative Medicine, 2015*, 1-13.

Shang, Z., Li, X., & Xiao, S. (2020). Two new bibenzyl compounds from *Dendrobium lindleyi*. *Records of Natural Products, 14*(6), 420.

Sharma, S., & Sharma, S. (2020). Obesity epidemic: striking the younger age group. *Medical Journal of Dr. DY Patil Vidyapeeth, 13*(4), 333-334.

Shi, Y., & Burn, P. (2004). Lipid metabolic enzymes: Emerging drug targets for the treatment of obesity. *Nature Reviews Drug discovery, 3*(8), 695-710.

Singh, G., Suresh, S., Bayineni, V. K., & Kadeppagari, R. (2015). Lipase inhibitors from plants and their medical applications. *International Journal of Pharmacy and Pharmaceutical Sciences 7*, 1-5.

Sridhar, S., Mutya, S., & Paul, A. T. (2017). Bis-indole alkaloids from *Tabernaemontana divaricata* as potent pancreatic lipase inhibitors: molecular modelling studies and experimental validation. *Medicinal Chemistry Research, 26*(6), 1268-1278.

Sritularak, B., Anuwat, M., & Likhitwitayawuid, K. (2011a). A new phenanthrenequinone from *Dendrobium draconis*. *Journal of Asian Natural Products Research, 13*(03), 251-255.

Sritularak, B., Duangrak, N., & Likhitwitayawuid, K. (2011b). A new bibenzyl from *Dendrobium secundum*. *Zeitschrift für Naturforschung C, 66*(5-6), 205-208.

Sritularak, B., & Likhitwitayawuid, K. (2009). New bisbibenzyls from *Dendrobium falconeri*. *Helvetica Chimica Acta, 92*(4), 740-744.

Sukhdev, S., & Singh, K. S. (2013). Therapeutic role of phytomedicines on obesity: Importance of herbal pancreatic lipase inhibitors. *International Research Journal of Medical Sciences, 1*(9), 15-26.

Sukphan, P., Sritularak, B., Mekboonsonglarp, W., Lipipun, V., & Likhitwitayawuid, K. (2014). Chemical constituents of *Dendrobium venustum* and their antimalarial and anti-herpetic properties. *Natural Product Communications, 9*(6), 825-827.

Sun, J., Zhang, F., Yang, M., Zhang, J., Chen, L., Zhan, R., Li, L., & Chen, Y. (2014). Isolation of α-glucosidase inhibitors including a new flavonol glycoside from *Dendrobium devonianum*. *Natural Product Research, 28*(21), 1900-1905.

Sun, M.-H., Ma, X.-J., Shao, S.-Y., Han, S.-W., Jiang, J.-W., Zhang, J.-J., & Li, S. (2021). Phenanthrene, 9, 10-dihydrophenanthrene and bibenzyl enantiomers from *Bletilla striata* with their antineuroinflammatory and cytotoxic activities. *Phytochemistry, 182*, 1-14.

Suzuki, R., Tanaka, T., Yamamoto, M., Sakagami, H., Tomomura, M., Tomomura, A., Satoh, K., & Shirataki, Y. (2012). In search of new biological activities of isolates from *Odontoglossum* Harvengtense 'Tutu'. *In Vivo, 26*(6), 993-999.

Tak, Y. J., & Lee, S. Y. (2021). Anti-obesity drugs: long-term efficacy and safety: an updated review. *The World Journal of Men's Health, 39*(2), 208-221.

Talapatra, B., Das, A. K., & Talapatra, S. K. (1989). Defuscin, a new phenolic ester from *Dendrobium fuscescens*: conformation of shikimic acid. *Phytochemistry, 28*(1), 290-292.

Tam, D. N. H., Mostafa, E. M., Tu, V. L., Rashidy, A. I., Matenoglou, E., Kassem, M., Soa, D. T., Bayumi, A., Emam, H. E. S., & Tran, L. (2020). Efficacy of chalcone and xanthine derivatives on lipase inhibition: a systematic review. *Chemical Biology & Drug Design, 95*(2), 205-214.

Tanagornmeatar, K., Chaotham, C., Sritularak, B., Likhitwitayawuid, K., & Chanvorachote, P. (2014). Cytotoxic and anti-metastatic activities of phenolic compounds from *Dendrobium ellipsophyllum*. *Anticancer Research, 34*(11), 6573-6579.

Tang, H., Zhao, T., Sheng, Y., Zheng, T., Fu, L., & Zhang, Y. (2017). *Dendrobium officinale* Kimura et Migo: a review on its ethnopharmacology, phytochemistry, pharmacology, and industrialization. *Evidence-Based Complementary and Alternative Medicine, 2017*, 1-19.

Tang, W., & Eisenbrand, G. (1992). *Dendrobium nobile* Lindl. *In Chinese Drugs of Plant Origin* (pp. 451-454): Springer, Berlin, Heidelberg.

Tek, C. (2016). Naltrexone HCl/bupropion HCl for chronic weight management in obese adults: patient selection and perspectives. *Patient Preference and Adherence, 10*, 751-759.

Teponno, R. B., Kusari, S., & Spiteller, M. (2016). Recent advances in research on lignans and neolignans. *Natural Product Reports, 33*(9), 1044-1092.

Thant, M. T., Chatsumpun, N., Mekboonsonglarp, W., Sritularak, B., & Likhitwitayawuid, K. (2020). New fluorene derivatives from *Dendrobium gibsonii* and their **α**-glucosidase inhibitory activity. *Molecules, 25*(21), 1-9.

Topaloglu, O., & Sahin, I. (2021). Pharmacological treatment of obesity in clinical practice. *Medicine, 10*(2), 651-657.

Tsai, A.-C., Pan, S.-L., Liao, C.-H., Guh, J.-H., Wang, S.-W., Sun, H.-L., Liu, Y.-N., Chen, C.-C., Shen, C.-C., & Chang, Y.-L. (2010). Moscatilin, a bibenzyl derivative from the India orchid *Dendrobrium loddigesii*, suppresses tumor angiogenesis and growth *in vitro* and *in vivo*. *Cancer Letters, 292*(2), 163-170.

Tuchinda, P., Udchachon, J., Khumtaveeporn, K., Taylor, W. C., Engelhardt, L. M., & White, A. H. (1988). Phenanthrenes of *Eulophia nuda*. *Phytochemistry, 27*(10), 3267-3271.

Vaddhanaphuti, N. (2005). A field guide to the wild orchids of Thailand. Chiang Mai, Thailand: Silkworm Books.

Veerraju, P., Rao, N. P., Rao, L. J., Rao, K. J., & Rao, P. M. (1989). Amoenumin, a 9,10-dihydro-5*H*-phenanthro-(4,5-b,c,d)-pyran from *Dendrobium amoenum*. *Phytochemistry, 28*(3), 950-951.

Wang, H., Zhao, T., & Che, C.-T. (1985). Dendrobine and 3-hydroxy-2-oxodendrobine from *Dendrobium nobile*. *Journal of Natural Products, 48*(5), 796-801.

Wang, L., Zhang, C.-F., Wang, Z.-T., Zhang, M., & Xu, L.-S. (2009). Five new compounds from *Dendrobium crystallinum*. *Journal of Asian Natural Products Research, 11*(11), 903-911.

Wang, P., Chen, X., Cai, C.-H., Kong, F.-D., Huang, S.-Z., Yuan, J.-Z., Xu, X.-L., Mei, W.-L., & Dai, H.-F. (2020). A new picrotoxane-type sesquiterpene from *Dendrobium nobile* Lindl. *Natural Product Research*, 1-6.

Wang, P., Chen, X., Wang, H., Huang, S., Cai, C., Yuan, J., Zhu, G., Xu, X., Mei, W., & Dai, H. (2019). Four new picrotoxane-type sesquiterpenes from *Dendrobium nobile* Lindl. *Frontiers in Chemistry, 7*, 1-8.

Wang, Y.-H. (2021). Traditional uses and pharmacologically active constituents of *Dendrobium* plants for dermatological disorders: a review. *Natural Products and Bioprospecting*, 1-23.

Wang, Y.-H., Avula, B., Abe, N., Wei, F., Wang, M., Ma, S.-C., Ali, Z., Elsohly, M. A., & Khan, I. A. (2016). Tandem mass spectrometry for structural identification of sesquiterpene alkaloids from the stems of *Dendrobium nobile* using LC-QToF. *Planta Medica, 82*(07), 662-670.

Warinhomhoun, S., Muangnoi, C., Buranasudja, V., Mekboonsonglarp, W., Rojsitthisak, P., Likhitwitayawuid, K., & Sritularak, B. (2021). Antioxidant activities and protective effects of dendropachol, a new bisbibenzyl compound from *Dendrobium pachyglossum*, on hydrogen peroxide-induced oxidative stress in HaCaT keratinocytes. *Antioxidants, 10*(2), 1-16.

Woodard, K., Louque, L., & Hsia, D. S. (2020). Medications for the treatment of obesity in adolescents. *Therapeutic Advances in Endocrinology and Metabolism, 11*, 1-12.

Wu, L., Lu, Y., Ding, Y., Zhao, J., Xu, H., & Chou, G. (2019). Four new compounds from *Dendrobium devonianum*. *Natural Product Research, 33*(15), 2160-2168.

Xiong, L., Cao, Z.-X., Peng, C., Li, X.-H., Xie, X.-F., Zhang, T.-M., Zhou, Q.-M., Yang, L., & Guo, L. (2013). Phenolic glucosides from *Dendrobium aurantiacum var. denneanum* and their bioactivities. *Molecules, 18*(6), 6153-6160.

Xu, F.-Q., Fan, W.-W., Zi, C.-T., Dong, F.-W., Yang, D., Zhou, J., & Hu, J.-M. (2017). Four new glycosides from the stems of *Dendrobium fimbriatum* Hook. *Natural Product Research, 31*(7), 797-801.

Xu, F.-Q., Xu, F.-C., Hou, B., Fan, W.-W., Zi, C.-T., Li, Y., Dong, F.-W., Liu, Y.-Q., Sheng, J., & Zuo, Z.-L. (2014). Cytotoxic bibenzyl dimers from the stems of *Dendrobium fimbriatum* Hook. *Bioorganic & Medicinal Chemistry Letters, 24*(22), 5268-5273.

Xu, J., Han, Q.-B., Li, S.-L., Chen, X.-J., Wang, X.-N., Zhao, Z.-Z., & Chen, H.-B. (2013). Chemistry, bioactivity and quality control of *Dendrobium*, a commonly used tonic herb in traditional Chinese medicine. *Phytochemistry Reviews, 12*(2), 341-367.

Xu, J., Zhao, W. m., Qian, Z. m., Guan, J., & Li, S. p. (2010). Fast determination of five components of coumarin, alkaloids and bibenzyls in *Dendrobium* spp. using pressurized liquid extraction and ultra performance liquid chromatography. *Journal of Separation Science, 33*(11), 1580-1586.

Xu, X., Chen, X., Yang, R., Li, Z., Zhou, H., Bai, Y., Yu, M., Li, B., & Ding, G. (2020). Crepidtumines A and B, two novel indolizidine alkaloids from *Dendrobium crepidatum*. *Scientific Reports, 10*(1), 1-8.

Xu, X., Li, Z., Yang, R., Zhou, H., Bai, Y., Yu, M., Ding, G., & Li, B. (2019). Crepidatumines C and D, two new indolizidine alkaloids from *Dendrobium crepidatum* Lindl. ex Paxt. *Molecules, 24*(17), 1-9.

Xue, Z., Li, S., Wang, S., Wang, Y., Yang, Y., Shi, J., & He, L. (2006). Mono-, bi-, and triphenanthrenes from the tubers of *Cremastra appendiculata*. *Journal of Natural Products, 69*(6), 907-913.

Yamaki, M., & Honda, C. (1996). The stilbenoids from *Dendrobium plicatile*. *Phytochemistry, 43*(1), 207-208.

Yang, D., Cheng, Z.-Q., Hou, B., Yang, L., Zi, C.-T., Dong, F.-W., Hu, J.-M., & Zhou, J. (2020). Two unusual dendrobine-type alkaloids from *Dendrobium findlayanum*. *Fitoterapia, 144*, 1-4.

Yang, D., Cheng, Z.-Q., Yang, L., Hou, B., Yang, J., Li, X.-N., Zi, C.-T., Dong, F.-W., Liu, Z.-H., & Zhou, J. (2018a). Seco-dendrobine-type alkaloids and bioactive phenolics from *Dendrobium findlayanum*. *Journal of Natural Products, 81*(2), 227-235.

Yang, D., Liu, L.-Y., Cheng, Z.-Q., Xu, F.-Q., Fan, W.-W., Zi, C.-T., Dong, F.-W., Zhou, J., Ding, Z.-T., & Hu, J.-M. (2015a). Five new phenolic compounds from *Dendrobium aphyllum*. *Fitoterapia, 100*, 11-18.

Yang, H., Chou, G. X., Wang, Z. T., Guo, Y. W., Hu, Z. B., & Xu, L. S. (2004). Two new compounds from *Dendrobium chrysotoxum*. *Helvetica Chimica Acta, 87*(2), 394-399.

Yang, H., Sung, S. H., & Kim, Y. C. (2007a). Antifibrotic phenanthrenes of *Dendrobium nobile* stems. *Journal of Natural Products, 70*(12), 1925-1929.

Yang, L., Han, H., Nakamura, N., Hattori, M., Wang, Z., & Xu, L. (2007b). Bio-guided isolation of antioxidants from the stems of *Dendrobium aurantiacum var. denneanum*. *Phytotherapy Research: PTR, 21*(7), 696-698.

Yang, L., Liu, S.-J., Luo, H.-R., Cui, J., Zhou, J., Wang, X.-J., Sheng, J., & Hu, J.-M. (2015b). Two new dendrocandins with neurite outgrowth-promoting activity from *Dendrobium officinale*. *Journal of Asian Natural Products Research, 17*(2), 125-131.

Yang, L., Qin, L.-H., Bligh, S. A., Bashall, A., Zhang, C.-F., Zhang, M., Wang, Z.-T., & Xu, L.-S. (2006a). A new phenanthrene with a spirolactone from *Dendrobium chrysanthum* and its anti-inflammatory activities. *Bioorganic & Medicinal Chemistry, 14*(10), 3496-3501.

Yang, L., Wang, Y., Zhang, G., Zhang, F., Zhang, Z., Wang, Z., & Xu, L. (2007c). Simultaneous quantitative and qualitative analysis of bioactive phenols in *Dendrobium aurantiacum var. denneanum* by high-performance liquid chromatography coupled with mass spectrometry and diode array detection. *Biomedical Chromatography, 21*(7), 687-694.

Yang, L., Wang, Z., & Xu, L. (2006b). Phenols and a triterpene from *Dendrobium aurantiacum var. denneanum* (Orchidaceae). *Biochemical Systematics and Ecology, 34*(8), 658-660.

Yang, L., Zhang, C., Yang, H., Zhang, M., Wang, Z., & Xu, L. (2005). Two new alkaloids from *Dendrobium chrysanthum*. *Heterocycles-Sendai Institute of Heterocyclic Chemistry, 65*(3), 633-636.

Yang, M., Chen, L.-J., Zhang, Y., & Chen, Y.-G. (2019). Two new picrotoxane-type sesquiterpenoid lactones from *Dendrobium williamsonii*. *Journal of Asian Natural Products Research, 21*(2), 129-133.

Yang, M., Zhang, Y., Chen, L., & Chen, Y. (2018b). A new (propylphenyl) bibenzyl derivative from *Dendrobium williamsonii*. *Natural Product Research, 32*(14), 1699-1705.

Ye, Q.-H., Zhao, W.-M., & Qin, G.-W. (2003). New fluorenone and phenanthrene derivatives from *Dendrobium chrysanthum*. *Natural Product Research, 17*(3), 201-205.

Ye, Q.-H., Zhao, W.-M., & Qin, G.-W. (2004). Lignans from *Dendrobium chrysanthum*. *Journal of Asian Natural Products Research, 6*(1), 39-43.

Ye, Q., Mei, Y., Yang, P., Cheng, L., & Kong, D. (2016). A new 9, 10-dihydrophenanthrene glycoside from *Dendrobium primulinum*. *Chemistry of Natural Compounds, 52*(3), 381-383.

Ye, Q., Qin, G., & Zhao, W. (2002). Immunomodulatory sesquiterpene glycosides from *Dendrobium nobile*. *Phytochemistry, 61*(8), 885-890.

Ye, Q., & Zhao, W. (2002). New alloaromadendrane, cadinene and cyclocopacamphane type sesquiterpene derivatives and bibenzyls from *Dendrobium nobile*. *Planta Medica, 68*(08), 723-729.

Ye, Z., Dai, J.-R., Zhang, C.-G., Lu, Y., Wu, L.-L., Gong, A. G., Xu, H., Tsim, K. W., & Wang, Z.-T. (2017). Chemical differentiation of *Dendrobium officinale* and *Dendrobium devonianum* by using HPLC fingerprints, HPLC-ESI-MS, and HPTLC analyses. *Evidence-Based Complementary and Alternative Medicine, 2017*, 1-9.

Ying, L., Jin-He, J., Yan, Z., & Ye-Gao, C. (2009). Chemical constituents of *Dendrobium aurantiacum var. denneanum*. *Chemistry of Natural Compounds, 45*(4), 525-527.

Yu, C.-L., Weng, M.-S., Chen, W.-C., Chien, K.-T., Chi, C.-W., Chung, C.-H., Huang, C.-W., Wang, P.-C., Chen, C.-C., & Tsai, A.-C. (2021). Moscatilin inhibits metastatic behavior of human hepatocellular carcinoma cells: a crucial role of uPA suppression via Akt/NF-**K**B-dependent pathway. *International Journal of Molecular Sciences, 22*(6), 1-16.

Zhang, C.-F., Wang, M., Wang, L., Iinuma, M., Zhang, M., Xu, L.-S., & Wang, Z.-T. (2008a). Chemical constituents of *Dendrobium gratiosissimum* and their cytotoxic activities. *Indian Journal of Chemistry Section B-Organic Chemistry Including Medical Chemistry, 47*(6), 952-956.

Zhang, C., Liu, S.-J., Yang, L., Yuan, M.-Y., Li, J.-Y., Hou, B., Li, H.-M., Yang, X.-Z., Ding, C.-C., & Hu, J.-M. (2017a). Sesquiterpene amino ether and cytotoxic phenols from *Dendrobium wardianum* Warner. *Fitoterapia, 122*, 76-79.

Zhang, G.-N., Zhong, L.-Y., Bligh, S. A., Guo, Y.-L., Zhang, C.-F., Zhang, M., Wang, Z.-T., & Xu, L.-S. (2005). Bi-bicyclic and bi-tricyclic compounds from *Dendrobium thyrsiflorum*. *Phytochemistry, 66*(10), 1113-1120.

Zhang, L., Fang, Y., Xu, X. F., & Jin, D. Y. (2017b). Moscatilin induces apoptosis of pancreatic cancer cells via reactive oxygen species and the JNK/SAPK pathway. *Molecular Medicine Reports, 15*(3), 1195-1203.

Zhang, X., Gao, H., Wang, N.-L., & Yao, X.-S. (2006a). Three new bibenzyl derivatives from *Dendrobium nobile*. *Journal of Asian Natural Products Research, 8*(1-2), 113-118.

Zhang, X., Gao, H., Wang, N., & Yao, X. (2006b). Phenolic components from *Dendrobium nobile*. *Chinese Traditional And Herbal Drugs, 37*(5), 652-655.

Zhang, X., Liu, H. W., Gao, H., Han, H. Y., Wang, N. L., Wu, H. M., Yao, X. S., & Wang, Z. (2007a). Nine new sesquiterpenes from *Dendrobium nobile*. *Helvetica Chimica Acta, 90*(12), 2386-2394.

Zhang, X., Tu, F.-J., Yu, H.-Y., Wang, N.-L., Wang, Z., & Yao, X.-S. (2008b). Copacamphane, picrotoxane and cyclocopacamphane sesquiterpenes from *Dendrobium nobile*. *Chemical and Pharmaceutical Bulletin, 56*(6), 854-857.

Zhang, X., Xu, J.-K., Wang, J., Wang, N.-L., Kurihara, H., Kitanaka, S., & Yao, X.-S. (2007b). Bioactive bibenzyl derivatives and fluorenones from *Dendrobium nobile*. *Journal of Natural Products, 70*(1), 24-28.

Zhang, X., Xu, J.-K., Wang, N.-L., Kurihara, H., & Yao, X.-S. (2008c). Antioxidant phenanthrenes and lignans from *Dendrobium nobile*. *Journal of Chinese Pharmaceutical Sciences, 17*(4), 314-318.

Zhang, Y., Wang, P., Song, X., Zuo, W., Wang, H., Chen, L., Mei, W., & Dai, H. (2018). Chemical constituents from *Dendrobium hainanense*. *Journal of Asian Natural Products Research, 21*(9), 873-880.

Zhang, Y., Zhang, L., Liu, J., Liang, J., Si, J., & Wu, S. (2017c). *Dendrobium officinale* leaves as a new antioxidant source. *Journal of Functional Foods, 37*, 400-415.

Zhao, C., Liu, Q., Halaweish, F., Shao, B., Ye, Y., & Zhao, W. (2003a). Copacamphane, picrotoxane, and alloaromadendrane sesquiterpene glycosides and phenolic glycosides from *Dendrobium moniliforme*. *Journal of Natural Products, 66*(8), 1140-1143.

Zhao, G.-Y., Deng, B.-W., Zhang, C.-Y., Cui, Y.-D., Bi, J.-Y., & Zhang, G.-G. (2018). New phenanthrene and 9,10-dihydrophenanthrene derivatives from the stems of *Dendrobium officinale* with their cytotoxic activities. *Journal of Natural Medicines, 72*(1), 246-251.

Zhao, H. L., & Kim, Y. S. (2004). Determination of the kinetic properties of platycodin D for the inhibition of pancreatic lipase using a 1,2-diglyceride-based colorimetric assay. *Archives of Pharmacal Research, 27*(10), 1048-1052.

Zhao, N., Yang, G., Zhang, Y., Chen, L., & Chen, Y. (2016). A new 9,10-dihydrophenanthrene from *Dendrobium moniliforme*. *Natural Product Research, 30*(2), 174-179.

Zhao, W., Ye, Q., Dai, J., Martin, M.-T., & Zhu, J. (2003b). Allo-aromadendrane-and picrotoxane-type sesquiterpenes from *Dendrobium moniliforme*. *Planta Medica, 69*(12), 1136-1140.

Zhao, W., Ye, Q., Tan, X., Jiang, H., Li, X., Chen, K., & Kinghorn, A. D. (2001). Three new sesquiterpene glycosides from *Dendrobium nobile* with immunomodulatory activity. *Journal of Natural Products, 64*(9), 1196-1200.

Zhen-jian, L., Wen-ya, Z., Bin, H., Yuan-cheng, W., Yi-yun, Z., Si-cong, L., & Zhen-yuan, S. (2020). Study on alkaloids from stems of *Dendrobium crepidatum* based on UPLC-Q-TOF-MS. *Natural Product Research and Development, 32*(3), 482-488.

Zhou, X.-M., Zhang, B., Chen, G.-Y., Han, C.-R., Jiang, K.-C., Luo, M.-Y., Meng, B.-Z., Li, W.-X., & Lin, S.-D. (2018). Dendrocoumarin: a new benzocoumarin derivative from the stem of *Dendrobium nobile*. *Natural Product Research, 32*(20), 2464-2467.

Zhou, X.-M., Zheng, C.-J., Wu, J.-T., Chen, G.-Y., Chen, J., & Sun, C.-G. (2016). Five new lactone derivatives from the stems of *Dendrobium nobile*. *Fitoterapia, 115*, 96-100.

Zhou, X.-M., Zheng, C.-J., Wu, J.-T., Chen, G.-Y., Zhang, B., & Sun, C.-G. (2017). A new phenolic glycoside from the stem of *Dendrobium nobile*. *Natural Product Research, 31*(9), 1042-1046.

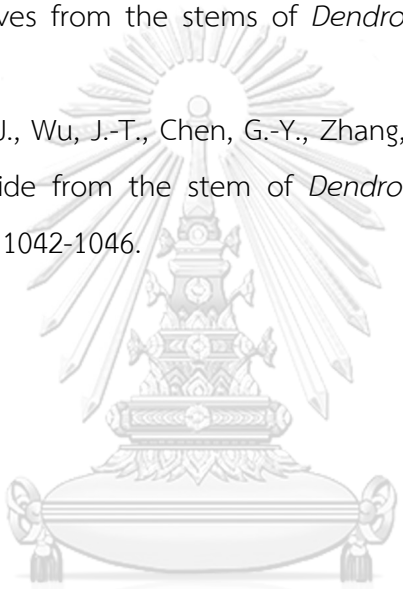

VITA

NAME	Ms. Myat Pann Phyu
DATE OF BIRTH	27 Feb 1997
PLACE OF BIRTH	Mandalay, Myanmar
INSTITUTIONS ATTENDED	University of Pharmacy, Mandalay
HOME ADDRESS	House no.72, 34th street, between 74th and 75th street, Molyagiwah quarter, Mandalay, Myanmar
PUBLICATION	Pann Phyu, M., Kongkatitham, V., Mekboonsonglarp, W., Likhitwitayawuid, K., & Sritularak, B. (2021). Phenanthrenes from Dendrobium senile and their pancreatic lipase inhibitory activity. Journal of Asian Natural Products Research, 1-6.